

Investigating controls on carbonate platform geometry using forward modelling, outcrop and synthetic seismic studies

Huw Davies Williams
MESci

Cardiff University and Shell
Submitted: July 2010



UMI Number: U517094

All rights reserved

INFORMATION TO ALL USERS

The quality of this reproduction is dependent upon the quality of the copy submitted.

In the unlikely event that the author did not send a complete manuscript and there are missing pages, these will be noted. Also, if material had to be removed, a note will indicate the deletion.



UMI U517094

Published by ProQuest LLC 2013. Copyright in the Dissertation held by the Author.
Microform Edition © ProQuest LLC.

All rights reserved. This work is protected against
unauthorized copying under Title 17, United States Code.



ProQuest LLC
789 East Eisenhower Parkway
P.O. Box 1346
Ann Arbor, MI 48106-1346

DECLARATION

This work has not previously been accepted in substance for any degree and is not concurrently submitted in candidature for any degree.

Signed Howell (candidate)
Date ...8.7.10.....

STATEMENT 1

This thesis is being submitted in partial fulfilment of the requirements for the degree of PhD.

Signed Howell (candidate)
Date ...8.7.10.....

STATEMENT 2

This thesis is the result of my own independent work/investigation, except where otherwise stated.

Other sources are acknowledged by explicit references.

Signed Howell (candidate)
Date ...8.7.10.....

STATEMENT 3

I hereby give consent for my thesis, if accepted, to be available for photocopying and for inter-library loan, and for the title and summary to be made available to outside organisations.

Signed Howell (candidate)
Date ...8.7.10.....

STATEMENT 4

I hereby give consent for my thesis, if accepted, to be available for photocopying and for inter-library loans **after expiry of a bar on access previously approved by the Graduate Development Committee.**

Signed Howell (candidate)
Date ...8.7.10.....

Summary

Combined outcrop and forward modelling studies have been used to test and develop the current classification scheme for carbonate platforms. End member platform types of ramp and flat-topped platform (FTP) are typically defined by their depositional gradient. However, many examples exist that do not conform to this simple classification. To investigate why this is and to better understand likely controls on platform development a series of 2D numerical forward models have been run to investigate how sediment production, transport and other controls such as tectonic subsidence, antecedent topography, and relative sea-level oscillation interact to determine platform geometry.

The modelling results suggest that rates of offshore sediment transport relative to rates of autochthonous production are a critical factor in maintaining a ramp profile in stable cratonic settings under a constant rate of relative sea-level rise. Type of carbonate production profile, for example euphotic versus oligophotic, is not a significant control in the model cases. Both euphotic and oligophotic production profiles produce FTPs when sediment transport rates are low relative to production rates, and ramps when sediment transport rates are relatively high. These results suggest a continuum of platform types, ranging from transport-dominated, low-gradient systems at one end of the spectrum, to in-situ accumulation dominated systems at the other.

Time evolution is also likely to be an important control on platform development. Initially low gradient systems will, in the absence of sufficiently high sediment transport rates, tend to evolve towards a high-gradient flat-topped steep-margined platform. Many observed or inferred platform geometries are therefore likely to be transient forms, and this could complicate interpretation.

Forward models investigating how basin bathymetry and style of subsidence control platform geometry suggest that in transport dominated systems strata simply drape the underlying topography, and that breaks of slope and differential fault subsidence are a stronger control on platform geometry for in-situ accumulation dominated systems. While rotational subsidence tends to create low-gradient transport-dominated systems when transport rates increase during rotation as topographic gradient increases and transport rate outpaces in-situ production rate.

Finally, forward models analysing the influence of relative sea-level oscillations on platform development illustrate how high-amplitude glacio-eustatic oscillations tend to move the locus of sediment production laterally along any gradient present on the platform, distributing sediment accumulation across the whole width of the platform, suppressing progradation and steepening, and so favouring the development of low-gradient ramp systems.

The forward modelling results suggest that carbonate platform classification into ramp and flat-topped platform types can be useful, however a more meaningful approach maybe to describe and predict platform strata in terms of a multidimensional parameter space (MPS) containing a continuum of geometries controlled by sediment production, sediment transport, subsidence effects, and relative sea-level oscillations.

Synthetic seismic investigating this continuum of platform geometries provides valuable information regarding potential hydrocarbon targets in these carbonate systems. The tramline like seismic expression of the low-gradient geometries precludes simple identification of reservoir prone facies. However, the combined forward modelling and field studies suggest that the presence of coarse, shallow water derived material in outer ramp wackestone/packstone beds may present previously overlooked prospective targets in the distal sections of these low angle carbonate geometries. High resolution seismic specifically targeting these areas may therefore prove beneficial in future assessments of a carbonate systems reservoir potential.

Outcrop and laboratory analysis of the South Wales carbonate ramp validated the model hypothesis that a high rate of sediment transport is likely a dominant control on the development of a low gradient carbonate geometry. Several other ramp examples are also shown to portray diagnostic features similar to the South Wales ramp example, implying significant magnitudes of sediment transport in each case and further supporting the hypothesis that ramps are transport-dominated systems.

Acknowledgements

I would firstly like to thank Shell for sponsoring this thesis, and for their continual support throughout the study.

My sincere thanks go to those who have provided me with assistance during fieldwork: Sid Howells for giving up his free-time time and invaluable experience and advice on the Castlemartin section of West Wales, and my fellow Cardiff University post-graduate student Ben Rabb for assisting me on the Pen-y-Holt sections. I am also extremely grateful to the Ministry of defence for granting me access to the Castlemartin Artillery range, without which my fieldwork would not have been possible, and I would not have been given the opportunity to work on the exceptional, untouched cliff sections located within the range.

In relation to the forward modelling aspect of the thesis I am very grateful to IFP, in particular Didier Granjeon, for permitting me the use of the Dionisos forward modelling software. While Henne Lammers provided me with invaluable information and discussion during my time in Rijswijk regarding the 'Analyse' code. Also thank you to Xavier Janson for his guidance and assistance with the Madagascar software.

I am deeply indebted to my supervisors, Paul Wright, Peter Burgess and Giovanna Della Porta for their guidance, without whom none of this would have been possible – thank you.

I would like to thank my family for their loving support throughout my studies, and finally a special thanks to Emily for her endless patience and encouragement when it was most required, and for always believing in me.

Contents

CHAPTER 1:	INTRODUCTION	
1.1	Rationale	1
1.2	Aims	2
1.3	Structure	2
<hr/>		
CHAPTER 2:	THE CARBONATE RAMP SYSTEM – OUR CURRENT UNDERSTANDING	4
2.1	The history of the carbonate ramp concept	4
2.2	Carbonate ramp classification and facies	6
2.3	Controls on carbonate ramp development	9
2.3.1	Carbonate productivity	9
2.3.2	Organic influence	14
2.3.3	Sediment dynamics	15
2.3.4	Sequence stratigraphic controls on ramp development	16
2.3.5	Tectonic setting	19
2.4	Carbonate ramp seismic character	23
2.5	The hydrocarbon and economic importance of carbonate ramps	26
2.6	Summary	29
<hr/>		
CHAPTER 3:	FORWARD MODELLING CARBONATE RAMP SYSTEMS	30
3.1	Stratigraphic forward modelling and the carbonate environment	30

3.2	SFM of carbonate ramp systems	34
3.3	The model-fit approach and the introduction of an alternative, new modelling method – ‘APE’	38
3.3.1	The APE method 1 – Construction of a Dionisos template	41
3.3.2	The APE method 2 – Use of the ANALYSE program	44
3.3.3	The APE method 3 – Formatting and illustration of results	51
3.4	Utilizing the APE modelling method	51
<hr/>		
CHAPTER 4:	UNDERSTANDING CARBONATE PLATFORM TYPES: USING ‘APE’ TO TEST THE ROLE OF SEDIMENT PRODUCTION AND TRANSPORT ON PLATFORM GEOMETRY	60
4.1	Introduction – Our current understanding of carbonate platform types	60
4.2	Modelling rationale and aims	63
4.3	Model formulation, initial conditions and parameters	64
4.3.1	Quantitative measurement of platform geometry	65
4.4	Euphotic, grain-dominated systems (M1 results)	66
4.4.1	Development of a slope break	72
4.5	Testing production profiles (M2) – <i>What kind of production profile creates a ramp?</i>	74
4.6	Grain composition (M3, M4, M5) – <i>What affect does it have on platform development?</i>	78
4.7	Discussion – Classifying a continuum of carbonate Platform types	84
<hr/>		
CHAPTER 5:	UNDERSTANDING CARBONATE PLATFORM TYPES: THE ROLE OF BATHYMETRIC, TECTONIC AND SEA-LEVEL VARIATIONS IN PLATFORM DEVELOPMENT	89
5.1	Introduction	89

5.2	Investigating the role of bathymetry on platform development	90
5.3	Investigating the influence of faulting and subsidence on platform development	93
5.3.1	Syn depositional Fault control on platform geometry (M7)	93
5.3.2	Platform geometry affected by rotational subsidence (M8)	95
5.3.3	Antecedent versus actively developing bathymetric geometries (M9-12)	97
5.4	Optimal tectonic conditions for ramp development	103
5.4.1	Passive margins	104
5.4.2	Foreland basin margins	106
5.4.3	Extensional basins – Fault block ramps	116
5.4.4	Intraplatform basins	126
5.4.5	Optimal tectonic conditions for ramp development – Summary	141
5.5	Investigating the influence of relative sea-level oscillations on platform development	142
5.5.1	Ice-house versus Greenhouse carbonate systems	143
5.5.2	Testing the role of relative sea-level on platform development with APE	145
5.5.3	Summary of relative sea-level oscillation control on platform development	149
5.6	The role of bathymetric, tectonic and sea-level variations in platform development – A synopsis and the ‘MPS’ concept	155
5.6.1	A Multidimensional Parameter Space for carbonate platform development: ‘MPS’	156

CHAPTER 6:	SEDIMENT DYNAMICS OF A CARBONIFEROUS (MISSISSIPPIAN) CARBONATE RAMP: THE SOUTH WALES RAMP	161
6.1	Introduction – Fieldwork Objectives	161
6.2	The South Wales carbonate ramp	163
6.2.1	The Arundian carbonate ramp	166
6.3	Field and Laboratory Analysis Methods	167
6.3.1	The Pen-y-Holt Limestone (PyH)	167
6.3.2	The High Tor Limestone	169
6.3.3	Laboratory Analysis	169
6.4	Field and Laboratory Analysis Results	171
6.4.1	The Pen-y-Holt Limestone (PyH)	171
6.4.2	The High Tor Limestone	177
6.4.3	Point count analysis of the Pen-y-Holt and High Tor	182
6.4.4	Scanning electron microscope analysis of the Pen-y-Holt Limestones	186
6.5	Sediment dynamics on the South Wales ramp – Interpretations and discussion	191
6.5.1.	The event deposits of the PyH	194
6.5.2.	The frequency of the PyH event deposits	197
6.6	Carbonate ramp sediment dynamics – Applications	201

CHAPTER 7:	THE SEISMIC VISIBILITY OF CARBONATE GEOMETRIES: CAN THE MPS PLATFORM GEOMETRIES BE VIEWED IN SEISMIC?	208
7.1	Introduction	208
7.2	Synthetic seismic	209
7.2.1.	Calculating synthetic seismic from sonic and density log Data – 1D convolution	209
7.2.2.	Velocity and density parameters	210
7.2.3.	Calculating synthetic seismic in Dionisos – 1D convolution	211
7.2.4.	Calculating synthetic seismic in Madagascar – 2D convolution	211
7.3	Synthetic seismic results and discussion	212
7.3.1.	1D convolution results	215
7.3.1.1	Ramp Geometries	215
7.3.1.2	FTP Geometries	215
7.3.1.3	RSL influenced examples	216
7.3.2.	2D convolution results	217
7.3.3.	Smaller-scale models and synthetic seismic	218
7.4	Synthetic seismic conclusions	221
CHAPTER 8:	CONCLUSIONS AND FUTURE WORK	224
8.1	Conclusions	224
8.1.1.	Forward modelling conclusions	224

8.1.2.	Forward modelling limitations and caveats	228
8.1.3.	Outcrop analysis conclusions	230
8.2	Wider implications of results	232
8.3	Future work	234
<hr/>		
REFERENCES		236
<hr/>		

APPENDICES		262
-------------------	--	------------

Appendix 1:	Sedimentary logs of the Pen y Holt Formation, Castlemartin, UK	262
-------------	--	-----

TABLES		
---------------	--	--

Table 3.1	Max and min Sediment Production Rates and Diffusion Coefficient values used in M1.	46
Table 3.2	Principal reference table for input parameters and purpose of each model produced in this study.	54
Table 4.1	New definitions for classification of large-scale carbonate deposystems	86
Table 5.1	Characteristic formations deposited in intraplatform basins	130
Table 7.1	Seismic parameters used for the creation of synthetic seismic in Dionisos and Madagascar.	210

LIST OF ABBREVIATIONS AND ACRONYMS

FTP - Flat-topped platform

LMA - Limestone-marl alternations

SEM - Scanning electron microscope

SFM - Stratigraphic forward modelling

APE - Assessing Platform controls using Experimental modelling

MPS - Multidimensional Parameter Space for carbonate platform development

Chapter 1: INTRODUCTION

1.1 RATIONALE

The rationale of this study was to use numerical forward modelling along with outcrop studies to gain a greater understanding for the controlling parameters and seismic character of carbonate ramp systems.

Despite their abundance and undoubted economic importance carbonate ramps have been the subject of surprisingly little focussed study and are still commonly misinterpreted and poorly understood. In general carbonate depositional systems are typically classified as one of a number of different platform types dependent on their large-scale geometry. This classification is important because many predictive elements of facies and sequence stratigraphic models vary between the different types. Unfortunately, as with many Earth surface systems, these definitions of carbonate depositional type are often difficult to apply because they are essentially simple geomorphic terms used to categorize potentially complicated ancient strata.

Of the several fundamental problems surrounding our understanding of the carbonate ramp system none are more poorly constrained than the controlling parameters on their development. Despite significant study of outcrop and subsurface examples there are limits to the insight that stratigraphy and sedimentary successions can provide regarding depositional conditions, and while the study of modern analogues can be informative neither method is perfect in enhancing our knowledge of the controls on these ancient environments. Numerical forward modelling provides a tool with which the controlling parameters of carbonate deposition in ancient environments can be evaluated in terms of their potential to produce recognisably equivalent sections to modern outcrop and subsurface examples.

A further problem is the lack of unique seismic character commonly portrayed by carbonate ramp systems, with successions typically appearing featureless and too thin for sequence geometries to be seen. Additional complications arise in the misinterpretation of slope breaks and platform margins in highly compressed seismic and many examples may simply be

missed all together due to the likely transitional nature of these systems into flat topped platforms.

The importance of these academic issues should not be underestimated. Important hydrocarbon reservoirs within carbonate ramp successions exist globally and an enhanced knowledge of their controlling parameters and seismic character will advance our appreciation of the distribution of reservoir prone facies in carbonate ramp systems. This study attempts to address the controls on the carbonate ramp system using a forward modelling approach.

1.2 AIMS

The individual objectives of every chapter are listed at the start of each, in addition to which three fundamental aims will be addressed throughout this study:

- 1.) To provide a new conceptual model (including terminology) of carbonate ramp development based on the combination of its controlling parameters.
- 2.) To produce a multidimensional platform parameter space for the prediction of carbonate platform development.
- 3.) To assess the seismic character and visibility of a range of carbonate platform geometries.

1.3 STRUCTURE

This thesis is organised into eight chapters, each of which initiate by outlining the aim of the chapter and conclude by summarizing the chapters' key results and outcomes. This Chapter introduces the fundamental themes and aims for the thesis, while Chapter two provides a review of our current knowledge of the carbonate ramp system, including a definition, global examples, our existing understanding surrounding their controls, seismic character, and their hydrocarbon and economic importance.

Chapter 3 discusses the use of stratigraphic forward models in understanding carbonate platform development, before introducing the 'APE' modelling method which is utilised throughout the thesis. Chapters 4 and 5

present a series of forward models which employ this method. Chapter 4 discusses model results illustrating the control sediment production and transport exert on carbonate platform geometry, while Chapter 5 investigates how platform geometry is influenced by additional controlling parameters including bathymetric variations, tectonic regimes and sea-level oscillations. Chapter 5 concludes with the construction of a multidimensional parameter space for carbonate platform development which summarizes and incorporates the forward modelling results of Chapters 4 and 5.

Chapter 6 tests the validity of these forward modelling results by means of an outcrop analysis of the Arundian aged South Wales carbonate ramp, while the Chapter 7 investigates the seismic visibility of the modelled geometries by creating and analysing a series of synthetic seismograms.

Chapter 8 is the final chapter and concludes the thesis by listing the major results and outcomes of the work, the wider implications of these results, and discussing the potential for future research.

Chapter 2: THE CARBONATE RAMP SYSTEM – OUR CURRENT UNDERSTANDING

At present a carbonate ramp is typically defined as a carbonate system which has a very low gradient depositional slope (commonly less than 1°) from a shallow-water shoreline or lagoon to a basin floor (Burchette and Wright, 1992). A large proportion of carbonate successions in the geological record were deposited on ramp like settings. However, in contrast to rimmed shelves and isolated build-ups where the factors which have controlled their development are by comparison, better understood, the controls on ramp development have rarely been clearly identified. The ramp setting therefore remains one of the more contentious carbonate platform types.

This chapter aims to review our current knowledge of the carbonate ramp system, including current definitions, providing numerous global examples, discussions about the existing understanding surrounding controls on ramp development, an outline of their seismic character, and their major hydrocarbon and economic importance.

2.1 The history of the carbonate ramp concept

Bishop's (1969) study of the Gulf of Mexico Smackover Formation and Purser's (1973) investigation in to the Persian Gulf prompted a critical review of the different types of carbonate platform and their accompanying facies patterns. This landmark study was conducted by Ahr (1973), in which the carbonate ramp concept was conceived. Ahr identified the key differences between the models for shelf and ramp environments, stating that the ramp model facies patterns are opposite to the shelf model in lateral relationships, whereby in the ramp model, grainstones and packstones outcrop as the landward facies and the sediments become muddy as you move seaward. This was in contrast to the shelf model, in which a muddy landward facies typical passes seaward into shelf-margin grainstones and boundstones. Ahr also noted the importance of the absence of continuous reefs, with patch reefs more probable to be locally present on carbonate ramps.

The carbonate ramp concept remained relatively unknown, probably because of the limited circulation of the journal in which the definition was first published. This was until Read (1982; 1985) made significant refinements to the ramp concept by dividing it into two subdivisions on the basis of slope gradient. The divisions were homoclinal and distally steepened ramps. Read classified the homoclinal ramp as having a relatively uniform slope which passes into basins with an absence of sediment gravity flow deposits or slumps in deep-water facies. Furthermore he made initial attempts at assigning a degree of slope to the surface, suggesting these relatively uniform slopes would only change one to a few metres in gradient over a kilometre (1982), and progressed (1985) to state that all ramps would generally have a slope less than 1°. The homoclinal ramp was comparable with Ahr's original ramp concept, however Read (1982; 1985) purposed a slightly different kind of ramp morphology also existed in the form of a distally steepened ramp. Read implied that such a ramp was in fact a transition between a ramp and rimmed shelf environment due to it sharing facies characteristics from both. He continued by stating that there was however a difference between the two depositional settings in that unlike the shelf system the major break in slope in a distally steepened ramp does not occur at the transition from wave-agitated lime sands to subwave-base muds, but many kilometres seaward of this zone.

In Read's 1985 study he also began to assess the relationship between the two ramp types with respect to their controlling factors which lead to one or the other being formed, these included sediment productivity, sediment dispersal, climatic fluctuations, and tectonic controls. In addition he briefly discussed ramp evolution, and stated the potential for a ramp to evolve into a rimmed shelf if given enough time. As in Ahr's initial paper (1973), Read also states the importance of the ramp setting with regards to petroleum exploration, notably their reservoir potential, and included examples such as the oolitic ramp reservoirs of the Jurassic Smackover and the Jurassic Arab A to D oolitic reservoirs of the Middle East.

2.2 Carbonate ramp classification and facies

Numerous attempts at a further subdivision of the carbonate ramp system have been made, with most classifications being based on the location of two critical interfaces: fair weather wave base (FWWB) and storm wave base (SWB). Using the Cambrian ramp in Virginia Markello and Read (1981) made an early attempt at such a subdivision, defining three distinct zones: peritidal platform, shallow ramp (located above FWWB), and deep ramp (below FWWB). Similar schemes were adopted by Aigner (1984) to describe the Triassic Upper Muschelkalk of Germany, Calvet and Tucker (1988) to describe the Catalan Basin, and Buxton and Pedley (1989) in reference to the Tertiary ramps of the Mediterranean.

In a synopsis of the ramp concept by Burchette and Wright (1992) these critical interfaces were once again invoked, which combined with recognition that ramps are morphologically and hydrodynamically similar to siliciclastic shelves a subdivision was devised (Fig. 2.1). The ramp was separated into four subdivisions: *Inner ramp* – the zone above FWWB, *Mid ramp* – the zone between FWWB and SWB, *Outer ramp* – the zone from the depth limit to which most storms influence to the basin plain, and the *Basin*. This scheme has since become the standard for classifying ramp subdivisions.

The typical facies associations found in carbonate ramps can also be described with reference to the Burchette and Wright (1992) ramp classification scheme. Carbonate ramp examples (Fig. 2.2) typically show the following associations; inner ramp facies are commonly composed of bioclastic or oolitic shoal, barrier, and back barrier sediments, with lagoonal sediments consisting of a range of mud-, wacke-, or packstone lithologies. Peritidal sediments are generally microbially laminated and any organic build ups in the inner ramp setting tend to be biostromal. The Mid-ramp environment is characterised by sediments deposited below FWWB and is usually dominated by lime or terrigenous mud, with associated grain or packstone sediments consisting of largely autochthonous bioclasts. While the outer ramp is commonly composed of argillaceous carbonate and terrigenous mud interbedded with event bed (packstone) deposits.

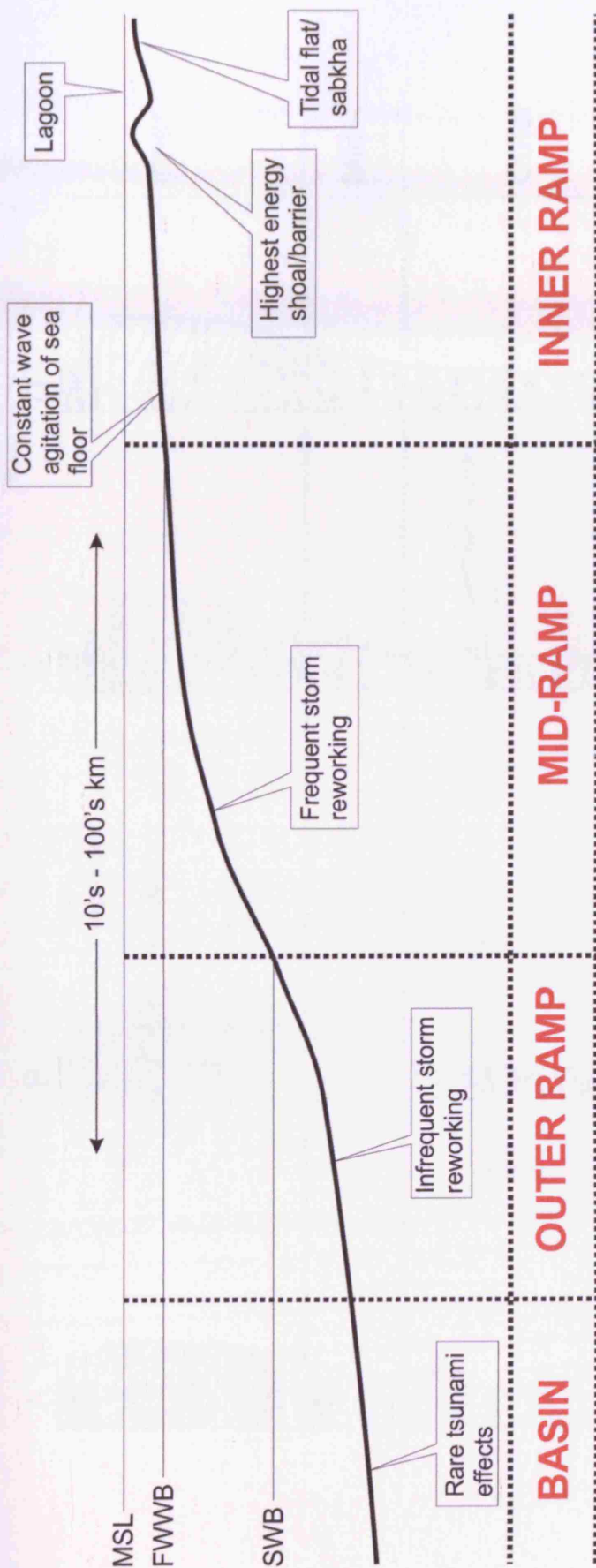


Figure 2.1. The classification of homoclinal ramp subdivisions after Burchette and Wright (1992). MSL = Mean Sea Level, FWWB = fair weather wave base, SWB = storm wave base.

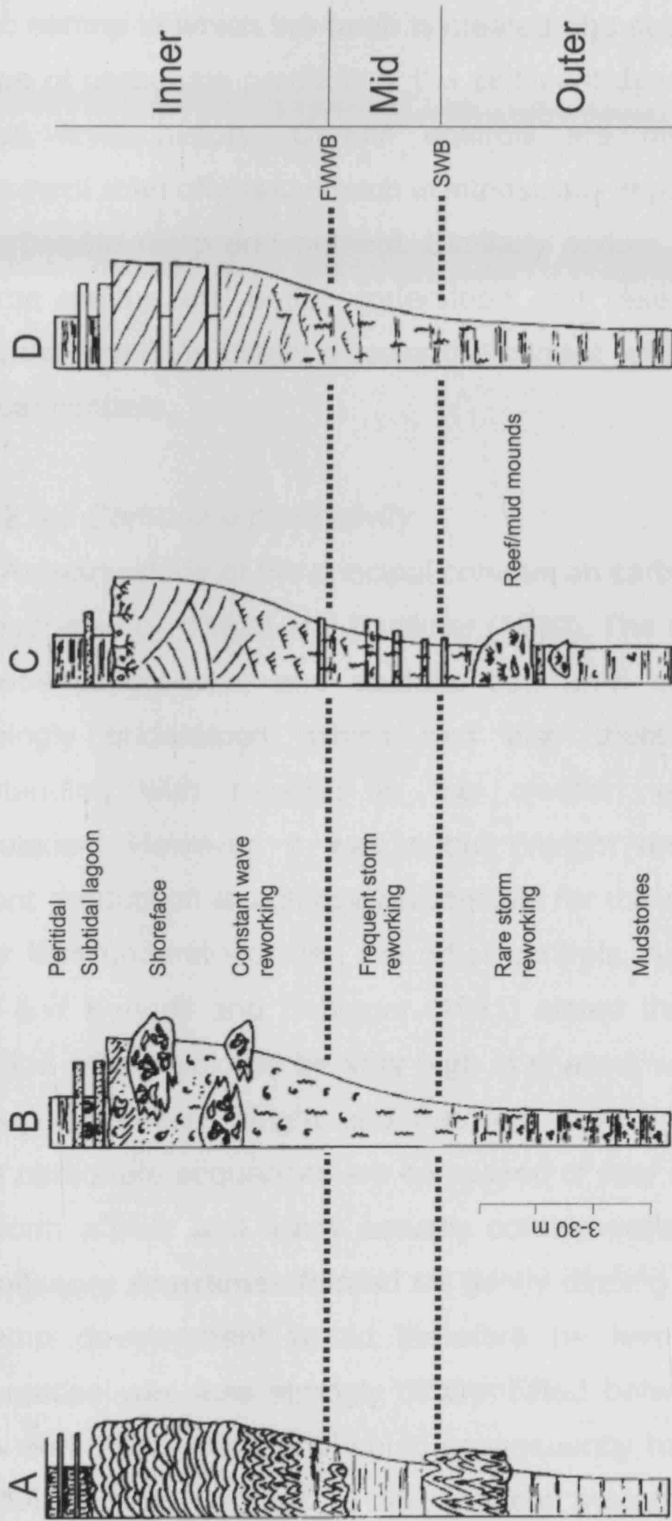


Figure 2.2. Representative facies successions for carbonate ramp examples, edited from Burchette and Wright (1992). A) Facies based on Proterozoic stromatolite-dominated ramp, Grotzinger (1989). B) Skeletal boundstone-dominated ramp, Burchette (1981) and Burchette and Britton (1985). C) Grainstone dominated ramp, Ahr (1973). D) Tertiary, large foraminiferan shoal-dominated ramp, Aigner (1983).

2.3 Controls on carbonate ramp development

The creation, development and lifespan of a carbonate ramp is the result of a wide range of interacting controls. Among others these include the tectonic setting in which the ramp is created, the subsidence regime, the rate and type of carbonate production, the sediment dynamics of the system, and the sea level history. Certain controls are more important in ramp development than others but each is intrinsically important in the development of a carbonate ramp environment. Similarly certain controls and their role in the ramp setting are better understood and researched than others; the subsequent sections briefly discuss the current level of knowledge on these individual controls.

2.3.1 Carbonate productivity

An early study of the principal controls on carbonate ramp development was conducted by Wright and Faulkner (1990). The rates and mechanisms of both tectonic process, and eustatic sea level changes were becoming increasingly understood, which had also therefore led to a greater understanding with regards to the creation of space for sediment accumulation. However, it was noted (Wright and Faulkner, 1990) that sediment production is actually responsible for the sediment record and this was far less understood than the other controls. Authors such as Schlager (1981) and Kendall and Schlager (1981) stated that the rate of carbonate production would typically be very high in shallow waters and much lower in the deep. However, Wright and Faulkner (1990) pointed out that not all ancient carbonate sequences are composed of very shallow water limestones of platform affinity and many actually contain varied shallow-to-moderately deep, offshore limestones formed on gently dipping slopes. They suggested that ramp development would therefore be favoured in settings where sedimentation was less strongly differentiated between production levels in shallow and deep water, and would consequently have a different carbonate productivity profile to that of the tropical system carbonate profile (i.e. Bosscher and Schlager, 1993) which had been derived from modern case studies. The production curve proposed by Wright and Faulkner (1990) implied that shallow water carbonate production on ramps would be lower

than that seen in modern reefal systems, and an elevated rate of production in deeper water was probably present, therefore suggesting more widespread carbonate production across the ramp system.

This idea of widespread carbonate productivity in ramp systems has subsequently been addressed in the work of Luis Pomar (2001a; 2001b; 2004), based predominantly on the Lower Tortonian ramp of Menorca. Pomar's approach at classifying the production across a ramp was by means of an analysis of the representative biota. The variables analysed included the type of sediment that was produced, the locus of sediment production, and the hydraulic energy. From these three variants Pomar implied that three carbonate-producing biota can then be distinguished (Fig. 2.3); (1) Euphotic in shallow, wave agitated areas; (2) Oligophotic in deeper, commonly non-wave-agitated areas; and (3) photo-independent biota in all water-depth ranges. Pomar used these divisions to assign the representative biota to respective platform types, be they rimmed or flat-topped platforms, and stated that oligophotic gravel-producing biota, such as some larger foraminifera and red algae are the most likely to generate distally steepened ramps, while mud-dominated carbonate production, in either euphotic or oligophotic zones would be likely to create a homoclinal ramp. Subsequently, Pomar (2004) suggested that changes in these carbonate producing biota could actually result in changes in the gross platform morphology, i.e. ramp to flat-topped platform evolution. Examples of this process in which ramp to platform evolution is ascribed to major changes in biota include the Lower to Middle Cambrian of the Appalachians (Barnaby and Read, 1990) and the Triassic of Central Europe (Torok, 1998). Pomar's genetic approach at classification may have simplified the many possible scenarios of platform architecture; however it was important in further emphasizing the potential for a varied carbonate-productivity profile with carbonate production not limited solely to the shallow waters.

In addition to the work of Pomar the role of the carbonate factory in platform development has also been assessed by Schlager (2000; 2003). In his re-analysis of the carbonate factory model Schlager proposed a new

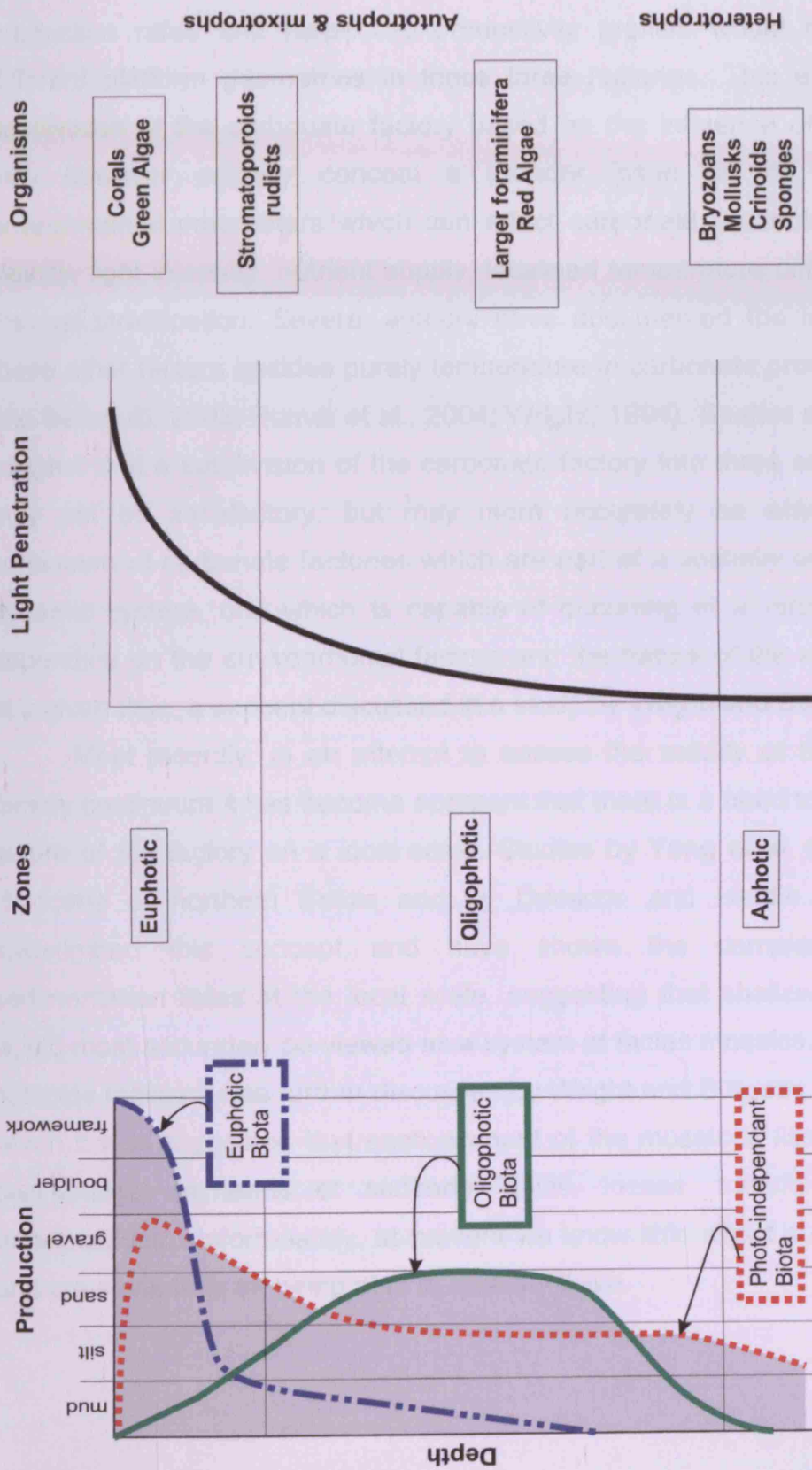


Figure 2.3. Classification of carbonate production across a ramp derived from its representative biota. Diagram modified after Pomar (2001a). Organism groups are controlled by their dependence on light penetration in the water column; euphotic = good light condition, oligophotic = poor light conditions, aphotic = no light.

subdivision of the carbonate factory into three main types; tropical shallow water, cool water, and mud-mound factory, and emphasized how the different production rates and respective productivity profiles would produce very different platform geometries in these three factories. This emphasis and subdivision of the carbonate factory based on the influence of temperature may however actually conceal a broader issue of the many other environmental parameters which can affect carbonate production, including salinity, light intensity, nutrient supply, localised temperature differences, and thermal stratification. Several authors have documented the importance of these other factors besides purely temperature in carbonate production (Mutti and Bernoulli, 2003; Pomar et al., 2004; Wright, 1994). Studies such as these suggest that a subdivision of the carbonate factory into three separate types may not be satisfactory, but may more accurately be envisaged as a continuum of carbonate factories which are part of a spatially and temporally dynamic system, one which is capable of occurring at a range of depths, depending on the environmental factors and the nature of the available biota at a given time, a concept discussed in a study by Wright and Burgess (2005).

Most recently, in an attempt to assess the validity of this carbonate factory continuum it has become apparent that there is a need to consider the nature of the factory on a local scale. Studies by Yang et al. (2004) on the Holocene of northern Belize and by Demicco and Hardie (2002) have investigated this concept and have shown the complex nature of sedimentation rates at the local scale, suggesting that shallow water areas would most accurately be viewed as a system of facies mosaics. This concept of facies mosaics was further discussed by Wright and Burgess (2005) during which it was suggested that each element of the mosaic is likely to have its own budget in terms of sediment gains, losses, transformations and translocations. Unfortunately, at present we know little about such processes and are some time off being able to quantify them.

2.3.1.1. Carbonate productivity- The affects of early diagenetic processes

An additional complication when assessing carbonate production in the carbonate ramp setting are the affects of early diagenetic processes. The previous section (2.3.1) examined the potential for variances in carbonate production related to changes in the depth and location of the carbonate factory, and hence the possibility of numerous depth-productivity profiles (e.g. Bosscher and Schlager, 1993; Pomar, 2001a; 2001b). However, a study by Wright and Cherns (2004) suggests that these variances within production profiles may actually be due to early diagenetic processes, the likelihood being that extensive dissolution of aragonite (and possibly high magnesian calcite) takes place during very early burial, even in relatively shallow tropical settings. If this is the case the established trends of diminishing carbonate productivity with depth could, for some settings such as ramps, be in part an artefact of selective, offshore dissolution more than simply due to reduced benthic production. In such a situation to therefore refer to profiles as 'production profiles' would be misleading, and they would maybe be more accurately described as net accumulation profiles, which have been affected by dissolution of carbonates either produced in situ or transported to those sites. Evidence for such processes have been shown (Cherns and Wright, 2000; Cherns et al., 2008) by massive skewing of the faunas through the removal of diverse aragonite components in Silurian and early Jurassic ramp successions. Hence, the possibility exists that what is now mud-grade carbonate in low energy deposits may not represent original material deposited from suspension but could actually represent transformed aragonite from in situ production by the skeletal fauna. In addition, studies by Walter and Bruton (1990) and Ku et al. (1999) have estimated that 50% of the annual carbonate produced in the Florida Bay lagoons is lost by dissolution.

At present it is not clearly documented how widespread such processes may be, although initial estimates would suggest it was possibly very extensive. It would however seem apparent that it is of increasing importance that we consider any effects of early diagenetic processes when attempting to assign a carbonate productivity profile to a ramp environment.

2.3.2 Organic influence

As important as the rate and location of carbonate production is (section 2.3.1), the significance of the specific type of carbonate producer should not be underestimated, as in all likelihood variations between carbonate producers could be a major controlling factor in the development of a carbonate ramp versus a flat-topped platform.

Carbonate ramps have developed throughout time but there are geological periods when they have been the most prominent platform type. Although the reasons for this are not clearly understood one explanation may be that changes in the dominant type of shallow water carbonate producer may control the development of platform architecture, whereby periods dominated by frame-building organisms have the stiff, rigid components required for the construction of a slope break on a flat-topped platform. Conversely periods characterised by a lack of frame-building organisms appear to have eliminated the ability of the carbonate system to develop steep platform morphologies and favoured ramp development.

Burchette and Wright (1992) suggested that major extinctions, oceanographic, or climatic factors may have been responsible for the exclusion of these frame-building organisms during time periods of abundant ramp development, with massive oolite production commonly occurring in their place. A trend illustrated by the widespread oolite dominated ramp examples of the Mississippian (e.g. Burchette et al., 1990, Al-Tawil et al., 2005, Sivils, 2005) and Jurassic (eg. Cabaleri et al., 2003, Hanford and Baria, 2007, Kastner et al., 2008), both of which correspond to periods when shallow-water framework reefs were globally absent or scarce. Furthermore the appearance of more effective frame builders in the later Mississippian saw a widespread transition to flat-topped platform morphologies (e.g. Cozar et al., 2006, Graham and Sevastopulo, 2008).

A similar relationship between the dominant carbonate producer and platform morphology can be seen in modern carbonate environments. The low angle geometry and lack of a significant slope break in the Trucial Coast ramp of the Arabian Gulf (Loiker and Steuber 2008) is to some extent likely due to the scarcity of corals (a result of the high ambient salinity) and other typical Late Cenozoic carbonate producers. Conversely the steep sided

margins of the open marine flat-topped platforms of the Bahamas or the Florida Shelf (Ginsburg et al., 2001) are characterised by rigid, framebuilding corals.

2.3.3 Sediment dynamics

The importance of sediment dynamics in the carbonate ramp setting is largely unevaluated. The earliest author to discuss the potential significance of such a process was Aigner (1984), who pointed out that the dynamics of ramp depositional systems make ramps extremely susceptible to the effects of swell, waves and storms. He suggested that the stratification and overall facies organisation of ramps are largely controlled by episodic high-energy processes, which by analogy to the modern, are most likely storms.

The implication of longshore and storm-generated currents in transporting sediment offshore from the inner to outer sections of the ramp was once more iterated by Burchette and Wright (1992) in their synopsis of the ramp system, during which they described these processes as 'potentially of major importance'. They continued in stating that detailed compositional studies of mid and outer ramp sediments were clearly required.

The first such study was conducted by Aurell et al. (1998) on the Kimmeridgian ramp from the Iberian Basin in northeast Spain. The composition of sand-sized grains found in the proximal and distal tempestites suggested that they had been produced in shallow ramp areas, while both the muddy facies associated with tempestites in the mid ramp zone and the muds and marls found in the outer ramp zone environment still contained quartz silt and other fine-grained detrital particles, along with a small proportion of well-preserved autochthonous skeletal grains. The presence of these continental-derived grains within the muddy facies was viewed as evidence of offshore transport, and Aurell et al. placed transport ranges as great as 10Km on these individual grains. The two mechanisms attributed to this significant erosion and resedimentation process were winter storm generated waves, and higher amplitude waves, generated by occasional events such as hurricanes. If these processes were responsible for the significant quantity of offshore transport in the Kimmeridgian ramp it is likely they are not solely limited to activity within this example but in all probability are a widespread processes which took

place across a range if not all carbonate ramps. In addition it is also important that lateral sediment transport is considered, as it is probable that processes such as geostrophic flows parallel to the isobaths could also be responsible for transporting considerable amounts of sediment (e.g. Hunter et al., 2007).

In contrast to studies such as Pomar's etc (refer to section 2.3.1) whereby the type and location of the carbonate factory is invoked as the dominant controlling parameter in the development of a carbonate ramp, the work of Aurell et al. (1998), inclines towards the notion that erosion of shallow water areas (these being the location of the dominant carbonate producing factory) and resedimentation into deeper areas is in fact a major control on the stratigraphic geometries and distribution of facies within the carbonate ramp environment.

The quantification of the sediment dynamics in the carbonate ramp setting is complicated by the potential for sediment production on each subdivision of the carbonate ramp. Benthic production is likely to dominate the shallow waters of the inner ramp, while pelagic sedimentation may take place on the middle and in some instances (section 2.3.1) outer ramp sections. A consequence of this potential for sediment production on each subdivision of the ramp is that it becomes vital that we understand where the sediment originated before we can assess where it may or may not have been transported from, and by what process.

2.3.4 Sequence stratigraphic controls on ramp development

The principle controls contributing to the initial growth of a carbonate ramp are a combination of the parameters discussed throughout section 2.3. However, it is probable that the most influential parameter on facies development, and to some extent ramp geometry is the relative sea-level history of the carbonate ramp. In contrast to the rapid flooding or exposure of the platform surface in a rimmed shelf setting during a relative sea-level change, the gentle depositional slope and absence of a slope break in the carbonate ramp environment means the major exposure and flooding surfaces are generally diachronous. A 1-2 metre fall in relative sea-level would expose a significant portion of most flat-topped platforms (e.g. Great Bahama Bank), but would have little effect on the character of a homoclinal

ramp (e.g. Southern Arabian Gulf). Similarly a 10 metre fall in relative sea level, the scale of many third-order cycles (Einsele et al., 1991), would likely expose the entire platform interior in a rimmed platform environment, while the same relative sea-level fall on a carbonate ramp would simply expose a 20-50 km tract of the former inner and mid ramp, with much of the mid and outer ramp remaining in or entering a favourable environment for lowstand shallow-water carbonate production. Therefore in comparison with carbonate flat-topped platforms the sequence stratigraphy of carbonate ramps is less complicated, whereby the somewhat simple geometry results in facies belts moving up or down the ramp in response to long-term relative sea-level changes.

The following paragraphs describe the response of depositional system tracts in an idealised ramp sequence:

Transgressive system tracts (TST):

The response of the systems tracts in a carbonate ramp setting during a transgressive phase varies according to the rate of sea-level rise when compared to the sedimentation rate. In a ramp setting where sea-level rise is much greater than the sedimentation rate, backstepping of the inner ramp will take place and a new shoreline of barrier-lagoon or beach ridge will likely be established. This facies jump will leave the former inner ramp sands drowned on the new outer ramp, which in turn will be buried by pelagic or hemipelagic muds, while much of the TST will be represented by condensed mid-outer ramp facies. Aggradation will commonly take place at the new shoreline before progradation during the HST. A sequence such as this is depicted in the two Great Oolite sequences of the Middle Jurassic Wessex Basin (Wyatt and Cave, 2002), where a thin, muddy TST is succeeded by a thick prograding oolite HST.

In conditions where sea-level rise is only just greater than carbonate sedimentation, retrogradation of the inner ramp sands will occur and the stratal package will onlap the ramp. The parasequences of the TST will form a parasequence set with a systematic upward change in character of the parasequences at any one locality, with slightly deeper water facies occurring in successive parasequences. An example of such a sequence is depicted in

the High Tor Limestone of the Lower Carboniferous ramp of South Wales, where a transgressive sheet grainstone is overlain by outer ramp mudrocks which were deposited when the ramp shoreline migrated landwards in response to a relative sea-level rise (Wright, 1986; Burchette et al., 1990).

Highstand systems tracts (HST):

In response to a HST, a ramp shoreline will likely undergo aggradation followed by progradation as the stillstand is reached and sea-level begins to fall. A lengthy phase of highstand deposition can lead to ramp carbonates offlapping considerable distances, the stratal packages of which are commonly seen in seismic as changing from oblique to sigmoidal in stratal geometry due to the preferential progradation of the inner-ramp over the outer-ramp facies. Numerous carbonate ramp examples exhibit well-developed prograding HST grainstones, one of the better known being the oolites of the Smackover Formation of the Gulf Coast rim (Hanford and Baria, 2007).

Lowstand systems tracts (LST):

There are no specific depositional environments created in relation to a relative sea-level fall during a LST on a carbonate ramp. Insufficient gradient on the ramp geometry is unlikely to generate slides, slumps, or rockfalls, which in contrast would be expected features on a similar LST siliciclastic shelf system (Van Wagoner et al., 1990). Generally there will be a basinward shift in facies belts, with inner ramp facies developing at the new shoreline over the previous mid-outer ramp setting, while exposure of the former inner-ramp during the lowstand may subject the sediments to erosion, karstic dissolution, calcretization, dolomitization or evaporite precipitation and replacement, depending largely on the climate.

2.3.4.1 Greenhouse versus Icehouse carbonate ramp development

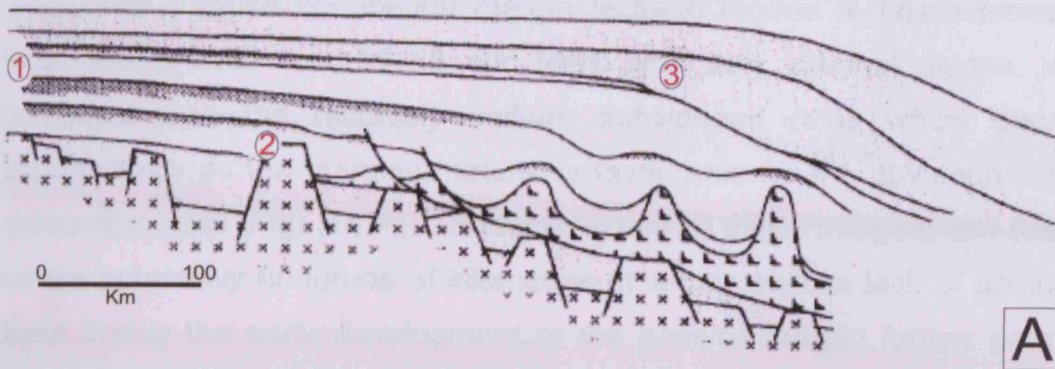
The aspects of sequence stratigraphy on an idealised ramp section have been described in the previous paragraphs, however it is important to understand that ramps that formed during differing global climatic conditions, greenhouse, ice-house and transitional times are likely to have distinctive

characteristics. The key differences of which may be presented by variations in slope, component parasequence make-up, stacking patterns and disconformity development.

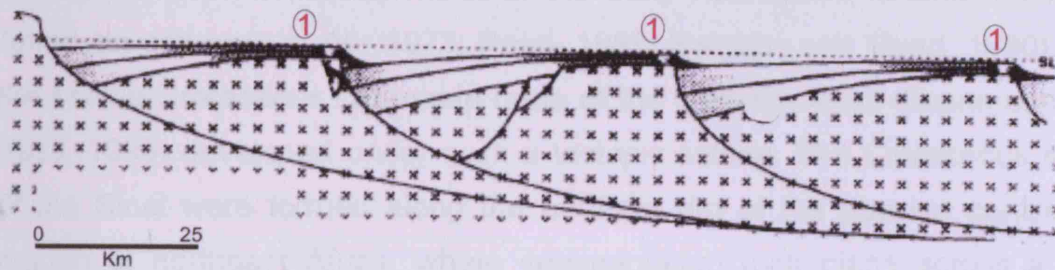
An integrated field and modelling study by Read (1998) approached some of the intrinsic differences seen in ramps formed at differing climatic conditions. Read postulated that carbonate ramps formed during greenhouse conditions likely developed under relatively small sea-level fluctuations, and as a consequence were likely to develop relatively flat tops that almost aggrade to sea level. In reference to ramps that formed under transitional climate conditions Read (1998) proposed that these will have moderate slopes, and consist of parasequences that are commonly a few metres thick, grainstone dominated, and range from upward-coarsening in the outer ramp to upward-fining in the inner ramp. While Ice-house ramps ascribed to development during times of continental glaciation and therefore under large sea-level changes are described as typically portraying relatively high gradients on their tops resulting from the large fluctuation in water depth.

2.3.5 Tectonic setting

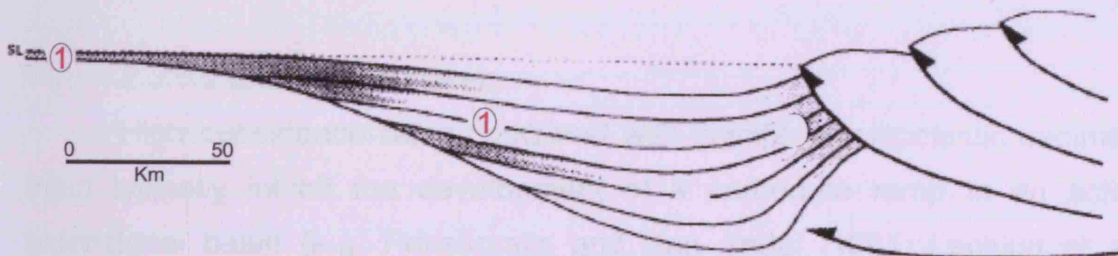
The uniform gently dipping geometry (commonly perceived to be less than 1°; Ahr 1973, Read 1985) which defines the carbonate ramp setting is likely a direct consequence of the initial bathymetry on which ramp development/growth initiated. Therefore it is paramount that initial tectonic conditions are suitable for the development of a carbonate ramp. Tectonic controls understood to promote optimal ramp development are a slight bathymetric gradient, and a relatively shallow basinal water depth (Burchette and Wright, 1992). Basin subsidence rate is also a crucial process in generating accommodation space for ramp development (e.g. Gilham and Bristow, 1998; Droste and Van Steenwinkel, 2004; and Contreras et al., 2010). Such tectonic regimes are characteristically portrayed in passive continental margins, and basins of extensional, compressional, and intraplateau type (Fig. 2.4). Numerous ramp examples from each of these settings are known.



A



B



C

Figure 2.4. Cross sections of carbonate ramp locations attributed to differing tectonic settings. Diagram modified after Burchette and Wright (1992). (A) Carbonate ramps forming within a passive margin tectonic setting; 1 - ramps develop as prograding wedges over older post-rift sequences; 2 - Remnant rift topography maybe location for the development of mid and outer ramp isolated shoals and reefs; 3 - ramp may depict a distally steepened character where it overlays the underlying shelf slope break. (B) Carbonate ramps forming within a extensional basin tectonic setting; 1 - ramps develop on the shallow slopes of fault blocks. (C) Carbonate ramps forming within a foreland, compressional basin tectonic setting; 1 - ramps develop on the gentle slope of the margin of the depressed foreland.

2.3.5.1 Passive continental margins

The passive continental margin tectonic regime is characterised by large areas over the old rift shoulders with very gradual slopes, which combined with the relatively uniform subsidence rates which decrease exponentially as the margins mature, is favourable for the development of a carbonate ramp (Fig. 2.4 A). The large extent of these margins can result in ramps potentially hundreds of kilometres in width, while a lack of siliciclastic input during the early development of the passive margin further promotes widespread carbonate deposition.

Numerous examples of carbonate ramps which developed in such a setting are known, notably much of the early Palaeozoic around the North American craton (e.g. Ahr 1973; Read, 1989; Barnaby and Read, 1990), and the Middle Cretaceous carbonate ramp of the northern Sinai (Bachmann and Kuss, 1998) developed under such a tectonic setting. The Cretaceous strata of the Sinai were formed along the northern rim of the passive continental margin of northeast Africa, where sedimentation took place across a very wide platform system which was influenced by major tectonic events during the Mesozoic-Early Tertiary times, coeval with the opening and closure of the Neotethys Ocean (Keeley, 1994).

2.3.5.2 Extensional basins

High subsidence rates combined with significant siliciclastic sediment input typically inhibit the development of a carbonate ramp in an active extensional basin (e.g. Perissoratis and Van Andel, 1991; Lachkar et al., 2009). A consequence of this lack of shallow-dipping substrate is that ramps which do develop in this tectonic setting are usually relatively small (a few kilometres or tens of kilometres across). Therefore these ramps are typically limited to development in transfer or fault tip-zones, where throws and gradients are minimal (Burchette and Wright, 1992), or on the dip slopes of tilted fault blocks where they prograde into the adjacent half-grabens (Fig. 2.4 B). Most ramps associated with extensional settings develop during quiescent phases or in the post-rift stage when subsidence becomes largely flexural.

The Miocene deposits in the Gulf of Suez (Burchette, 1988) represent one such example of a ramp developing in an extensional setting. The

deposits were controlled by an extensional fault-block topography in which they were deposited around the exposed block crests and in marginal half-grabens. The Paleocene deposits of the Sirte Basin, Libya (Fiduk, 2009) also represent a similar setting. Rifting of the Late Paleozoic age Sirt Arch beginning in the Triassic led to its collapse in the Middle to Late Cretaceous, forming the Sirte Basin (Anketell, 1996). The margins of the Sirte Basin descend from the shoreline across a series of platforms, troughs, ridges and slopes into deeper water. It is on these shallow, gently dipping surfaces that carbonate deposition has taken place and the development of ramp like carbonate geometries. These deposits are of significant economic importance with the Sirte Basin petroleum province being ranked 13th in the world with proven reserves of 43.1 billion barrels of oil equivalent (Alhbrandt, 2001).

2.3.5.3 Compressional basins

A low slope gradient and lack of subsidence commonly results in the development of carbonate ramps (Fig. 2.4 C) as linear belts along the peripheral bulge of marine foreland basins (Burchette and Wright, 1992). This location in the compressional basin setting also experiences relatively low rates of terrigenous siliciclastic input due to its separation by the foredeep from the main siliciclastic source area in the thrust zone. Ramps developed within this setting can be over a hundred kilometres across. The classic modern example of a carbonate ramp formed within this tectonic regime is the Arabian Gulf (Lokier and Steuber, 2008). Additionally ramps can also develop in compressional back-arc basins where depositional gradients on the cratonward side are gentle.

Numerous examples of carbonate ramps in the foreland basin setting exist throughout the geological record including the Upper Ordovician Lourdes Formation, Newfoundland, Canada (Batten Hender and Dix, 2008), the Lower Mississippian Mission Canyon Formation, Montana and Idaho (Reid and Dorobek, 1993), the Upper Pennsylvanian Las Llacerias Formation, NW Spain (Merino-Tome et al., 2009), and the Lower Eocene Sierra del Cadi of the SE Pyrenees, Spain (Gilham and Bristow, 1998).

2.3.5.4 Intraplatform basins

Intraplatform basins are a common feature within extensive, epeiric carbonate platforms. Although no modern examples exist, epeiric carbonate platforms were widespread in the past, particularly in the Middle East (Murriss, 1980; Burchette, 1993; Van Buchem et al., 2002) where some of the world's largest hydrocarbon accumulations are to be found in carbonates deposited in settings of this type. Epeiric platforms were vast entities, spanning hundreds to thousands of kilometres across, covering millions of square kilometres, and in the majority of cases developing on relatively stable cratonic interiors or on wide, flooded continental shelves. Characteristically these extensive platforms often portrayed one or in some examples a series of shallow depressions within the boundaries of the platform. These shallow depressions are commonly referred to as intraplatform basins.

The margins of these basins typically depict a gradual coarsening of facies along the margin as it shallows progressively away from the basin centre. The geometry of these basin margins can vary from flat-topped platforms to both homoclinal and distally steepened ramps. These margins commonly contain coarse grained facies of the shallow water shoals and biostromes, which combined with their close proximity to potential source prone strata in the restricted basin centre, results in this tectonic setting being of considerable economic importance.

The margins of numerous intraplatform basins have been described as displaying a carbonate ramp geometry, including the Mishrif Formation of the Southern Arabian Gulf, which is commonly described as having a homoclinal ramp geometry (Burchette, 1993). While the Natih Formation of Northern Oman (Van Buchem et al., 2002), the Las Plias Formation of Northern Mexico (Osleger et al., 2004), and the Southern Istria section of Croatia (Buckovic et al., 2003), have all been described as distally steepened ramps on account of the coarse grained, high angled clinofolds contained within each of the formations.

2.4 Carbonate ramp seismic character

Field outcrops are rarely large enough to view major portions of ramp depositional systems; therefore gross ramp geometries are predominantly

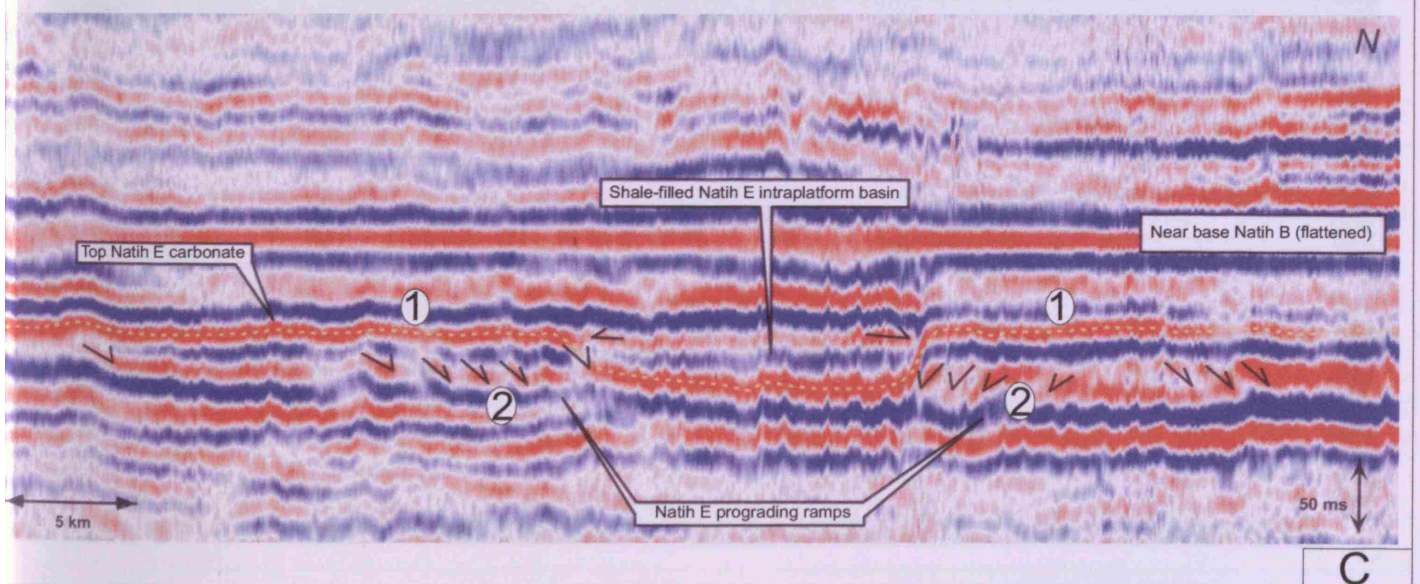
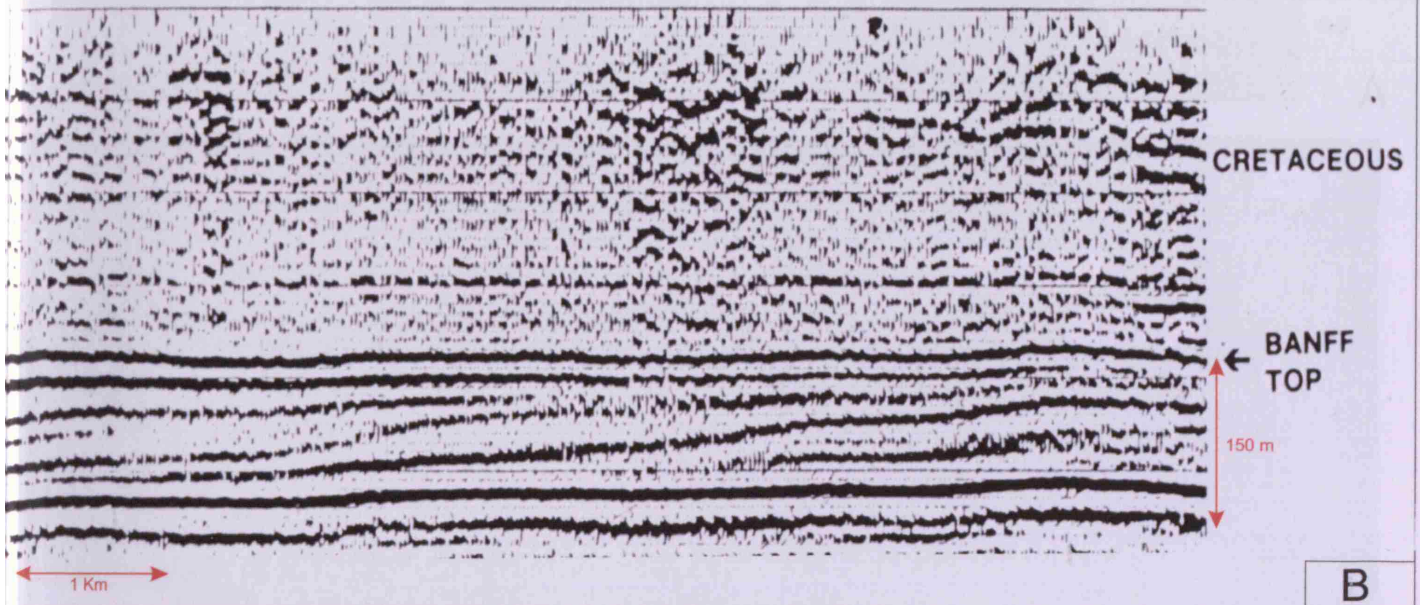
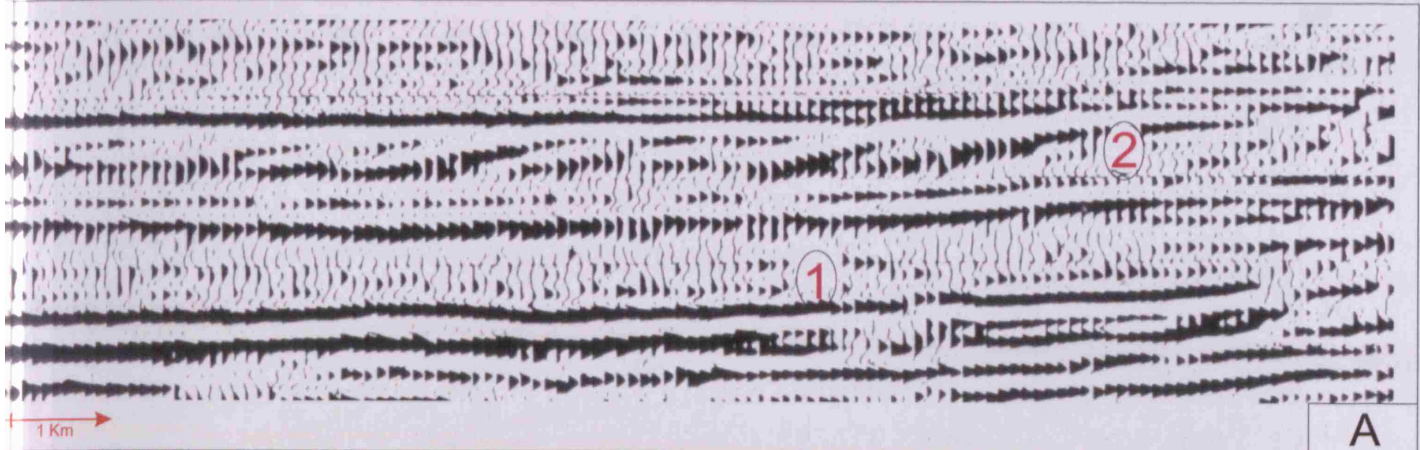


Figure 2.5. Seismic expressions of carbonate ramps. (A) Jurassic Smackover Formation seismic lines from South Texas (Sassen et al., 1987). 1 - The ramp successions show typical tram-line like seismic character. 2 - Progradational character shown by prograding bodies. (B) Banff Formation Northeast British Columbia (Chatellier, 1988). Formation shows near parallel seismic reflectors with some progradational character in the centre of the Formation. (C) Middle Cretaceous Natih Formation (Droste and Van Winkler, 2004). 1 - Highlighted interval (yellow dashed line) shows near parallel reflectors on the North and South margins of the intraplatform basin. 2 - Steepened reflectors represent the clinoform bearing margins of the basin as the ramp passes into the intraplatform basin

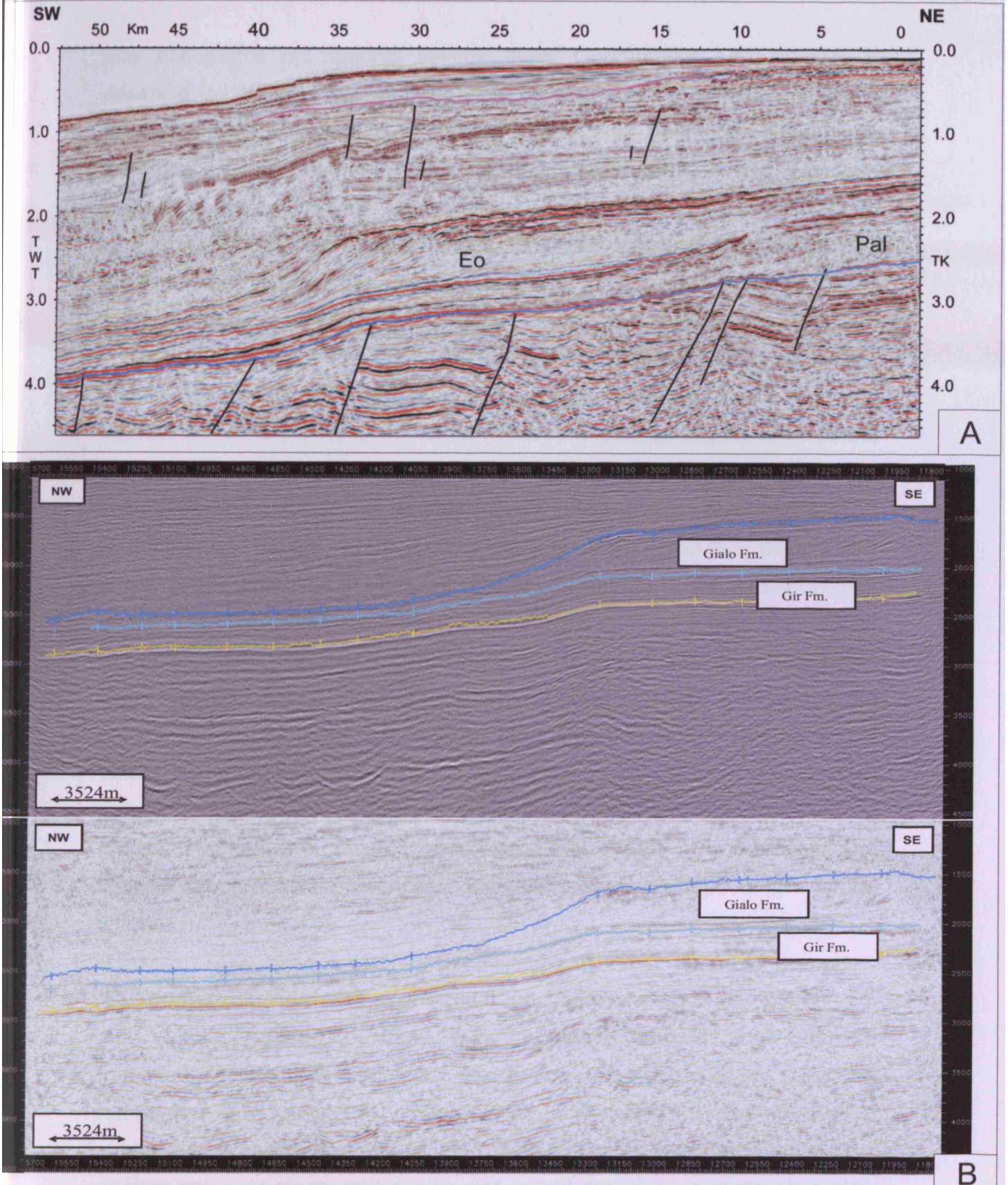


Figure 2.6 . (A) Seismic profile of Paleocene and Eocene ramp like margins prograding into the Sirte Embayment Libya (Fiduk 2009). The Paleocene (Pal) interval depicts near horizontal reflectors, while clinofolds can be seen in the Southwest of the Eocene (EO) Strata. The clinofolds and steepening are a likely consequence of the underlying faulted topography and give the Eocene succession a more distally steepened ramp like geometry. (B) Seismic profiles of Eocene successions on the margins of the extensional Sirte basin, Libya (Shell E&P, 2008). A homoclinal ramp geometry is illustrated by the lower of the highlighted intervals (Gir Fm), depicted with its near horizontal like strata. Underlying fault control is the probable cause for the development of a steepened margin in the overlying (Gialo) formation, illustrating a more distally steepened like geometry.

only observable on regional seismic lines. Good-quality seismic data is essential for the effective analysis of ramp geometry however many ramps are extensive, featureless and too “thin” for sequence geometries to be seen. Examples where geometries can be determined from seismic lines are typically sheet or lens-like, up to several hundred meters thick and tens to hundreds of kilometres across, thinning gently towards both the basin centre and basin margin (Burchette and Wright, 1992).

Carbonate ramps have no unique seismic characters, and are commonly referred to as portraying ‘tram-line’ like seismic (Fig. 2.5, 2.6). Inner-ramp seismic reflectors tend to be parallel, relatively continuous and regular, as are outer ramp reflectors which may diverge slightly towards the basin margin. The outer ramp to basinal sections generally consist of parallel, continuous character or may be a seismically unresolvable condensed section (Burchette and Wright, 1992). Thicker sections of the ramp may display low-angle, gently sigmoidal or shingled clinoforms (Fig. 2.5 C, 2.6 A) with distinct toplap and little resolvable topset, as illustrated in many intraplateau basin examples, e.g. The Natih (Van Buchem et al., 2002) and Smackover (Handford and Baria, 2007) Formations. These clinoform geometries are commonly misinterpreted as parallel or subparallel continuous reflectors unless these subtle geometries are viewed on highly vertically exaggerated data sets. Finally mid or outer ramps areas of reflection free, mounded, or chaotic character are commonly associated with basement or salt highs and indicate the probable presence of discrete organic buildups or grainstone shoals.

2.5 The hydrocarbon and economic importance of carbonate ramps

Large isolated buildups and carbonate rimmed shelves have traditionally been key petroleum exploration targets, however carbonate ramps also form major reservoir zones. They offer different, commonly more subtle play types than many rimmed platforms, with wide opportunities for stratigraphic and structural trapping and lateral variations in reservoir quality. The reservoir potential in low-energy ramps is low unless outer ramp buildups develop or they lie in situations where the timing of diagenesis in relation to petroleum migration has been particularly favourable. Conversely high-energy

ramps have significant reservoir potential, the location of which are predominately found in either organic buildups or carbonate sandbodies.

Petroleum reservoirs located within organic buildups on carbonate ramps are common and have been discovered within a wide range of organic and sedimentary facies, of notable mention are the prolific mid-ramp petroleum reservoirs attributed to the texturally varied phylloid and related algae buildups of West Texas and New Mexico in the USA (Doherty et al., 2002; Saller et al., 2005; Tinker et al., 2005) and the Timan Pechora and North Caspian Basins in Russia and Kazakhstan (Weber et al., 2003). Reservoirs also occur in the outer ramp coral-algal buildups in the Jurassic aged Smackover Formation of the US Gulf Coast (Handford and Baria, 2007; Mancini et al., 2008).

Hydrocarbon reservoirs composed of grainstones are widespread in the carbonate ramp setting and occur in a number of configurations. Reservoir facies can range from shoreline carbonate sandbodies to major detached shoal complexes or shoal complexes over offshore highs, and are generally characterized by a relatively thin or layered reservoir facies geometry which is seldom more than a few tens of metres thick. Examples of such reservoirs include the Early Cretaceous of the Neuquen Basin, Argentina (Hogg, 1993; Urien and Zambrano, 1994), the Mississippian Mission Canyon Formation of the Williston Basin (Lindsey and Kendall, 1985) and the Jurassic of the Paris Basin (Purser, 1985; Mougnot, 1999).

The margins of intraplatform basins are commonly described as carbonate ramps, and due the considerable reservoir prone potential of these margins this setting is also of significant economic importance. The reservoir quality of the margins, and their respective porosity and permeability are largely facies dependent, with the highest reservoir potential again occurring in the coarse shoal, biostromal, and uppermost-slope facies. Reservoir heterogeneity tends to be very low due to the commonly localized distribution of the coarse facies on basement highs, while reservoir quality is significantly enhanced in highstand carbonates which have been exposed to meteoric leaching, and hence potential formation of mouldic porosity. The coarse molluscan (largely rudistid) packstone-grainstone slope facies of the Middle East Mishrif Formation (Burchette, 1993) underwent such a process, in which

large volumes of mouldic porosity (maximum 35 % , mostly 10-25 %) were created during meteoric leaching. Furthermore, incomplete cementation by meteoric cements in the Mishrif Formation resulted in excellent permeabilities (maximum several darcys, mostly 10-1000 md). The development of mouldic porosity by leaching of rudists and other skeletal fragments is also documented in both the Natih (Van Buchem et al., 2002) and Shuaiba (Alsharhan, 1995) Formations.

The intraplatform basin setting not only has proven reservoirs on its margins but the potential for preservation of organic material within the basin is also very high. The presence of poorly oxygenated to anoxic bottom water, along with potential salinity stratification facilitates the preservation of organic matter. Several authors (Kirkland and Evans, 1981; Sonnenfeld, 1985; Warren, 1986) have commented on the source rock potential of carbonates deposited in restricted, saline to hypersaline settings, where the organic productivity and the total organic carbon content can typically be very high. The preservation potential of organic matter in these settings (typically shallow evaporitic pans) is rather poor; as account of their shallow nature they are typically subaerially exposed and/or exposed to oxidising fresh waters. However, these sediments are less likely to be oxidised in subsiding/deepening intraplatform basins. The result is very organic rich basin sediments, which illustrate TOC values for example of 6% in the basinal sediments of the Hanifa Formation (Droste, 1990) and as much as 15% in the Natih E and B Members of the Natih Formation (Terken, 1999). This excellent potential for the preservation of organic matter has resulted in numerous intraplatform basins providing the hydrocarbon source to prospective plays. These include the Basque Cantabrian Basin which is understood to provide the source to Spain's only onshore oil field, the Ayoluengo field (Quesada et al., 1997), a minor hydrocarbon source is provided by the basinal facies of the Middle East Shuaiba Formation (Alsharhan, 1985), while the Hanifa Formation (Droste, 1990), Natih E and B Members of the Natih Formation (Van Buchem et al., 2002), and the Shilaif basinal deposits of the Mishrif Formation are all major hydrocarbon source providers in multiple plays in the Middle East.

It also significant that a major rise in sea level across the intraplateau basin setting can result in the formation of an adequate seal to the basin margin reservoirs by means of a basinal shale infilling the basin. Examples of such a seal are the Nahr Umr shale which was deposited above the basin slope reservoirs of the Shuaiba (Alsharhan, 1995) and Natih (Droste and Van Steenwinkel, 2004) Formations, and the overlying Laffan Formation (Burchette and Britton, 1985) which provides an adequate structural-stratigraphic seal to the Mishrif Formation. It is this potential combination of source (basin deposits), reservoir (basin margins), and seal (overlying shales) triplet, and their close proximity to one another in the intraplateau basin environment that provides this setting with excellent potential for hydrocarbon accumulation and subsequent exploration. This triplet has been exploited with major hydrocarbon production from the Mishrif Formation reservoirs in offshore U.A.E., Oman, and Southern Iraq (Alsharhan, 1995), and significant production from the intraplateau basin margin reservoirs of both the Natih (Van Buchem et al., 2002) and Shuaiba (Alsharhan, 1985) Formations of the Middle East.

2.6 Summary of our current understanding of the carbonate ramp system

Our current level of knowledge with regards to the carbonate ramp system has been outlined throughout chapter 2, while our present understanding of the principle controls on these systems was summarized in section 2.3. Many of these controls were originally defined from simple cartoon like models and lacked proper investigation via quantitative testing. The recent advances in stratigraphic forward modelling are beginning to offer tools with which these controls can begin to be tested. The following chapter examines some of these initial forward modelling investigations, before introducing a new stratigraphic forward modelling procedure which aims to quantifiably test if our current understanding of the controls on ramp growth (outlined in this chapter), are in fact correct, and which controls (i.e. sediment production, sediment transport, tectonic influence, changes in relative sea-level etc) impart the most significant influence on overall ramp development.

Chapter 3: FORWARD MODELLING CARBONATE RAMP SYSTEMS

The previous chapter discussed the carbonate ramp concept and the current level of knowledge of controls on ramp development. This chapter aims to review how understanding of these controls has progressed in recent years by the use of stratigraphic forward models. A brief synopsis of several attempts at modelling the carbonate ramp system is provided, before a new alternative modelling approach, used in the subsequent chapters of this thesis, is introduced. A detailed description of the methods, inputs, outputs, procedures and modelling package used in this new modelling approach is presented.

3.1 Stratigraphic forward modelling and the carbonate environment

A forward model is defined as the simulation of a product from the known response of a process to a given set of input parameters (Cross, 1990; Watney et al., 1999). If this method is applied to stratigraphy the process is commonly referred to as Stratigraphic Forward Modelling (SFM), a process which combines various numerical and algorithmic methods to create synthetic strata based on simulated tectonic and stratigraphic processes such as subsidence, sediment supply variations, and the various processes of sediment transport and deposition (Burgess, 2009 in press). Numerical SFMs thus represent a quantitative expression of our ideas about how certain Earth-surface systems work (Watney et al., 1999; Paola, 2000).

In contrast to siliciclastic systems much of the material that accumulates and is preserved as strata in a carbonate system was produced in-situ by living organisms, the skeletal elements of which are then commonly disarticulated and broken down to create carbonate sediment. The production of this sediment is therefore typically modelled to depict the depth dependence of the production rate relating to known functions for light attenuation in the ocean (Bice, 1991; Bosscher and Schlager 1992, 1993; Bosscher and Southam, 1992; Galewsky, 1998). Other factors influencing production rate including turbidity, temperature (Lerche et al., 1987) and rate

of sea-level rise (Watney et al., 1991) have also been modelled, while production rates have also been directly inferred from modern or ancient carbonate accumulations (Pomar, 2001). The transport of this produced sediment is a key process in carbonate systems, and SFM illustrating variations in platform geometries typically account for such features by including geometric treatment of sediment redistribution by physical transport.

The majority of carbonate stratigraphic forward models focus on either replicating one type of carbonate platform architecture (e.g. a flat-topped platform), which in many cases target individual examples (e.g. the Miocene reef-rimmed platform of Mallorca, Bosence et al., 1994) or on replicating a sub-system within a particular platform type (e.g. platform interior strata, Goldhammer et al., 1987; Burgess et al., 2001; Burgess, 2006). Models targeting platform architecture have generally concentrated on flat-topped platform development. Of the numerous attempts at modelling a carbonate platform depositional system one of the earliest was made by Bice (1988), whose simple depositional system model attempted to analyse the role of a depth dependant factory, crustal subsidence, and sea-level fluctuations on platform development, with a series of simple synthetic cross sections presented to illustrate the results (Figure 3.1 A). Refinements to Bices' early model were suggested by Bosence and Waltham (1990) whose model differed by the introduction of subaerial and submarine erosion to the system, and the potential for both lateral and vertical variability of the carbonate system (Figure 3.1 B). These early models by Bice, and Bosence and Waltham presented relatively simple results, however both were the starting point for carbonate system modelling, highlighting the importance of computer modelling as an experimental tool, to permit analysis of carbonate platform evolution unavailable using more traditional outcrop and qualitative modelling approaches.

Bosence and Waltham's model was further modified during a study of the Miocene carbonate platform of Mallorca, Spain (Bosence et al., 1994), whereby the way in which erosion and the redeposition of sediment was modelled were altered. Primarily the study modelled the Cap Blanc Platform of Mallorca by integrating field data obtained from the well-exposed cliff sections of the reef-rimmed platform. The modelled cross sections simulate

Figure 3.1

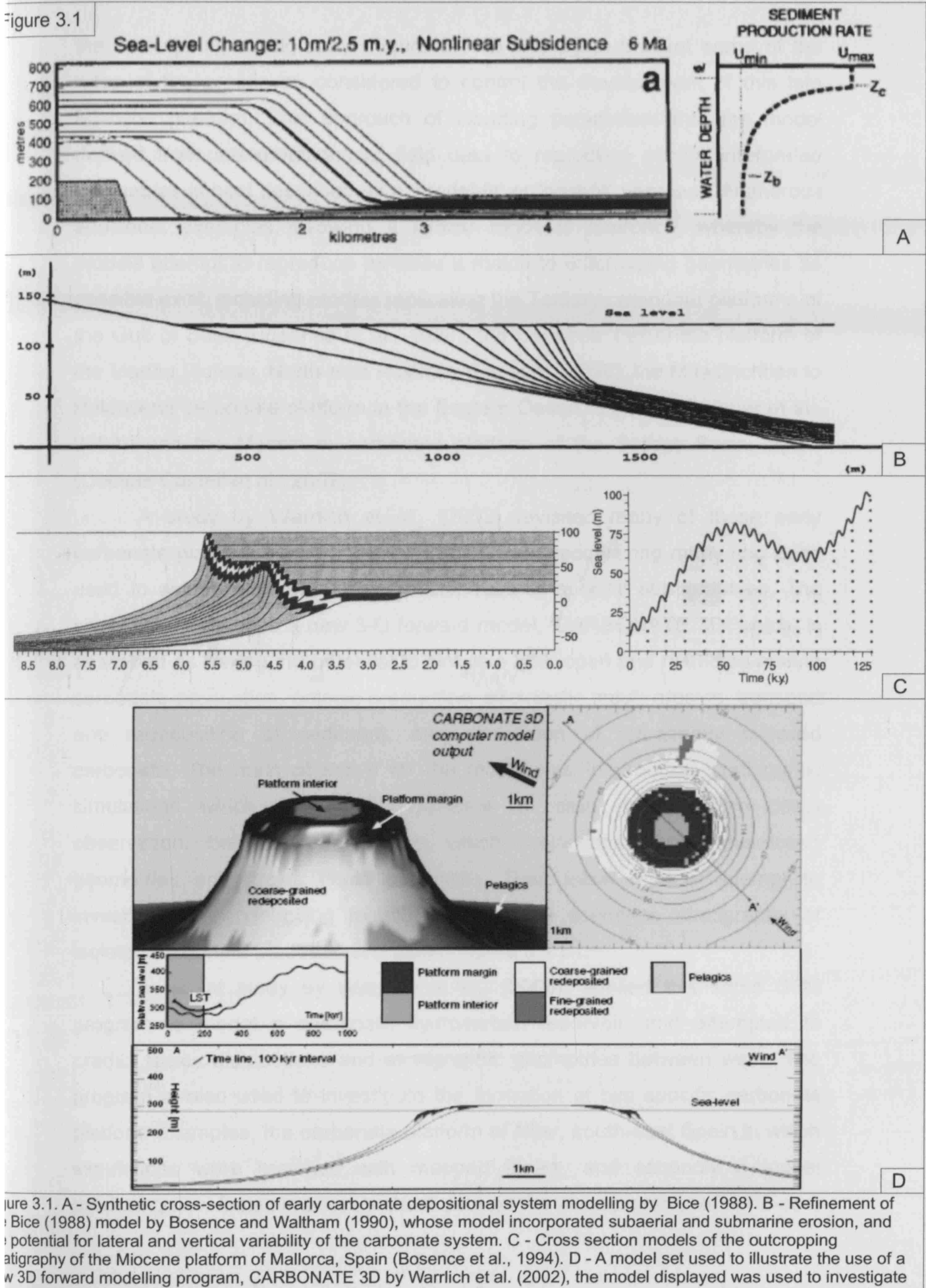


Figure 3.1. A - Synthetic cross-section of early carbonate depositional system modelling by Bice (1988). B - Refinement of Bice (1988) model by Bosence and Waltham (1990), whose model incorporated subaerial and submarine erosion, and the potential for lateral and vertical variability of the carbonate system. C - Cross section models of the outcropping stratigraphy of the Miocene platform of Mallorca, Spain (Bosence et al., 1994). D - A model set used to illustrate the use of a new 3D forward modelling program, CARBONATE 3D by Warrlich et al. (2002), the model displayed was used to investigate the controlling mechanisms on the sequence stratigraphy of an atoll.

the outcropping stratigraphy (Figure 3.1 C) and try to bracket some of the rates of the processes considered to control the development of this late Miocene platform. This approach of inputting parameters into the model derived from interpretations of field data to reproduce similar interpreted geometries is best described as a 'model-fit' or 'best-fit' approach. Numerous additional examples following a similar model-fit approach, whereby the models attempt to reproduce as close a match to outcropping geometries as possible exist, including models replicating the Tertiary carbonate platforms of the Gulf of Suez (Bosence et al., 1998), the Cenozoic carbonate platform of the Mariou Plateau, North-east Australia (Liu et al., 1998), the Maastrichtian to Paleocene carbonate platform in the Eastern Desert, Egypt (Scheibner et al., 2003), and the Messinian carbonate platform of the Sorbas Basin, Spain (Cuevas Castell et al., 2007).

A study by Warrlich et al., (2002) revisited many of these early carbonate platform stratigraphic forward models, recognizing many had been used to simply understand the development of specific stratigraphies. The study also introduces a new 3-D forward model, 'CARBONATE 3D' which is described as having the potential to simulate both open and restricted marine carbonate production, pelagic production, siliciclastic input, erosion, transport and redeposition of sediment, and dissolution of subaerially exposed carbonate. The main objective for the model was to produce stratigraphic simulations which were not dependant on data derived from direct observation, but simulations from which predictions about unexposed geometries and facies could be made. Their initial models attempt to investigate the controlling mechanisms on the sequence stratigraphy of isolated carbonate platforms and atolls (Figure 3.1 D).

A recent study by Warrlich et al., (2008), applied this same SFM program to model a carbonate hydrocarbon reservoir, and attempted to predict facies distributions and stratigraphic geometries between wells. The program is also used to investigate the formation of two specific carbonate platform examples; the carbonate platform of Nijar, south-east Spain in which simulations were matched with mapped facies, and secondly a model predicting new facies in areas without data on the Jurassic ramp of north-east

Spain, which in doing so the authors suggest aid the understanding of carbonate ramp evolution.

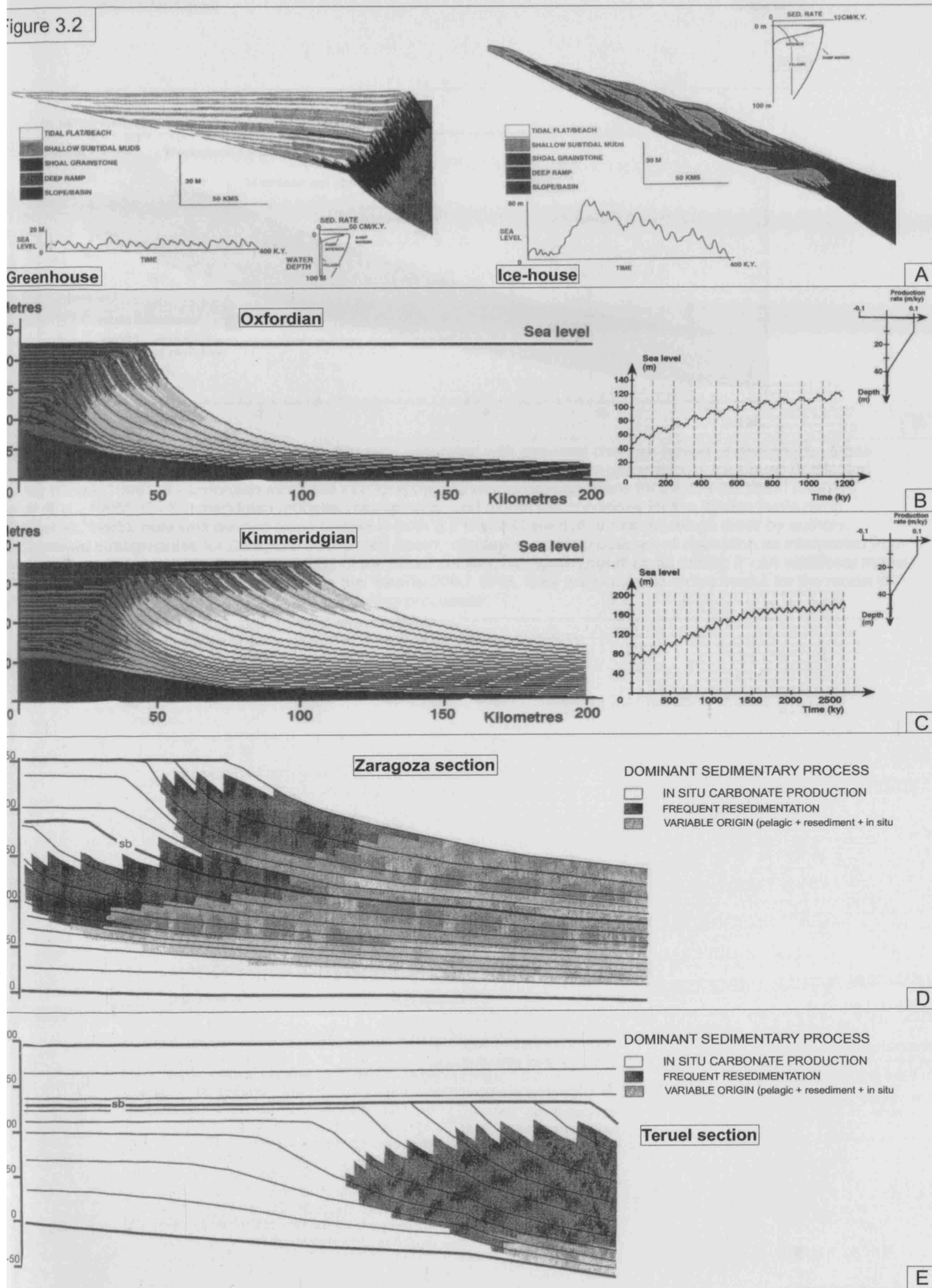
This SFM study of a carbonate ramp by Warrlich et al., (2008) helps illustrate some of the key processes occurring within the ramp environment. However, prior to this the carbonate ramp setting, with the exception of the examples discussed in the subsequent section, has been the focus of very few SFM studies, which may go some way to explaining why our understanding of their formative processes has remained relatively poor.

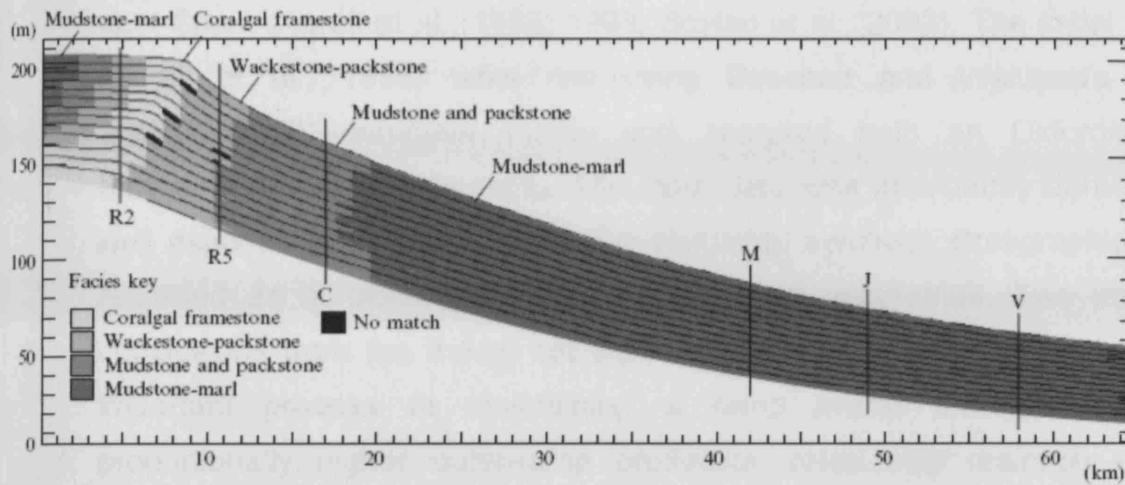
3.2 SFM of carbonate ramp systems

The carbonate platform setting has generally been the dominant focus of carbonate SFM studies, with few models investigating the ramp environment. The reasons for this remain unclear, it may be that as early SFM (e.g. Bice 1988; Bosence and Waltham 1990) focused on the platform environment subsequent studies have simply refined and replicated these concepts and models, or could be due the significant interest in the hydrocarbon bearing potential of these platform systems, however as our awareness of the hydrocarbon importance of the ramp setting grows our need for a greater understanding on their controlling processes increases, hence a SFM approach to the ramp system may prove beneficial in gaining a greater appreciation for these controls.

Few studies have directly attempted to model the ramp environment; work by Read (1998) using Scott Bowman's basin modelling program Phil^R, was one of the earliest. The models were principally run to illustrate parasequence packaging on greenhouse, transitional and ice-house ramp systems (Figure 3.2 A), with generated geometries compared to field examples, many of which were from Palaeozoic sequences in the United States. The model set provides an interesting insight into the potential stacking patterns of cycles in the ramp setting, and presents data to suggest the presence of compartmentalization in carbonate ramp reservoirs, neither of which significantly advance our fundamental understanding of ramp development, but may however provide a useful tool in refining the sea-level history under which specific ramp geometries developed.

Figure 3.2





F

Figure 3.2. A - Left model: Synthetic ramp stratigraphy generated with sea-level changes typical of greenhouse times. Right model: Synthetic ramp stratigraphy, analogous to Pennsylvanian cyclothem generated by ice-house dominated eustasy (Read, 1998). B - Oxfordian modelled stratigraphy, and model run conditions for the Iberian basin ramp (Aurell et al., 1995). C - Kimmeridgian modelled stratigraphy, and model run conditions for the Iberian basin ramp (Aurell et al., 1995), note well defined slope breaks in both 3.2 B and C are defined as the 'slope crest' by authors. D - Simulated stratigraphies for Zaragoza section NE Spain, displaying major processes of deposition as interpreted from field data (Aurell et al., 1998). E - As for 3.2D but for Teruel section, NE Spain (Aurell et al., 1998). F - An additional model for the Late Jurassic Iberian Basin ramp using the 'SedTec2000' SFM. Note the simulated facies output for the model is defined by a range of values for each of the controlling processes.

The carbonate ramp example which has probably received the most focused SFM is the Late Jurassic carbonate ramp of the Iberian basin, north-east Spain (Aurell et al., 1995; 1998; Boylan et al., 2002). The initial models (Aurell et al., 1995) were run using Bosence and Waltham's (1990) 'CARBONATE' computer model and analysed both an Oxfordian and Kimmeridgian carbonate ramp. The input data was dominantly derived from well exposed field sections and the simulated synthetic stratigraphies were regarded as a 'close match' to the observed geometries. Two important conclusions from the model set were that resedimentation by storms is an important process in maintaining a ramp profile through time, and proportionally higher outer-ramp production rates help maintain a ramp geometry. It should however be noted that their simulated geometries (Figure 3.2 B & C) do not closely resemble a typical uniform, gently dipping slope geometry as originally defined for the ramp system by Ahr (1973), and later refined by Wright and Burchette (1992) (see Figure 2.1). The modelled geometries actually portray well defined slope breaks which are typically more synonymous with the flat-topped platform setting. The authors attribute these geometries to the enigmatic 'slope crest' of ramps which they suggest are consequence of a combination of higher, shallow water production and erosion rates, together with loss of accommodation during highstands and high-stillstands in their modelled sea-level curves. Furthermore the presence of the ramp 'slope crest' in these examples highlights the potential difficulty of maintaining low angle ramp profiles over significant periods of geological time.

The validity of the model matching technique used within this study is discussed by the authors. The very well-constrained, outcrop derived time frame, facies analysis and stratal thicknesses and geometries which act as the input for the model are suggested to be the reason for such a close match between the observed and modelled stratigraphies. However the authors do suggest that whether they are correctly deducing the controlling parameters is another question, and state that there "may be other solutions to our known stratigraphy that we have not discovered, or that the program is not able to model".

A subsequent study (Aurell et al., 1998) on the same stratigraphies further analysed the role of offshore transport in the carbonate ramp setting by

means of investigating the origin of offshore carbonate mud. Synthetic stratigraphies modelled to closely replicate two observed cross-sections (Figure 3.2 D & E) near Zaragoza and Teruel in north-east Spain, implied that most of the offshore mud was produced by re-sedimentation from inshore areas, as opposed to pelagic sedimentation, and that offshore transport would have been highest during periods of sea-level highstands. Further analysis of the Jurassic carbonate ramp of the Iberian Basin was conducted by Boylan et al., (2002), with the aid of a new SFM model, 'SedTec2000'. The model is able to output simulated facies which are defined by a range of values for each of the controlling processes and thereby predict rock textures within simulated stratigraphies (Figure 3.2 F). Applied to the Jurassic ramp example it was suggested it could provide a more accurate output regarding the processes that were simulated in these ramp models, therefore allowing more direct comparisons to be made with the facies observed in the field and providing potential for a more rigorous method for assessing the 'goodness of fit' of the simulated stratigraphies.

3.3 The model-fit approach and the introduction of an alternative, new modelling method – 'APE'

The modelling method used for the analysis of the Iberian basin ramp, along with the numerous carbonate platform SFM studies described in section 3.1 predominantly rely on data derived from direct outcrop observations and measurements. This data is applied to the model in order to replicate the observed stratigraphy as closely as possible, using a typical 'model-fit' or 'best-fit' modelling approach. However, there is an outstanding question - what are we gaining from using this approach? Are these methods advancing our understanding of the ramp system as a whole or just replicating specific examples under specific assumptions, with a significant danger of circular reasoning? Moreover how could these methods be applied to subsurface or poorly exposed ramp examples? This seems likely to be difficult. In general best-fit modelling approaches have tended to suffer from issues of an overly-simple objective function and potentially circular reasoning whereby parameters derived from interpretations of data were input into the model, which then rather unsurprisingly reproduced the same interpreted geometries.

As stated in a recent review of SFM (Burgess 2009, in press) it remains unclear what this modelling approach actually demonstrates, or what predictive power a single best-fit model of this type actually has.

It would therefore seem that there is a need for an alternative modelling approach in order to better understand the dynamics of a ramp system. Experimental approaches constructing models to formulate hypotheses of the form “if a carbonate system works as follows what resultant geometries will we observe?” may represent a more useful approach to carbonate morphometric modelling. Numerous, varied examples of experimental modelling exist for siliciclastic systems (e.g. Gerber et al., 2008), suggesting the technique has become well established and has yielded some important results. While examples of such experimental modelling are sparse with regards to carbonate systems (and non-existent with regards to ramps), two notable examples exist. The first was a study conducted by Drummond and Dugan (1999) whose experimental modelling approach used a cellular automata to reproduce negative exponential thickness-frequency relationships observed in outcrop successions, while Burgess et al., (2001), Burgess (2001), Burgess and Wright (2003), Burgess and Emery (2004), and Burgess (2006) used a 3D model to investigate interaction of auto and allocyclic processes. This thesis proposes an additional example of carbonate modelling using an experimental approach whereby the interplay of controlling parameters on carbonate platform development will be investigated.

This new approach *Assessing Platform controls using Experimental modelling* will be referred to from here in as the ‘APE’ method. The APE method differs from the ‘model-fit’ approach in that the models run are unconstrained by comparison to any specific example. The key point to this new modelling method is that the models are not constrained by data derived from specific outcrops, and are therefore not trying to replicate specific geometries from which field data has been derived. The principal purpose and importance of the APE method is that multiple model suites can be run with a range of different controlling parameters to systematically test the response of the model to these various parameter combinations and evaluate the response in terms of generated stratal geometries. Importantly not only can

the effect the various parameters have on platform generation be analysed, but for each individual parameter a range of values can also be tested.

The APE method follows a three step procedure (Figure 3.3). Each step is described in detail below. The example used for the APE method description shall be referred to as Model 1 (M1), and is the model discussed in Chapter 4 which investigates the role of sediment production and transport on carbonate platform geometry. M1 is the principal model used throughout this study on the controlling parameters of the carbonate ramp setting, and all additional models are either derived from this model suite or are tested against and compared with it. All models are listed in table 3.2 along with their input parameters, their variation from M1, and a description highlighting the purpose of each model suite.

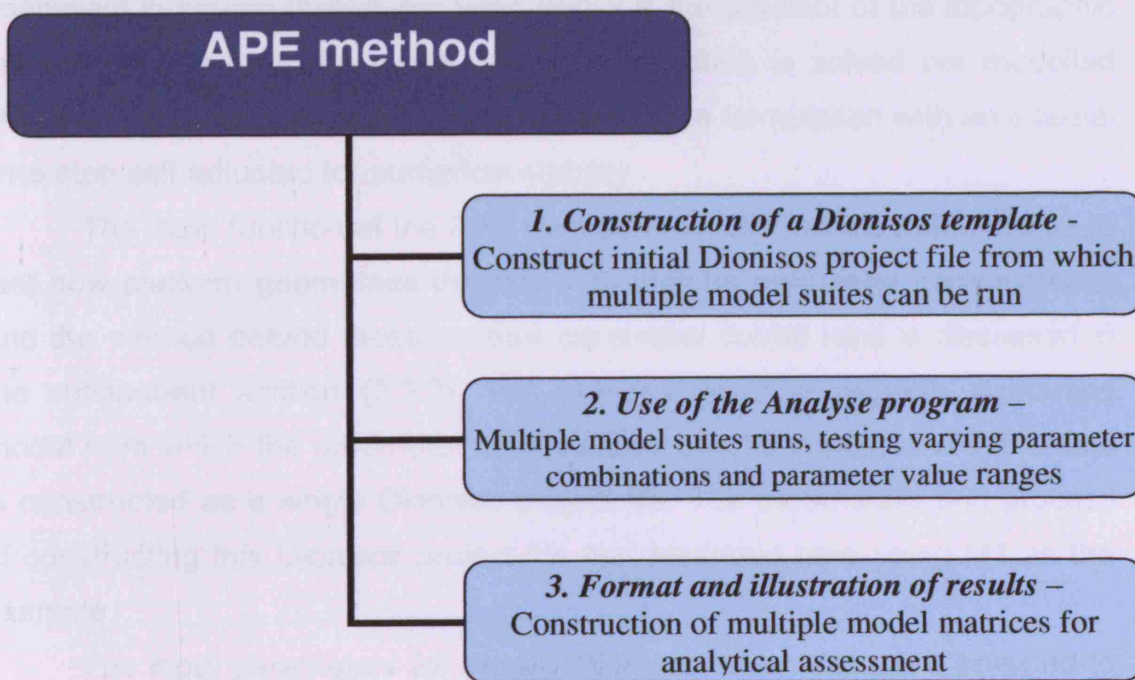


Figure 3.3. The 3-step procedure for the APE method.

3.3.1 The APE method 1 – Construction of a Dionisos template

The APE method uses the three-dimensional numerical stratigraphic forward modelling program Dionisos. The program has been developed by the Institut Francais Petrole, and includes a number of different sedimentary and tectonic processes capable of producing complicated three-dimensional models (Granjeon and Joseph, 1999; Granjeon et., 2002). Dionisos is based on a generalized, modified diffusion formulation of sediment transport, where transport rate is dependent on topographic slope, diffusion coefficient, and water discharge volume. Gravity driven sediment flux is calculated per model cell from

$$Q_s = \kappa S$$

where Q_s is the sediment flux in square meters per year, κ is the diffusion coefficient in square meters per year, and S is the gradient of the topographic surface at a point in the model grid. This equation is solved per modelled strata surface using a fully implicit finite difference formulation with an internal time-step self-adjusted for numerical stability.

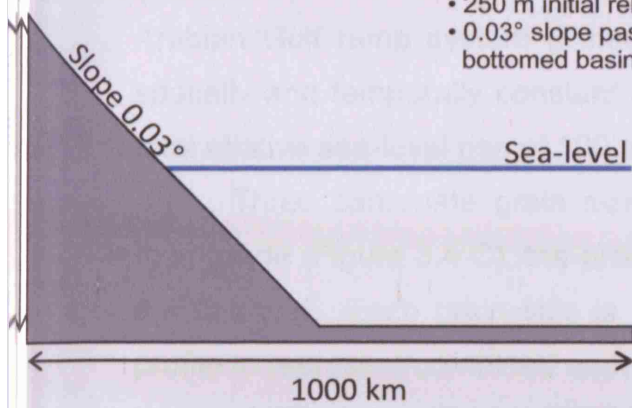
The main function of the APE method is to run multiple model suites to test how platform geometries develop with various parameter combinations, and the method behind these multiple parameter model runs is discussed in the subsequent section (3.3.2). The process however requires a starting model from which the parameter combinations can be varied, and this model is constructed as a single Dionisos project file. The parameters and process of constructing this Dionisos project file are described here using M1 as the example.

The input parameters for the M1 Dionisos project file were selected to represent a generic cratonic ramp and basin system of the type interpreted to occur at various points in the Phanerozoic history of North America, the Middle East and Europe (Cutler, 1983; Aigner, 1984; Watts, 1990; Burchette, 1993). The model runs on a 1000 km long two-dimensional grid with 10 km grid cells (Figure 3.4 A) for a total duration of 5 million years (Figure 3.4 B) and starts with a 250 m relief 0.03° slope that passes distally into a 125 m deep flat-bottomed basin. This configuration is broadly comparable with

Figure 3.4

M1 Input Parameters

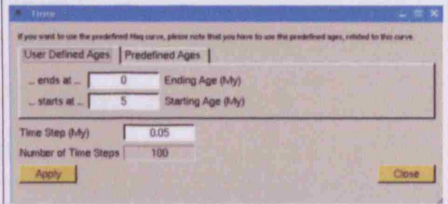
- Bathymetry at 5 Ma
- 1000 Km long 2D grid with 10 Km grid cells
- 250 m initial relief
- 0.03° slope passing into 125 m flat bottomed basin



```
Compute Map using the following formula ...
Bathymetry[3] = ((x+500)*(x/2-125)+(y-500)*(125))
```

A. Initial basement bathymetry

B. Model Duration



- 5 to 0 My = 5 My model duration
- 0.05 My time step

D. Angle of repose

Lithology Name	1	2	3
Grain Size (mm)	0.2	0.02	0.006
Critical Slope (m/100m)	600	200	50

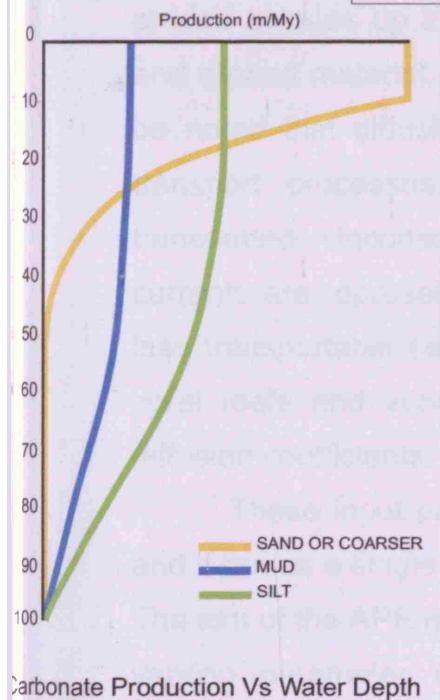
C. Modelled Lithologies

- Carbonate sand or coarser
- Silt
- Mud

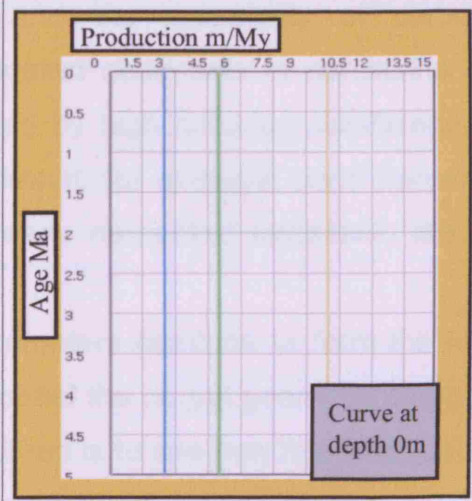
Name	1	2	3	4	5	6	7
Color	Sand	Silt	Mud				

The color is used only to enhance 1D displays such as production or supply curves

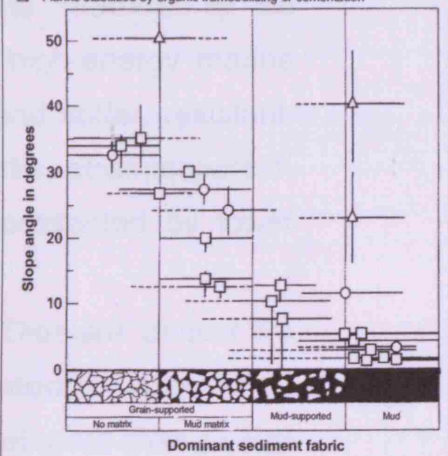
GRAIN	GRAIN SIZE	CRITICAL SLOPE
Sand or coarser	0.2 mm	3°
Silt	0.02 mm	12°
Mud	0.006 mm	30°



Age (My)	1	2	3
litho ->	Sand or coars	Silt	Mud
	0	10	5
	5	10	5

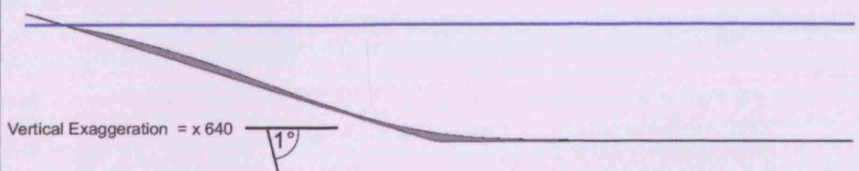


- Well documented examples
- Examples lacking precise control on geometry
- △ Flanks stabilized by organic framebuilding or cementation



E. Initial model rates

GRAIN	Initial Sediment Production Rate m/My	Initial Diffusion Coefficient Km ² /ky
Sand or coarser	10	0
Silt	5	0
Mud	2.5	0



F. M1 Resultant geometry

Figure 3.4 Input parameters for M1

- A - Initial basement bathymetry from which M1 is modelled. Dionisos interface image shows formula used to create bathymetry.
- B - M1 model duration.
- C - Dionisos interface image shows three modelled lithologies, production curves depict carbonate production versus time for each lithology, and production versus time interface shows constant production rates throughout duration of model
- D - Angle of repose values for each lithology. Grain sizes are derived from the Udden-Wentworth scale (Nichols, 1998) and angle of repose values estimated from Kenter (1990).
- E - Initial production and diffusion coefficient rates for M1
- F - Resultant Dionisos geometry for M1.

gradients inferred from ancient cratonic interior systems and from the modern Arabian Gulf ramp system (Purser, 1973; Walkden and Williams, 1998). A spatially and temporally constant rate of subsidence of 20 mMy^{-1} leads to a total relative sea-level rise of 100 m during each model run.

Three carbonate grain sizes are modelled sand or coarser, silt and mud-grade (Figure 3.4 C), the production rate of which can be seen in Figure 3.4 C and E. Each grain size is modelled with a different production-depth profile to represent combined euphotic and oligophotic factories inhabited by a range of different producers (Pomar, 2001), while all three grain sizes have an angle of repose (Kenter, 1990) beyond which the sediment will become unstable and collapse (Figure 3.4 D). Sediment transport is calculated using a generalized modified diffusion formulation, and the diffusion coefficient values used in M1 are shown in Figure 3.4 E. Previously deposited sediment can be eroded at rates up to 100 m/My , depending on local topographic gradient S and eroded material is then available to be transported by diffusion. It should be noted that diffusion coefficients encompass both efficiency of sediment transport processes, and the propensity of carbonate material to be transported. Unconsolidated sediments in conditions of high-energy marine currents are represented by high diffusion coefficients, and stiffer, resistant, less transportable sediment, for example coral frameworks, stromatoporoid-coral reefs and very early cemented sediment, are represented by lower diffusion coefficients.

These input parameters combine to form the M1 Dionisos project file and if run as a single model the output geometry can be seen in Figure 3.4 F. The aim of the APE method is to see how this initial geometry will change with varying parameter combinations, and section 3.3.2 describes how this procedure is conducted.

3.3.2 The APE method 2 – Use of the ANALYSE program

The single geometry output (Figure 3.4 F) provided by the M1 Dionisos project file is the starting point for the multiple model runs, the idea of which is to investigate the role changing parameter and parameter values has on platform architecture. If we use the parameters of carbonate production and transport as an example, in order to investigate the control they impose on platform development (and therefore in this example their impact on geometry M1, Figure 3.4 F) it appears logical that increasing the rate of each parameter by a fixed increment will provide a clear illustration of their influence on the system. However if we manually increase the parameter rate in the Dionisos interface and continue to run the model as single model sets, taking into account model run time and the time spent manually changing the parameter values the procedure will not only be extremely time consuming but is also unlikely to be an exhaustive analysis of the parameters control. A program was therefore written in the C programming language to automate this process, and is called the ANALYSE program.

ANALYSE was written originally by Didier Granjeon (IFP), and subsequently modified by Henne Lammers (Shell E&P), Peter Burgess (Shell E&P) and the author. ANALYSE contains just over 1500 lines of code and its main purpose is to automate the running of the multiple model suites. In essence the program takes the original Dionisos project file and runs a series of model runs, each of which is slightly different to the previous model run due to an increased parameter value (either sediment transport or production rate). A detailed workflow of how the ANALYSE program works is provided in Figure 3.5. The program can run as many iterations of the model as specified in the code by the user, however for ease of analysis end member values should be identified and the number of model runs between these values decided. To determine these end member values a systematic approach of trial model runs can be conducted whereby parameter values are set accordingly high that beyond which no major change in platform architecture is likely to occur. For example, with regards to sediment transport the highest diffusion coefficient should be a value which effectively transports the majority, if not all of the sediment into the deepest distal parts of the system,

ANALYSE program workflow

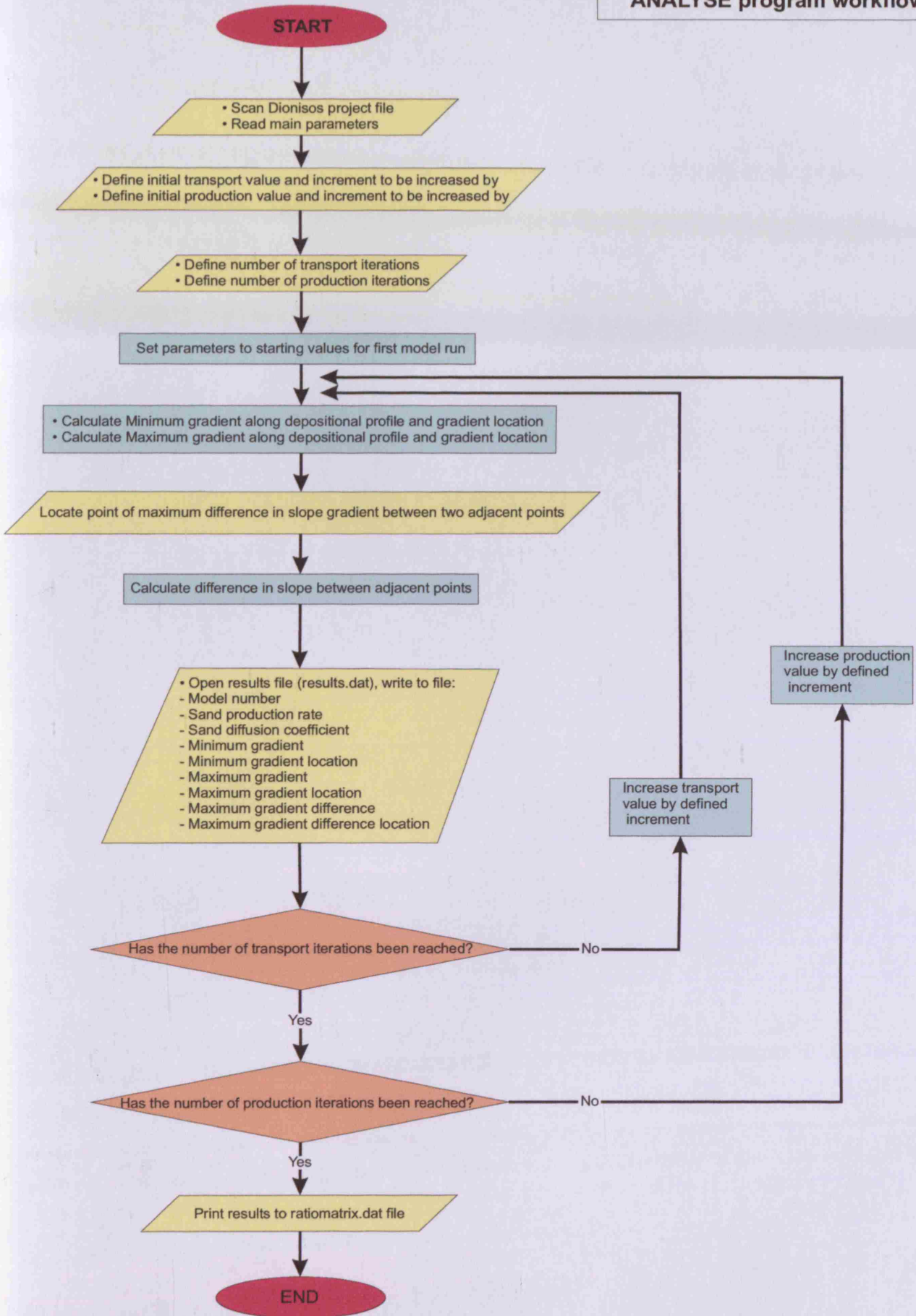


Figure 3.5. Workflow depicting the ANALYSE program procedure.

thus diffusion coefficient values higher than this value need not be considered because they will produce the same basic geometry.

For M1 many (>1000) models were run to determine end member values, the rates of which can be seen in Table 3.1, with diffusion coefficients reaching 50 Km²/ky and combined sediment production exceeding 450 m/My, a maximum rate which is comparable with modern production rates (Lokier and Steuber, 2008). With high end member values identified and low end member values set at Zero the number of iterations of M1 was set at 200, and value ranges divided by this to calculate the increment increases for each parameter (Table 3.1).

M1 Model Iteration	Grain type	Sediment Production Rates m/My			Diffusion Coefficient Km ² /ky		
		Minimum rate	Maximum rate	Increment increase	Minimum rate	Maximum rate	Increment increase
200	Sand or Coarser	10	280	13.5	0	5	0.25
	Silt	5	140	6.75	0	10	0.5
	Mud	2.5	70	3.375	0	50	2.5

Table 3.1. Max and min Sediment Production Rates and Diffusion Coefficient values used for M1.

Once all values have been ascertained and the code edited to provide the required number of model iterations the ANALYSE program is run via the command terminal on a PC running a Linux operating system. The command issued in the terminal opens the ANALYSE program, fetches the specified Dionisos project file and must state the starting value and increment increase for each of the three grain types. The Terminal command is formatted as follows:

1. Open ANALYSE program
2. Fetch specified Dionisos project file
3. Define initial Sand Production rate
4. Define Sand Production increase increment
5. Define initial Silt Production rate
6. Define Silt Production increase increment
7. Define initial Mud Production rate
8. Define Mud Production increase increment
9. Define initial Sand Diffusion Coefficient
10. Define Sand Diffusion Coefficient increase increment
11. Define initial Silt Diffusion Coefficient
12. Define Silt Diffusion Coefficient increase increment
13. Define initial Mud Diffusion Coefficient
14. Define Mud Diffusion Coefficient increase increment

The terminal command for example M1 would therefore be:

```
ANALYSE, M1.pro, 10.0, 13.5, 5.0, 6.75, 2.5, 3.375, 0, 0.25, 0, 5.0, 0, 2.5
```

If this procedure is followed the ANALYSE code will run the 200 model iterations. The data which is output is also specified within the ANALYSE program. If the data is output as a series of 200 platform geometry diagrams, such as the one seen in Figure 3.4 F, these provide a visual component from which platform architecture development can be assessed. However, considering the scale of the models (1000 Km) and the vertical exaggeration required to view the resultant geometries (at least x 320) such assessment will be somewhat subjective dependant on the individual viewing the geometries. Analysis of the resulting geometries based on their visual character alone is therefore unsatisfactory and an alternative system is required with which the resultant models can be numerically and quantitatively assessed. The ANALYSE program provides this by systematically evaluating each individual model and outputting a string of data derived from a series of measurements obtained from the top surface of the resultant geometry. The basic output measurements provided are:

1. The Model number
2. The Sand or coarser production rate (used to ascertain from which parameter value the model is derived)
3. The Sand or coarser diffusion coefficient (used to ascertain from which parameter value the model is derived)
4. The Minimum gradient observed within a cell across the top surface of the resultant geometry
5. The location of this minimum gradient on the top surface
6. The Maximum gradient observed within a cell across the top surface of the resultant geometry
7. The location of this maximum gradient on the top surface

The series of output data provides numerical values for each of the resultant architectures, but does not directly infer the type of platform geometry being created, for example either a ramp or flat-topped platform system. As the purpose of the APE method is to evaluate what geometrical type of carbonate system is created by varying parameter values, an automated platform type classification system is also incorporated within the ANALYSE program. The classification system is derived from the surface

gradients of the resultant geometries, and three separate methods of evaluation have been utilized:

Automated platform type classification 1 – Minimum gradient

Minimum gradient values of zero degrees indicates presence of a flat surface, most likely a platform top, thus implying a flat-topped platform system. It should be noted that this method is unreliable in high transport examples due to potential distal ponding, so the position of the zero-gradient points should also be considered to differentiate proximal flat-top platform from distal sediment ponding.

Automated platform type classification 2 – Gradient ratio (R)

A significant difference between a carbonate ramp and a carbonate flat-topped platform system is the difference between its Max (So) and Min (Si) surface gradient (Figure 3.6). Using the gradient output data derived from the ANALYSE program a gradient ratio (R) for each model can be calculated by:

$$R = \frac{S_i}{S_o}$$

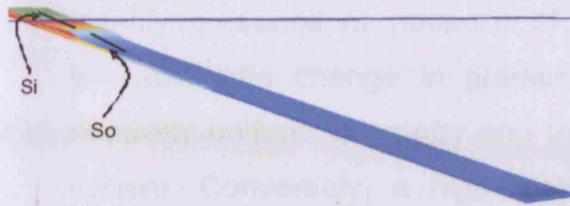
High ratio values indicate a relatively uniform gradient, indicating in turn a possible homoclinal ramp system. Conversely a low gradient ratio will indicate a large difference in maximum and minimum gradient, and thus a major change in gradient within the system potentially indicating a flat-topped platform environment. As with the minimum gradient method, the location in which the maximum or minimum gradients occur should also be considered in order to distinguish proximal flat-top platforms from distal ponded strata.

Automated platform type classification 3 – Maximum gradient difference (Max ΔS)

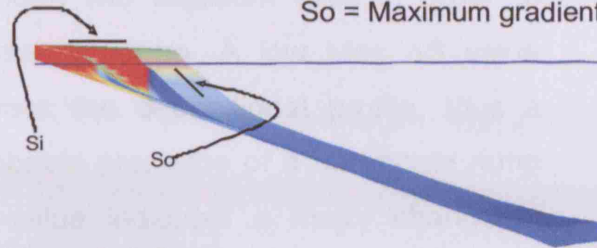
The final and most accurate scheme for automated platform classification is identifying the maximum gradient difference (Max ΔS) along the modelled depositional profile. This method is incorporated within the ANALYSE program, and systematically examines the gradient in each individual cell

Automated platform type classification 2 - Gradient Ratio (R)

Homoclinal Ramp



Si = Minimum gradient
So = Maximum gradient

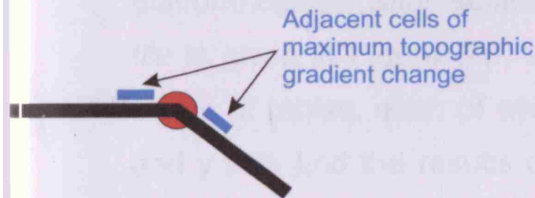


Flat topped platform

Figure 3.6. Automated platform classification system derived from calculating a gradient ratio between the Max (So) and Min (Si) gradient, which are ascertained from the top surface of the modelled depositional profile.

Automated platform type classification 3 - Maximum gradient difference (Max ΔS)

Identify point on modelled depositional profile with largest difference in slope gradient between two adjacent cells
Gradient of both adjacent cells is measured and difference between both calculated



Point of maximum topographic gradient change (Max ΔS)



Low (Max ΔS) ≈ Homoclinal ramp
High (Max ΔS) ≈ Flat topped platform

Figure 3.7. Automated platform classification system derived from calculating the maximum gradient difference between adjacent cells along the modelled profile. The process can be viewed as identifying the lack, or presence of a slope break.

A	B	C	D	E	F	G	H	I	J	K
n	SandProd	SandDiffCoeff	MinGrad	X	MaxGrad	X	MaxGradD	X	GradientRatio	minimumWD
0	91	0	0	39	17.57888	41	17.5788784	40	0	0
1	91	0.25	0	36	3.40772	41	1.800675	40	0	0
2	91	0.5	0	36	2.623206	42	1.762527	40	0	0
3	91	0.75	0	36	2.138077	42	1.2291081	40	0	0
4	91	1	0	36	1.84329	43	0.934039	40	0	0
5	91	1.25	0	35	1.65345	43	0.752213	40	0	0
6	91	1.5	0	35	1.50552	43	0.625109	40	0	0
7	91	1.75	0	35	1.394417	44	0.537467	40	0	0
8	91	2	0	35	1.306522	44	0.469857	40	0	0
9	91	2.25	0	35	1.232426	44	0.416946	40	0	0
10	91	2.5	0	35	1.170828	44	0.375368	40	0	0
11	91	2.75	0	35	1.116091	45	0.341799	40	0	0
12	91	3	0	35	1.069551	45	0.314406	40	0	0
13	91	3.25	0	35	1.028664	45	0.29168	40	0	0
14	91	3.5	0	35	0.989581	45	0.271669	40	0	0
15	91	3.75	0	35	0.954343	46	0.253881	40	0	0
16	91	4	0	34	0.922535	46	0.25	4	0	0
17	91	4.25	0	34	0.894556	46	0.25	4	0	0
18	91	4.5	0	34	0.868739	46	0.25	4	0	0
19	91	4.75	0	34	0.844612	46	0.25	4	0	0
20	91	5	0	34	0.821722	47	0.25	4	0	0

Figure 3.8. Example of output data file from the ANALYSE program when following the APE method. Column values represent: A - Model number, B - Sand production rate, C - Sand Diffusion coefficient, D - Minimum gradient along the modelled depositional profile, E - Cell number location of minimum gradient, F - Maximum gradient along the modelled depositional profile, G - Cell number location of the maximum gradient, H - The maximum gradient difference value, I - Cell number location that the maximum gradient difference was measured, J - Gradient ratio value, K - Minimum water depth of the system.

along the modelled depositional profile and determines the maximum change in topographic gradient occurring between two adjacent cells in order to identify presence or absence of a break of slope. A low Max ΔS value indicates little change in gradient across the depositional profile, thus a relatively uniform geometry and the probable presence of a carbonate ramp system. Conversely, a high Max ΔS value indicates a major change in gradient within the system, has identified the location of a break of slope, and implies a flat-topped platform environment (Figure 3.7).

3.3.3 The APE method 3 – Formatting and illustration of results

The APE method outputs various data, including the automated platform classification schemes listed in section 3.3.2. An example output data file is given in Figure 3.8. Values from this data file can be formatted into a series of tables, each of which displays increasing parameter values on its x and y axis and the results of a corresponding third parameter, i.e. maximum gradient, at that parameter range (Figure 3.9). The tables can be imported into either Excel or Matlab and further manipulated to create graphical plots of the matrices incorporating 3 colour formatted parameters. The matrices integrate each of the 200 model results and display how changes in sediment production and down-dip sediment transport affect the third plotted parameter (typically one of the automated platform type classification schemes), providing a clear dataset for analytical interpretation (Figure 3.10).

3.4 Utilizing the APE modelling method

The subsequent chapters utilize the APE modelling method described in this chapter to produce a series of models from which the control a multitude of parameters and parameter ranges exert on platform development can be analyzed. Table 3.2 lists each of these models, the purpose of each model, and is the main reference table for specific input data values for each of the models.

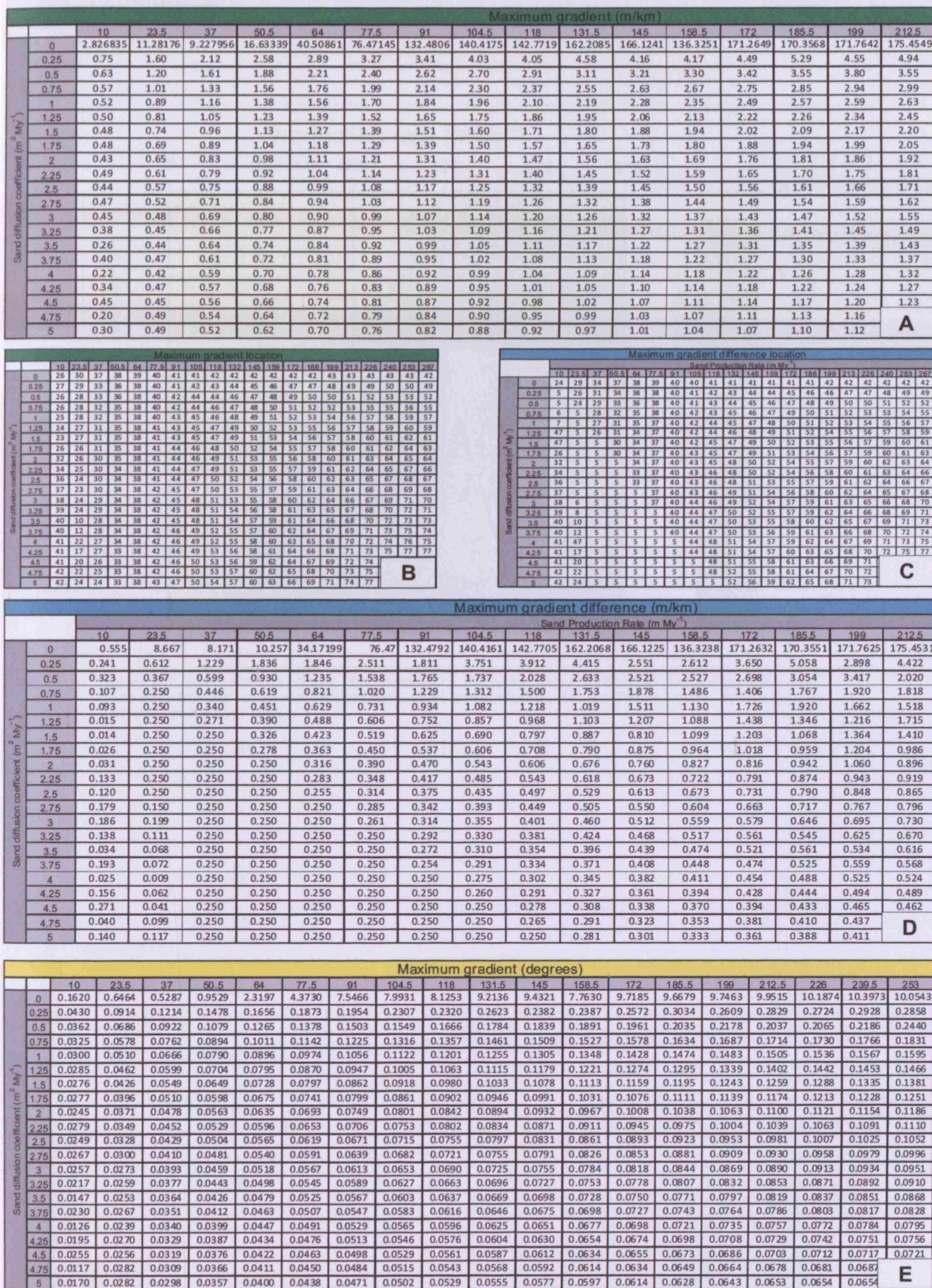
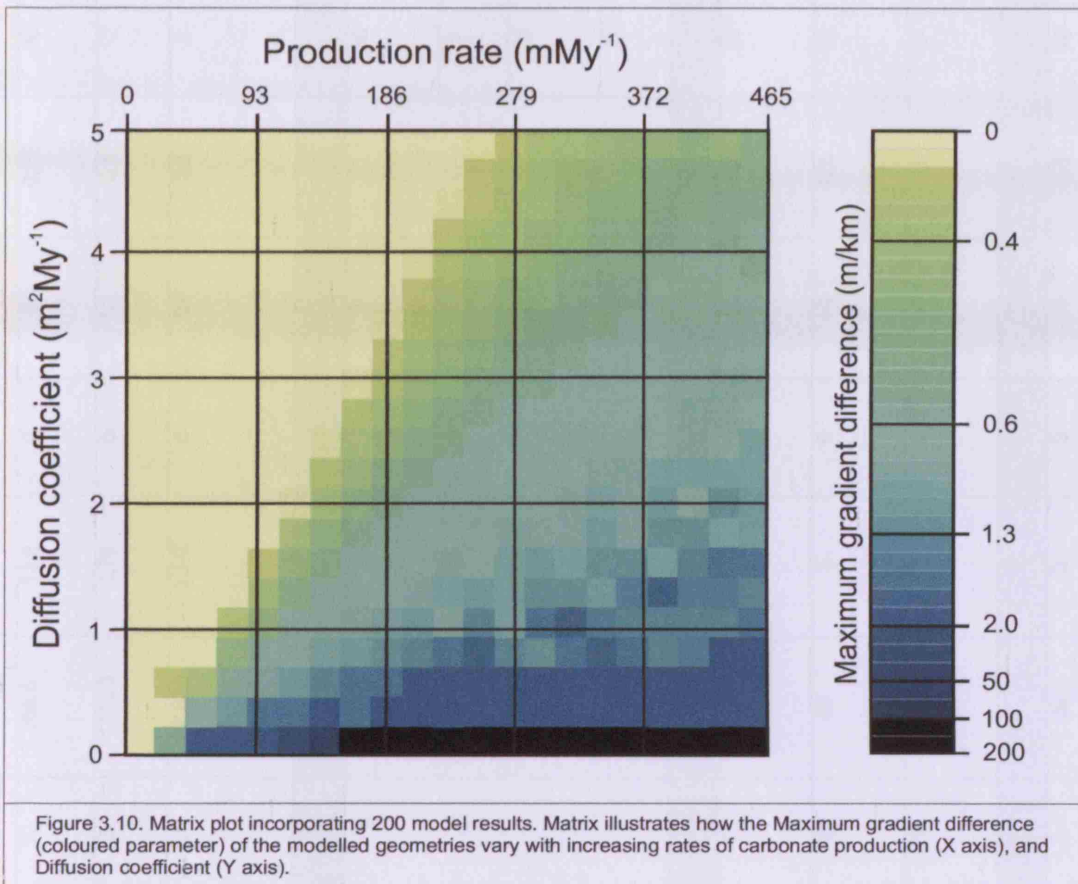


Figure 3.9. Formatted excel tables containing results for complete 200 model APE method model run. All tables have increasing Diffusion coefficient on Y axis, and increasing production rate along X axis. Value illustrated within each table represents a different parameter but for the same model set: A - Maximum gradient m/km, B - Maximum gradient cell location number, C - Maximum gradient difference cell location number, D - Maximum gradient difference m/km, E - Maximum gradient in degrees.



Model Model	'APE' Model Iterations	Duration My	Initial Bathymetry	Subsidence mMy ⁻¹	Sea-level History	Grain Type	Sediment Production Rates mMy				Diffusion Coefficient Km ² /ky				Angle of Repose °	Purpose of Model
							Minimum rate	Maximum rate	Increment increase	Minimum rate	Maximum rate	Increment increase	Minimum rate	Maximum rate		
M1	200	5	<ul style="list-style-type: none"> • 1000Km • 250m initial relief • 0.03° slope passing into 125m flat bottomed basin • Refer to Fig. 3.4A 	20	Relative sea-level rise of 100m	Sand or Coarser	10	266.5	13.5	0	5	0.25	30	Investigate influence of sediment production and transport on carbonate platform geometry.		
						Silt	5	133.25	6.75	0	10	0.5	12			
						Mud	2.5	66.625	3.375	0	50	2.5	3			
M2	2	5	<ul style="list-style-type: none"> • 1000Km • 250m initial relief • 0.03° slope passing into 125m flat bottomed basin • Refer to Fig. 3.4A 	20	Relative sea-level rise of 100m	Ramp Sand or Coarser	100				3		30	Investigate the control production profile exerts on platform geometry. Fixed rates of production and transport for ramp and FTP prone conditions.		
						Ramp Mud	25				30		3			
						FTP Sand or Coarser	100			0.25		30				
						FTP Mud	25			2.5		3				
M3	200	5	<ul style="list-style-type: none"> • 1000Km • 250m initial relief • 0.03° slope passing into 125m flat bottomed basin • Refer to Fig. 3.4A 	20	Relative sea-level rise of 100m	Sand or Coarser	1	28.5	1.5	0	5	0.25	30	Identify the control grain composition exerts on platform geometry. Grain composition of M3 = Sand or coarser 8%, Silt 15%, Mud 77%.		
						Silt	2	59	3	0	10	0.5	12			
						Mud	10	295	15	0	50	2.5	3			
M4	200	5	<ul style="list-style-type: none"> • 1000Km • 250m initial relief • 0.03° slope passing into 125m flat bottomed basin • Refer to Fig. 3.4A 	20	Relative sea-level rise of 100m	Silt	2	59	3	0	10	0.5	12	Identify the control grain composition exerts on platform geometry. Grain composition of M4 = Silt 17%, Mud 83%.		
						Mud	10	295	15	0	50	2.5	3			

M5	200	5	20	Relative sea-level rise of 100m	Sand or coarser	100	3	30	control grain composition exerts on platform geometry. Grain composition of M5 = Mud 100%.
M6	5	5	20	Relative sea-level rise of 100m	Sand or coarser	100	3	30	Investigate the control changing initial basement bathymetry exerts on platform geometry
					Silt	50	6	12	
					Mud	25	30	3	
M7	1	5	20	Relative sea-level rise of 100m	Sand or coarser	100	3	30	Identify effect of localised faulting on platform development
					Silt	50	6	12	
					Mud	25	30	3	
M8	9	5	100	Relative sea-level rise of 100m	Sand or Coarser	280	5	30	Identify effect of differential subsidence on platform development
					Silt	140	10	12	
					Mud	70	50	3	

ID	6	5	• 1000Km bathymetry • Antecedent bathymetry • Shallow 100m deep basin	20	Relative sea-level rise of 100m	Sand or Coarser		FTP Silt	FTP Mud	FTP Sand or Coarser	6	30	3	12	control an antecedent bathymetry may exert on platform development
						Ramp Silt	Ramp Mud								
M9							30	150			6		3		
							15	75			30		3		
							60	300			0.25		30		
							30	150			0.5		12		
							15	75			2.5		3		
M10			• 1000Km • Antecedent bathymetry • Deep 500m basin	20	Relative sea-level rise of 100m	60	300				3		30	Investigate the control an antecedent bathymetry may exert on platform development	
						30	150			6		12			
						15	75			30		3			
						60	300			0.25		30			
						30	150			0.5		12			
M11			• 1000Km • Active differential subsidence forming a shallow 100m deep basin at conclusion of model	20	Relative sea-level rise of 100m	60	300				3		30	Investigate the control syndepositional subsidence may exert on platform development	
						30	150			6		12			
						15	75			30		3			
						60	300			0.25		30			
						30	150			0.5		12			
						15	75			2.5		3			

Model ID	Model Name	Relative sea-level rise of 100m	Coarser	FTP	Mud	Production rates based on Steuber (2000)	Coarser	FTP	Mud	Production rates based on Steuber (2000)
M12	Active differential subsidence forming 500m deep basin at conclusion of model	20	Ramp Silt	30	150	6	30	12	3	
			Ramp Mud	15	75	30	15	3	3	
			FTP Sand or Coarser	60	300	0.25	60	30	30	
			FTP Silt	30	150	0.5	30	12	12	
			FTP Mud	15	75	2.5	15	3	3	
M13	Two subsidence regimes modelled A) Differential subsidence simulating typical foreland basin type B) Same as A but maximum rate of 1mm/yr after Dorobek (1995)		Sand or Coarser	160	80	3		30	12	Model simulating carbonate ramp growth in the foreland basin tectonic setting. Ramp is based on the Arabian Gulf example incorporating data derived from literature and the results of previous model sets
			Silt	40		6		3	3	
			Mud		Production rates from Lokier and Steuber (2008)	30				
M14	Differential accentuates basin, maximum basin depth reaches 100m		Sand or Coarser (Rudists)	250	125	0.25		30	12	Model simulating carbonate ramp growth in the intraplatform basin tectonic setting. Ramp is based on the Natih Formation incorporating data derived from literature and the results of previous model sets
			Silt	62.5		0.5		3	3	
			Mud		Production rates based on Steuber (2000)	2.5				

Case	M	A	B	C	D	E	F	G	H	I	J	K	L	M			N	O	P	Q	R	S	T									
														1	2	3																
M15	6	1	20	<ul style="list-style-type: none"> • 1000Km • 250m initial relief • 0.03° slope passing into 125m flat bottomed basin • Refer to Fig. 3.4A 	20	Amplitude = 2 m ii) Period = 40 Ky Amplitude = 2 m B - Icehouse i.) Period = 400 Ky Amplitude = 20 m ii) Period = 100 Ky Amplitude = 70m C - Icehouse i.) Period = 400 Ky Amplitude = 70 m ii) Period = 100 Ky Amplitude = 20 m	Coarser	50	25	100	6	12	3	30	Investigate the role of relative sea-level change on platform development	12	3	30	Investigate the role of relative sea-level change on platform development	12	3	30	Investigate the role of relative sea-level change on platform development									
																								Sand or Coarser	100	25	100	6	12	3	30	Investigate the role of relative sea-level change on platform development
																								Ramp Silt								
																								Ramp Mud								
																								FTP Sand or Coarser								
																								FTP Silt								
FTP Mud																																
M16	200	1	20	<ul style="list-style-type: none"> • 1000Km • 250m initial relief • 0.03° slope passing into 125m flat bottomed basin • Refer to Fig. 3.4A 	20	Period = 100 Ky Amplitude Min (M) Min (M) Iterations Increment	Sand or Coarser	50	25	100	5	12	3	Investigate the role of relative sea-level change on platform development	12	3	30	Investigate the role of relative sea-level change on platform development	12	3	30	Investigate the role of relative sea-level change on platform development										
																							Silt									
																							Mud									
																							Sand or Coarser	100	25	100	5	12	3	30	Investigate the role of relative sea-level change on platform development	
																							Sand or Coarser									
																							Silt									
Mud																																
Sand or Coarser																																
M17	200	1	20	<ul style="list-style-type: none"> • 1000Km • 250m initial relief • 0.03° slope passing into 125m flat bottomed basin • Refer to Fig. 3.4A 	20	Period = 400 Ky Amplitude Min (M) Min (M) Iterations Increment	Sand or Coarser	50	25	100	5	12	3	Investigate the role of relative sea-level change on platform development	12	3	30	Investigate the role of relative sea-level change on platform development	12	3	30	Investigate the role of relative sea-level change on platform development										
																							Silt									
																							Mud									
																							Sand or Coarser	100	25	100	5	12	3	30	Investigate the role of relative sea-level change on platform development	
																							Sand or Coarser									
																							Silt									
Mud																																
Sand or Coarser																																

M18	200	1	<ul style="list-style-type: none"> • 250m initial relief • 250m initial • 0.03° slope passing into 125m flat bottomed basin • Refer to Fig. 3.4A 	20	<p>Iterations Min (M) Min (M) Increment</p> <p>200 0 100 5</p> <p>Amplitude</p> <p>Silt</p>	50					0	10	0.5	12		
						25					0	50	2.5	3		
M19	200	1	<ul style="list-style-type: none"> • 1000Km • 250m initial relief • 0.03° slope passing into 125m flat bottomed basin • Refer to Fig. 3.4A 	20	<p>Period = 500 Ky Sand or Coarser</p> <p>Iterations Min (M) Min (M) Increment</p> <p>200 0 100 5</p> <p>Amplitude</p> <p>Silt</p> <p>Mud</p>	100					0	5	0.25	30		
						50					0	10	0.5	12		
						25					0	50	2.5	3		

Table 3.2. A complete listing of the input parameters for each of the forward models produced in this study. The principal purpose of each model is also listed.

Chapter 4: UNDERSTANDING CARBONATE PLATFORM TYPES: USING 'APE' TO TEST THE ROLE OF SEDIMENT PRODUCTION AND TRANSPORT ON PLATFORM GEOMETRY

Chapter 4 presents forward modelling results investigating the control sediment production and transport exert on carbonate platform geometry. The modelling is conducted using the APE method discussed in Chapter 3. The chapter outlines the rationale behind the modelling before extensively testing the role sediment production and transport play in carbonate depositional systems, and concludes with a discussion surrounding the implications and possible uses of the model results presented here.

4.1 Introduction – Our current understanding of carbonate platform types

Carbonate depositional systems are typically classified as one of a number of different platform types dependent on their large-scale (10's kms) geometry. This classification is important because many predictive elements of facies and sequence stratigraphic models vary between the different types. To classify a particular system its large scale depositional geometry can either be observed directly, for example in modern settings such as the Arabian Gulf (Purser, 1973), imaged by seismic data in subsurface examples (Chatellier, 1988; Droste and Van Steenwinkel, 2004; Handford and Baria, 2007), reconstructed from large outcropping geometries such as the Sierra del Cuera, NW Spain (Bahamonde et al., 2004) and the Mut Basin, Turkey (Janson et al., 2007), or inferred from more indirect evidence such as outcrop facies belt distributions and absence of diagnostic evidence such as a visible platform margin geometry (Burchette and Wright, 1992).

The two main types of carbonate systems are flat-top platforms (FTP) and ramps. FTPs, as the name suggests, have a very low gradient top surface that passes seaward into a much steeper slope (i.e. $> 1^\circ$, typically greater than 3°). Ramp systems, in contrast, lack the steep slope found seaward of the platform margin on FTPs (Ahr, 1973; Read, 1982; Burchette and Wright, 1992). Instead of flat-tops and steep margins, homoclinal ramps

have a distally dipping surface with approximately constant regional gradients of 0.1 to 1.0 degrees (Burchette and Wright, 1992). Distally steepened ramps are less uniform and show a break of slope, with a distal steeper portion (Read, 1985), but the gradient on this distal portion is assumed to be significantly less than gradients on a rimmed margin slope (Burchette and Wright, 1992). Ramps may also differ from FTPs in that the development of high-energy facies belts in ramps is limited to the littoral zone close to the shoreline, unlike rimmed flat-topped platforms which often have a high-energy belt offshore on the platform margin (Burchette and Wright, 1992; Schlager, 2005).

Unfortunately, as with many Earth surface systems, these definitions of homoclinal and distally steepened ramp are often difficult to apply because they are rather simple geomorphic terms used to categorize potentially complicated ancient strata. Direct observational evidence of large scale geometry is often lacking, and where depositional systems are sufficiently variable in space and time, for example in terms of facies belt development, they often do not fit easily into one simple category. The original classification of the ramp model (Ahr, 1973) cited the slopes of the Western Trucial Coast (Southern Arabian Gulf) as a type example for the carbonate ramp model, but several case studies of "low-relief" deposystems have since shown numerous geometrical variations on this uniformly dipping surface model. In fact many carbonate platforms classified as ramps actually resemble "flattened" rimmed shelves with a platform top with a subtle break of slope, for example the Upper Jurassic to Lower Cretaceous strata of the Neuquen Basin, Argentina, (Mitchum and Uliana, 1985), the Nisku Formation of the Western Canadian Basin (Burchette and Wright, 1992), and the Smackover Formation of the U.S. Gulf Coast (Handford and Baria, 2007). This change in gradient is commonly referred to as the ramp slope crest which is also frequently the location of seismically resolvable sigmoidal clinoforms with complex internal geometries, for example the Banff Formation of the West Canada Basin (Chatellier, 1988), the Natih Formation of Northern Oman (Droste and Van Steenwinkel, 2004), and the Las Plias Formation of Northern Mexico (Osleger et al., 2004). Even the Arabian Gulf, the classic example of a modern carbonate ramp, used by

Ahr (1973) in his original classification, may not actually be a ramp system (Walkden and Williams, 1998).

Part of the problem regarding identification and definition of ramp systems is a lack of detailed understanding about what processes and external controls determine ramp morphology (Wright and Burchette, 1998). For example, it is likely that many ramp systems represent a transient phase of accumulation between initial marine flooding of a topographic surface, and evolution of a flat-topped platform (Burchette and Wright, 1992). In addition it has long been hypothesized that a continuum of geometries exist between these ramp and FTP end members, with numerous authors (e.g. Wilson, 1975; Read, 1982; Schlager, 2005) providing illustrative sketches attempting to depict this evolutionary trend from ramp to FTP (Fig. 4.1). Moreover, examples of lateral changes in geometry on modern platform margins have been observed on the Quaternary margins of Western Australia (James et al., 1999), Southeast Australia and Eastern Florida (Ginsburg and James, 1974). However, there is no quantitative explanation of how and why this transition from ramp to platform might occur.

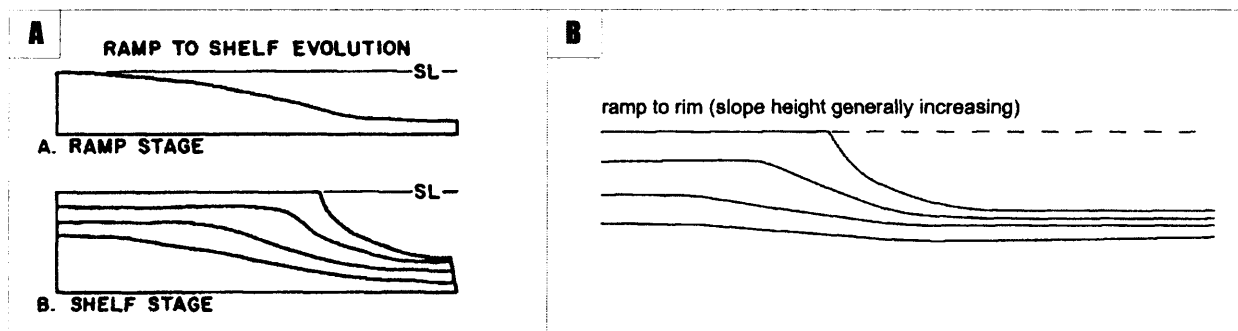


Figure 4.1. A – Evolution of ramp to rimmed shelf after Read (1982). B – Transition from ramp to rimmed platform with a sharp shelf break after Schlager (2005).

It also seems likely that ramp systems differ from FTPs in that they require an interaction of sediment production and sediment transport to maintain their form, a principle previously invoked by Wilson (1975), and James and Kendall (1992) to explain differences in platform geometries. However, it is not clear what these sediment transport processes are, nor exactly how they interact with sediment production in the various carbonate factories to maintain a ramp profile. Furthermore, the importance of offshore sediment transport has previously been highlighted by Aurell et al. (1998) during the modelling of a Kimmeridgian ramp system.

An additional parameter commonly attributed to controlling platform geometry is the carbonate production curve. Production curves define the relationship between water-depth and carbonate production rate, and a large variety of production curves have been published, and variations in platform geometry are commonly ascribed to differences in curve morphology. Euphotic production curves consisting of dominantly shallow water production are generally thought to construct FTP geometries (e.g., Bosscher and Schlager, 1992; Bowman and Vail, 1999). Conversely, oligophotic curves in which production is more widespread, occurring at both shallow and deeper water depths (e.g. Wright and Faulkner, 1990; Pomar, 2001) are frequently stated to form ramp systems. Unfortunately many of these curves are conceptual in nature, explained with simple illustrative diagrams, often without scales, and are generally insufficient to properly investigate the interactions of controls and dynamic processes likely involved.

4.2 Modelling rationale and aims

In an attempt to advance our understanding of how these multiple controls determine carbonate platform geometry the models presented in this chapter illustrate the investigation of a selection of dynamic processes that lead to ramp formation. A stratigraphic forward model is used to determine which combinations of sediment production and sediment transport generate morphologies that can be quantifiably identified as ramp systems. The models aim to for the first time, illustrate in a quantitative way the evolution of a ramp to a FTP geometry, and demonstrate the continuum of geometries which until now has been hypothesized exist in between. With the aid of the models the

role of the carbonate production curve on platform evolution will also be critically assessed.

The concept of in-situ accumulation versus transport dominated systems controlling platform geometry has been suggested previously (Burchette and Wright, 1992; Aurell et al., 1998; Pomar, 2001; Schlager, 2005) but it has not been systematically investigated in a quantitative way using numerical experiments, nor defined with appropriate terminology. Thus the overall aim of this chapter is to test some of these current ideas about what controls carbonate platform geometry, and to enhance understanding of ramp system dynamics.

4.3 Model Formulation, initial conditions and parameters

For a full description of the model formulation refer to the previous chapter. The model results were compiled following the APE method outlined in section 3.3, and the first model investigating the role of sediment production and transport on carbonate platform geometry is referred to as Model 1 (M1). All changes and parameter variations from the principle M1 model are described where necessary.

The two key parameters being investigated in M1 are sediment production and transport. Each of the three modelled grains types in M1 has a different maximum rate (Table 3.2), each of which is comparable with modern production rates (Lokier and Steuber, 2008; Warrlich et al., 2008). Non slope-failure related sediment transport in M1 is calculated using a generalized modified diffusion formulation of sediment transport where transport rate is dependent on topographic gradient and diffusion coefficients (Granjeon and Joseph, 1999; Granjeon et al., 2002). Diffusion coefficient are poorly constrained due to a lack of data, particularly in carbonate systems, and this often leads to doubts about the validity of a particular single diffusion coefficient for replicating a specific stratal geometry. However, what matters in M1 (and subsequent models) is the range of diffusion values used, not specific values. The model runs for M1 span a wide range of values and situations, from cases dominated by in-situ accumulation, with very little transport, to transport dominated cases where all the sediment produced is

transported into the basin. Estimates of diffusion coefficients from natural systems range from $560\text{km}^2\text{ky}^{-1}$ in the Mississippi delta (Kenyon and Turcotte, 1985) to $0.007\text{km}^2\text{My}^{-1}$ in pelagic strata on the flanks of the Galapagos spreading center (Mitchell, 1996), suggesting that the range used in M1 (Table 3.2) is reasonable, albeit poorly constrained by data from shallow-marine carbonate systems. By spanning the range of transport rates likely to be operating in different shallow-marine settings, and making simple general observations about resulting geometries, it is possible to avoid drawing conclusions that depend on specific diffusion coefficient values that would be difficult to defend given the lack of available data, and hopefully gain some insight into the likely controls on different types of platform systems.

4.3.1 Quantitative Measurement of Platform Geometry

The purpose of running many models (e.g. >1000 to generate Figure 4.2) with different production and transport values was to determine what types of platform architecture result from the various combinations of sediment transport and sediment production. The quantitative scheme used to illustrate the results of M1 is outlined in section 3.3.2, with maximum topographic gradient (max S), and the maximum change in topographic gradient (max ΔS) selected for automated platform classification (type 3 – refer to section 3.3). For each model run (in M1) after 5 My of elapsed model time max S and max ΔS were measured from the output synthetic strata and recorded to summarize the depositional geometry. Max S should be higher for steep-margined FTPs, and low for lower-gradient ramp systems. Max ΔS should be small for homoclinal ramps, which show little change in gradient down dip, and high for FTPs, which show a pronounced change of gradient between the platform top and the platform margin and slope. Running the forward model systematically with a range of sediment production and diffusion coefficient values allows creation of matrices (outlined in section 3.3.3) of max S and max ΔS values showing how they vary with changes in sediment production and down-dip sediment transport rates (Fig. 4.2).

4.4 Euphotic, grain-dominated systems (M1 results)

M1 incorporates two hundred model cases, with total sediment production rates ranging from 17.5 to 466.375 mMy⁻¹ (Table 3.2). The models were run with a euphotic depth-production curve (Fig. 4.2D), and higher rates for sand or coarser production than mud production (Table 3.2). Sand or coarser diffusion coefficients in M1 range from 0 to 5 Km²ky⁻¹, and mud transport rates are an order of magnitude greater than sand transport rates (Table 3.2). The value of max S and max ΔS was calculated at the end of each model run and plotted in colour-coded matrices along with selected depositional profiles (Fig. 4.2A & 4.2B).

The M1 results illustrate that at relatively low production rates transport tends to move all sediment basinward preventing any aggradation in shallow water (Fig. 4.2C profiles II & III). Conversely, higher rates of production combined with low transport rates lead to development of extensive FTPs with progressive steepening of the marine portion of the profile as production rate increases (Fig. 4.2C profiles, IV and VII). For higher rates of sediment production, increasing the transport rate tends to decrease max ΔS by enhancing development of platform margin slope clinoforms and increasing progradation rates (Fig. 4.2C profiles VII, VIII and IX). Over the range of production and transport rates modelled in this example, max S ranges from 0.01° to 12°.

All the examples with non-zero transport rates for the coarsest grain type (sand or coarser grade), have maximum gradients less than 1° and hence classify as ramps as defined by Burchette & Wright (1992). These low gradients are also partly a consequence of the initial bathymetry (refer to section 5.2 for a discussion on initial bathymetry), but the initial bathymetry used here is realistic based on values calculated from the bathymetry of the modern Arabian Gulf (Purser 1973; Walkden and Williams, 1998; Lokier and Steuber, 2008). Grain repartition in these high-transport examples (Fig 4.2C profiles II and III) illustrate a fining outward trend of grains towards the basin (Fig. 4.3A), with the coarsest fraction (sand grade or coarser) dominantly located in the shallows. High angled, steep-margin development in this coarse

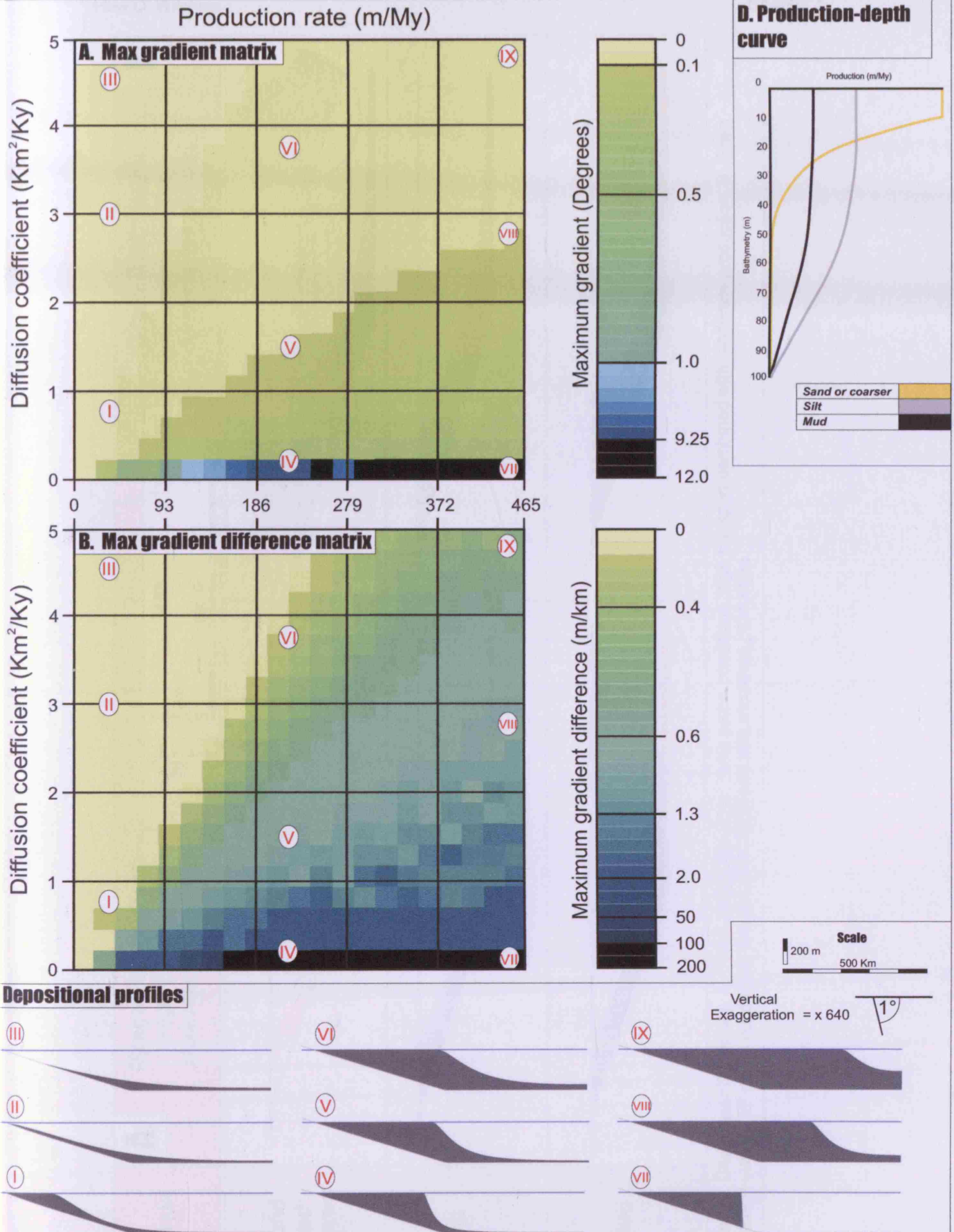


Figure 4.2. M1 results. A: Matrix representing topographic gradient (max S) obtained along the modeled depositional profiles. B: Matrix representing the maximum change in topographic gradient (max $S\Delta$), or break of slope, occurring between two adjacent cells on the depositional profiles. For matrices A and B the production rate is a total combined value of sand or coarser, silt and mud production rate values. Diffusion coefficients correspond to sand or coarser grade, refer to table 3.2 for silt and mud values. C: Cross-sectional view of modeled depositional geometries, profile locations correspond with matrices A and B. D: Euphotic, grain dominated production-depth curve.

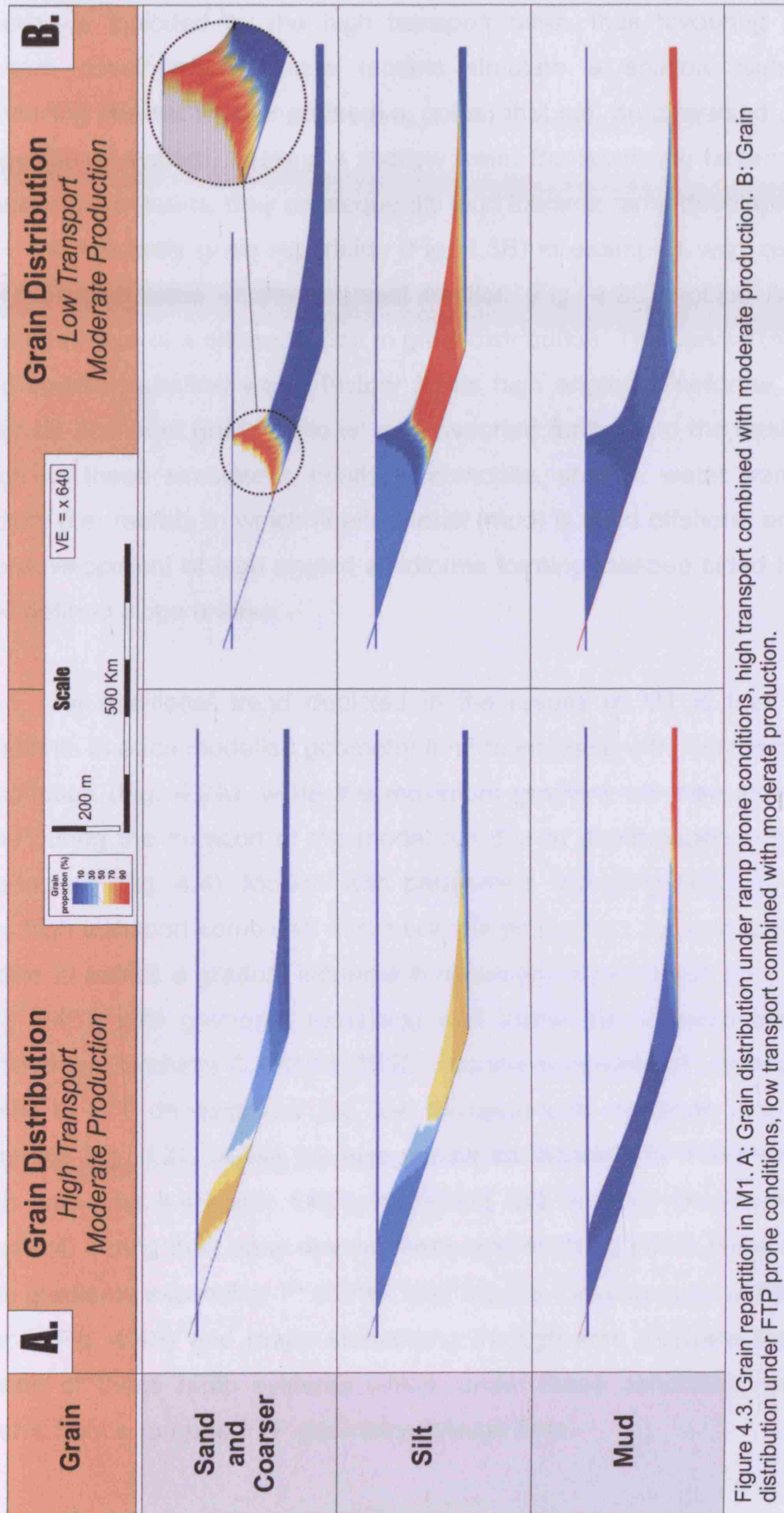


Figure 4.3. Grain repartition in M1. A: Grain distribution under ramp prone conditions, high transport combined with moderate production. B: Grain distribution under FTP prone conditions, low transport combined with moderate production.

fraction is inhibited by the high transport rates, thus favouring low angle system development. These models simulate a shallow water factory producing coarse, mobile grains (i.e. ooids) that can be dispersed across the depositional system. Lacking a shallow water framebuilding factory, and with transportable grains, they consequently tend towards ramp development.

Conversely grain repartition (Fig. 4.3B) in examples with zero to very low transport rates of the coarsest fraction (Fig. 4.2C profiles IV and VII) illustrate more of a differentiation in grain distribution. The coarse (sand grade and coarser) shallow water factory forms high angled clinoforms, while the finer silt and mud grade material is transported further into the basin. Models such as these simulate a relatively immobile, shallow water framebuilding factory (i.e. reefal), in which finer material (mud) is shed offshore, and favours the development of high angled clinoforms forming steeped sided FTP's with well defined slope breaks.

An additional trend depicted in the results of M1 is that maximum gradients in each modelled geometry tend to increase with increasing rates of production (Fig. 4.2A), while the maximum gradient will also increase over time during the duration of the model run due to depth-dependent sediment production (Fig. 4.4). Models with parameters favouring ramp development (i.e. high transport combined with moderate production, for example Fig. 4.2C profile II) exhibit a gradual increase in maximum gradient with time (Fig. 4.4A and 4.4C), with gradients remaining well below the 1° ramp threshold as defined by Burchette & Wright (1992). Models consisting of parameters more suited to FTP development (i.e. low transport with moderate production, for example Fig. 4.2C profile IV) also exhibit an increase in maximum gradient with time (Fig 4.4B and 4.4D), beginning with a ramp like character ($<1^\circ$ gradient) during their early development, and evolving into a steep sided FTP with gradients exceeding 7° at their later stages. Development of this break of slope (Fig. 4.4E) and major steepening through time illustrate the transient nature of these ramp systems which, under these conditions, will tend to evolve from a ramp to FTP geometry through time.

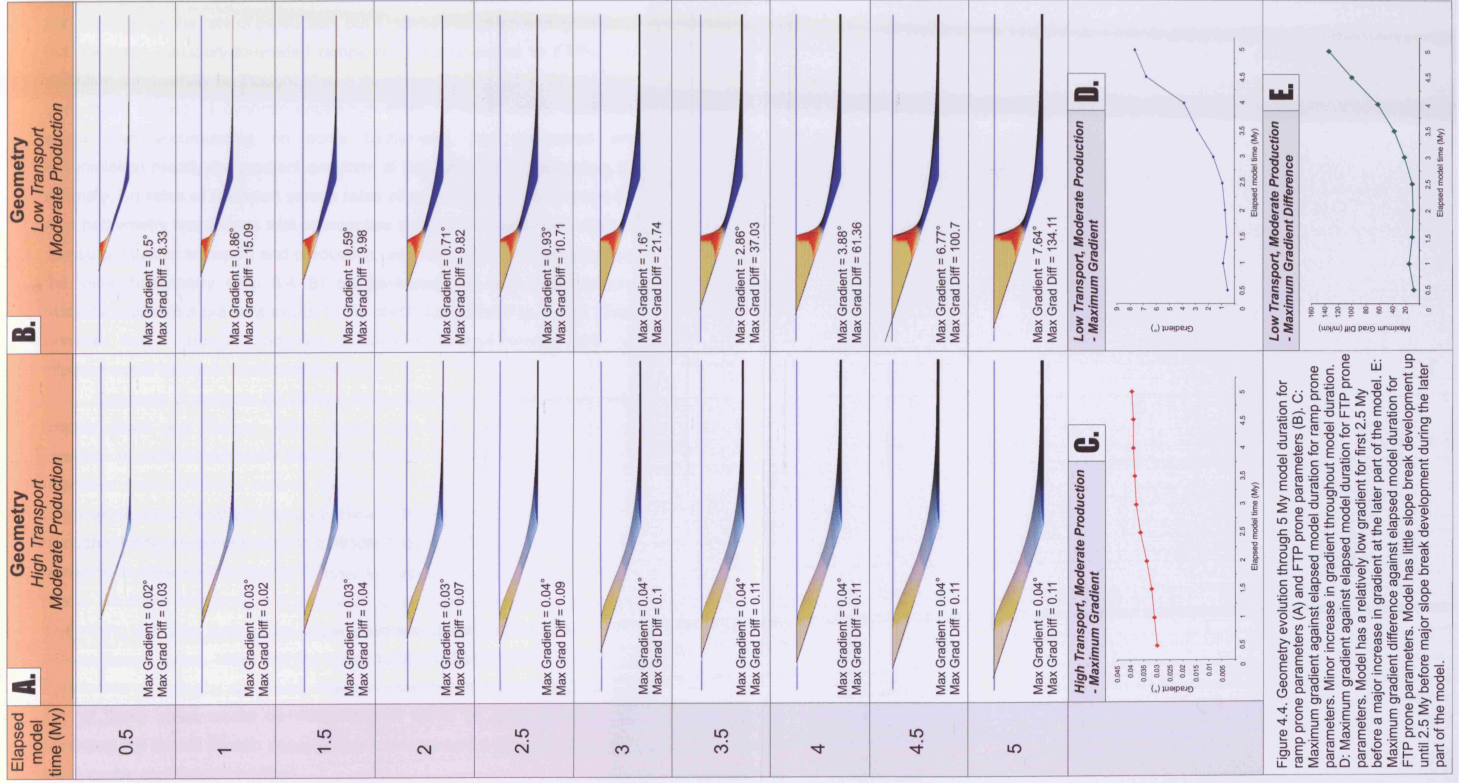


Figure 4.4. Geometry evolution through 5 My model duration for ramp prone parameters (A) and FTP prone parameters (B). C: Maximum gradient against elapsed model duration for ramp prone parameters. Minor increase in gradient throughout model duration. D: Maximum gradient against elapsed model duration for FTP prone parameters. Model has a relatively low gradient for first 2.5 My before a major increase in gradient at the later part of the model. E: Maximum gradient difference against elapsed model duration for FTP prone parameters. Model has little slope break development up until 2.5 My before major slope break development during the later part of the model.

It is likely that in the absence of sufficient sediment transport and assuming a healthy carbonate factory, carbonate platforms will always tend to evolve like this, from a ramp to FTP geometry because of in-situ accumulation. How long this evolution takes will depend on the rate of transport versus the rate of production, but it may be that given enough time all but the most transport-dominated ramps will tend to evolve to FTPs. This evolution can usefully be thought of as a development from an initial condition bathymetry towards a dynamic equilibrium state. In other words, carbonate strata start accumulating on some bathymetry, and production and accumulation modify the gradient and form of the bathymetry, depending, for example, on rates of transport versus rates of production. At some point the new bathymetry has a form that approaches a dynamic equilibrium state for particular rates of transport and production, and may differ considerably from the initial bathymetry (Fig. 4.4 B) or, particularly in high transport rate systems, maintain a gradient similar to the starting gradient (Fig. 4.4 A). Note, however, that if rates of production or transport change through time, the situation could be much more complicated.

Concepts of dynamic equilibrium have been applied in siliciclastic shelf models (Swift and Thorne, 1991; Thorne and Swift, 1991) and a similar evolution of platform geometry towards a dynamic equilibrium state has been described from carbonate outcrop studies. For example, the Lower Triassic ramp sequence of Northern Hungary (Hips, 1998) evolved from a homoclinal through distally steepened ramp to a Middle Triassic FTP, and a ramp to FTP transition is preserved in Upper Triassic to Upper Jurassic Adriatic platform strata, Southern Montenegro (Cadjenovic et al., 2008). Other examples of steepening with time include the Upper Devonian Grosmont Formation of the Alberta Basin (Cutler, 1983) and the Lower to Middle Cambrian of the Virginia Appalachians (Barnaby and Read, 1990). A snapshot of platform geometry in any of these cases could be misleading in terms of understanding and predicting the overall system because it would represent a transition form, not the dynamic equilibrium condition.

Based on the analysis and results of M1 alone (Fig 4.2, 4.3, and 4.4), ramps develop when transport rates are high enough to prevent development

of a steep platform margin. In other words, the essential process determining distinction between platform geometries typically referred to as ramps and FTPs is the effective action of sediment transport of sufficient magnitude and over sufficient distance to move sediment away from its area of production and prevent buildup of steep platform margin gradients. High sediment transport rates relative to production rate remove carbonate sediment that would otherwise accumulate in shallow water and prevent progradation and steepening by redistributing sediment with a more even thickness across the underlying topography (e.g. Fig. 4.2C II). When transport of the coarser grain types is ineffective, due to low energy, low gradients, or the resistance of sediment grains due to being entrained, autochthonous accumulation will tend to quickly build steep-margined flat-topped platforms. Maximum stable gradient will depend on sediment composition, degree of sediment binding, but also on rates and types of transport processes operating.

The results also suggest that in the absence of sufficiently high transport rates, either due to low-energy conditions or presence of transport-resistant sediment, platform margins will steepen as they prograde, and the 1° gradient cut-off will be exceeded. If we define a ramp as a carbonate system with a regional gradient of less than 1° (e.g. Ahr, 1973; Burchette and Wright, 1992), then these examples would not be classified as ramps, and presumably therefore they would be flat-topped steep-margined platforms. However, looking at the model results in more detail suggests that this distinction between ramp and FTP may be an over simplification, because many of the low-gradient examples in Figure 4.2 do show a distinct slope break (e.g. Fig. 4.2C I), often in a proximal position on the depositional profile, and often prograding into deeper water and increasing in magnitude with time. The existence and development of these slope breaks is addressed in the following section.

4.4.1 Development of a slope break

Considering the development of slope breaks in M1, generally max ΔS increases with increasing rates of sediment production and decreases with increasing rates of sediment transport (Fig. 4.2B). Modelled profiles for all but

the highest-transport lowest-productivity cases show proximal aggradation to sea-level forming a break of slope and a seaward-dipping subtidal ramp (e.g. Fig. 4.2C profile I). This suggests that most carbonate platforms, even very low-gradient systems, will commonly develop a break of slope (Mitchum and Uliana, 1985; Chatellier, 1988; Handford and Baria, 2007). This will tend to become more pronounced with time even in low-gradient systems (Fig. 4.4A), making it problematic to use a break of slope as a feature to distinguish ramps and FTPs. A break of slope feature will only be absent in ramp systems when rates of sediment transport are very high relative to rates of production (e.g. Fig. 4.2C profiles II and III), or when relative sea-level rise outpaces accumulation, for example during high-frequency high-amplitude glacio-eustatic transgression (see section 5.5).

In outcrop examples, identification of a slope break where a flat surface passes seaward into a surface dipping at $>0.5^\circ$ should be straight forward, assuming time lines can be traced over a distance of 1km or more, because a depositional surface with a gradient of $>0.5^\circ$ traced over 1 km will show a water depth difference of >8.7 m and this should translate into observable facies changes even accounting for substitutable facies in shallow water (Rankey, 2004). Seaward dipping surfaces with a dip of less than 0.5° may be more problematic, requiring tracing of assumed time lines over longer distances to identify, and raising the issue that most correlations of this type are model-driven interpretation, not fact-based observation.

In the subsurface, using seismic data, examining a typical seismic line with a vertical resolution of ~ 30 m over a distance of 10 km should allow resolution of any surface dipping at 0.2° or more (Sheriff, 1991). Burchette and Wright (1992) noted that some ramps possess subtle changes of slope, recognizable on some regional seismic lines, which they termed the ramp slope crest. Examples include the Nisku Formation, Frasnian, Western Canadian Basin (Burchette and Wright, 1992), and the Upper Jurassic to Lower Cretaceous carbonate platform of the Neuquen Basin, Argentina (Mitchum and Uliana, 1985). These are large scale examples (>10 kms) comparable with the modelling presented here, and should not be confused with smaller meter-scale features visible in outcrop e.g. the bedforms of the Lower Permian, San-Andreas of West Texas occur over length scales of a

few kilometres (Kerans et al., 1994), while the clinoforms in the Upper Jurassic Smackover carbonates of Louisiana are developed over a distance of <10 km (Handford and Baria, 2007).

4.5 Testing Production Profiles (M2) - *What kind of production profile creates a ramp?*

Much previous work has ascribed formation of ramp geometries to operation of a particular relationship between water-depth and production rate, where carbonate production is more widespread across the system occurring in both shallow (inner to middle ramp) and deeper (middle to outer) waters (e.g. Wright and Faulkner, 1990; Pomar, 2001). These conceptual models were derived from simple cartoon production profiles and the proposed relationships have never been validated with a quantitative test. A second model suite (M2) tests the influence of the production profile on platform geometry by running Dionisos models with fifteen different types of carbonate production curve (Fig. 4.5), each of which has been published by various authors over the last twenty years. Curves vary from dominantly euphotic based production (Fig. 4.5A – 4.5I), such as Bosscher and Schlager's (1992) curve (Fig. 4.5B) in which production is focused to shallower waters, to the more oligophotic type curves (Fig 4.5K – 4.5O) in which production occurs in deeper water and is more widespread across the system, for instance Pomar's (2001) curve (Fig. 4.5O).

Each of the fifteen production curves in M2 was modelled with the same initial model conditions as M1 (refer to Table 3.2). However, a range of production and transport rates was not modelled in M2, but two sets of values were derived from the results of M1 depicted in Figure 4.2. The first parameter combination represents high transport combined with moderate production, conditions shown most likely to produce a ramp geometry in Figure 4.2. The second parameter combination represents low transport rates combined with moderate production rates that tend to generate a FTP. Maximum gradient and break of slope position (based on maximum gradient difference) was calculated at the conclusion of each model run and are plotted for reference (Fig. 4.5P and 4.5Q).

Production Profile	High Diffusion, Moderate Production Example	Low Diffusion, Moderate Production Example
A	 Max Gradient = 0.027 Max Grad Diff = 0.01	 Max Gradient = 3.157 Max Grad Diff = 55.156
B	 Max Gradient = 0.022 Max Grad Diff = 0.011	 Max Gradient = 3.157 Max Grad Diff = 55.16
C	 Max Gradient = 0.028 Max Grad Diff = 0.011	 Max Gradient = 3.766 Max Grad Diff = 41.946
D	 Max Gradient = 0.025 Max Grad Diff = 0.011	 Max Gradient = 3.181 Max Grad Diff = 55.58
E	 Max Gradient = 0.023 Max Grad Diff = 0.011	 Max Gradient = 3.177 Max Grad Diff = 55.415
F	 Max Gradient = 0.029 Max Grad Diff = 0.023	 Max Gradient = 7.353 Max Grad Diff = 125.046
G	 Max Gradient = 0.028 Max Grad Diff = 0.023	 Max Gradient = 6.150 Max Grad Diff = 107.759
H	 Max Gradient = 0.027 Max Grad Diff = 0.021	 Max Gradient = 6.150 Max Grad Diff = 107.759
I	 Max Gradient = 0.027 Max Grad Diff = 0.01	 Max Gradient = 5.077 Max Grad Diff = 77.15
J	 Max Gradient = 0.027 Max Grad Diff = 0.014	 Max Gradient = 6.238 Max Grad Diff = 144.781
K	 Max Gradient = 0.031 Max Grad Diff = 0.024	 Max Gradient = 6.894 Max Grad Diff = 156.494
L	 Max Gradient = 0.027 Max Grad Diff = 0.012	 Max Gradient = 6.238 Max Grad Diff = 144.78
M	 Max Gradient = 0.031 Max Grad Diff = 0.027	 Max Gradient = 10.545 Max Grad Diff = 186.151
N	 Max Gradient = 0.038 Max Grad Diff = 0.048	 Max Gradient = 10.873 Max Grad Diff = 182.072
O	 Max Gradient = 0.039 Max Grad Diff = 0.037	 Max Gradient = 6.689 Max Grad Diff = 170.734

Production Profile

- A - Williams et al. (2009)
- B - Bosscher and Schlager (1992)
- C - Warrlich et al. (2008)
- D - Warrlich et al. (2002)
- E - Boylan (2002)
- F - Bowman and Vail (1999)
- G - Aurell et al. (1995)
- H - Bosence and Waltham (1990)
- J - Bice (1988)
- J - Goldhammer et al. (1991)
- K - Read (1998)
- L - Demicco (1998)
- M - Pomar et al. (2004)
- N - Pomar et al. (2004)
- O - Pomar (2001)

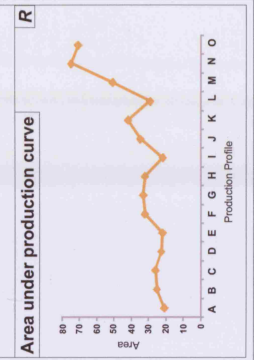
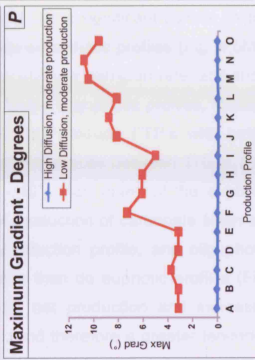


Figure 4.5. A-O: M2 depositional profiles for 15 different published production curves. Each curve is modeled under ramp prone conditions; *high diffusion, moderate production*, and FTP prone conditions; *low diffusion, moderate production*. P: Plot of maximum gradient for each of the 15 production curves, under both ramp and FTP prone conditions. Q: Same as P but a plot of maximum gradient difference. R: Plot for the area under each of the 15 production curves

Results from these model runs (Fig. 4.5) demonstrate that the shape and dominant production loci of the profile is not a significant control on the large-scale platform geometry. Even strongly oligophotic profiles (Fig. 4.5M – 4.5O) evolve towards FTPs when combined with low transport rate, and show platform margin gradients as high as 10° . These oligophotic profiles, formally thought to favour ramp development, actually produce FTP's with better developed slope breaks (maximum gradient differences between 170 to 192) and higher maximum slope gradients ($9 - 10^\circ$) than many of the euphotic profiles. This occurs because magnitude of production of carbonate sediment is determined by the area beneath the production profile, and oligophotic profiles have a greater area under the curve than do euphotic profiles (Fig. 4.5R). Increased area results in a greater net production and increased progradation rate for a given transport rate, and therefore a greater tendency to create a steep-margin FTP. The increased net production and progradation results in a steepening of the platform margin (Fig 4.6A), while the inflection point or break of slope on the FTP will become more distal along the modelled profile as the area beneath the production curve increases (Fig 4.6B). Some support for rapid oligophotic progradation comes from outcrop examples interpreted to represent strong upper-slope progradation driven by a microbial carbonate (Della Porta et al., 2003 & 2004; Kenter et al. 2005).

Model runs with high transport rate combined with moderate production rates tend to create ramp profiles with less variation of maximum gradient than the lower transport rate examples (Fig. 4.5). The maximum gradient displayed for the fifteen models under these higher transport rate conditions is actually very close to 0.03° , the gradient of the initial topographic surface in each example. This shows an important correlation between initial bathymetric conditions and the overall ramp gradient, demonstrating that ramp systems likely tend to drape the underlying topography (refer to section 5.2 for discussion on bathymetric controls).

In summary, model runs with high transport rate relative to production rate tend to create ramp profiles, regardless of which production profile is used (Fig. 4.5), suggesting that sediment transport rate, in this model determined by diffusion coefficient and topographic gradient, is a more dominant control on platform geometry than the type of production profile. The

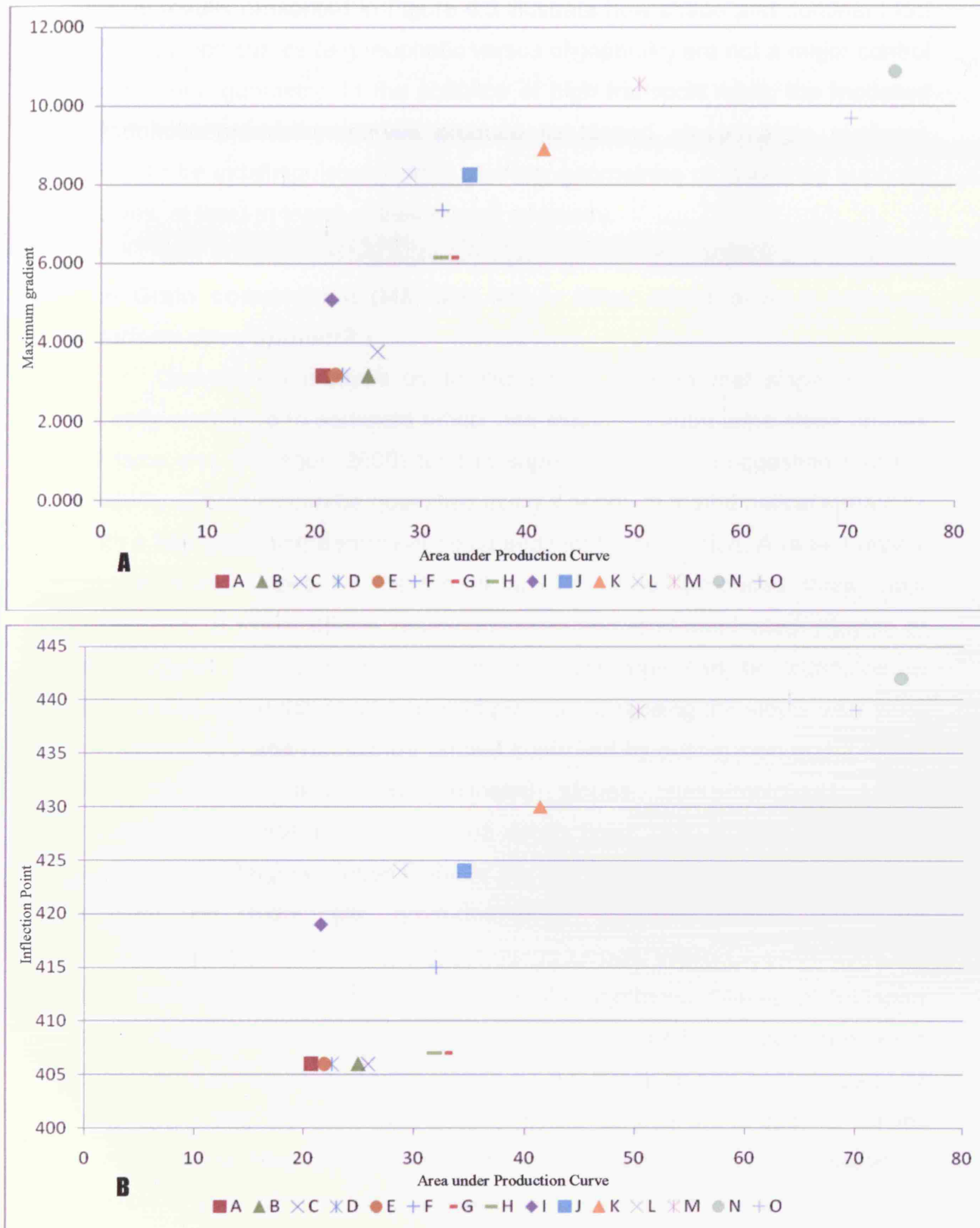


Figure 4.6. Letters correspond to production profiles of Fig. 4.5. A – Plot of maximum gradient against area under production curve for the 15 curves of Figure 4.5. Gradient values are for examples modelled under FTP prone conditions (low diffusion, moderate production). B – Same as A, but illustrating inflection point, or break of slope location for each of the 15 modelled examples.

model results presented in Figure 4.5 illustrate how shape and dominant loci of production curves (e.g. euphotic versus oligophotic) are not a major control on platform geometry. In the absence of high transport rates, the modelled oligophotic production curves produce flat-topped steep-margin platforms likely to be indistinguishable from platform geometries produced by euphotic curves, at least in terms of their overall geometry.

4.6 Grain composition (M3, M4, M5) – *What affect does it have on platform development?*

Quantitative analysis by Kenter (1990) showed that slope angle is directly correlated to sediment fabric, and studies of submarine slope profiles (Adams and Schlager, 2000) tend to support this view, suggesting that the majority of profiles can be quantified using a series of mathematical equations with a key governing parameter being sediment composition. A recent review of carbonate slopes by Playton et al., (in press) proposed three main categories of slope; debris, grain-dominated and mud-dominated. Playton et al., suggest that differences in slope morphology can be attributed to differences in the dominant transport process controlling the slope, with mud-dominated systems (principally ramps) controlled by suspension and turbidity flow processes, and grain-dominated slopes (steep-margined FTPs) controlled by concentrated grain and debris flows derived from the shallow platform top. Margin collapse features are also important components typically present on high-angle grain-dominated platform slopes and are characteristically absent on mud-dominated slopes. While Dionisos does not explicitly represent all these processes, the combined diffusional transport and critical-angle slope failure processes included in all the model runs are a reasonable generalized representation for the temporal and spatial scales of large-scale platform evolution. It is possible to use the model to further investigate the Playton et al. (in press) classification scheme, and therefore the role of grain composition on platform geometry development.

The models of M1 and M2 both use the same grain size component (Table 3.2), with a composition dominated (57%) by the coarsest sand or coarser grade grain type, therefore simulating a relatively coarse, grainy system. Three additional model runs (M3, M4 and M5) have been conducted

in which the composition of the system has been altered to simulate a finer grained, muddier system (Table 3.2). The models become gradually finer; M3 is composed of 8% sand or coarser, 15% silt and 77% mud, M4 does not have the coarsest fraction and is composed of 17% silt and 83% mud, while M5 is a mud dominated system composed of 100% mud. The same production curves used in M1 for each of the respective grain types are used, as is the same range of diffusion coefficients. The 3 models were run following the APE method (section 3.3) with both maximum gradient and development of slope break (maximum gradient difference) calculated for each and plotted as matrices (Fig 4.7, 4.8, 4.9). As the only change in parameter from M1 is the grain composition percentage, the matrices (Fig 4.7, 4.8, 4.9) of M3, M4 and M5 can be directly compared with those representing a grainer system (Fig 4.2).

The finer, muddier composition of M3, M4 and M5 results in the generation of lower gradient geometries (Fig. 4.7A, 4.8A, 4.9A) when compared with the grainer models of M1 of similar diffusion coefficient (Fig. 4.2A). The grainy geometries of M1 develop platform margin slopes exceeding 10° (Fig. 4.2A); in contrast the maximum gradient observed in the muddy model runs is a gradient of just 1.12° in M3, with gradients not exceeding 1° in either M4 or M5. The maximum gradient of the modelled geometries also decreases as the systems become gradually muddier from M3 through to M5. The development of a slope break (Fig. 4.7B, 4.8B, 4.9B) is also limited as a result of increased slope failure at the platform margin due to a lower angle of repose of the dominant grain type (mud). This lack of slope break development also increases as the systems become muddier from M3 through to M5, with the mud dominated system of M5 portraying very low maximum gradient difference values (<40 m/Km), thus indicating little to no slope break development in the geometries of M5 (Fig. 4.9B). These muddy systems therefore tend towards the generation of ramp geometries. This occurs, even at the lower end of the range of transport rates modelled, with this tendency towards ramp generation a combined consequence of a greater proportion of easily transported sediment being produced, thus leaving little material to accumulate in situ, and the lack of a coarse, framebuilding grain type inhibiting the development of a steep platform margin and slope break.

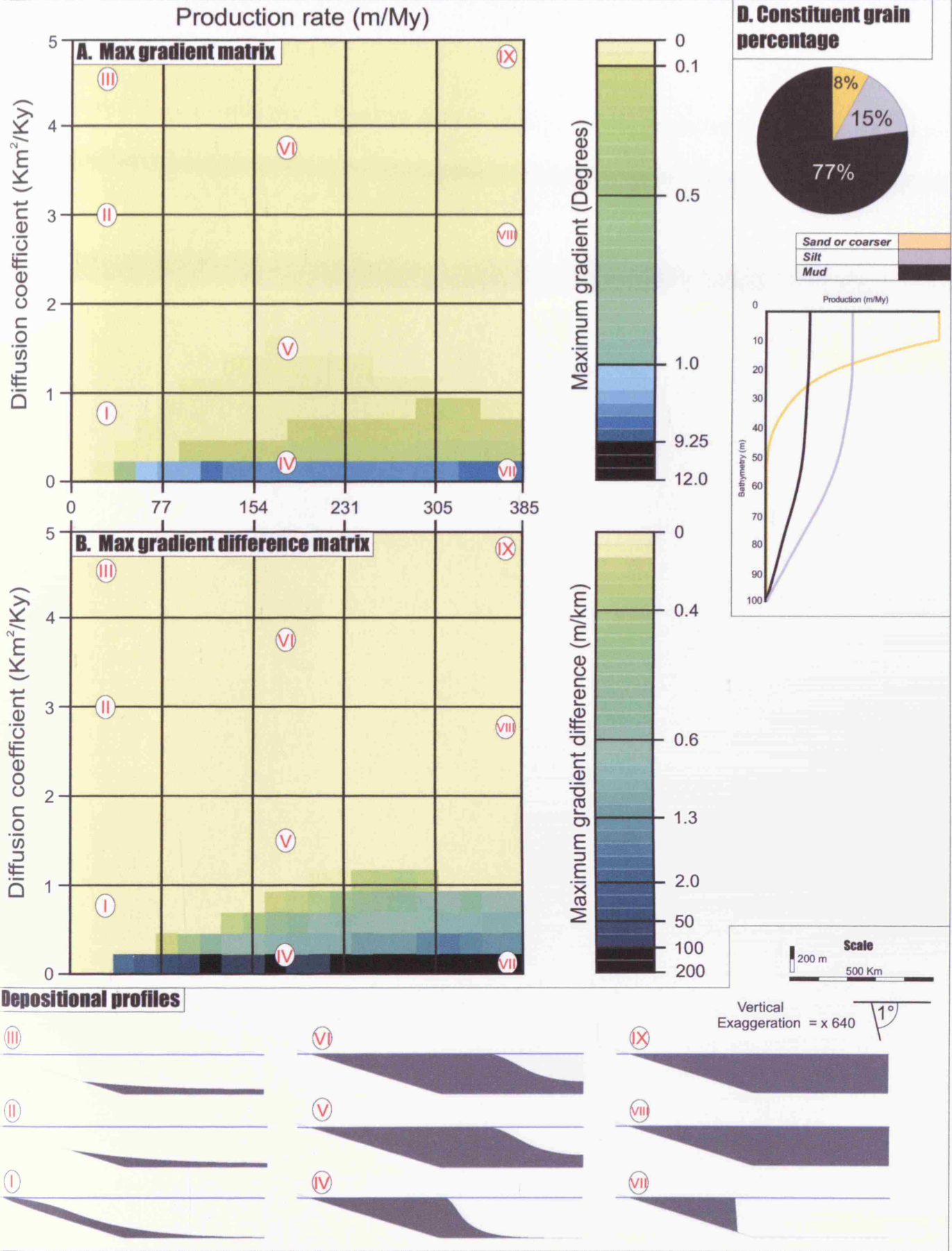
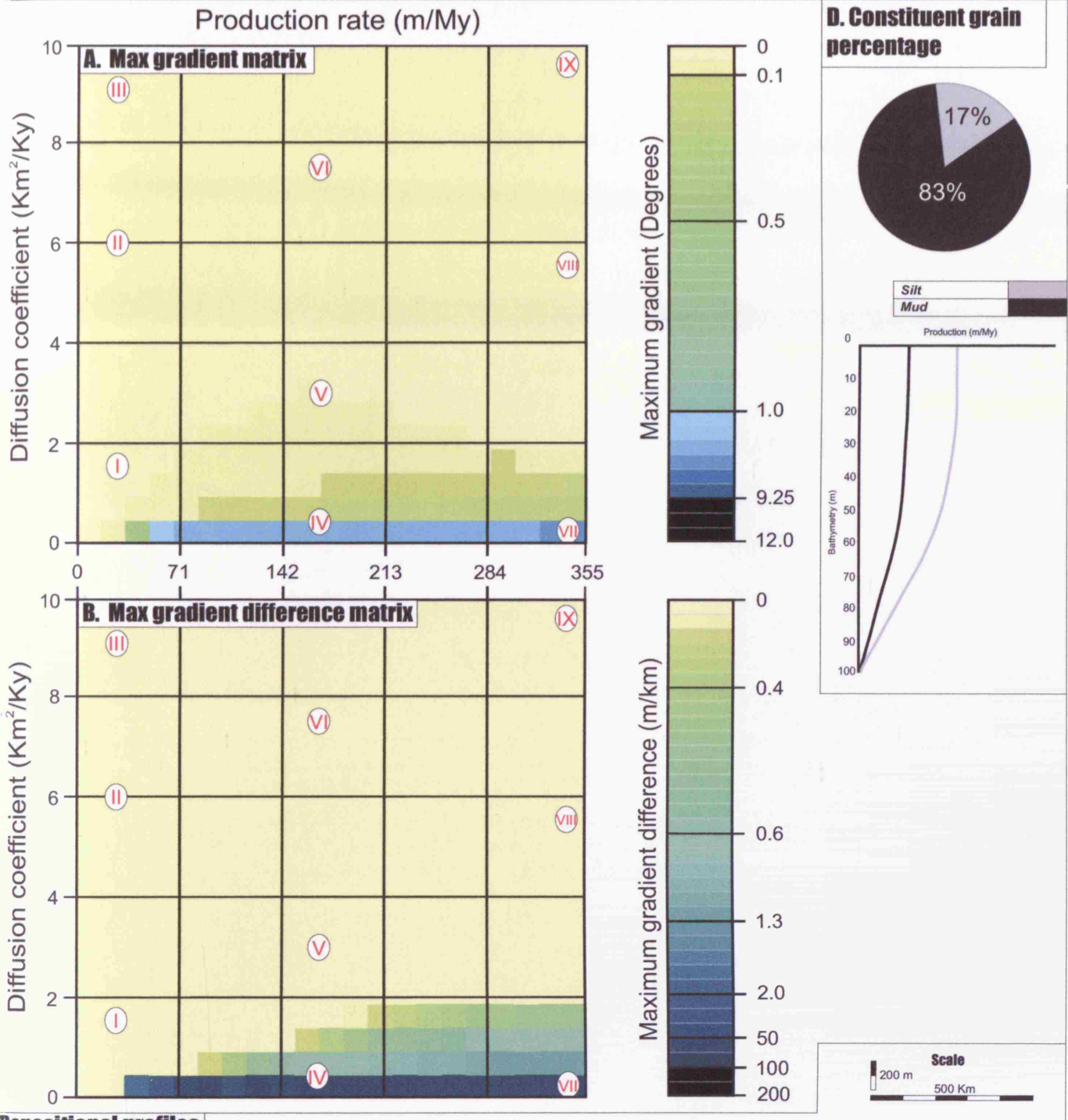


Figure 4.7. M3 results. A: Matrix representing topographic gradient ($\max S$) obtained along the modeled depositional profiles. B: Matrix representing the maximum change in topographic gradient ($\max S\Delta$), or break of slope, occurring between two adjacent cells on the depositional profiles. For matrices A and B the production rate is a total combined value of sand or coarser, silt and mud production rate values. Diffusion coefficients correspond to sand or coarser grade, refer to table 3.2 for silt and mud values. C: Cross-sectional view of modeled depositional geometries, profile locations correspond with matrices A and B. D: Grain composition percentages of M3.



Depositional profiles

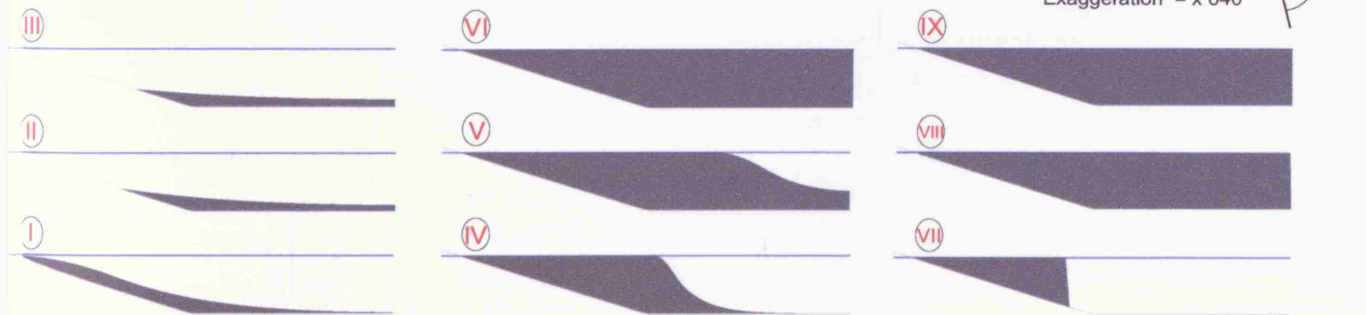


Figure 4.8. M4 results. A: Matrix representing topographic gradient ($\max S$) obtained along the modeled depositional profiles. B: Matrix representing the maximum change in topographic gradient ($\max S\Delta$), or break of slope, occurring between two adjacent cells on the depositional profiles. For matrices A and B the production rate is a total combined value of silt and mud production rate values. Diffusion coefficients correspond to silt grade, refer to table 3.2 for mud values. C: Cross-sectional view of modeled depositional geometries, profile locations correspond with matrices A and B. D: Grain composition percentages of M4.

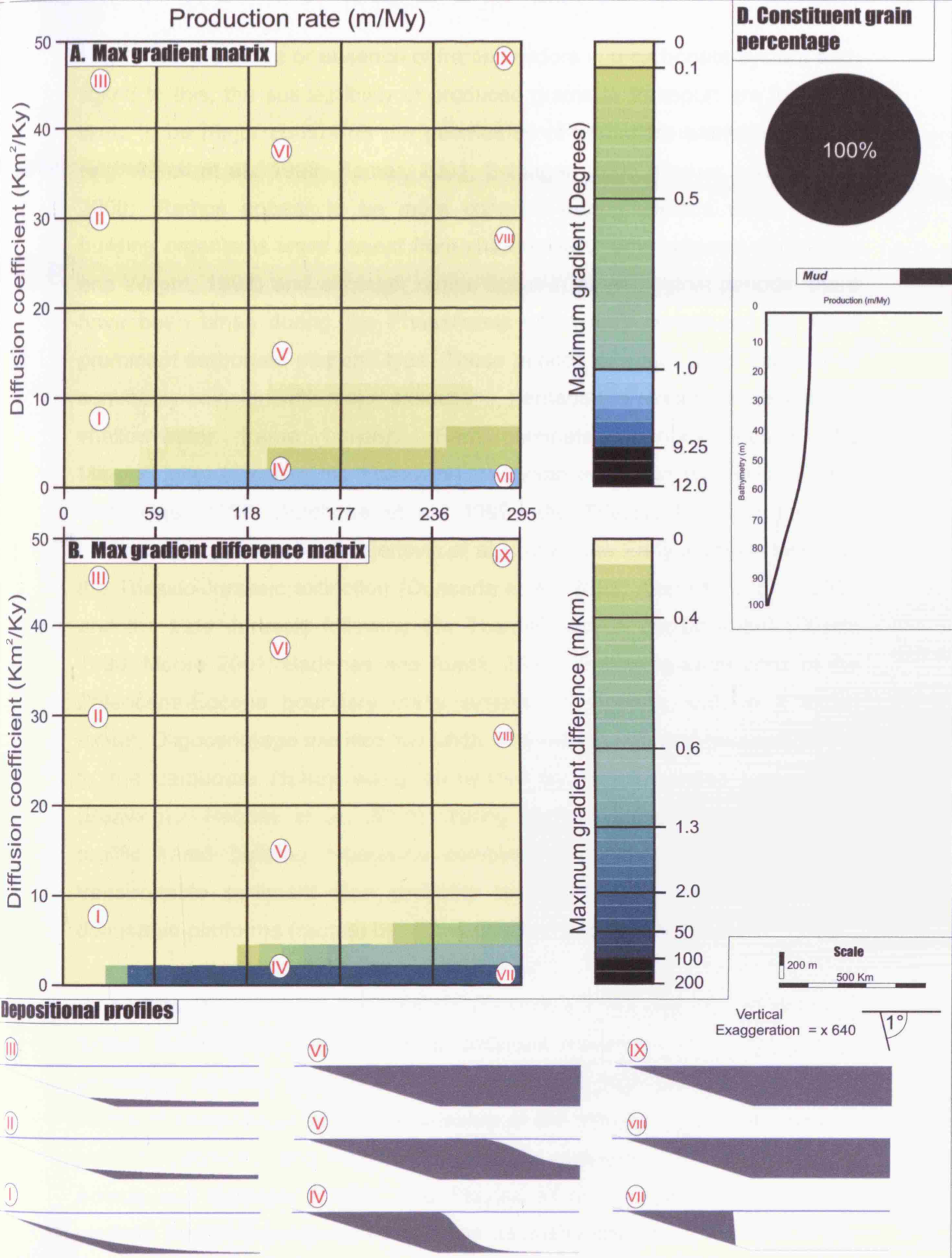


Figure 4.9. M5 results. A: Matrix representing topographic gradient (max S) obtained along the modeled depositional profiles. B: Matrix representing the maximum change in topographic gradient (max $S\Delta$), or break of slope, occurring between two adjacent cells on the depositional profiles. For matrices A and B the production rate represents mud production, and diffusion coefficients correspond to mud transport rates. C: Cross-sectional view of modeled depositional geometries, profile locations correspond with matrices A and B. D: Grain composition percentages of M5.

The presence or absence of frame builders in a carbonate system and, linked to this, the susceptibility of produced grains to transport are therefore likely to be major control on the geometries of carbonate platform systems (e.g. Aurell et al., 1998; Pomar, 2001; Schlager, 2005; Pomar and Hallock, 2008). Ramps appear to be more common during periods when frame-building organisms were absent from shallow-water environments (Burchette and Wright, 1992) and although ramps occur in all geological periods, there have been times during the Phanerozoic when they constituted the most prominent carbonate platform type. These periods of major ramp occurrence commonly coincide with major extinctions, perhaps the reason for absence of shallow-water frame builders. Ramp-dominated periods include the Mississippian following the Frasnian-Famennian extinction (Chatellier, 1988; Gutteridge, 1989; Burchette et al., 1990), the Triassic following the P-T extinction (Aigner, 1984; Cadjenovic et al., 2008), the Early Jurassic following the Triassic-Jurassic extinction (Quesada et al., 2005; Azeredo et al., 2009), and the Late Jurassic following the Toarcian ocean anoxic event (Droste 1990; Moore 2001; Badenas and Aurell, 2010). Following extinctions at the Paleocene-Eocene boundary many systems of Eocene and, to a lesser extent, Oligocene age are also low-angle transport dominated geometries due to the carbonate factory being dominated by larger benthic foraminifera (Beavington-Penney et al., 2005). During each of these periods a lack of prolific frame building organisms combined with dominance of a highly transportable sediment type probably resulted in low-gradient transport-dominated platforms (ramps) being the principal depositional system.

The results of M3, M4, and M5 (Figures 4.7, 4.8 and 4.9 respectively) further illustrate the importance of sediment dispersion and transport on controlling platform geometry. The results also highlight the effect that sediment composition and transportability of the dominant grain type has on platform geometry, and support the previous conclusions of Kenter (1990), Adams and Schlager (2000), and Playton et al. (in press). Variations in platform margin development and slope geometry caused by changes in the grain composition are likely to be an important additional control on the continuum of platform geometries (discussed in the subsequent section). At a

fixed diffusion coefficient and production rate, the models of M3, M4 and M5 illustrate how dominant grain size is an additional controlling variable, with grain-dominated and mud-dominated systems representing the end members of a grain size continuum.

4.7 Discussion – *Classifying a continuum of carbonate platform types*

The model results presented throughout Chapter 4 suggest that the essential process determining the distinction between a ramp and a FTP is the effective action of sediment transport over a length scale of sufficient magnitude to move sediment away from its area of production and prevent buildup of steep platform margin gradients. The efficiency of sediment transport is the main control on creating and maintaining a ramp profile (M1), while the type of production profile appears to exert little influence on platform development (M2). When transport of the coarser grain types is ineffective, due to low-energy or the resistance of sediment grains due to being entrained, autochthonous accumulation will tend to quickly build flat-topped platforms. It is also important to note that gradients will tend to increase with time if production gradually outpaces transport (Fig 4.4), and given sufficient time many low-gradient ramp systems will likely evolve into steep-margined FTPs.

The profiles generated in the modelling cases presented in Chapter 4 represent a gradational series of geometries created by essentially the same interacting processes of production and transport (Fig. 4.10). This process continuum results in a continuum of platform geometries that extend beyond the two end-members of a transport dominated ramp (Fig. 4.10, Geometry I, comparable to Trucial Coast ramp) versus the low transport FTP (Fig. 4.10, Geometry IV, comparable to Bahamian FTP) with in situ light-dependent production. Intermediate geometries which are not comparable with these end member geometries therefore likely exist (i.e. Geometries II and III, Fig 4.10). These geometries lack the high angle slope break of an FTP (i.e. Geometry IV, Fig 4.10), however the presence of a less prominent slope break (discussed in section 4.4.1) and the development of relatively flat tops that almost aggrade to sea level (i.e. Geometry III, Fig 4.10, akin to the Iberian basin ramp) suggest it would be inaccurate to describe them as homoclinal

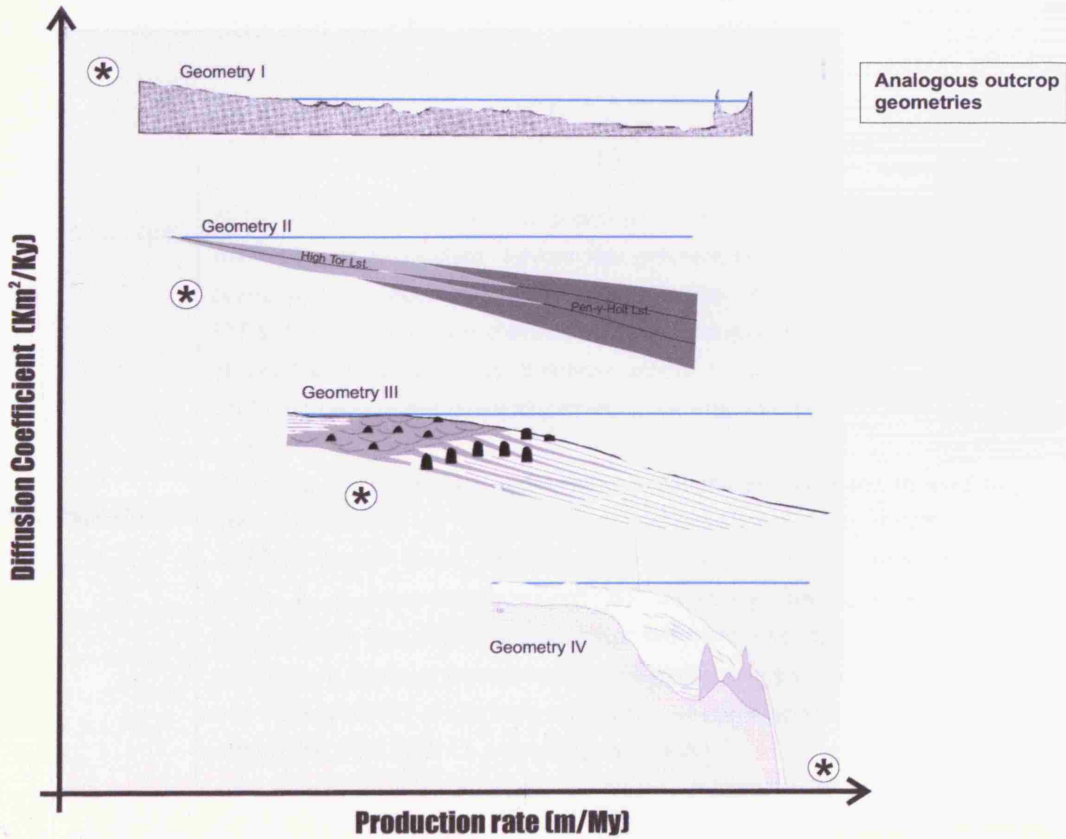
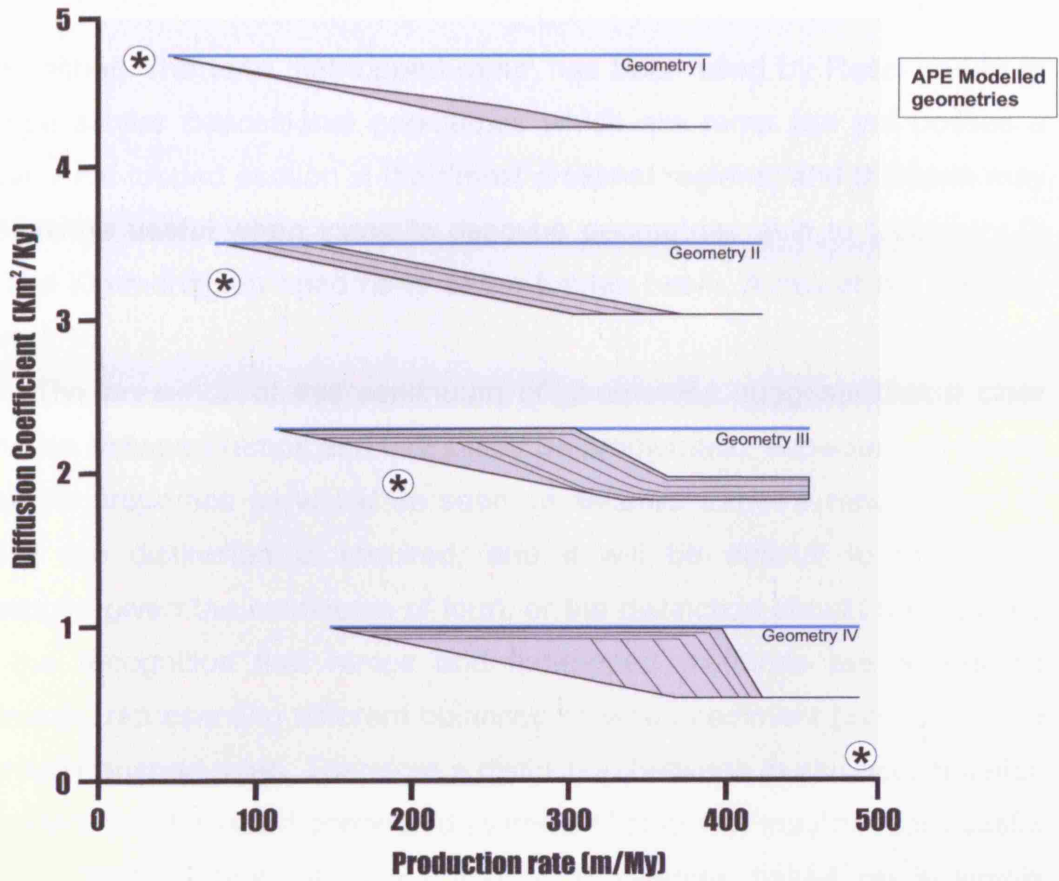


Figure 4.10. Upper parameter space illustrates representative gradational geometries created by interaction of production and transport using the APE forward modelling method. Lower parameter space illustrates outcrop geometries which are analogous to the modelled geometries. Geometry I: The low angle homoclinal ramp is comparable with the Trucial Coast ramp (image modified from Purser, 1973). Geometry II: Low angle ramp geometry akin to the Arundian aged South Wales ramp (image modified from Simpson, 1987). Geometry III: An intermediate geometry (flat-topped ramp) akin to the Kimmeridgian aged ramp of the Iberian basin (image modified from Aurell et al., 1998). Geometry IV: FTP geometry comparable with the Great Bahama Bank (image modified from Schlager, 2005).

ramps either. The term ‘flat-topped ramp’ has been used by Read (1998) to describe similar depositional geometries which are ramp like yet possess a relatively flat-topped section in their most proximal regions, and this term may therefore be useful when trying to describe geometries akin to Geometry III (i.e. The Kimmeridgian aged ramp of the Iberian basin, Aurell et al., 1998) of Figure 4.10.

The presence of this continuum of geometries suggests that a clear distinction between ramps and FTPs may be problematic, especially on purely geometric properties as would be seen on seismic. Either a new method of making the distinction is required, and it will be difficult to make this meaningful given the continuum of form, or the distinction should be replaced with the recognition that ramps and flat-topped platforms are a process continuum, representing different balances between sediment production and sediment transport rates. Therefore a distinction between in-situ accumulation dominated, and transport dominated systems (Table 4.1) may be more useful than the differentiation of ramps from FTP systems based on a simple gradient cut-off (Burchette and Wright, 1992).

<i>Transport dominated</i>	Platforms where sediment is prone to be transported away from the main sites of production. Favour low gradient ramp systems, normally preventing the accumulation and aggradation of sediment to produce FTP's. Such systems are characterized by a paucity of organisms capable of producing large in-situ buildups unless in deeper waters, and by sediment types more easily dispersed by normal marine processes.
<i>In-situ accumulation dominated</i>	Platforms where enough sediment is produced and retained to lead to the development of flat-topped depositional profile separated from adjacent deeper water areas by a prominent break of slope beyond which is a zone characterized by instability and gravity flows. Deposystems are likely to also shed sediment into deeper water but sufficient is retained to produce a topographically elevated margin. In-situ accumulations are prominent feature of these systems such as reef complexes, reef mounds and microbial mounds.

Table 4.1. New definitions for classification of large-scale carbonate deposystems.

However, a critical consideration is that, although the modeling produces a continuum of geometries, distinctly different processes may operate in particular real cases. For example, on an FTP with high-angle slope-margins sediment instability could result in erosion and collapse of the margin and deposition down dip of slides, slumps, debris flows, and turbidity currents, with the possible development of a significant bypass surface on the slope (Schlager, 2005). Low-gradient ramp systems should lack such collapse, erosion and bypass features but excluding pelagic and hemipelagic deposits, subtidal ramp strata should be dominated by material transported by any of a variety of down-ramp processes. For example, storm-triggered density currents are commonly invoked as the means for redistributing sediments from shallow waters to offshore settings (Aurell et al., 1998; Pedley, 1998). Recognition of this transport may also be complicated in some systems where mud-grade offshore strata are the product of diagenetic remobilization of benthic skeletal aragonite (Wheeley et al., 2008). This is then complicated further by other controlling factors such as initial bathymetry, differential subsidence and relative sea-level oscillations that are also likely to be important controls in any particular example.

The process continuum described in this chapter can usefully be thought of as platform types that exist in a parameter space of controlling variables. A parameter space is a space in which all possible combinations of controlling variables for a system are represented. The space may have many dimensions, depending on how many controlling variables or parameters it is considered to have, but each possible parameter combination corresponds to one unique point in the parameter space. A parameter space defining the models presented in this chapter would consist of two axes; sediment transport rate and sediment production rate (Fig. 4.10). End-members on these axes would be a transport-dominated ramp (Fig. 4.10, Geometry I) and an in-situ dominated FTP (Fig. 4.10, Geometry IV), with a continuum of geometries between (e.g. Fig. 4.10, Geometries II and III). However, as mentioned previously this continuum of geometries are likely to be complicated by other controlling factors such as initial bathymetry, differential subsidence and relative sea-level oscillations. Therefore an accurate

parameter space for overall platform development would not be constructed from only the two controls discussed in this chapter (sediment production and transport), but would likely incorporate these additional controlling factors in a multidimensional parameter space. The concept and construction of a *Multidimensional Parameter Space for carbonate platform development*, referred to from here on as 'MPS' will be addressed in the subsequent chapter. The controls factors such as relative sea-level oscillations exert on platform development will be investigated and representative parameter spaces constructed. These additional parameter spaces can be combined with the parameter space for sediment transport and production presented here to produce a MPS.

Chapter 5: UNDERSTANDING CARBONATE PLATFORM TYPES: THE ROLE OF BATHYMETRIC, TECTONIC AND SEA-LEVEL VARIATIONS IN PLATFORM DEVELOPMENT

Chapter 5 presents forward modelling results investigating how bathymetric variations, tectonic regimes and sea-level oscillations control carbonate platform geometry. The previous chapter presented results identifying optimal sediment production and transport regimes for ramp and for FTP formation. The same approach continues in this chapter with analysis of additional controls that may also affect the type of carbonate platform generated. The chapter presents Dionisos models illustrating the influence changes in bathymetric conditions, such as faulting and differential subsidence, can exert on platform morphology. Dionisos models are also presented demonstrating the optimal tectonic conditions for carbonate ramp generation along with seismic and outcrop examples. Finally, sea-level control on platform geometry is examined, with the influence exerted on platform morphology by greenhouse versus icehouse global conditions investigated using the APE method. The chapter concludes with the construction of a multidimensional parameter space for carbonate platform development (MPS) incorporating the results of chapters 4 and 5.

5.1 Introduction

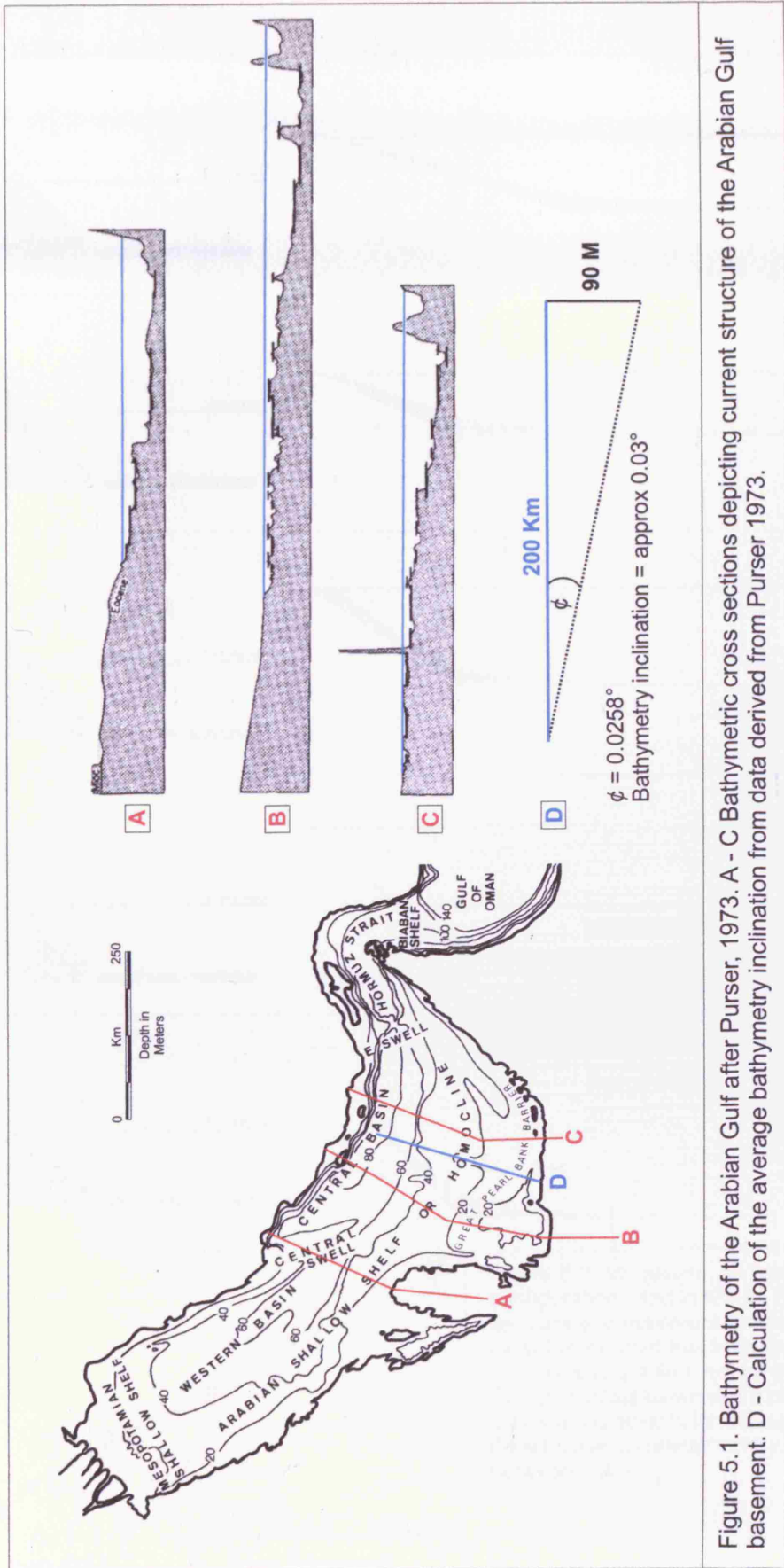
The aim of the five model sets (M1-5) used in chapter 4 was to identify the optimal sediment transport and production rates for the creation of ramp and FTP systems, and the continuum of geometries between. In M1-M5 the bathymetry, tectonic regime and sea-level history parameters were kept constant (see table 3.2), so that influence of variations in sediment transport and production on platform geometry could be assessed. However variations in these parameters may also exert a control on platform development. Therefore parameters fixed in model sets M1 to M5 in chapter 4 are varied in this chapter in model sets 6 to 12 (M6 - M12) and the influence variations in initial bathymetry, tectonic regime and sea-level oscillations exert on platform geometry are analysed.

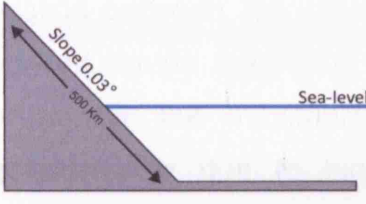
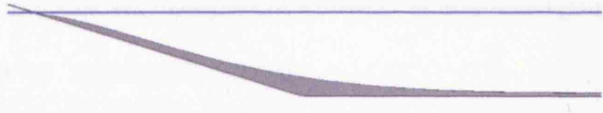
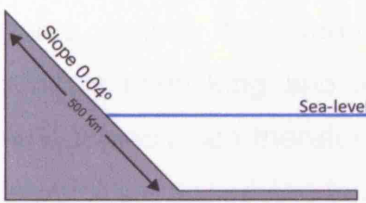
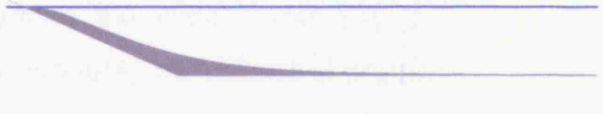
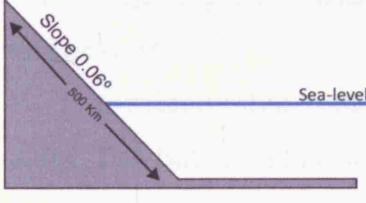
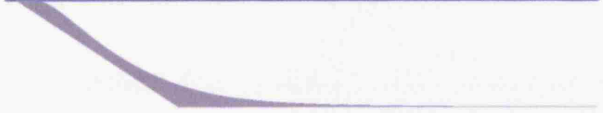
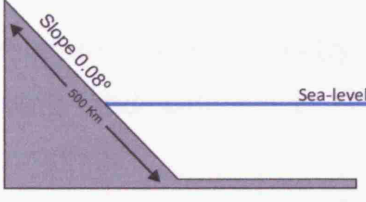

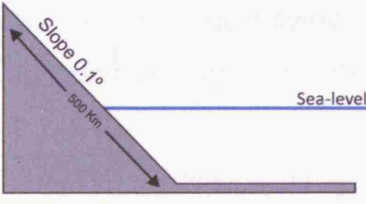
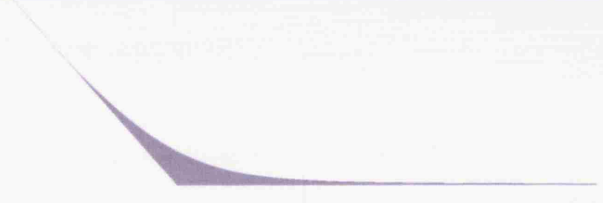
Model Set 6 (M6) investigates the relationship between platform geometry and the initial basement bathymetry, while model sets 7-12 (M7-12) analyse how changes to this bathymetry, for example faulting or differential subsidence, affect platform development. Results from each of these models are then used to suggest the optimal bathymetric and tectonic conditions for carbonate ramp development. The final section of the chapter uses the APE modelling method to analyse how variations in sea-level can effect platform development.

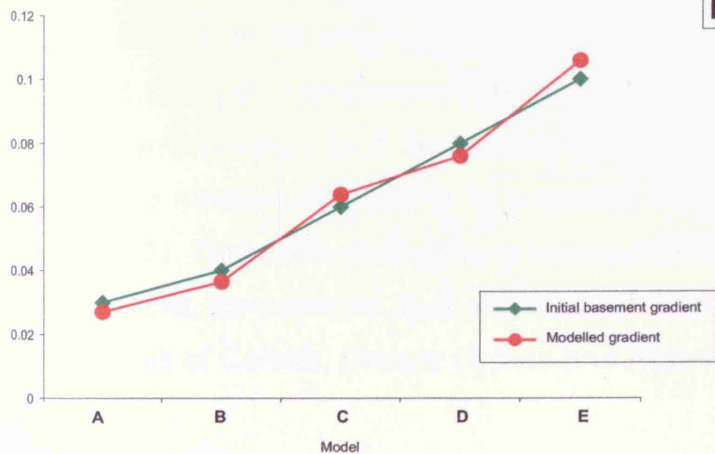
5.2 Investigating the role of bathymetry on platform development

A constant bathymetry (Fig. 3.4A) was used in each of the previous five model sets (M1-5), with an initial basement bathymetry derived from the basement structure of the Arabian Gulf (Fig. 5.1) and Purser (1973). The average Arabian Gulf basement bathymetric gradient has been calculated as 0.03° (Fig. 5.1D). The initial basement bathymetry used for M1-M5 is consistent with this, with a 0.03° slope over 250 Km slope giving 125 metres of bathymetric relief passing into a flat bottomed basin at 125 meters of water depth. In each of the ramp geometries seen in the results of M1 (Fig. 4.4A), and particularly the fifteen models of M2 (Fig.4.5) simulating platform development under ramp prone conditions (high diffusion rates, moderate production rates), the value of the maximum gradient observed is very close to the 0.03° gradient which was assigned to the initial basement bathymetry. Several of the modelled geometries (e.g. Fig. 4.5 K and M) have a maximum gradient of exactly 0.03° , while each of the remaining geometries deviate by less than 0.01° from this value. There appears to therefore be a close match between the gradient assigned to the initial basement bathymetry and the maximum gradient observed in the modelled ramp geometries.

To investigate this match an additional set of model runs was conducted; model set 6 (M6), in which the gradient of the initial basement bathymetry was varied. The parameters used in M6 were identical to those of M1 (refer to Table 3.2 for M1 and M6 parameters), while sediment production and transport were set at ramp prone rates (high diffusion, moderate production), and the initial basement bathymetry set at increasingly higher gradients. The results of M6 (Fig. 5.2) show a very clear correlation between



Basement slope gradient (°)	Basement Bathymetry	Modelled Geometry (VE = x640)	Maximum gradient of modelled geometry (°)
0.03			0.027 ≈ 0.03°
0.04			0.036411 ≈ 0.04°
0.06			0.063894 ≈ 0.06°
0.08			0.0759 ≈ 0.08°
0.1			0.106152 ≈ 0.1°



F. Figure 5.2. M6 results. A) Initial basement configuration used in M1-5. B-E) Modelled cross sections and maximum gradient values obtained from modelled geometries. Initial basement bathymetry increases in gradient from A through to E. F) Plot of initial basement bathymetry and modelled maximum gradients for examples A to E. Gradients depict close correlation with minimal variation between values.

the gradient assigned to the initial bathymetry and the maximum gradient of the modelled geometry (Fig. 5.2F). In each of the examples there is little deviation between the values of these two gradients (Fig. 5.2A-E), with the modelled ramps appearing to inherit the gradient of the initial bathymetry. Furthermore the maximum ramp gradients never exceed the basement gradient value due to high transport values precluding steepening and development of a break of slope. These results suggest that gradient of ramp systems reflect the geometry and gradient of underlying bathymetry, commonly mimicking and inheriting the initial basement gradient, and that ramp geometry can therefore reasonably be viewed in many cases simply as a drape of the underlying topography.

5.3 Investigating the influence of faulting and subsidence on platform development

The relationship outlined in section 5.2 is valid for the relatively low-gradient, flat bathymetric conditions used in M1 to M6. However, carbonate platforms also form on more complex bathymetries. Bathymetric features such as basement highs or shallow depressions and basins commonly influence carbonate stratal geometry. While syndepositional processes such as active faulting and differential subsidence may also affect developing platform geometries.

The models sets 7 to 12 (M7 to M12) investigate some of these processes by identifying the control faulting, subsidence, antecedent topography and syndepositional processes exert on platform development.

5.3.1 – Syndepositional Fault control on platform geometry (M7)

M7 models a developing carbonate platform with localized faulting (Fig. 5.3). All other parameters are the same as those in M1 (refer to table 3.2), with ramp-prone sediment transport and production rates, and a syndeposition fault developing at a fault slip rate of 0.02 m kyr^{-1} throughout the model run resulting in a vertical downthrow of 100 meters at 5 My (Fig. 5.3). This scale of faulting is representative of several Quaternary extensional faults, for example fault slip rates of 0.25 m kyr^{-1} have been calculated in the Gulf of Corinth, Greece (Cowie and Roberts, 2001), and a rate of 0.62 m kyr^{-1}

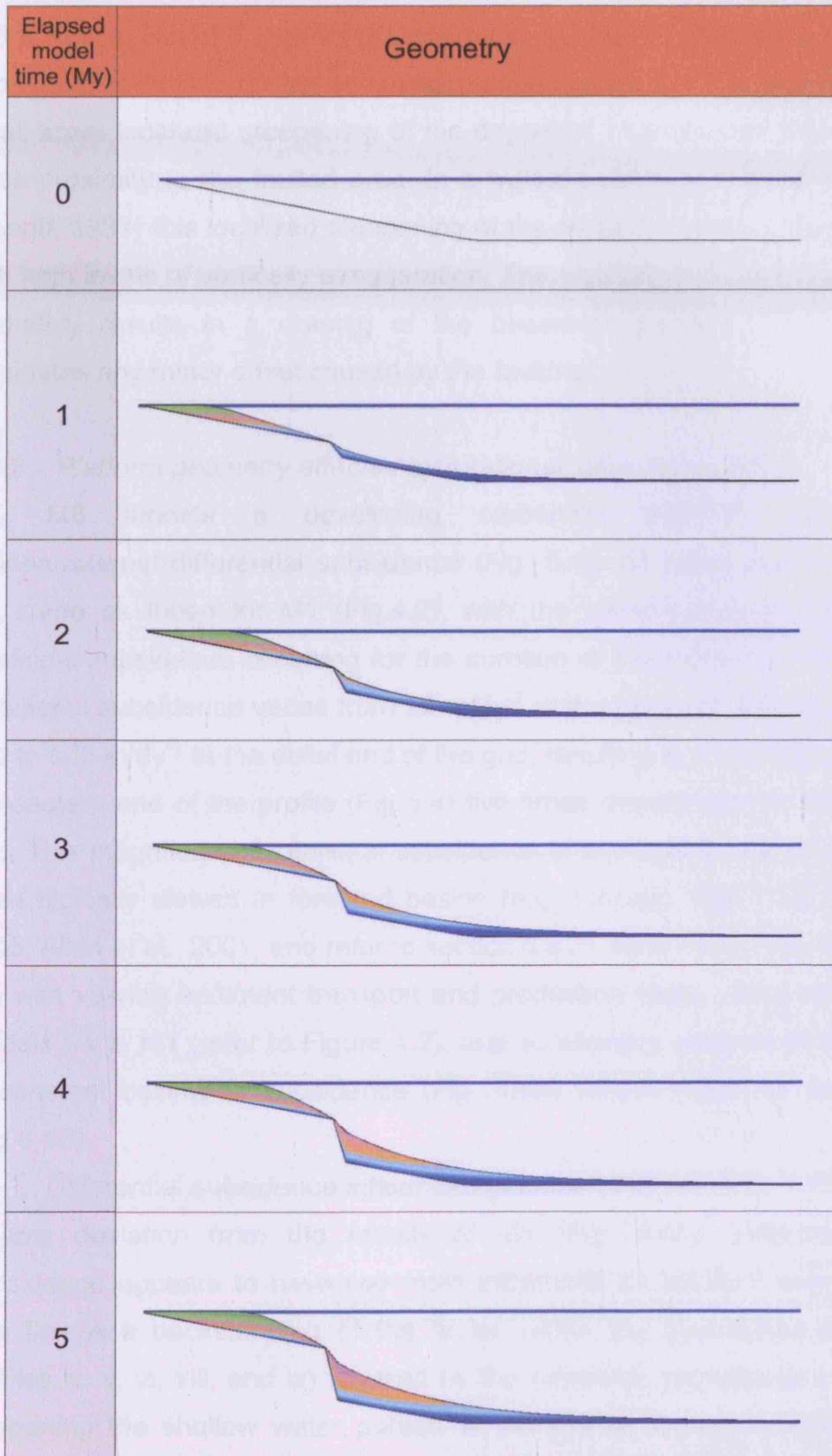


Figure 5.3. M7 results. Model depicting geometry development of carbonate system affected by faulting. Fault is occurring syndepositionally and has a downthrow at 5 My of 100m.



in the Rukwa Rift of Tanzania (Kjennerud et al., 2001). This scale of faulting appears to exert little control on overall platform geometry (Fig. 5.3). However, small scale localized steepening of the deposited material can be seen in close proximity to the faulted area. In a typical seismic line of 10 km length (Sheriff, 1991) this localized steepening of the strata is probably recognizable with high levels of vertically exaggeration. The high diffusion coefficient of M7 ultimately results in a draping of the basement bathymetry and quickly eliminates any minor offset caused by the faulting.

5.3.2 – Platform geometry affected by rotational subsidence (M8)

M8 models a developing carbonate platform affected by syndepositional differential subsidence (Fig. 5.4). All parameters were kept the same as those for M1 (Fig.4.2), with the exception of a high rate of rotational subsidence occurring for the duration of the model run (Table 3.2). Rotational subsidence varies from 20 mMy^{-1} at the proximal end of the model grid to 100 mMy^{-1} at the distal end of the grid, resulting in a subsidence rate at the eastern end of the profile (Fig 5.4) five times greater than at the western end. This magnitude of rotational subsidence is analogous to the subsidence rates typically viewed in foreland basins (e.g. Sinclair, 1997; Allen & Allen, 2005; Allen et al., 2001, and refer to section 5.4.2). Nine model iterations were run with varying sediment transport and production rates, using values from models i-ix in M1 (refer to Figure 4.2), and so allowing analysis of the impact of constant basinwide subsidence (Fig. 5.4A) versus rotational subsidence (Fig 5.4B).

Differential subsidence influenced geometries of M8 (Fig. 5.4B) show a notable deviation from the results of M1 (Fig. 5.4A). Laterally varying subsidence appears to have two main influences on platform development. The first is a backstepping of the facies within the geometries (Fig. 5.4B profiles iv, v, vi, viii, and ix), caused by the rotational subsidence continually deepening the shallow water portion of the profile, forcing retrogradational migration of the coarse, shallow water facies (also seen in Fig. 5.7B). Secondly the profiles (with the exception of profile vii) depict a more ramp like character than the original models (Fig. 5.4A), with a more uniform, gently dipping morphology and a less prominent slope break or ramp crest (i.e.



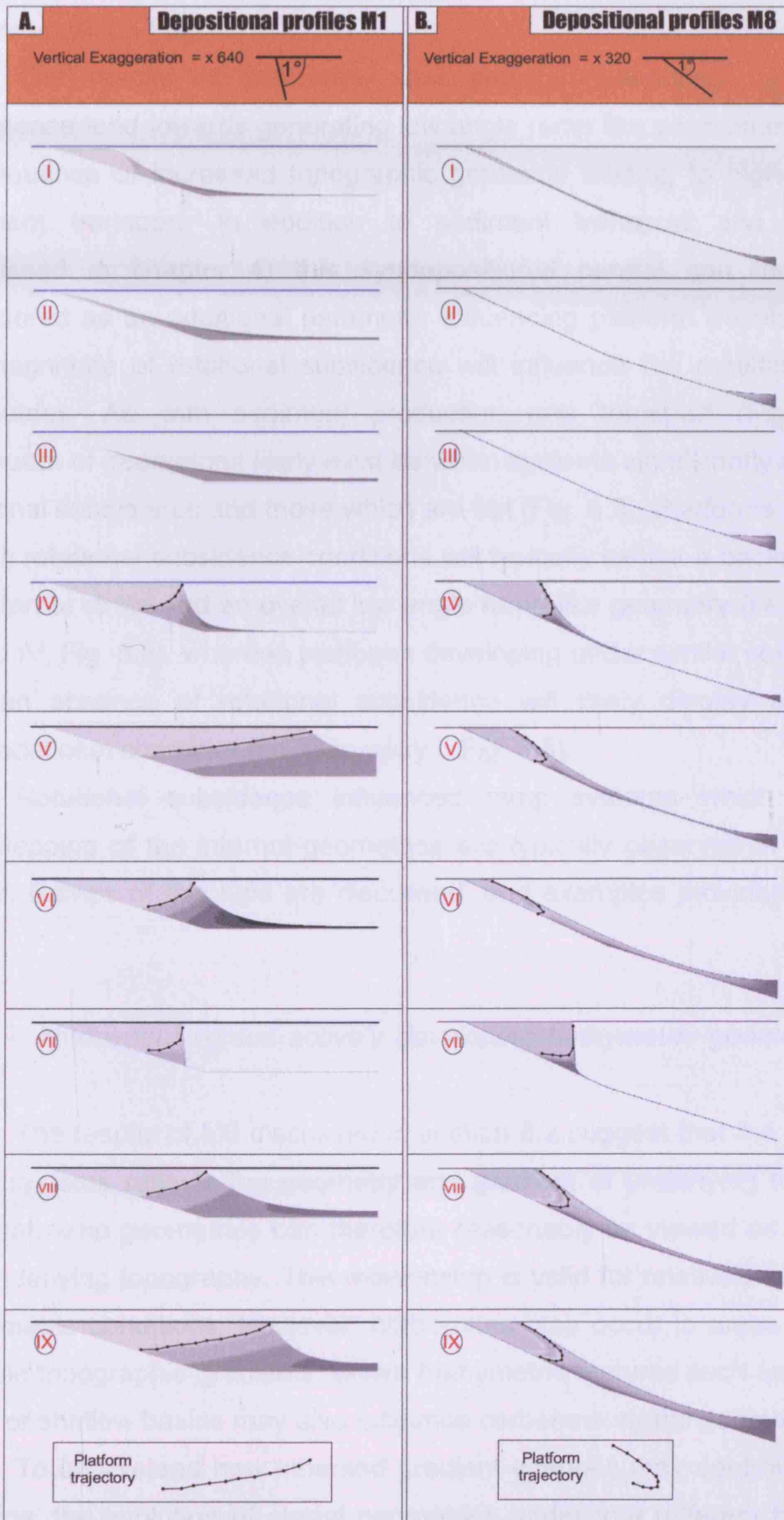


Figure 5.4. Comparison of depositional geometries under differing subsidence regimes. A) Original depositional profiles from M1 (Fig. 4.2) with basin wide subsidence of 20 mMy⁻¹. B) M8 depositional profiles depicting platform development with differential subsidence. Subsidence is 5 times the magnitude at eastern end of profile compared to western end. For production and transport values of profiles i - ix refer to Figure 4.2.

profiles vi, viii and ix).

The results of M8 imply that settings influenced by rotational subsidence tend towards generating low angle ramp like geometries. This is a consequence of increased topographic gradients leading to higher rates of sediment transport. In addition to sediment transport and production (discussed in chapter 4) this syndepositional control can therefore be considered as an additional parameter influencing platform development, as the magnitude of rotational subsidence will influence the resulting platform geometries. As with sediment production and transport (Fig. 4.10) a continuum of geometries likely exist between systems significantly affected by rotational subsidence and those which are not (Fig. 5.5). Platforms developing in high rotational subsidence conditions will typically exhibit a backstepping of the internal strata and an overall low angle ramp-like geometry (i.e. Geometry III and IV, Fig. 5.5), whereas platforms developing under similar conditions but with an absence of rotational subsidence will likely display a far more progradational character (i.e. Geometry I, Fig. 5.5).

Rotational subsidence influenced ramp systems which display a backstepping of the internal geometries are typically observed in fault block ramps. Ramps of this type are discussed, and examples provided in section 5.4.3.

5.3.3 – *Antecedent versus actively developing bathymetric geometries (M9-12)*

The results of M6 discussed in section 5.2 suggest that the gradient of ramp systems reflects the geometry and gradient of underlying topography, and that ramp geometries can therefore reasonably be viewed as a drape of the underlying topography. This relationship is valid for relatively low-gradient bathymetric conditions. However, carbonates also occur in areas with more variable topographic-gradients, where bathymetric features such as basement highs or shallow basins may also influence carbonate stratal geometry.

To understand how inherited gradient changes may control carbonate systems, the evolution of stratal geometries under four different bathymetric scenarios has been modelled in model sets 9, 10, 11, and 12 (M9 to 12) (Table 3.2). M9 and M10 (Fig. 5.6A and 5.6B) simulate carbonate deposition

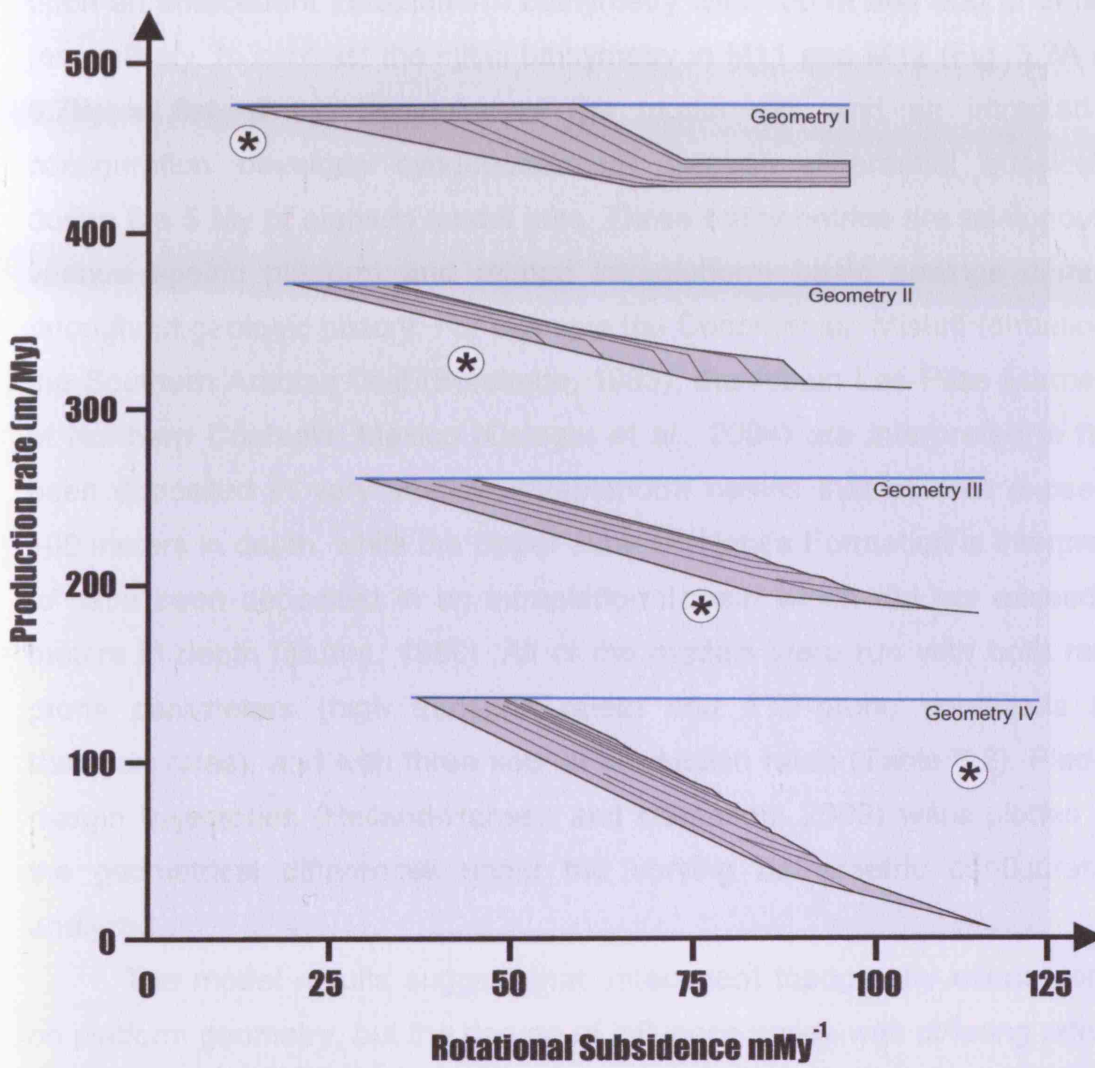


Figure 5.5. Representative gradational geometries created by interaction of sediment production rate and rotational subsidence. Subsidence values (mMy^{-1}) represent maximum rotational subsidence value at distal end of grid. Geometries I and II display a progradational character. As the magnitude of rotational subsidence increases (Geometry III and IV) geometries depict a retrogradational character as the strata begin to backstep, resulting in an increasingly low angle geometry. The low angle ramp geometries are a consequence of increased topographic gradients leading to higher rates of sediment transport.

upon an antecedent intraplatform bathymetry with 100 m and 500 m of relief respectively. In contrast the initial bathymetry in M11 and M12 (Fig. 5.7A and 5.7B) is flat at the beginning of the model run, and an intraplatform configuration develops syndepositionally through differential subsidence during the 5 My of elapsed model time. These bathymetries are analogous to various epeiric platform and related intraplatform basin settings common throughout geologic history. For example the Cenomanian Mishrif formation of the Southern Arabian Gulf (Burchette, 1993), the Albian Las Plias Formation of Northern Coahuila, Mexico (Osleger et al., 2004) are interpreted to have been deposited in very shallow intraplatform basins that seldom exceeded 100 meters in depth, while the Upper Jurassic Hanifa Formation is interpreted to have been deposited in an intraplatform basin which did not exceed 60 meters in depth (Murriss, 1980). All of the models were run with both ramp-prone parameters (high transport rates) and FTP-prone conditions (low transport rates), and with three sets of production rates (Table 3.2). Platform margin trajectories (Helland-Hansen and Hampson, 2009) were plotted and the geometrical differences under the varying bathymetric configurations analyzed.

The model results suggest that antecedent topography exerts control on platform geometry, but the degree of influence varies with differing rates of production and transport, and for different amounts of basinal relief. For example, under relatively low sediment production and sediment transport conditions, rates of progradation of an FTP margin decrease markedly across the 100 m relief intraplatform basin margin in Figure 5.6A but shows little change when transport and production rates are higher. Increasing the relief on the intraplatform basin margin (Fig. 5.6B) stalls FTP progradation in the low transport rate case, and creates a bypass slope with little or no accumulation, except in the higher production rate case. In all these low transport cases, FTP progradation is stalled at the intraplatform basin margin. This occurs because the euphotic production curve used in these models is unable to create sediment in deeper water, so accumulation only occurs in shallow water and progradation stalls at the basin margin.

All the examples modelled here are best considered as FTPs because they all have a clear break of slope where the flat platform top passes

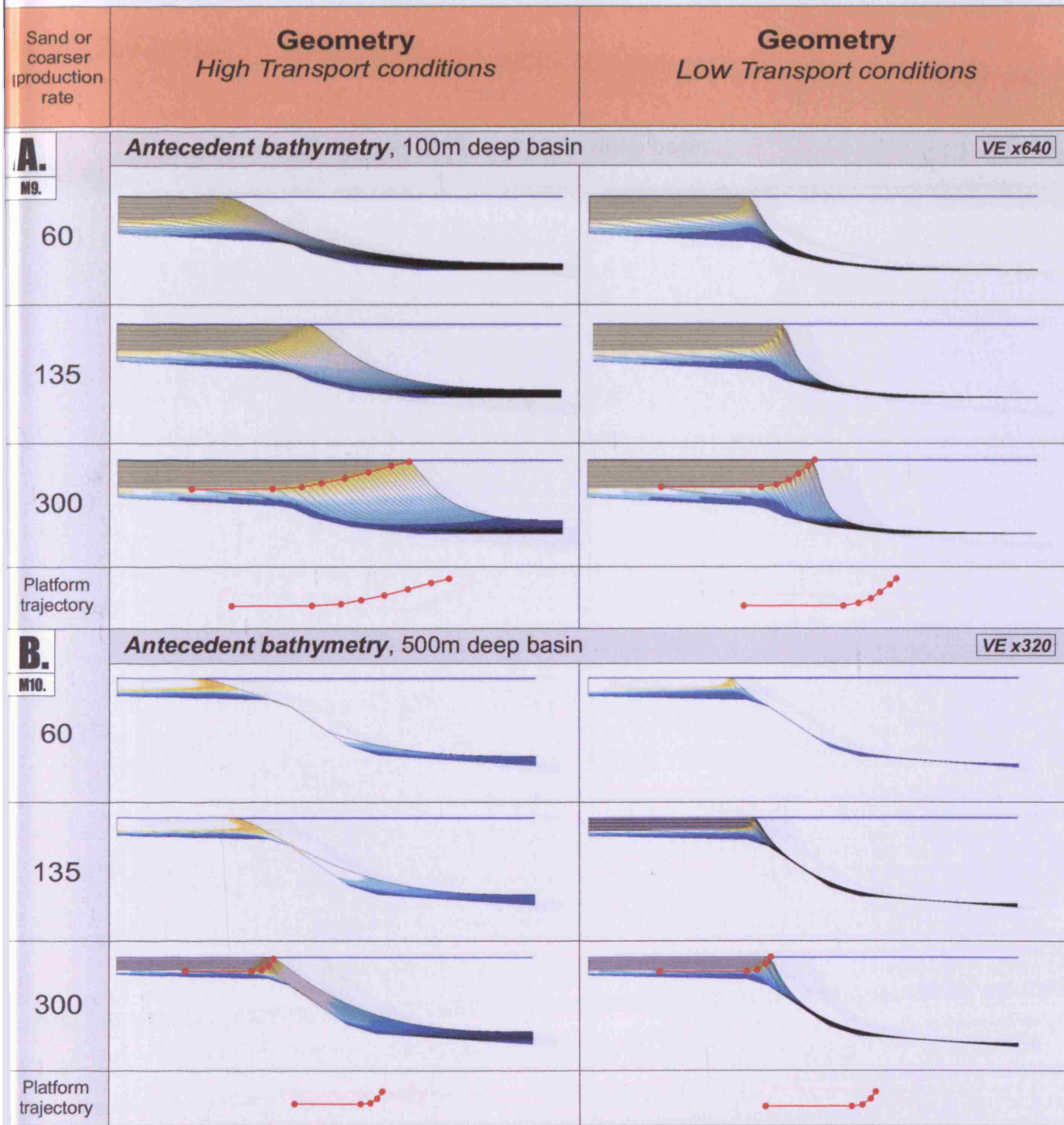


Figure 5.6. Cross sections from M9 and M10 illustrating the impact of antecedent bathymetry on platform architecture. In both A) and B) results from six models runs are shown. In each case three model runs have relatively low transport rates, and three have high transport rates, and for each set of low or high transport cases sediment production rate is either 60, 135 or 300 m My⁻¹. In A) from M9 an initial shallow-water platform bathymetry passes to the right into a 100 m deep basin. The modelled architectures suggest that the basin margin has some influence on the final position of the carbonate platform margin, but this influence is reduced with higher production and transport rates, both of which tend to facilitate progradation into the basin. In B) the relief on the basin margin is 500 m and in these cases the platform margin is clearly influenced by the position of the basin margin, which, even under the high production and transport cases, inhibits progradation of the platform margin and forces a change in stacking from progradation to aggradation.

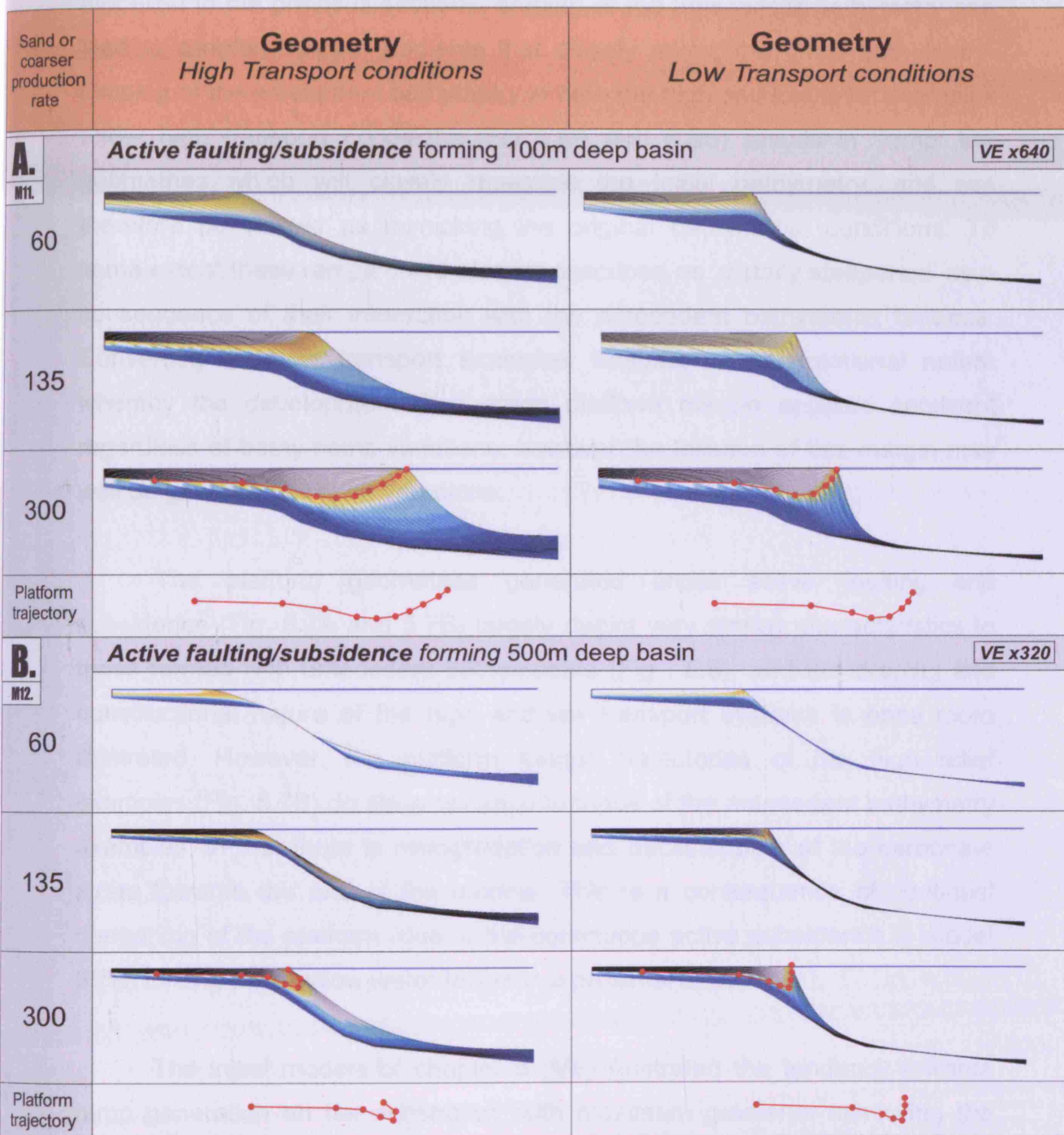


Figure 5.7. Cross sections from M11 and M12 illustrating the impact of syndepositional faulting on platform architecture. In both A) and B) results from six models runs are shown. In each case three model runs have relatively low transport rates, and three have high transport rates, and for each set of low or high transport cases sediment production rate is either 60, 135 or 300 m My⁻¹. The initial bathymetry in both models is a flat substrate before syndepositional faulting throughout the duration of the model forms the bathymetries viewed here. In A) syndepositional faulting creates a basin 100 m deep during the 5 My duration model runs. As in Fig 5.6A, 100 m of bathymetric relief is insufficient to prevent progradation in all but the lowest production rates modelled. In B) syndepositional faulting creates a 500 m deep basin during the 5 My duration model runs, and in this case, as in Fig 5.6B accommodation creation across the fault is sufficient to prevent progradation.

seawards into a platform margin slope. However, as in the ramp examples modelled in the previous sections, draping of the antecedent bathymetry can lead to clinoform slope gradients that closely mimic the initial bathymetry. Draping of the antecedent bathymetry in both the high and low relief examples under high transport conditions (Fig 5.6A and 5.6B) results in 'ramp' like geometries which will closely resemble the initial bathymetry, and can therefore be viewed as mimicking the original bathymetric conditions. To some extent these ramps could also be described as 'distally steepened' as a consequence of their interaction with the antecedent bathymetric features. Conversely the low transport examples illustrate a constructional nature whereby the development of a steep platform margin appears imminent regardless of bathymetric variations; however the location of this margin may well be governed by such variations.

The platform geometries generated under active faulting and subsidence (Fig. 5.7A and 5.7B) largely depict very similar characteristics to those formed with antecedent bathymetries (Fig . 5.6), and the draping and constructional nature of the high and low transport systems is once more illustrated. However, the platform margin trajectories of the high relief examples (Fig. 5.7B) do show variation to those of the antecedent bathymetry examples, in that there is retrogradation and backstepping of the carbonate strata towards the end of the models. This is a consequence of continual deepening of the platform (due to the continuous active subsidence in model 5.7B) forcing the shallow water facies in a proximal direction.

The initial models of chapter 5 (M6) illustrated the tendency towards ramp generation on flat substrates, with maximum gradients mimicking the gradient of the original bathymetry. The models (M7-12) analysing how changes to this flat substrate effected platform development depicted the draping nature of ramp systems, commonly inheriting underlying features, and the constructional character seen in FTP geometries. These characteristics may therefore provide a good indicator for the tectonic conditions in which ramp development will succeed. It is evident from the models that ramp systems require relatively low-gradient bathymetric conditions to develop,

supporting the view of Burchette and Wright (1992) who suggested that ramp development is most likely where gradients are slight, in tectonic locations such as the dip slopes of extensional fault blocks, cratonic foreland basin margins and epeiric seas in cratonic interiors. The following section addresses this idea by incorporating the results of M7-12 into an investigation of the optimal tectonic conditions for ramp development.

5.4 Optimal tectonic conditions for ramp development

A recent review of carbonate platform classification by Bosence (2005) stated that “the basinal and tectonic setting of carbonate platforms is shown to control their occurrence, the overall 3-D platform morphology, and depositional sequences”. Bosence continues by suggesting that the occurrence and development of specific platform types, for example carbonate ramps, is therefore directly correlated to the tectonic setting upon which the carbonate is deposited. Hence specific tectonic environments will favour ramp development, which according to the classification of Bosence (2005) will be; upon fault blocks, subsiding or passive margins, and the margins of foreland basins.

It is likely that ramp development will favour these tectonics settings; however it is unlikely that the tectonic setting itself is actually a principle control on platform type, as has been suggested by Bosence, but more probable the set of characteristics shared by the tectonic settings commonly attributed to ramp creation. The models presented earlier in this chapter and those of chapter 4 have highlighted the controlling parameters which favour ramp system development. These include a flat, low gradient substrate for the sediment to drape, a lack of large scale fault influence, and a rotational subsidence regime. Therefore any tectonic setting which possesses one or more of these characteristics maybe prone to ramp development. The presence of these controlling parameters does not however automatically result in ramp creation, it simply facilitates development should other parameters be suitable, and an important caveat to this relationship is the sediment production and particularly transport regime influencing the tectonic setting, because as was discussed in chapter 4 a lack of sediment redistribution will likely result in the development of an FTP regardless of the

other characteristics (i.e. a flat, low gradient substrate) present in the tectonic setting.

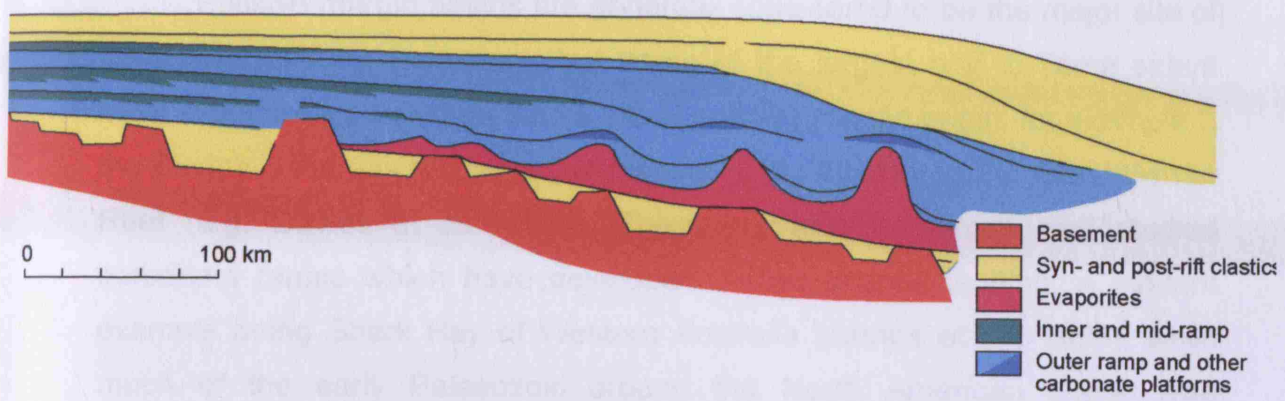
The concept that the geotectonic setting provides a major control on gross platform morphology has also been used prior to the classification of Bosence. The idea was introduced by Read (1985) and further discussed by Tucker and Wright (1990); however a major review of the carbonate ramp concept by Burchette and Wright (1992) specifically discussed the key tectonic settings for ramp development. The review reiterated the requirement of a low gradient substrate, and continued by suggesting additional optimal conditions for ramp growth would be provided in settings with relatively shallow basinal water depths, and those in which subsidence is continuously or episodically slow. Therefore suggesting ramp occurrence would favour the dip-slopes of extensional fault blocks, passive margins, foreland basin margins, and the margins of shallow intracratonic basins. These tectonic settings suggested by Burchette and Wright (1992) correlate with the classification of Bosence (2005), with the exception of the intracratonic setting which was not directly addressed in Bosences' work.

The subsequent sections investigate the tectonic settings in which ramp growth is commonly attributed using a series of Dionisos models. Each of the models is based on either a modern or ancient example with data sourced from both literature and the results and understanding gained from the previous sections of this chapter and each of the sections of chapter 4. The purpose of conducting these models is to ascertain why ramps may favour development in these settings, and to test the tectonic settings suggested by Bosence (2005) and Burchette and Wright (1992).

5.4.1 Passive margins

The passive margin tectonic setting (Fig 5.8) is characterised by low, relatively uniform subsidence rates, which typically decrease as the passive margin matures (Allen and Allen 2005). Once syn-rift relief has been buried or denuded this tectonic setting typically portrays large areas with very gradual slopes and little relief, which as shown in the previous models is ideal conditions for ramp development. The large extent of these margins can result

A



B

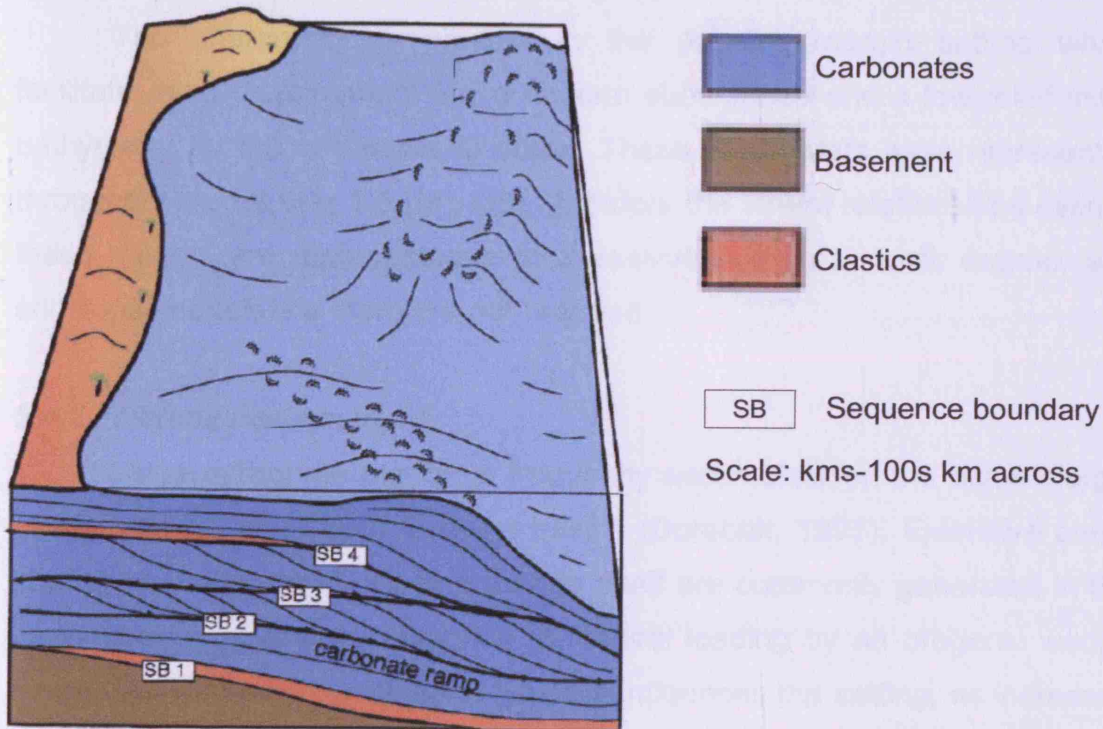


Figure 5.8. Ramp development on passive margins. A) Location of ramp growth in passive margin setting seen in green and blue coloured region of diagram (modified after Burchette and Wright, 1992). B) Carbonate ramp growth in a passive margin setting modified after Bosence, (2005). Note relatively flat initial basement bathymetry, and evolution of ramp to FTP geometry through time.

in ramps potentially hundreds of kilometres in width.

Passive margin basins are generally considered to be the major site of carbonate platform formation, thus some of the largest and to some extent most extensively studied platforms are of passive margin origin; for example the Florida-Bahamas region (e.g. Ginsburg et al., 2001) and the Great Barrier Reef (e.g. Davies et al., 1989). There are also numerous well studied carbonate ramps which have developed in this tectonic setting, a modern example being Shark Bay of Western Australia (James et al., 1999), while much of the early Palaeozoic around the North American craton also developed upon a passive margin (e.g. Ahr 1971; Read, 1989; Barnaby and Read, 1990). At a smaller scale, a Tortonian aged ramp outcrops on the island of Menorca, which formed on the passive, subsiding margins of an eroded Alpine basement (Pomar et al., 2002).

The characteristics present in the passive margin setting which facilitate ramp development are a uniform subsidence and a low-relief initial bathymetry for the carbonate to drape. These parameters were represented throughout model sets 1-5 (M1-M5), therefore the stratal relationships seen in these models are representative of a passive margin tectonic regime, and additional models are therefore not required.

5.4.2 Foreland basin margins

Large carbonate platforms frequently accumulate on the distal margin of low-latitude, underfilled foreland basins (Dorobek, 1995). Extensive areas of shallow water, gently dipping marine shelf are commonly generated in the foreland basin setting in response to flexural loading by an orogenic wedge (Fig. 5.9). Rotational subsidence typically influences the setting, as increased loading results in the distal portion of the shallow marine shelf subsiding at a significantly greater rate than the proximal portion, commonly resulting in a backstepping of the deposited strata. A low angle marine shelf for the carbonate to drape, combined with a rotational subsidence regime has previously been shown in model set 8 (M8, Fig. 5.4 and 5.5) to favour ramp growth when sediment transport and production rates are favourable. Hence the presence of these two characteristics in the foreland basin tectonic setting facilitates ramp development, many of which are frequently over a hundred

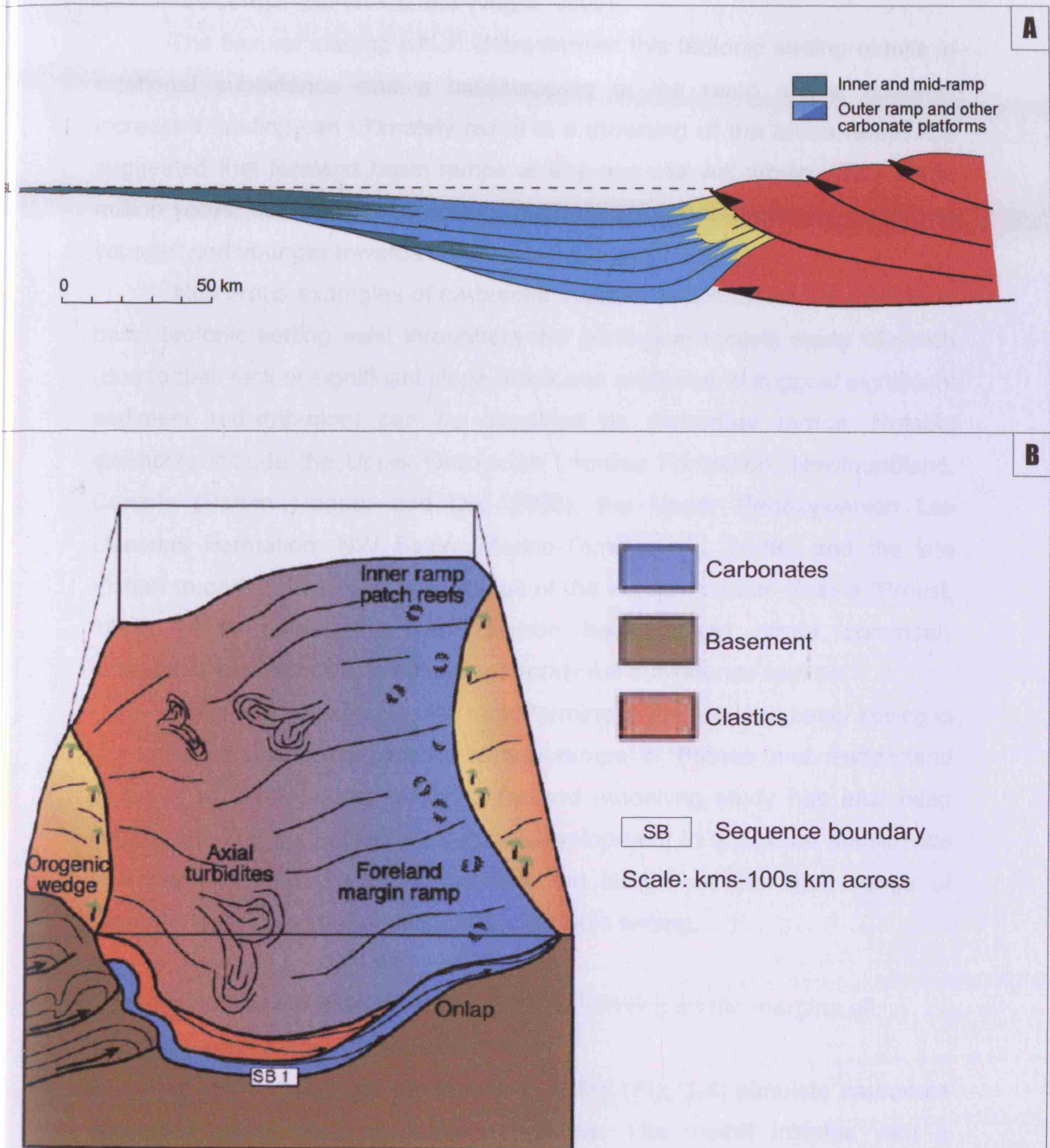


Figure 5.9. Ramp development on foreland basin margins. A) Location of ramp growth on a foreland basin margin is seen in green and blue coloured region of diagram. Ramps initiate on gentle slope at margin of depressed foreland and prograde to the basin. (modified after Burchette and Wright, 1992). B) Carbonate ramp growth on a foreland basin margin setting (modified after Bosence, (2005).

kilometres across (Burchette and Wright, 1992).

The flexural loading which characterises this tectonic setting results in rotational subsidence and a backstepping of the ramp strata, however increased loading can ultimately result in a drowning of the entire ramp. It is suggested that foreland basin ramps at any one site will drown within a few million years, but that the composite platform will be diachronous, becoming younger and younger towards the foreland (Dorobek, 1995).

Numerous examples of carbonate systems which formed in a foreland basin tectonic setting exist throughout the geological record, many of which (due to their lack of significant slope break and evidence to suggest significant sediment redistribution) can be classified as carbonate ramps. Notable examples include the Upper Ordovician Lourdes Formation, Newfoundland, Canada (Batten Hender and Dix, 2008), the Upper Pennsylvanian Las Llacerias Formation, NW Spain (Merino-Tome et al., 2009), and the late Viséan to early Moscovian aged ramps of the Western Urals, Russia (Proust, 1998) which depict the characteristic backstepping strata commonly associated with ramps formed under a rotational subsidence regime.

An additional example of a ramp forming in the foreland basin setting is the early Tertiary Perialpine carbonate ramps of France and Switzerland (Allen et al., 2001), upon which a forward modelling study has also been conducted. The study illustrates ramp development in a flexural subsidence controlled foreland basin and provides an insight on the likely range of geodynamical parameters affecting the tectonic setting.

5.4.2.1. Forward modelling carbonate ramps forming on the margins of foreland basins – The Arabian Gulf

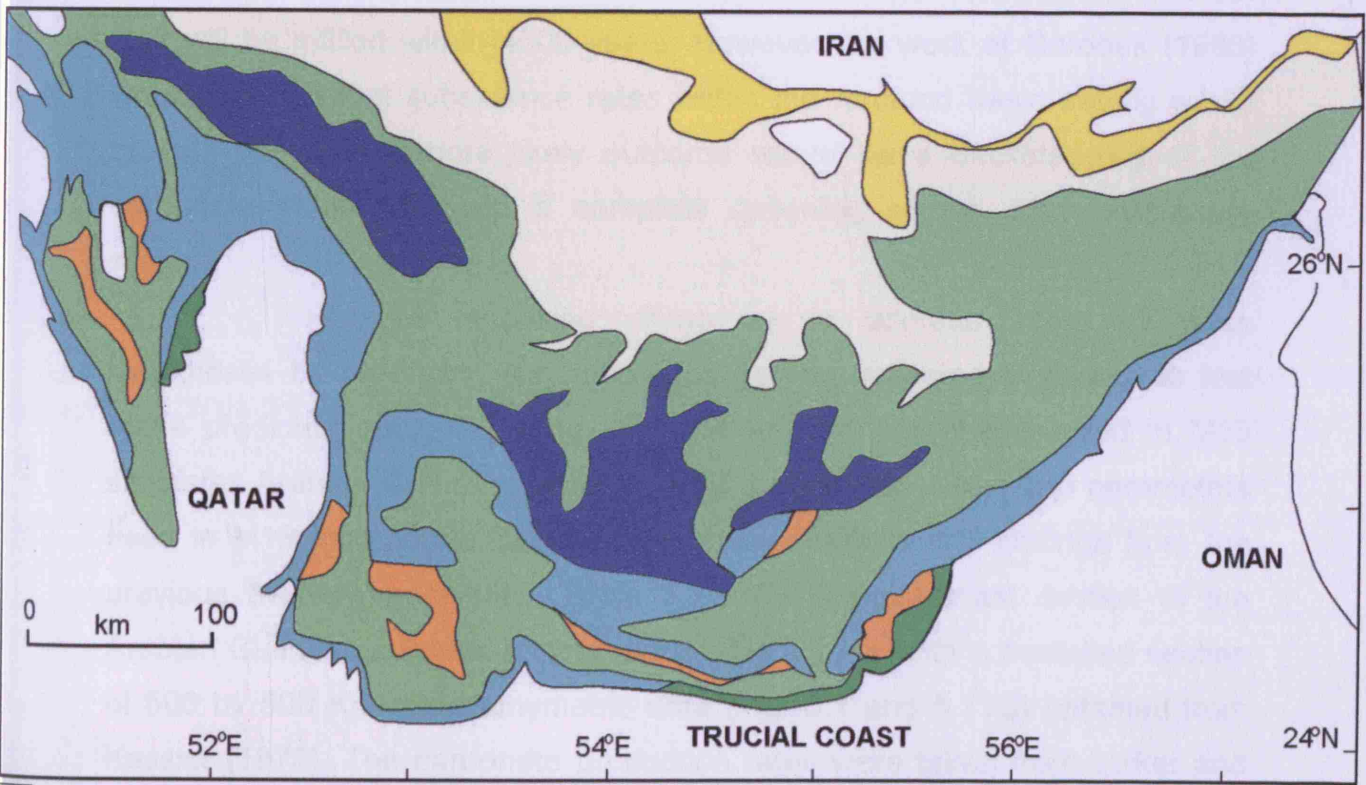
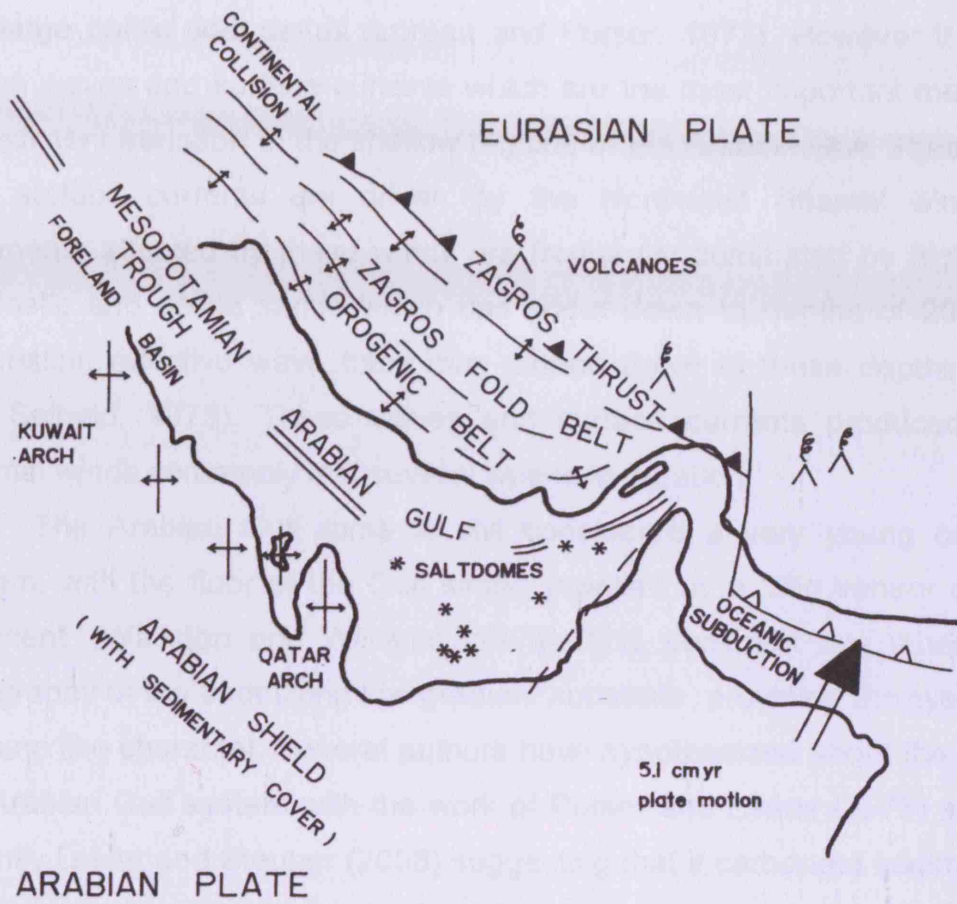
To some extent the models seen in M8 (Fig. 5.4) simulate carbonate deposition under foreland basin conditions. The model initiates with a relatively low gradient bathymetry which then rotates due to differential subsidence; magnitude of the rotational subsidence occurring at the eastern end of the profile is five times that of the subsidence occurring at the west. This is analogous with increasing rates of subsidence towards the orogenic load (e.g. Sinclair, 1997; Allen & Allen, 2005; Allen et al., 2001); in the model example the loading would be taking place on the east end of the model

profile. Results from M8 illustrate a backstepping retrogradational platform, consistent with characteristics commonly seen in foreland basin ramps (e.g. Sinclair, 1997; Allen et al. 2001).

A classic modern example of a carbonate ramp formed within a foreland basin tectonic regime is the Arabian Gulf ramp (Purser, 1973; Lokier and Steuber, 2008). The Arabian Gulf is a foreland basin lying between the Arabian Shield to the southwest and the Zagros fold mountain belt to the northeast (Fig. 5.10A). It is a small remnant of the northwest-southeast Tethyan basin in which a thick series of hydrocarbon-rich deposits accumulated, often in depositional environments very similar to those found in the present Arabian Gulf (Murriss, 1980). The Pleistocene-Holocene bathymetric profile (Fig. 5.1) owes its origin to the Zagros Orogeny, which began in Miocene time, the continuation of which is often given as the cause of underthrusting along the Zagros line and consequently the earthquakes and volcanoes in Iran (Glennie, 1995). The Hajar (Oman) Mountains, a related orogen, exist across the Straits of Hormuz on the Arabian Peninsula, while the UAE are essentially located on the peripheral bulge of this orogenic belt (Loosveld et al., 1996).

The distribution of Holocene sediments in the Arabian Gulf depicts a characteristic ramp grading of lithology, with grain types becoming progressively finer towards the distal, deeper regions of the ramp (Fig. 5.10B). The Arabian Gulf Sea floor grades from skeletal, oolitic and pelletoidal sands and fringing reefs at its most proximal locations, passing into widespread skeletal muddy sands, and finally into basin centre muds at its most distal locations, where water depths do not exceed 100 m (Seibold et al., 1973). It is likely that this sediment grading and the low angle ramp geometry displayed by the present Arabian Gulf is due to significant sediment redistribution across the system (as discussed in chapter 4). This sediment grading and redistribution of grains in the Arabian Gulf is driven by several environmental factors. The first is the regional and tidal currents which affect the Gulf. These typically attain velocities exceeding 50 cm per second, and influence sediment textures even in the deepest parts of the basin (Purser and Seibold, 1973). It is these bi-directional currents which are attributed to the local development of

A.



- Bioclastic muddy sand
- Aggregate grains
- Bioclastic sand
- Pelletoidal
- Peloidal
- Siliciclastic sand
- Bivalve marl

B.

Figure 5.10. A) General tectonic setting of the Arabian Gulf, modified after Evans (1995). B) Regional distribution of principal sedimentary grain types in the Trucial Coast region of the Arabian Gulf, modified after Wagner and Van der Togt (1973).

the large oolitic tidal deltas (Loreau and Purser, 1973). However it is wind-driven waves and surface currents which are the most important mechanism of sediment transport in the shallow regions of the Arabian Gulf. These waves and surface currents are driven by the Northwest Shamal winds. The sediments affected by these winds are frequently dominated by high-energy bioclastic and oolitic sands which can occur down to depths of 20 metres, suggesting effective wave base may extend down to these depths (Purser and Seibold, 1973). These waves and surface currents produced by the Shamal winds commonly last several weeks in duration.

The Arabian Gulf ramp is still considered a very young carbonate system, with the floor of the Gulf simply mantled by a 'thin veneer of recent sediment' (Walkden and Williams, 1998). This sediment has inherited the topography of the underlying low gradient substrate, providing the system with its ramp like character. Several authors have hypothesized about the future of the Arabian Gulf system with the work of Purser and Evans (1973) and more recently Lokier and Steuber (2008) suggesting that if carbonate sedimentation continues at its current rate much of the shallow water areas of the Arabian Gulf will be infilled within 4000 years. However the work of Dorobek (1995) would suggest that subsidence rates within the foreland basin setting would prevent this and a more likely outcome would be a backstepping of the carbonate strata, or even a complete drowning of the entire carbonate system.

Forward modelling allows us to address some of these hypotheses by producing simulations containing collected field data to test these predicted outcomes. The Dionisos forward model presented in M13 simulates Arabian Gulf ramp development for the next 1 My. The parameters used in M13 incorporate data derived from literature and findings from the previous twelve model sets (Table 3.2). The Trucial coast section of the Arabian Gulf was selected for the model (Fig.5.11A), with a modelled section of 500 by 500 Km and bathymetric data (Fig. 5.1 and 5.11B) obtained from Kassler (1973). The carbonate production rates were taken from Loiker and Steubers (2008) recent investigation into carbonate ramp sedimentation rates on the Abu Dhabi shoreline (Table 3.2), while the carbonate production profiles used were the same as those of M1, since results of M2 illustrated the

A.



B.

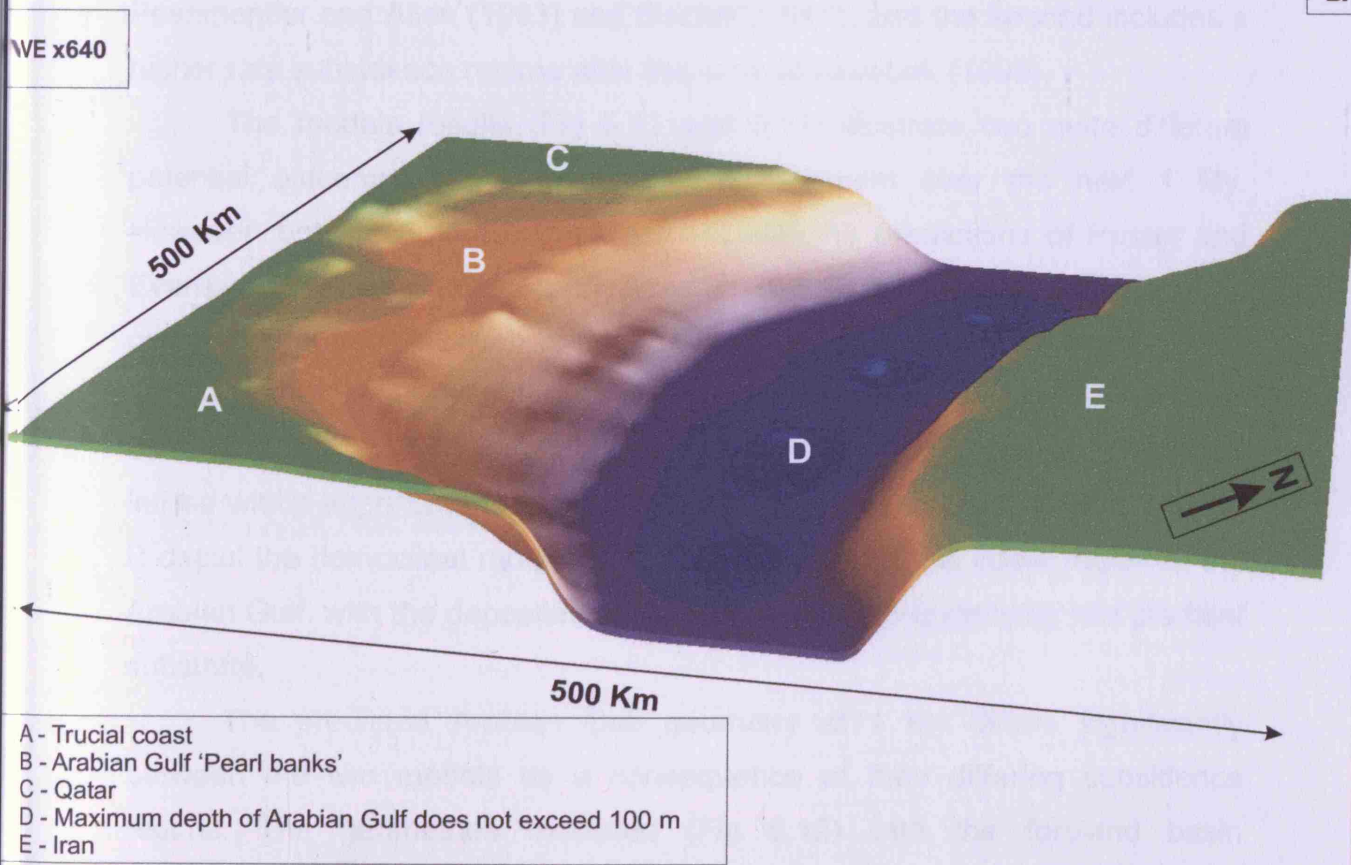


Figure 5.11. Parameters for Arabian Gulf Dionisos forward model. A) Aerial view of Arabian gulf. Dashed box indicates selected region for forward model. Image courtesy of Google Maps (2010). B) Initial basement bathymetry simulated for Arabian Gulf forward model using the Dionisos modelling package. Bathymetric data obtained from Kassler (1973).

lack of control these production curves exert on overall platform geometry.

As described above, distribution of Holocene sediments displays a marked distal fining of grain types, characteristic of ramp systems, and interpreted to be due to transport by tidal and Shamal wind derived currents. Given this evidence for operation of significant sediment transport processes, M13 is assumed to have 'typical' ramp like sediment transport parameters, and diffusion coefficient were derived from the results of M1, and fall within the ramp-prone space of the parameter plots seen in the results and figures of M1 (Fig. 4.2).

Unfortunately there is little constraint on the present subsidence rates occurring within the Arabian Gulf foreland basin. Therefore subsidence rates for other foreland basin types assumed to be similar were used, and two separate models run, each simulating a differing subsidence regime. The first run incorporates data derived from the work on underfilled foreland basins by Posamentier and Allen (1993) and Sinclair (1997), and the second includes a higher rate subsidence regime after the work of Dorobek (1995).

The models results (Fig 5.12 and 5.13) illustrate two quite different potential outcomes for Arabian Gulf development over the next 1 My. However, both models are in agreement with the predictions of Purser and Evans (1973), and Lokier and Steuber (2008) that at present rates of carbonate production much of the shallow water regions of the Arabian Gulf will be infilled. Analysis of the modelled geometries suggests that, if present conditions persist, the entire 'Pearl banks' region of the Arabian Gulf will be infilled within approximately 20ky. The modelled cross sections in M13 A and B depict the homoclinal ramp-like character of the Trucial coast region of the Arabian Gulf, with the deposited sediment draping the underlying low-gradient substrate.

The predicted Arabian Gulf geometry at 1 My differs significantly between the two models as a consequence of their differing subsidence regime. The geometries modelled (Fig 5.12) with the foreland basin subsidence rates of Posamentier and Allen (1993) and Sinclair (1997) predict a total infill of the Arabian Gulf within 0.98 My if parameter values were to continue at their current rates. The rapid infilling of the basin may however be a consequence of the model parameters, in that the model simulates a closed

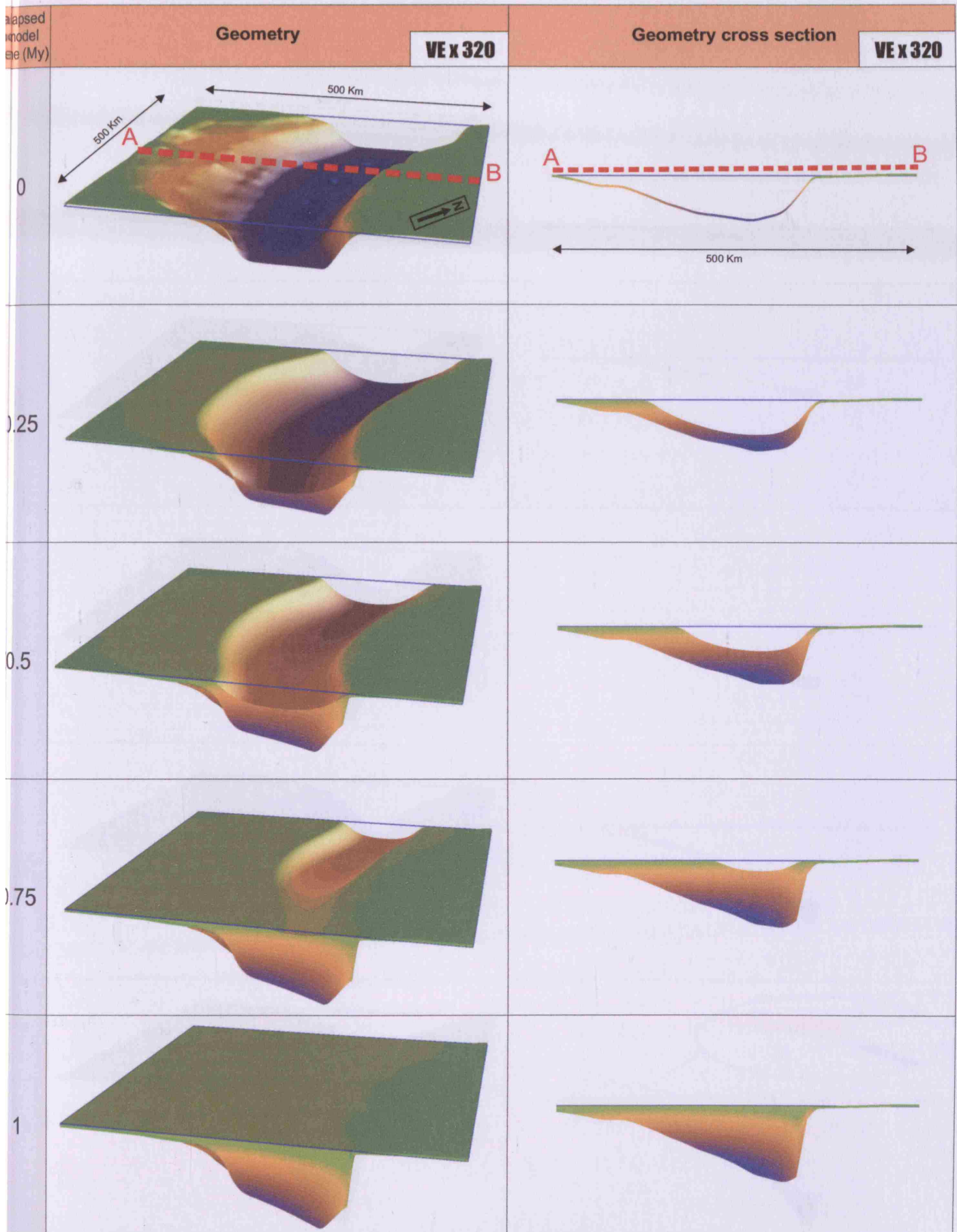
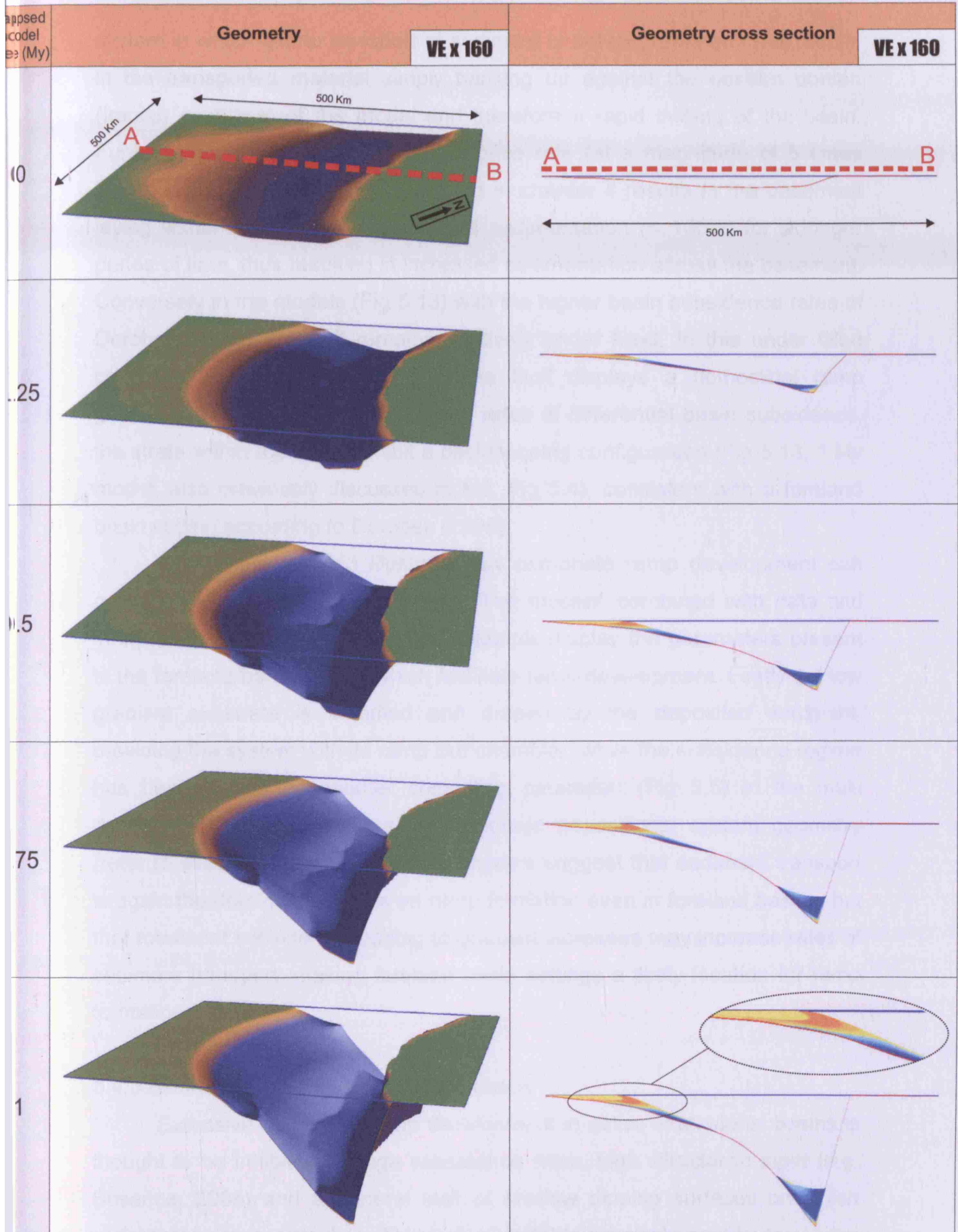


Fig 5.12. M13A results. Dionisos models simulating Arabian Gulf developed for the next 1My under a maximum foreland basin subsidence rate of 0.2 mm/yr, after Sinclair (1997). Model results illustrated for both gross Arabian Gulf geometry development and cross section profiles. Basin orientation and location of cross section shown in 0My result. Basin colour illustrates bathymetry evolution.



5.13. M13B results. Same a figure 5.12 but modelled with a maximum foreland basin subsidence rate of 1mm/yr after Tobek (1995).

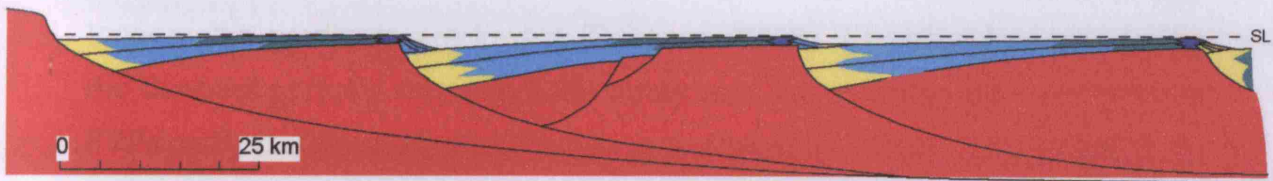
system in which lateral transport of sediment is not incorporated. This results in the transported material simply banking up against the eastern portion (Iranian coastline) of the model and therefore a rapid infilling of the basin. Furthermore a lower modelled subsidence rate (at a magnitude of 5 times smaller) than that of models presented in chapter 4 results in the basement laying within the zone of pelagic mud sedimentation (< 100M) for a longer period of time, thus resulting in increased sedimentation across the basement. Conversely in the models (Fig 5.13) with the higher basin subsidence rates of Dorobek (1995) the Gulf remains relatively under filled. In this under filled case the Trucial Coast region of the Gulf displays a homoclinal ramp geometry. However, due to increased rates of differential basin subsidence, the strata within the ramp exhibit a backstepping configuration (Fig 5.13, 1 My model, also previously discussed in M8, Fig 5.4), consistent with a foreland basin setting according to Dorobek (1995).

The results of M13 illustrate how carbonate ramp development can occur within a foreland basin setting. The models, combined with data and interpretation from the Arabian Gulf example display the parameters present in the foreland basin setting which facilitate ramp development. Firstly the low gradient substrate is inherited and draped by the deposited sediment, providing the system with its ramp like character, while the subsidence regime has been shown as another controlling parameter (Fig 5.5) in the multi dimensional parameter space for carbonate depositional system geometry (refer to section 5.6.1). However the models suggest that sediment transport is again the dominant process on ramp formation even in foreland basins, but that rotational subsidence leading to gradient increases may increase rates of sediment transport, making foreland basin settings a likely location for ramp formation.

5.4.3 Extensional basins – Fault block ramps

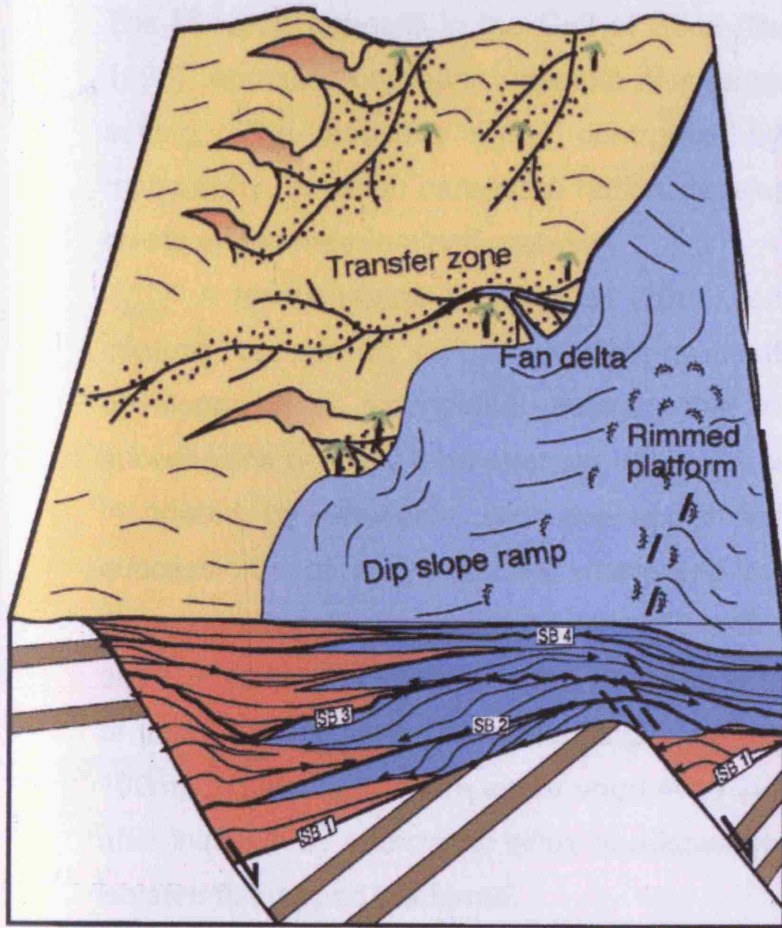
Extensive carbonate ramp development in active extensional basins is thought to be inhibited by high subsidence rates, high siliciclastic input (e.g. Bosence, 2005) and a general lack of shallow dipping surfaces on which carbonates can accumulate. This lack of suitable substrate contributes to the characteristically small size (a few kilometres or tens of kilometres across) of

A



- Basement
- Syn- and post-rift clastics
- Inner and mid-ramp
- Outer ramp and other carbonate platforms

B



- Carbonates
- Pre-rift
- Clastics
- SB Sequence boundary

Scale: kms-10s km across

Figure 5.14. Ramp development in an extensional basin setting. A) Location of ramp growth within extensional basin is shown in green and blue coloured region of diagram. Ramps initiate on the gentle dip slopes of faulted blocks (modified after Schette and Wright, 1992). B) Carbonate ramp growth in the extensional basin setting modified after Bosence, (2005). Dip slope ramps are seen forming on tilted fault blocks.

ramps formed in extensional basins. Ramp growth in extensional tectonic settings is often restricted to development in fault transfer or fault tip-zones, or on the dip slopes of tilted fault blocks (Fig. 5.14), where fault throws and topographic gradients are lowest (Bosence, 2005). Elevated footwalls facing the deepest portions of half-grabens may also be occupied by small rimmed FTPs or by distally steepened ramps (e.g. Chatellier, 1988). Low gradient dip slope examples may provide an excellent substrate for ramp development, but antithetic faulting, or the development of sub-basins, may disrupt the topography and limit the distance ramps can prograde, or may result in a distal steepening of the ramp geometry as the carbonate deposystem responds to the developing tectonic topography (Burchette and Wright, 1992). The Miocene deposits in the Gulf of Suez (Burchette, 1988; Bosence et al., 1998) represent one such example of a ramp developing in an extensional setting. The deposits were controlled by an extensional fault-block topography, in which carbonate ramps developed around the exposed block crests and in marginal half-grabens.

A recent review by Dorobek (2008), on the tectonic and depositional controls on syn-rift carbonate platform sedimentation re-examined ramp development in extensional basins. The review states that thin ramp successions typically form after syn-rift fault-bounded highs have been initially inundated by seawater; with the updip limit of the initial syn-rift ramp succession commonly reflecting where sea-level intersected the hanging-wall dip slope during progressive flooding. As with the reviews of Bosence (2005) and Burchette and Wright (1992) Dorobek suggests the extent and thickness of these onlapping and backstepping ramp packages will be typically thin (< 100m), indicating they are either short-lived systems that are terminated soon after initiation by siliciclastic influx or relative sea-level rise, or they evolve into isolated flat topped platforms.

The models presented in chapter 4 would suggest that a transition from a ramp to FTP geometry is the most likely cause of these short lived ramp systems. Chapter 4 (section 4.4) discussed the transient nature of ramps (Fig. 4.4), in that in the absence of sufficient sediment transport and assuming a healthy carbonate factory, carbonate platforms will always tend to evolve from a ramp to FTP geometry because of in-situ accumulation. How long this

evolution takes will depend on the rate of transport versus the rate of production. This evolution can be thought of as a development from an initial condition bathymetry towards a dynamic equilibrium state. In the case of fault block ramps, carbonate strata begins to accumulate on the low relief fault block bathymetry, and production and accumulation modify the gradient and form of this system until a certain point at which the new system has a form that approaches a dynamic equilibrium state, which would appear to be a FTP, differing considerably from the initial ramp like bathymetry. This ramp to platform transition and attempt to reach a dynamic equilibrium state may explain the short lived nature and relative thinness of fault block ramps. An excellent example of this exact process can be seen in a Miocene outcrop from offshore Vietnam (Dorobek, 2008). The syn-rift strata were constructed on a half-graben high, and an interpretation of the stratal geometries viewed on seismic (Fig. 5.15) allow us to interpret platform growth in this extensional example. The near horizontal, tram like seismic viewed directly above the 'base carbonate' (yellow region in Fig. 5.15) suggests initial carbonate deposition simply draped the underlying fault block, resulting in the early system to have a ramp-like geometry. The transition of this ramp stage to a more FTP like geometry (green region in Fig. 5.15) likely occurred as production and accumulation modified the gradient and form of the geometry as the system approached a dynamic equilibrium state.

5.4.3.1. Forward modelling carbonate ramps forming on fault blocks– The Sirte Basin

In addition to the Vietnam example (Dorobek, 2008) the Paleocene strata of the Sirte Basin, Libya (Fiduk, 2009) is another excellent example of a carbonate ramp deposited within an extensional basin. Triassic rifting of the Late Palaeozoic Sirt Arch led to its collapse in the Mid to Late Cretaceous, forming the Sirte Basin (Anketell, 1996). The Sirte Basin margins are composed of a series of platforms, troughs, ridges and slopes marking the transition into deeper water (Fig. 5.16). Carbonate ramp development occurred on this margin, and the ramp strata host some significant hydrocarbon accumulations (Alhbrandt, 2001).

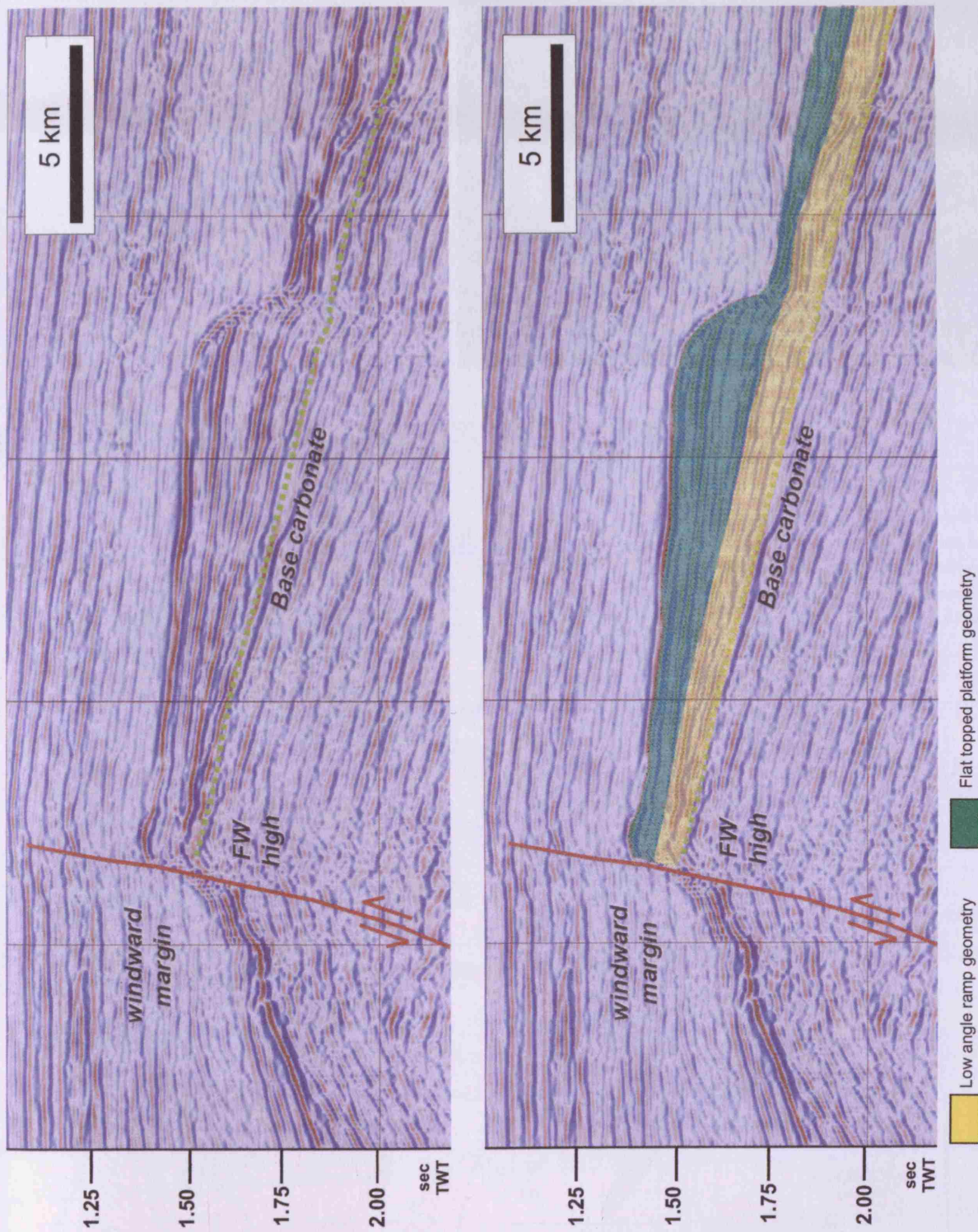


Figure 5.15. Syn-rift carbonate deposition on a half-graben high. This Mioene aged example is from the subsurface of offshore Vietnam (edited from Dorobek, 2008). Lower image displays interpreted carbonate geometries based on the stratal geometries observed in the upper seismic section. Initial carbonate deposition on the fault block appears to have a ramp-like character, before the development of a significant slope break and a more FTP type deposition, refer to text for discussion on these changes in platform type.

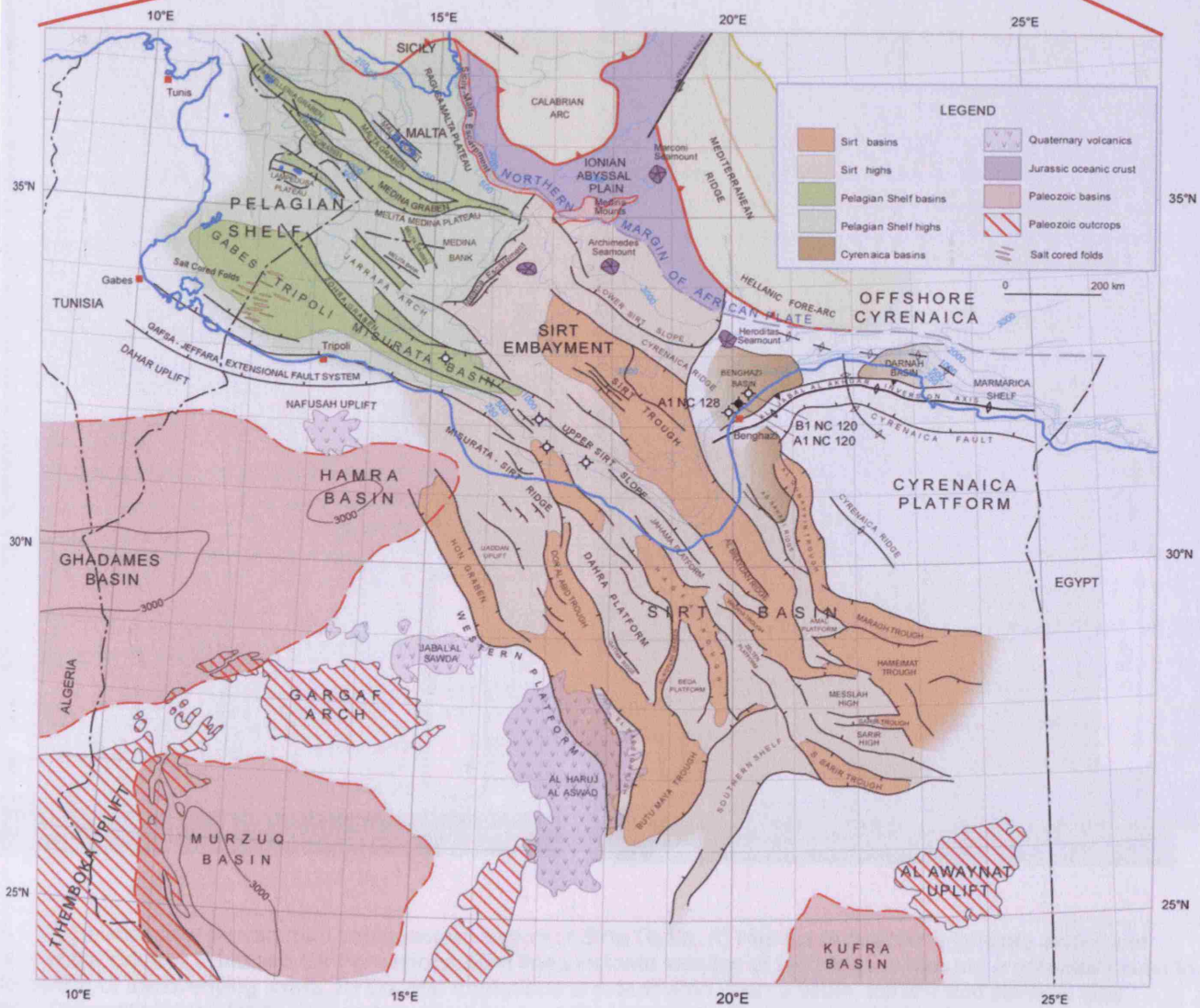
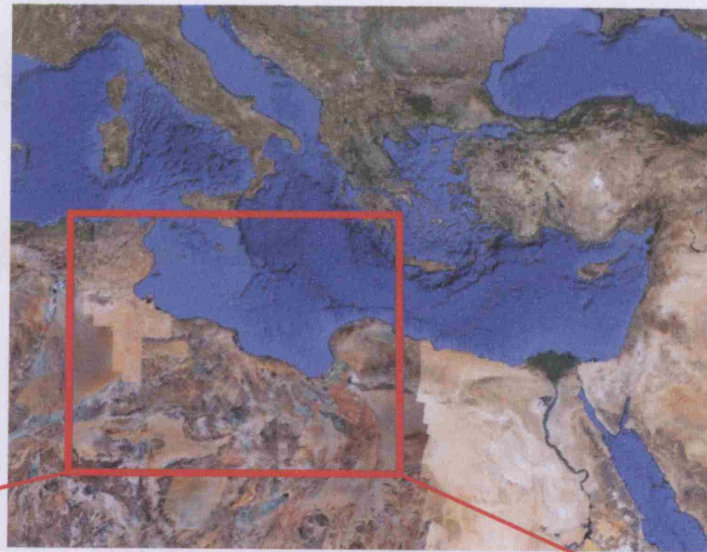


Figure 5.16. Location of Libya and Sirte Basin shown in aerial photograph. (Image courtesy of Google maps, 2010). Tectonic and structural elements map for Libya and surrounding offshore areas. Location and extent of the Sirte Basin and its offshore extension; the Sirte Embayment, are shown by light brown colour. Map modified from Fiduk (2009).

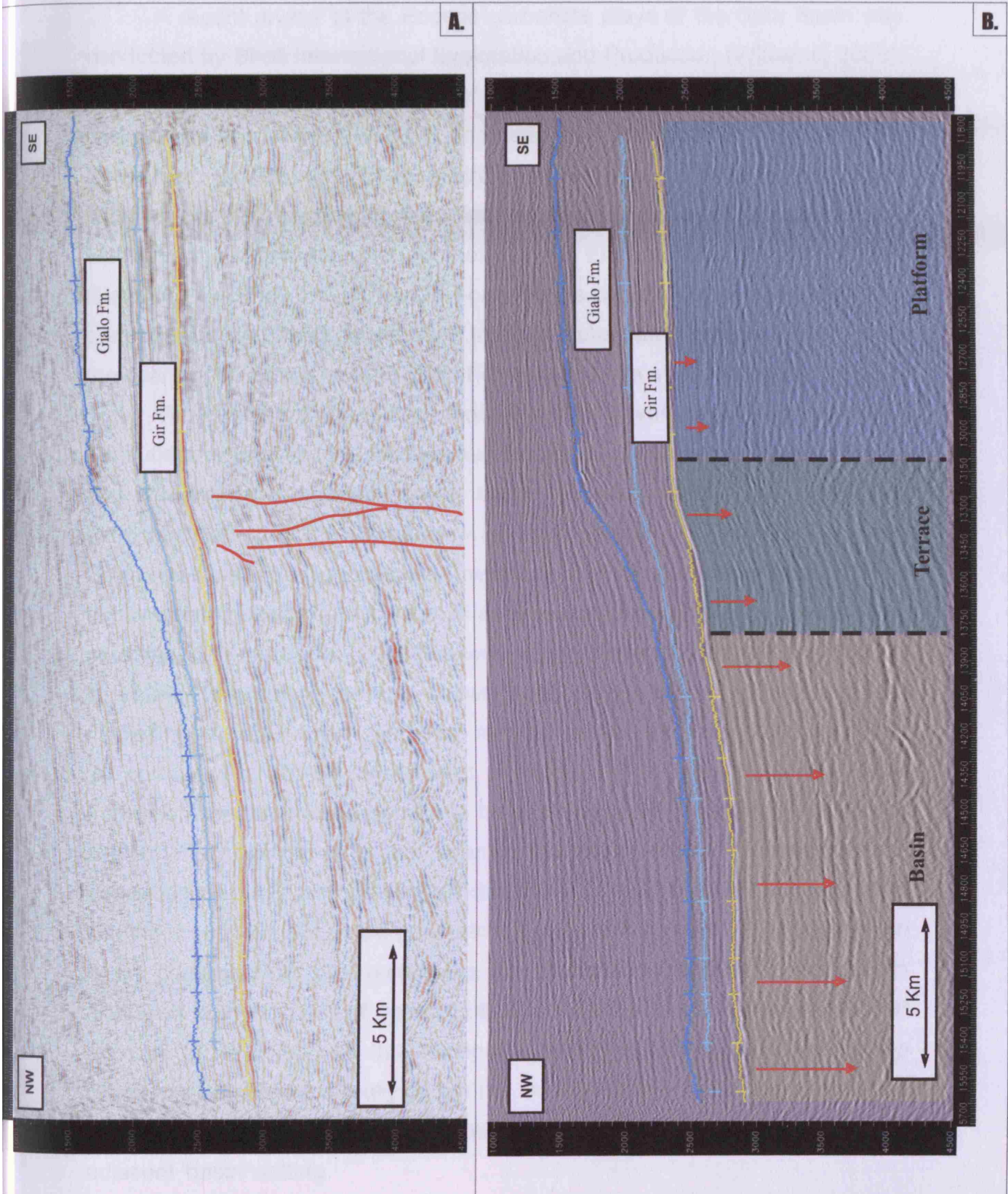


Figure 5.17. Seismic line derived from southeastern region of Sirte Basin. A) Highlighted sections indicate extent and geometry of the Eocene Gialo and Gir Formations. Red lines indicate location of fault lines, which are a potential cause for the steepening of the overlying strata. B) Eocene formations are deposited upon a basin, terrace and platform type geometry. Differential subsidence caused by underlying Late Cretaceous faulting has resulted in this present basement configuration.

A recent review of the Eocene carbonate plays of the Sirte Basin was conducted by Shell International Exploration and Production (Williams, 2008). The review included interpretation of several 2D seismic lines. The example seismic line used here (Fig. 5.17) originates from the southeast corner of the Sirte Basin, and images Eocene strata deposited on a tilted faulting block situated on the margins of the Sirte extensional basin. The seismic line highlights the distribution and geometry of two Eocene aged Formations, the Gialo and Gir (Fig. 5.17). The Gir Formation is dominantly composed of fine grained mud and chalk, interpreted to be of outer ramp pelagic origin, while the coarser, clinoform-bearing Gialo Formation is of a shallower water origin.

The basement upon which these formations were deposited was not a flat substrate due to Late Cretaceous faulting that formed a basin, terrace, and platform type geometry (pers. comm. Baaske, 2008). This underlying bathymetry affected the depositional geometries seen in both the Gialo and Gir Formations. The Gir Formation, believed to be of outer ramp origin is likely to have been subject to high rates of sediment transport (refer to chapter 4 for reasoning), therefore the sediment was simply deposited across this change in underlying gradient (as was shown in M9-12), in doing so inheriting and mimicking the steepened geometry, and hence this ramp could be described as portraying a distally steepened character. With regards to the Gialo Formation the thickness appears to be significantly different in the 'platform' setting when compared to that seen in the 'basin' region. Furthermore the Formation displays well developed clinoforms in the 'platform' setting, which combined with the displayed geometries suggests a more FTP like deposition when compared to the underlying Gir Formation. Similar to the results displayed in the models of figure 5.6B and 5.7B the progradation of this FTP appears to be limited by this change in underlying bathymetry, with steep clinoforms developing directly above the location of this underlying steepening (evidenced by the high amplitude reflectors) which fail to prograde into the adjacent 'basin' setting.

The overall platform geometry of the combined Gir and Gialo Formations is very similar to those seen in the offshore Vietnam example (Fig. 5.15). As with the Vietnam platform the margins of the Sirte basin appear to depict an initial period of ramp-like sedimentation (Gir Formation) before

transition to a more FTP like mode of deposition (Gialo Formation). This ramp to FTP evolution likely occurred as production and accumulation modified the gradient and form of the geometry as the system approached a dynamic equilibrium state, a similar process to that evoked from the evolution of the Vietnam platform. The position of the FTP margin is dictated by the location of underlying faulting, as progradation of the clinoforms appears to be halted by the change in underlying bathymetry (as shown in M9-12, Fig. 5.6 and 5.7).

A forward modeling study of the geometries seen on the margins of the Sirte basin was conducted by Shell International (Williams, 2008), the aim of which was to investigate facies distribution and reservoir potential in these Eocene carbonate ramps. The forward modelling was conducted using the Dionisos modelling software, with the majority of data and parameters obtained from internal Shell reports. These values included the recognised durations for both the Gir and Gialo Formations, 6 My and 10 My respectively, both Eocene and therefore deposited from 54.5 to 38.5 My (Ogg et al., 2008). Initial basement bathymetry incorporated the Late Cretaceous faulting, and the bathymetry was modified syndepositionally via differential subsidence to create the current basin, terrace and basin configuration as observed on seismic (Fig. 5.17).

The resultant Dionisos model and synthetic seismic created with these parameters is a reasonable match to the geometries imaged on the seismic line (Fig. 5.18). The model results suggest that the interpretation of initially higher transport rates, decreasing with time, and significant control on geometries by underlying fault-controlled bathymetry (Fig. 5.18, 2 and 4), are reasonable if not a unique explanation of the observed geometry. The model results illustrate the ramp to FTP transition as the system approaches dynamic equilibrium. The results, including the synthetic seismic, also demonstrate the occurrence and location of maximum flooding surfaces (Fig. 5.18, 1), backstepping sequences (Fig. 5.18, 3), and most importantly the location, distribution and relationship to one another of both potential seal (maximum flooding surfaces) and potential reservoir (coarser shallower water facies) units.

The models and examples presented for ramp development on fault blocks once more illustrate the requirement of a relatively flat substrate for the

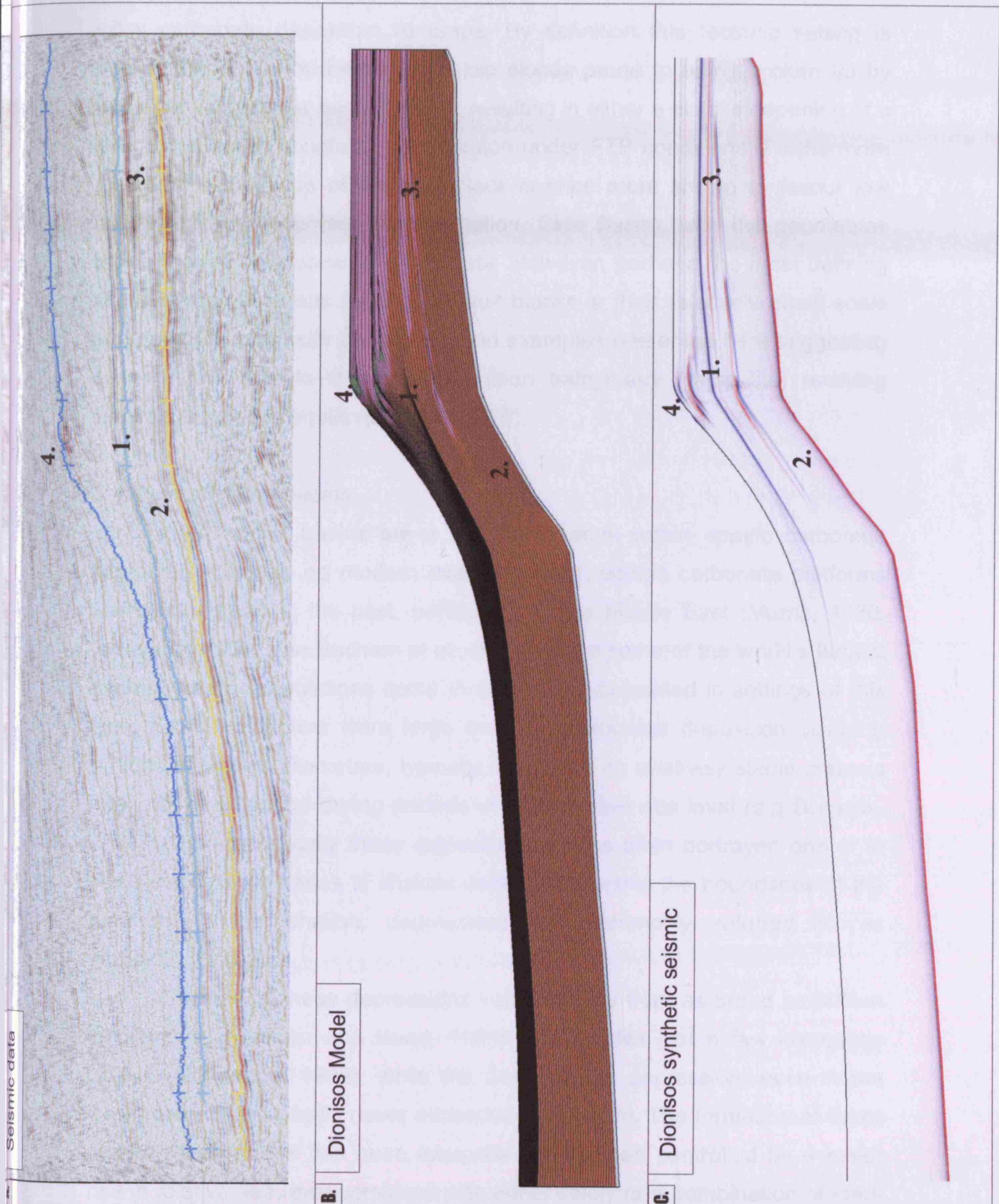


Figure 5.18. A) Selected seismic line of Eocene strata from southeast margin of Sirte Basin. B) Dionisos model of geometries seen in seismic (A). C) Synthetic seismic of Dionisos model seen in B. Numerical labels correspond to A, B and C -

1. Maximum flooding surface at contact between Gir and Gialo Formations
2. Gir Formation displays near horizontal reflectors for entire Formation, note the steepening of the strata as it passes over the underlying faulted bathymetry
3. Minor backstepping sequence at conclusion of Gir Formation prior to major flooding
4. Steep clinofolds within the Gialo Formation are consequence of progradation into adjacent basin

initial carbonate deposition to drape. By definition this tectonic setting is heavily influenced by faulting, with dip slopes prone to being broken up by further faulting as the basin evolves, resulting in either a distal steepening of a ramp or effecting clinoform progradation under FTP conditions. Furthermore rotational subsidence of the fault block is once more shown to favour low angle ramp development (Gir Formation, Sirte Basin), with the geometries typically displaying backstepping strata. However, perhaps the most defining characteristic of ramps formed on fault blocks is their relatively small scale and short lifespan, with the models and examples presented here suggesting this may be due to the initial condition bathymetry (ramp-like) evolving towards a dynamic equilibrium state (FTP).

5.4.4 Intraplatform basins

Intraplatform basins are a common feature within epeiric carbonate platforms. Although no modern examples exist, epeiric carbonate platforms were widespread in the past, particularly in the Middle East (Murriss, 1980; Burchette, 1993; Van Buchem et al., 2002) where some of the world's largest hydrocarbon accumulations occur in carbonates deposited in settings of this type. Epeiric platforms were large areas of carbonate deposition covering millions of square kilometres, typically developed on relatively stable cratonic interiors, and flooded during periods of high relative sea-level (e.g Burgess, 2008). Characteristically these extensive platforms often portrayed one or in some examples a series of shallow depressions within the boundaries of the platform. These shallow depressions are commonly referred to as intraplatform basins.

The size of these depressions varied greatly from as broad as 800km in diameter (Markello and Read, 1981) to examples just a few kilometres across (Gutteridge, 1989), while the depth of the depression, even in the larger examples typically never exceeded 100-200 m. The formation of these shallow depressions has been interpreted to of been controlled by a major rise in relative sea level combined with either solely or a combination of load-induced isostatic sagging, salt tectonics, differential subsidence, localised tectonism or spatially and temporally varying carbonate production.

Intraplatform basin infill typically consists of storm generated, fine grained sediments derived and transported from the surrounding shallow platform environment. An excellent illustration is the basinal Hanifa Formation (Droste, 1990) composed of laminated strata, interbedded with coarse intervals and benthic bioclastic deposits interpreted as storm units. The characteristics seen in the margins of these basins are not as homogenous as in the basin centres, but vary greatly depending on the extent and shape of the basin, as does the respective facies development. In general the smaller, shallower basins portray a lack of margin facies development before passing into the platform proper (Murriss, 1980), while the larger/deeper examples commonly depict a gradual coarsening of facies along the margin as it shallows progressively away from the basin centre. These coarsening upward sequences typically include the coarse grained facies of the shallow water shoals and biostromes, of obvious hydrocarbon reservoir-prone potential. The geometry of these margins have been interpreted to vary from rimmed shelves to both homoclinal and distally steepened ramps, while frequently the margins typically portrayed both shelf and ramp characteristic at one time or another as the margins were continually evolving through the span of the basins existence.

Intraplatform basins generally developed in stable tectonic conditions and due to their relatively shallow nature their sedimentary successions were highly dependent on high frequency sea-level changes. This dependency on sea-level cyclicity meant the basins tended to be geologically short-lived, with the basin often filled by fine grained basinal carbonates during a subsequent sea-level cycle. Conversely a change to more arid conditions may have resulted in extensive evaporite deposits within the basin, in doing so providing a potential impermeable seal to the system. It is this source (basin deposits), reservoir (coarse margins); seal (evaporites) triplet and their close proximity to one another within the intraplatform basin environment which makes this setting of such economic importance. The source rocks of the Hanifa intraplatform basin show a comparative example, which combined with the Arab A to D reservoirs, and sealing anhydrites of the Qatar and Hith formations constitute one the worlds richest single oil habitats (Murriss, 1980).

Intraplatform basin deposits occur on a global scale within strata of various ages. Figure 5.19 depicts the distribution of some of these deposits (14 examples), particularly concentrating on the location of the examples discussed here. The distribution map illustrates how many examples are concentrated around major hydrocarbon producing regions, particularly the Middle East, further demonstrating the importance of this setting and its association with hydrocarbon occurrence. A synopsis of the characteristics depicted by the formations deposited in key intraplatform basin examples is given in table 5.1.

5.4.4.1 Carbonate ramp development on the margins of intraplatform basins

The geometrical and platform type classification of the margins of intraplatform basins varies significantly between basin examples, with authors commonly describing these margins as portraying either an FTP, or a homoclinal or distally steepened ramp geometry (refer to 'Margin development' in table 5.1). Examples include the Mishrif Formation of the Southern Arabian Gulf, which is commonly described as having a homoclinal ramp geometry (Burchette, 1993), while the Natih Formation of Northern Oman is frequently referred to as portraying a distally steepened ramp geometry (Van Buchem et al., 2002) as a consequence of the steepening and clinoforms which are present within the Formation. Additional examples formed within the intraplatform basin setting and described as having a distally steepened ramp character are the Las Plias Formation of Northern Mexico (Osleger et al., 2004), and the Southern Istria section of Croatia (Buckovic et al., 2003), both of which contain coarse clinostratified bodies at the margins of the basin.

These classifications may however be unsatisfactory in light of the work and models presented in this and the previous chapter. It is likely that the classification of these systems has been based on a single component of the system and does not account for the system as a whole, in that the classification is made by analysing only the basin margins (commonly clinoform foresets) and does not include the more proximal sections located on the epeiric platform top (commonly platform interior facies) or the more distal sections (commonly basinal) in the overall platform classification. It is

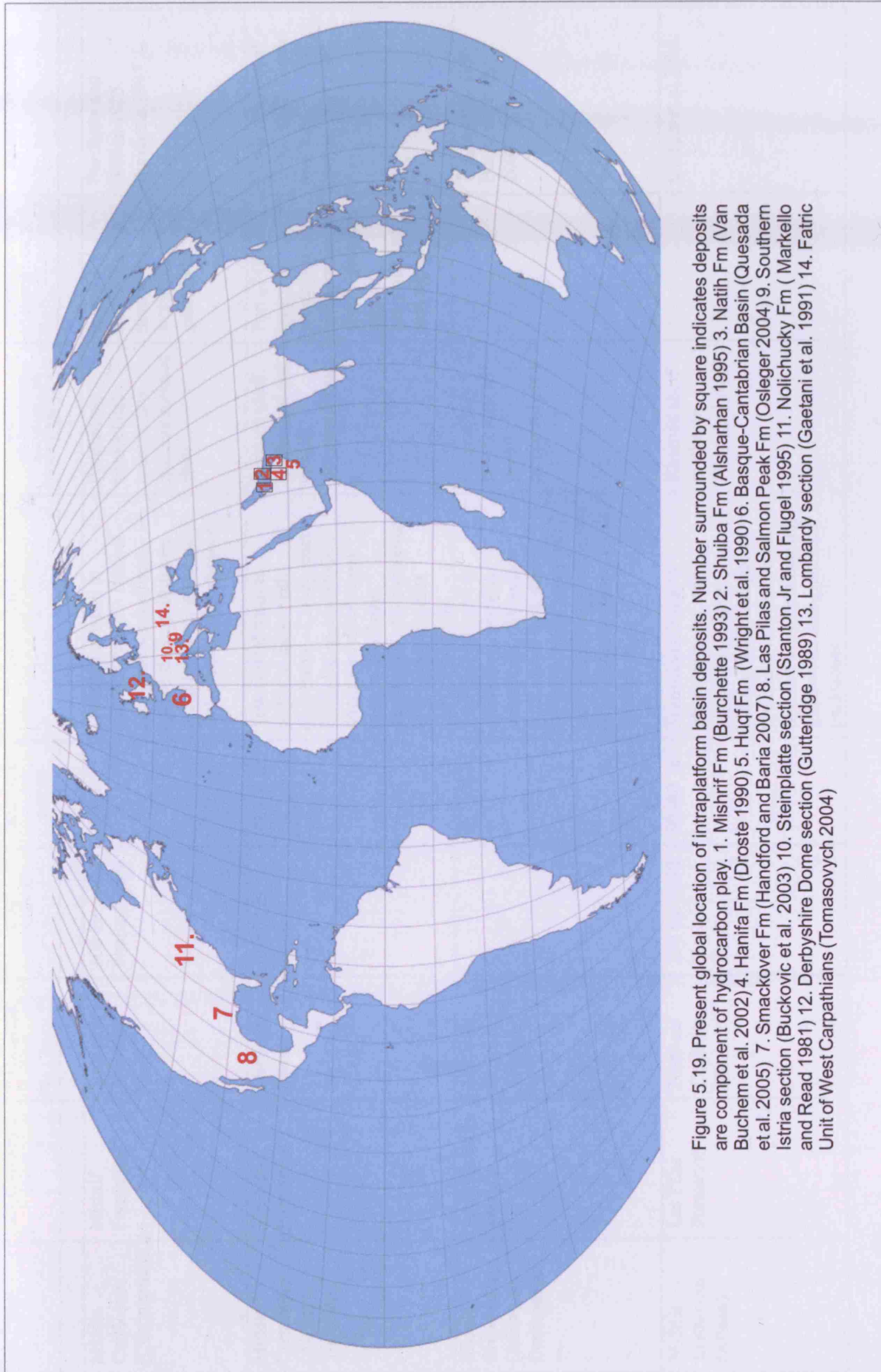


Figure 5.19. Present global location of intraplatform basin deposits. Number surrounded by square indicates deposits are component of hydrocarbon play. 1. Mishrif Fm (Burchette 1993) 2. Shuiba Fm (Alsharhan 1995) 3. Natih Fm (Van Buchem et al. 2002) 4. Hanifa Fm (Droste 1990) 5. Huqf Fm (Wright et al. 1990) 6. Basque-Cantabrian Basin (Quesada et al. 2005) 7. Smackover Fm (Handford and Baria 2007) 8. Las Pias and Salmon Peak Fm (Osleger 2004) 9. Southern Istria section (Buckovic et al. 2003) 10. Steinplatte section (Stanton Jr and Flugel 1995) 11. Nolicucky Fm (Markello and Read 1981) 12. Derbyshire Dome section (Gutteridge 1989) 13. Lombardy section (Gaetani et al. 1991) 14. Fatric Unit of West Carpathians (Tomasovych 2004)

AGE	STRATIGRAPHIC NAME	LOCATION	BASIN PROPERTIES	MAXIMUM BASIN DEPTH	FACIES TYPES	MARGIN DEVELOPMENT ACCORDING TO SOURCE REFERENCE	HYDROCARBON IMPORTANCE	SOURCE REFERENCE
Middle Cretaceous (Cenomanian)	Mishrif Formation	Southern Arabian Gulf	300 km width Shailaif basin	200 m	Transitional basin to platform facies – Basinal packstone/wackestones, coarse slope grainstones, rudist biostromes and patch reefs, lagoonal mudstones.	Prograding homoclinal ramp to low gradient rimmed shelf	Forms reservoirs in a number of world class giant fields	Burchette and Britton 1985. Burchette 1993.
Middle Cretaceous (Albian to Turonian)	The Nath Formation	Northern Oman.	≈ 250 km width	80-100 m	Transitional basin to platform facies with clinoforms - Clayey marl Basinal facies, mudstone dominated distal shoal margin, bioclastic grainstones of the proximal shoal margin, rudist dominated shoal.	Rimmed shelf, homoclinal and distally steepened ramp	Part of Oman's largest producing hydrocarbon field – provides source, reservoir and seal triplet	Van Buchem et al, 1996, 2002. Droste and Van Steenwinkel 2004.
Middle Cretaceous (Albian to Cenomanian)	Southern Istria Section	Southern Istria, Croatia		80 - 100 m	Transitional basin to platform facies with clinoforms - Shoreface grainstones with micro HCS. Intensely bioturbated carbonate sand bar. Foresets of subaqueous dunes, rudist biostromes	Prograding homoclinal to distally steepened ramp.		Tisjar et al, 1998. Buckovic et al, 2003.
Middle Cretaceous (Albian)	Las Plias Formation	Northern Coahuila, Mexico	250 km width Maverick Basin	50 - 80 m	Transitional basin to platform facies with clinoforms - Basin globigerinid calcisphere mudstone to wackestone, massive clinoform bearing grainstones and grain-rich packstones	Rimmed shelf to distally steepened ramp		Osleger et al 2004.

AGE	STRATIGRAPHIC NAME	LOCATION	BASIN PROPERTIES	MAXIMUM BASIN DEPTH	FACIES TYPES	MARGIN DEVELOPMENT ACCORDING TO SOURCE REFERENCE	HYDROCARBON IMPORTANCE	SOURCE REFERENCE
Lower Cretaceous (Aptian)	Shuaiba Formation	Southern Arabian Gulf	≈ 120 km width Abu Dhabi Basin	> 50 m	Transitional basin to platform facies – Basinal argillaceous dense lime mudstones, platform slope rudistid packstones, rudist barrier rudistid grainstones/boundstones	Rimmed shelf	Reservoir units contain ≈ 12.6 billion bbl of oil reserves, minor source rocks in thin kerogen rich layers	Alsharhan 1985, 1995.
Late Jurassic (Upper Oxfordian to Lower Kimmeridgian)	Hanifa Formation	Arabian Peninsula	250 – 300 km diameter	≈ 60 m	Basin dominated facies – Dark organic rich laminated lime mud/wackestone of basin fill, some patches of nodular and massive anhydrite	Poor margin development - low gradient ramp	Major source rock of Middle East, combined with Arab reservoirs and Qatar and Hith sealing anhydrites as much as 100 x 10 ⁹ bbl of recoverable reserves	Murris 1980, Droste 1990.
Late Jurassic (Oxfordian)	Smackover Formation	South Texas	4 basins S. Texas, E. Texas, N. Louisiana, Mississippi	< 300 m	Basin dominated facies – Organic rich laminated mudstone and siltstone	Fringing bank/homoclinal ramp?	Major exploration over 80 years, 4 major oil and gas reservoirs	Budd and Loucks 1981. Moore 2001. Handford and Baria 2007.
Lower Jurassic	Basque Cantabrian Basin	Northern Spain	System of Smooth troughs	100 m	Basin dominated facies – Dark grey/black organic rich marls and paper laminated black shale's in suboxic troughs	Undefined margin	Provides source for Ayoluengo oil field, Spain's only onshore oil field	Quesada et al, 2005. Rosales et al, 2006.

AGE	STRATIGRAPHIC NAME	LOCATION	BASIN PROPERTIES	MAXIMUM BASIN DEPTH	FACIES TYPES	MARGIN DEVELOPMENT ACCORDING TO SOURCE REFERENCE	HYDROCARBON IMPORTANCE	SOURCE REFERENCE
Upper Triassic	Oberthalk Formation	Austria	> 40 km wide Kossen Basin	200 m	Transitional basin to platform facies – Restricted basinal shales, skeletal packstones, rudstones, with boundstone patches on mid ramp, inner ramp cyclic subtidal strata	Homoclinal to distally steepened ramp		Stanton and Flugel 1993.
Middle Carboniferous (Brigantian)	Station Quarry beds	Derbyshire, England	5-10 km wide	25 m	Dominated by basinal bioclastic (platform derived) grainstone/packstones	Homoclinal ramp to distally steepened ramp		Gutteridge 1989.
Upper Cambrian	Nolichucky Formation	Appalachian Valley, Virginia, USA	Up to 800 km long, 300-400 km wide	≈ 50 m	Transitional basin to platform facies – Shale dominated basin facies, ribbon carbonates of outer ramp, Ooid/oncolitic carbonates of mid/inner ramp, inner ramp cycles	Prograding homoclinal ramp		Markello and Read 1981, 1982.
Late Precambrian	Huqf Group - Khufai and Buah Formations	E. Central Oman	≈ 150 km long, 30 km wide		Transitional basin to platform facies – Khufai – Basinal dark bituminous dolomites, prograding grainstone shoal, beach sand flats, peritidal back shoal with stromatolites Buah – Basinal lime mudstones, grainstones and stromatolites of active shoal, evaporitic lagoons	Prograding homoclinal ramp		Wright et al, 1990.

important to assess the system as a whole before classifying it, and the origin of the clinoforms may provide evidence for the controlling parameters in this system. The clinoforms situated on the margins of these intraplateau basins are commonly high angle, for example clinoform gradients of 8 to 15° have been recorded in the Las Plias Formation of Northern Mexico (Osleger et al., 2004), up to 35° in the Natih Formation of Northern Oman (Droste and Van Steenwinkel, 2004), and 4 to 7° in the Smackover Formation of South Texas (Handford and Baria, 2007). Their formation is commonly attributed to decreased accommodation on the epeiric platform top leading to transport and shedding of sediment into the subsidence created, adjacent intraplateau basin. Therefore the magnitude of sediment redistribution in the system is going to have a significant control on the overall platform geometry. While the geometry of this deposited material will to some extent be influenced by the underlying bathymetry upon which it is deposited.

The examples run in model sets 9, 10, 11 and 12 (M9 to M12, Fig 5.6 and 5.7) investigate this exact process of sediment being deposited upon the margins of shallow basins, under a varying degree of transport (refer to section 5.3.3 for full description of models). The model results illustrate variances in bathymetry do exert a control on platform geometry, but the degree of influence varies with differing rates of production and transport, and for different amounts of basinal relief. The models run under low transport conditions (Fig. 5.6 and 5.7) illustrate a constructional nature whereby the development of a steep platform margin appears imminent regardless of bathymetric variations; however the location of this margin appears to be governed by such variations, in that FTP progradation is stalled at the intraplateau basin margin forming high angle clinoforms at this location. Conversely a draping of the underlying basinal bathymetry in the models run under high transport conditions (Fig. 5.6 and 5.7) results in 'ramp' like geometries which closely resemble the initial bathymetry, and can therefore be viewed as mimicking the original bathymetric conditions. To some extent these ramps could also be described as 'distally steepened' as a consequence of their interaction with the antecedent bathymetric features.

The model results illustrate how the interaction of the underlying bathymetry and magnitude of sediment redistribution can influence the

geometry of the resultant platform. The results would suggest that if the entire intraplatform basinal system (epeiric platform top, basin margins and basin) is analyzed, it is highly unlikely that any sediment package deposited in this setting could accurately be described as displaying a homoclinal ramp geometry. By definition the intraplatform basin will display some degree of steepening, which under ramp-prone (high sediment transport) conditions will be draped and mimicked by the deposited sediment, which would therefore more accurately be described as a distally steepened ramp, with this distal steepening initiating at the break between the epeiric platform top and intraplatform basin. Examples which have previously been ascribed as having a homoclinal ramp-like character, therefore lacking high angled clinofolds and a well defined break of slope, (e.g. the Nolichucky Formation, Markello and Read 1982; the Mishrif Formation, Burchette 1993; the Hanifa Formation, Droste 1990) are surely more accurately described as distally steepened ramps due to this interaction with the underlying bathymetry. Evidence to verify the significant sediment redistribution in such examples is provided by the fine grained storm units commonly found in the basinal sections of these systems, which are interpreted to have been derived and transported from the surrounding shallow platform environment by storm and wave reworking (e.g. The Hanifa Formation; Droste, 1990).

In contrast, intraplatform basinal settings where sediment redistribution is lower will be prone to FTP development, with the site of the high angled clinofolds likely influenced by the steepening associated with the epeiric platform top to intraplatform basin transition. It should be noted that many intraplatform basins may well have experienced low rates of sediment redistribution, evidenced by the high content of organic material often associated with their deposits (e.g. the Shuaiba Formation, Alsharhan, 1995; the Natih Formation, Van Buchem et al., 2002). The presence of the organic material suggests that these sediments must have deposited in a restricted regime in which turbulence and circulation was low, resulting in poorly oxygenated waters. Therefore tidal exchange between the epeiric platform top and intraplatform basin must have been minimal resulting in almost isolated basin conditions. Under such conditions redistribution of any sediment produced on the platform top would have been minimal, resulting in the

formation of the coarse, high angle clinoforms which are viewed in many intraplateform basin Formations (e.g. the Natih Formation, Van Buchem et al., 2002; Droste and Van Steenwinkel, 2004; the Las Plias Formation, Osleger et al., 2004; the Shuaiba Formation, Alsharhan, 1995; the Oberrhalkalk Formation, Stanton and Flugel, 1995). In these examples if the entire system (epeiric platform top, basin margins and basin) is considered the deposited geometry will most accurately be described as an FTP, and not a distally steepened ramp.

5.4.4.2. Forward modelling carbonate ramps formed on the margins of intraplateform basins – The Natih Formation

As discussed the models of M9 to M12 are representative of sediment deposition in the intraplateform basin setting. M9 and M11 (Fig. 5.6 and 5.7) are representative of an intraplateform basin environment with shallow depressions that do not exceed 100 metres in depth. The models (M9 and M11) illustrate how a distally steepened ramp geometry can develop as carbonate is deposited across the gently dipping basin margins. However, this only occurs when sediment transport rates are sufficiently high to suppress clinoform development. In model runs with lower transport rate, clinoforms develop and prograde, possibly passing into aggradational stacking if the gradient of the underlying bathymetry increases (Fig 5.6 and 5.7).

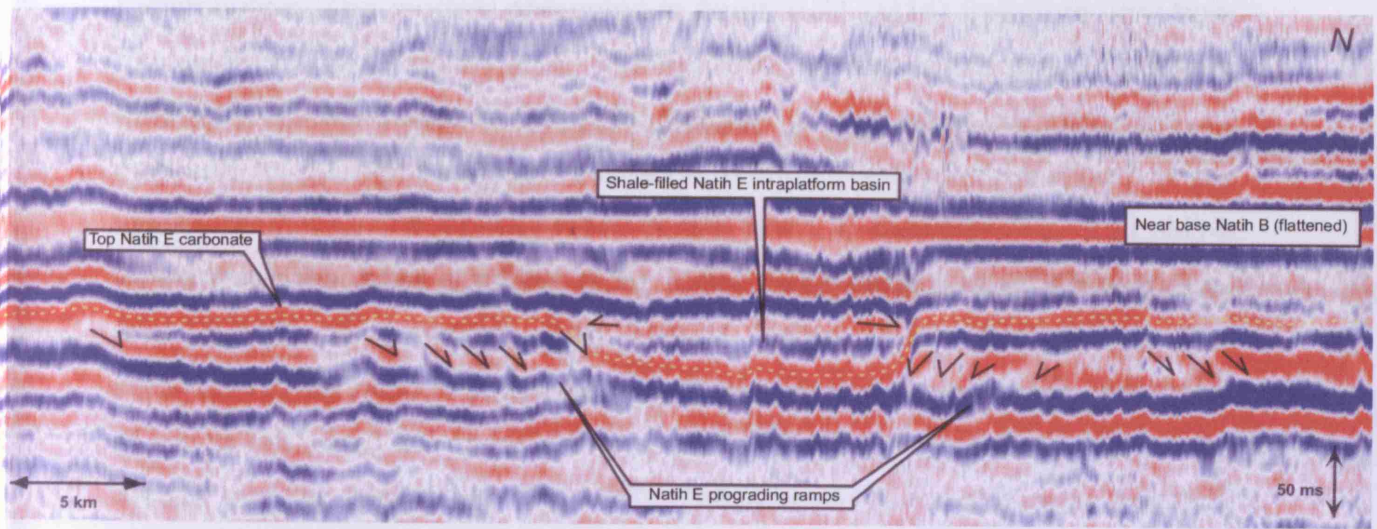
Individual examples of Formations deposited in an intraplateform basin setting can provide us with a more specific insight into the controlling processes on platform development in these settings. The Albian to Turonian aged Natih Formation (Van Buchem et al., 2002; Droste and Van Steenwinkel, 2004) of Northern Oman formed within an intraplateform basin setting, and the Formation is frequently described as displaying a distally steepened ramp geometry. The Formation is of major economic importance due to the coexistence of both reservoir facies and source rocks in the same depositional sequences; the reservoir provided by the coarse, commonly rudist abundant shoals located on the basin margins, and the source provided by the organic-rich basinal facies. Natih reservoirs in Oman's largest oilfield (the Fahud field), have been producing oil for more than 37 years, with remaining reserves estimated at several billion barrels (Van Buchem et al.,

2002). Consequently, the Natih Formation has been the focus of extensive analysis, seismic (Fig. 5.20 A), stratigraphic (Fig. 5.20 B) and lithological data for the Formation are readily available, and Natih strata are therefore a good example to model in order to better understand carbonate deposition in the intraplatform basin setting.

Input parameters for model 14 (M14) were obtained from logs, seismic and stratigraphic data from several published sources (Table 3.2). M14 concentrates on modelling the E member of the Natih Formation over a 4.6 My span (Van Buchem et al., 2002). The model initiates on the top surface of the Natih F member (bathymetry sourced from Van Buchem et al., 1996 and Droste and Van Steenwinkel, 2004). Initial basement bathymetry is a shallow water environment in which water depth does not exceed 30 m (Fig 5.21A). Water depth increases throughout the model run due to differential subsidence, but never exceeds 100 m. Information regarding the key grain types in the Natih Formation was taken from the extensive logs of Van Buchem et al., (1996; 2002), with composite production curves constructed for mud, silt and sand or coarser grain types. The dominant carbonate producers in the Natih Formation were rudists, represented in the model by the sand or coarser production curve, with maximum production rates obtained from the work of Steuber (2000) on Cretaceous rudist bivalve growth rates. A pulse of siliciclastic influx into the system is also modelled, the timing and location of which is taken from Van Buchem et al., (1996). While sea-level oscillations for the Natih E member were based on a short term Haq type curve (Haq et al., 1988, Haq and Al-Qahtani, 2005).

A depositional model (Fig. 5.20) for the development of the Natih E member was constructed from the high resolution outcrop investigation conducted by Van Buchem et al., (1996; 2002). An analysis of the geometries formed by the deposited sediments in this model suggest an early low angle ramp phase before the development of a margin with high angle clinoforms and a more FTP like geometry (Fig. 5.20). Van Buchem et al., (1996; 2002) account for these changes in geometry and overall stratigraphic organisation by means of sea-level oscillation control, the data for which is obtained from their sequence stratigraphic mapping. The understanding obtained from this and the previous chapters work suggest an alternative control could also

A.



B.

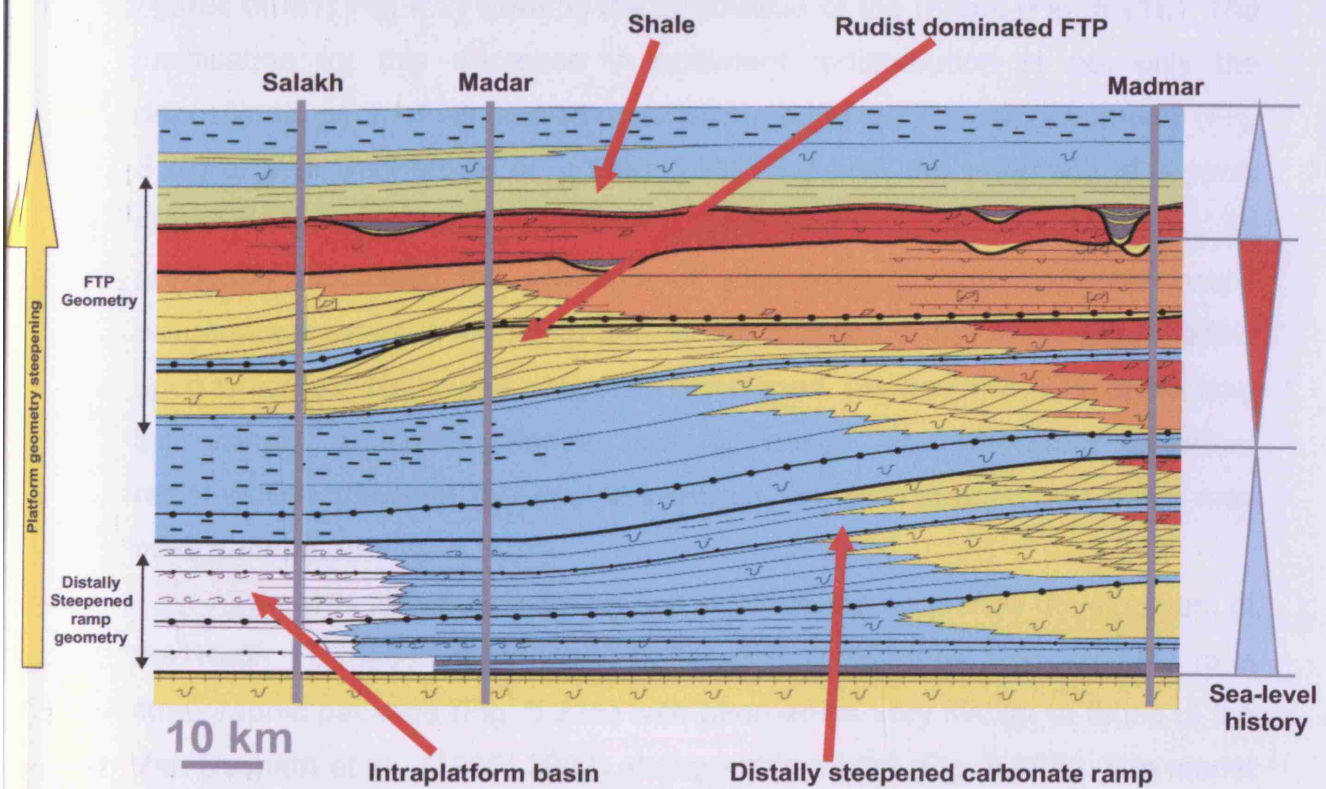
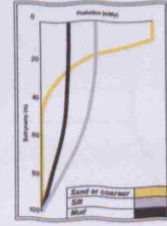
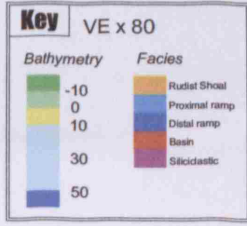
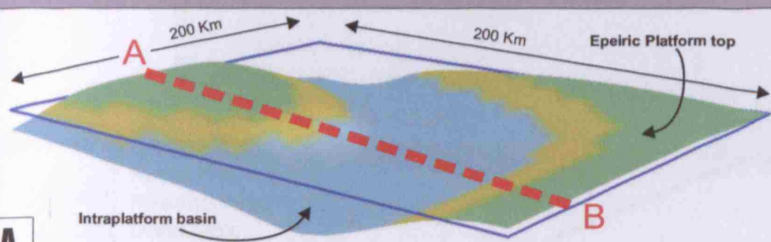


Figure 5.20. Seismic and stratigraphic data for the Middle Cretaceous Natih Formation. A) Seismic line of the Natih Formation displaying high angle clinoforms prograding into the intraplateform basin. Clinoforms have a maximum recorded gradient of 35°, which is commonly much less. Seismic modified from Droste and Van Steenwinkel (2004). B) Natih Formation depositional environments and facies. Modified from Van Buchem et al., (1996).

account for these changes in platform geometry, that of sediment redistribution. The models presented in figure 5.21 (M14) therefore vary from the work of Van Buchem et al., (1996; 2002) in that basin margin platform geometry is controlled by the magnitude of sediment redistribution as opposed to overall sea-level oscillation control. Sediment transport in the model simulating the development of the Natih E member (Fig 5.21, M14) varies throughout the duration of the model. The early part of the sequence (Fig. 5.21B) is modelled with 'typical' ramp like sediment transport parameters, the rates of which were derived from the results of M1, the values of which fall within the ramp prone space of the parameter plots seen in the results and figures of M1 (Fig. 4.2). The magnitude of sediment transport decreases throughout the remainder of the model before reaching 'typical' FTP like sediment transport parameters (again derived from the results and figures of M1, Fig. 4.2) towards the conclusion of the model (Fig. 5.21E). The justification for this decrease in sediment redistribution is not only the depositional geometries viewed on seismic and in the depositional model (Fig. 5.20) of Van Buchem et al., (1996; 2002) but also the presence of organic material within the Natih Formation (Droste and Van Steenwinkel, 2004). As previously discussed the presence of such material likely indicates poorly oxygenated waters, suggesting that as the margins of the intraplatform basin upon which the Natih was deposited developed, the basin may have become increasingly restricted, hence tidal exchange and therefore sediment redistribution between the epeiric platform top and intraplatform basin may have decreased.

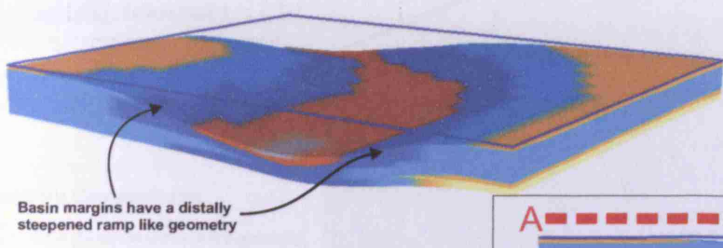
The M14 forward model results illustrate the sequence development of the Natih Formation from initial bathymetric conditions (Fig. 5.21A), to a stratigraphic package (Fig. 5.21F) with geometries very similar to those of the Van Buchem et al., (1996; 2002) stratigraphic model (Fig. 5.20B). The model depicts an early phase in which the sediment deposited upon the margins of the basin closely mimics the underlying bathymetry (refer to Fig. 5.6 and 5.7) forming a geometry which is most accurately described as a distally steepened ramp (Fig. 5.21B). A decreasing magnitude of sediment redistribution results in a steepening of the sediment deposited on the basin margins (Fig. 5.21D) ultimately resulting in the development of a FTP

Modelled Geometries

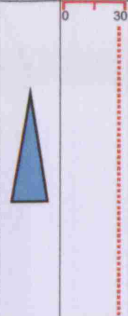
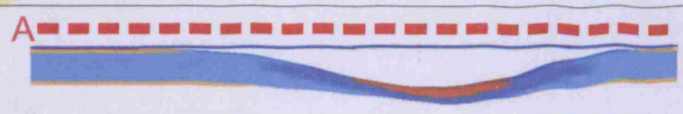


Sea-level trend
Sand or coarser diffusion coefficient (Km²/Ky)

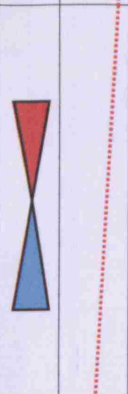
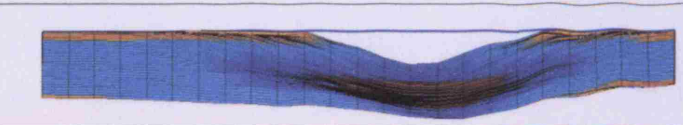
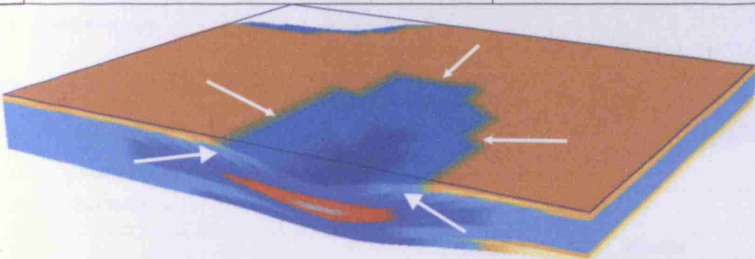
A.



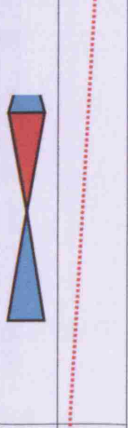
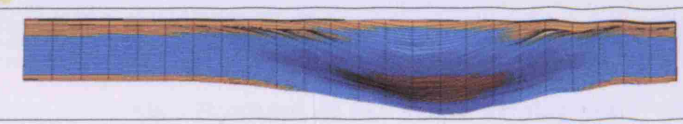
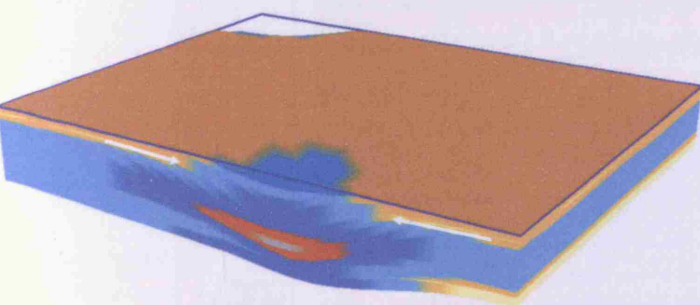
Basin margins have a distally steepened ramp like geometry



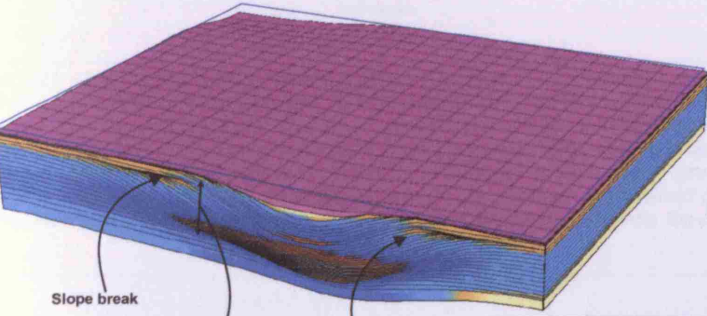
B.



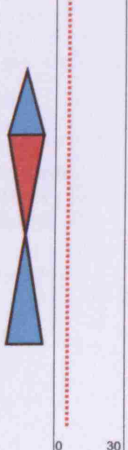
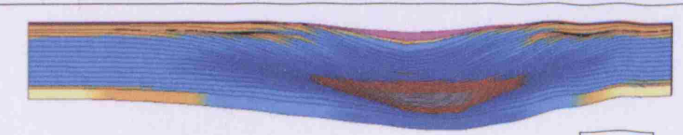
C.



D.



Slope break
FTP geometry
Clinoforms



E.

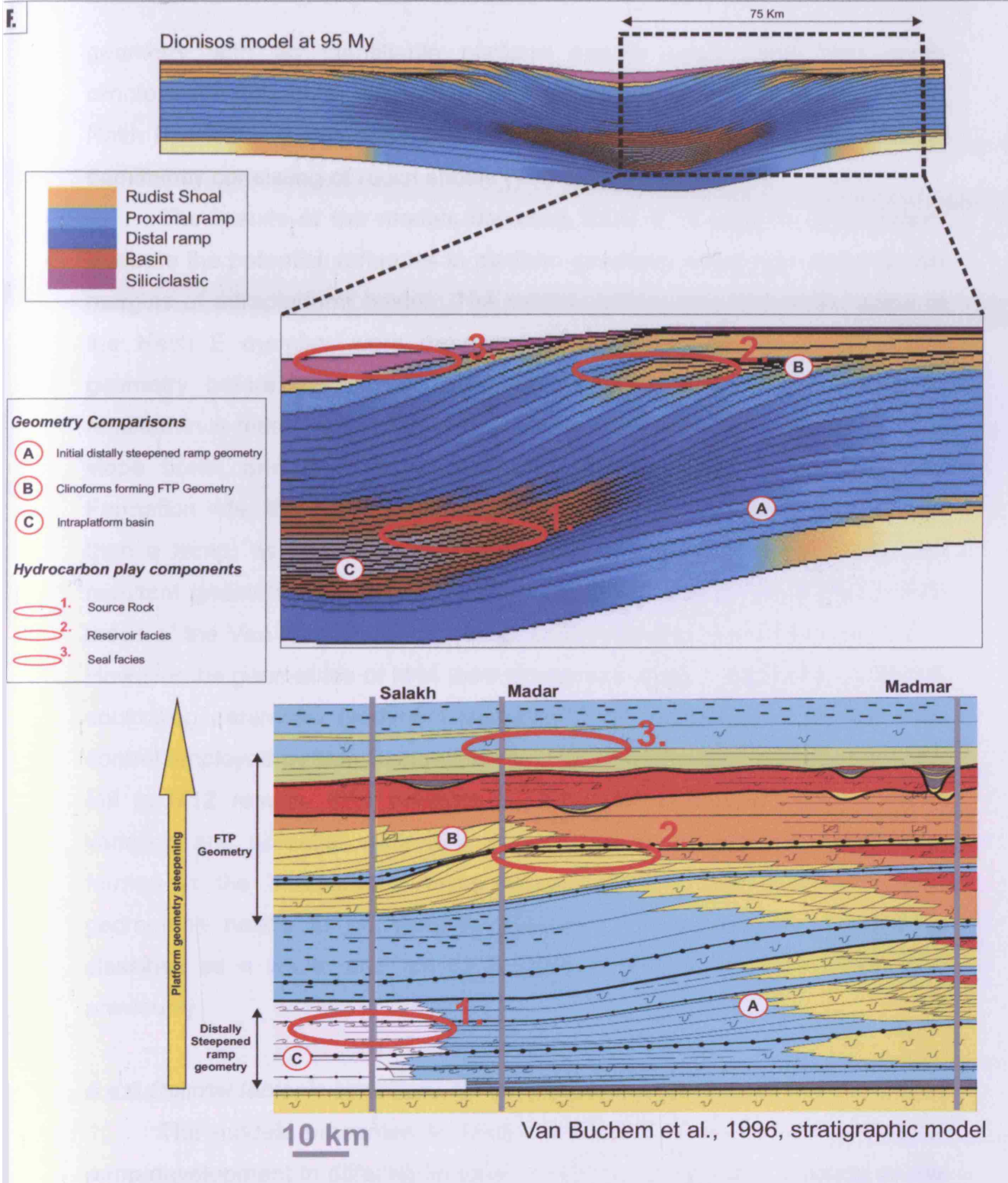


Figure 5.21. M14 forward model results. A) Initial basement bathymetry for forward model is based on the top surface of the Natih F member, basin depth does not exceed 30 m. Cross section location applicable for B-E. B) High sediment diffusion coefficients result in deposited sediment closely mimicking the underlying bathymetry upon the margins of the intraplatform basin. Platform geometries are most accurately described as a distally steepened ramp. C-D) Decreasing magnitude of sediment redistribution results in the steepening of the sediment deposited on the basin margins, ultimately resulting in the development of a FTP geometry (E) with an identifiable platform margin break of slope, and high angle clinoforms. F) Comparison of modelled geometries (top 2 diagrams) with the stratigraphic model of Van Buchem et al., (1996) displays a good correlation. Model also depicts the distribution and heterogeneities of source, reservoir and seal facies.

geometry with an identifiable platform margin break, and high angle clinoforms. It should be noted that the development of these clinoforms in the Natih Formation is facilitated by the coarse nature of the carbonate factory, dominantly consisting of rudist shoals (Van Buchem et al., 1996; 2002).

The results of the models depicting Natih E Formation development illustrate the potential variances in platform geometry which can occur on the margins of intraplateau basins. The models portray how the initial strata of the Natih E member were deposited in a distally steepened ramp like geometry before basin restriction and decreased sediment redistribution resulted in a more FTP mode of deposition. The presence of a well defined slope break and high angle clinoforms throughout the majority of the Formation infer the Natih E member would be better described as an FTP, than a ramp, as has been previously done. It is also significant that the resultant geometries developed in M14 are a reasonably close match with those of the Van Buchem et al., (1996; 2002) depositional model (Fig. 5.21). However the geometries of M14 were developed using a significantly different controlling parameter (sediment transport) than the sequence stratigraphic control employed by Van Buchem et al., (1996; 2002). In combination with the M9 to M12 results, M14 provides a useful insight into the development; variation and potential controlling parameters on the platform geometries formed in the intraplateau basin setting. Future classification of these geometries needs to be carefully assessed as these systems need to be classified as a whole and not as a single component as has been done previously.

5.4.5 Optimal tectonic conditions for ramp development – Summary

The models presented in section 5.4 enhance our understanding for ramp development in differing tectonic conditions, specifically focusing on the controls which facilitate ramp growth in each tectonic setting. Ramp development is shown to be possible in a number of tectonic settings, including passive margins, foreland, extensional and intraplateau basins, and the combination of tectonic characteristics which facilitate ramp growth in each of these settings has been outlined. The models suggest sediment deposited under ramp prone conditions act as drapes; therefore a necessity in

each of the tectonic settings is an initial flat substrate upon which the ramp can develop and drape. The subsidence regime affecting this substrate is also shown to be of importance, as rotational subsidence appears to favour ramp development, as seen in the foreland basin and fault block systems, while differential subsidence forming shallow depressions can affect platform progradation, or under suitable sediment transport and production rates form distally steepened ramp geometries, as seen in the intraplatform basin setting. The control these tectonic characteristics exert on the development of platform geometry are additional parameters (to those of sediment production and transport discussed in Chapter 4, Fig. 4.10) in the multidimensional parameter space for carbonate platform development. These parameters and their influence on the multidimensional parameter space are discussed in section 5.6.1.

In addition to these parameters, the influence exerted on such a parameter space by sea-level oscillations has not previously been investigated. Considerable work has been conducted on assessing the influence changes in relative sea-level exert on well developed platform systems, however little has been done to understand the control these changes may have on overall platform geometry. The following section aims to investigate this with the aid of the APE modelling method, in an attempt to add an additional dimension to the multidimensional parameter space for carbonate platform development.

5.5 Investigating the influence of relative sea-level oscillations on platform development

Numerous studies have investigated the effects of sea-level oscillations on well developed FTP systems (Goldhammer et al., 1993; Read, 1998; Barnett et al., 2002; Schlager, 2005). We understand that relatively minor sea-level changes can cause rapid flooding or exposure of platform surfaces in developed FTP settings, while the gentle depositional slope and absence of a major slope break in the carbonate ramp environment means the major exposure and flooding surfaces are generally diachronous under similar rates of change. Moreover, in comparison with FTP's the sequence stratigraphy of

carbonate ramps tends to be somewhat straightforward, with relatively simple geometries produced by facies belt migration up or down the ramp in response to long-term relative sea-level changes. However, the majority of these studies concentrate on well developed systems and do not investigate or discuss what control sea-level change may exert on overall platform geometry if oscillations are occurring from the onset of carbonate deposition.

5.5.1 *Ice-house versus Greenhouse carbonate systems*

An investigation into the control these oscillations exert on overall platform geometry can be conducted by analysing the geometries formed during differing global climatic conditions. A similar approach was adopted by Read (1998), who identified key differences in the ramp geometries formed under greenhouse versus ice-house conditions, classifying the resultant geometries as either 'low-gradient' or 'high-gradient' ramps. Read's (1998) models which imply that sea-level change can exert a control on overall platform geometry are investigated in Model set 15 (M15), which models three different systems simulating differing global climatic conditions; a greenhouse system (Fig. 5.22A) and two ice-house systems (Fig. 5.22B and 5.22C). M15 was run with a shorter model duration (1 My), but all other parameters remained constant with those used in M1 (Table 3.2), and using the results obtained in the previous sections the models were run under both ramp prone (high transport, moderate production) and FTP prone (low transport, moderate production) conditions (Table 3.2), and the resultant geometries analysed. The platform geometries modelled under greenhouse conditions (Fig. 5.22A) follow the same relationships illustrated in the initial models sets 1 and 2; high transport results in the development of low angle ramp systems, while a lack of transport results in the development of a steep margin and an FTP geometry. The platform-interior facies in the FTP example (Fig. 5.22A) depicts characteristic greenhouse layer-cake stacking patterns (i.e. Lehrmann and Goldhammer, 1999). Conversely the ice-house examples (Fig. 5.22B and 5.22C) depict quite different results to those seen previously, illustrating a tendency towards ramp generation regardless of the transport regime. As expected high transport conditions create a ramp geometry. However low transport conditions do not result in FTP generation but also result in ramp

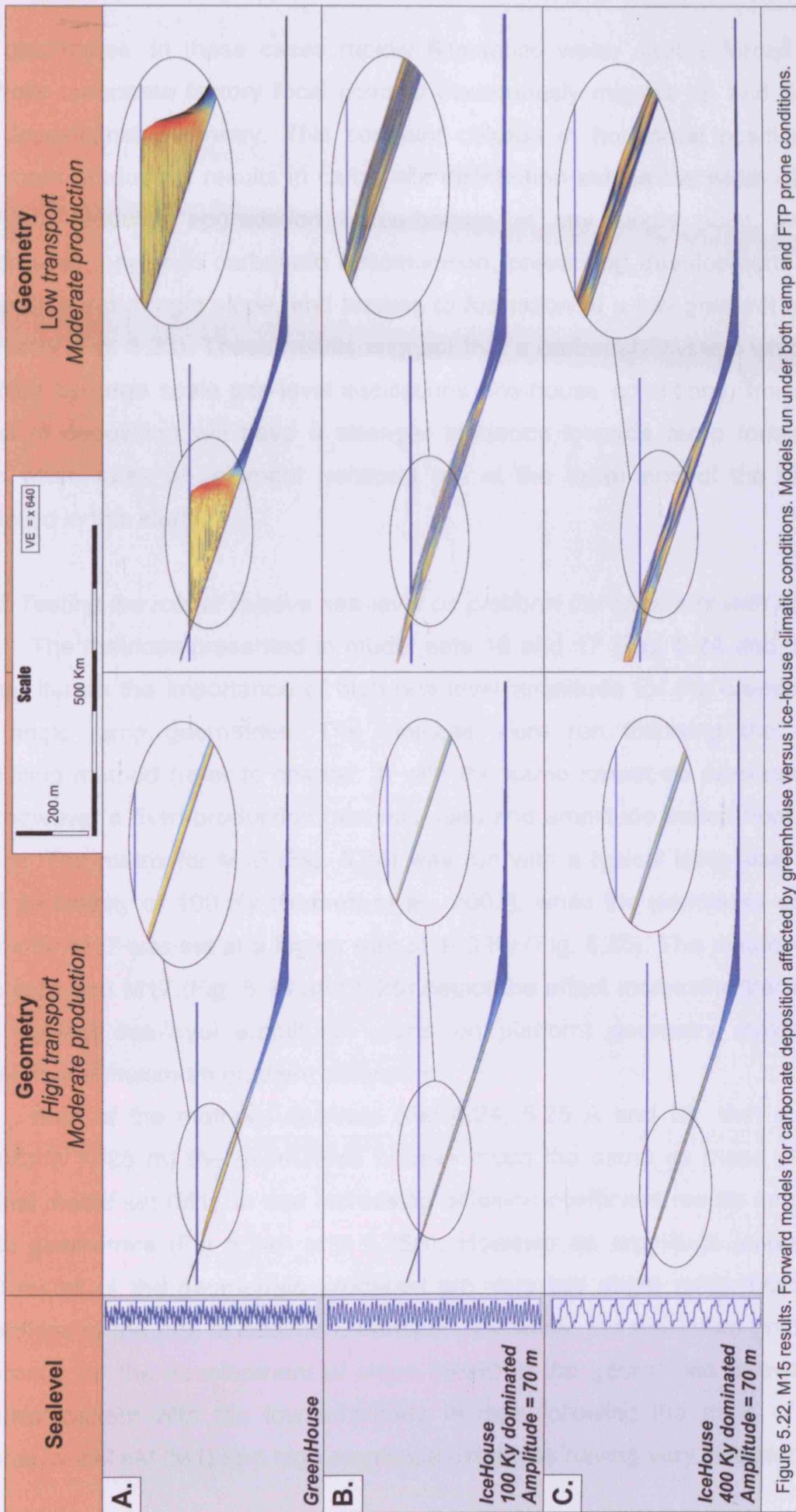


Figure 5.22. M15 results. Forward models for carbonate deposition affected by greenhouse versus ice-house climatic conditions. Models run under both ramp and FTP prone conditions.

like geometries. In these cases rapidly fluctuating water depths forced the euphotic carbonate factory focal point to continuously migrate up and down the depositional geometry. This constant change in horizontal position of maximum production results in carbonate distribution across the width of the platform, reducing aggradation of carbonate at any single point, which suppresses long-term carbonate accumulation, preventing development of a steep platform-margin slope, and leading to formation of a low gradient ramp geometry (Fig. 5.23). These results suggest that a carbonate system which is affected by large scale sea-level oscillations (ice-house conditions) from the onset of deposition will have a stronger tendency towards ramp formation even when rates of sediment transport are at the lower end of the range modelled in this study.

5.5.2 Testing the role of relative sea-level on platform development with APE

The matrices presented in model sets 16 and 17 (Fig. 5.24 and 5.25) further iterate the importance of high sea level amplitude for the creation of low angle ramp geometries. The matrices were run following the APE modelling method (refer to chapter 3) with the same format as presented in M1, however a fixed production rate was used and amplitude varied from 0 to 100 m. The matrix for M16 (Fig. 5.24) was run with a typical ice-house sea-level periodicity of 100 Ky (Barnett et al., 2002), while the periodicity of the matrix for M17 was set at a higher rate of 400 Ky (Fig. 5.25). The matrices for both M16 and M17 (Fig. 5.24 and 5.25) depict the effect increasing transport rate against sea-level amplitude exerts on platform geometry maximum gradient and maximum gradient difference.

Both of the matrices illustrate (Fig 5.24, 5.25 A and B) that at low amplitude (0-25 m) the geometries behave much the same as those of the original model set (M1), in that increasing diffusion coefficient results in lower angle geometries (Fig 5.24A and 5.25A). However as amplitude increases (>50 m) all of the geometries produced are very low angle ramp systems, regardless of the rate of sediment transport. Likewise, the maximum gradient difference (or the development of slope break) of the geometries follows an identical pattern with the low amplitude models following the trend of the original model set (M1) and high amplitude examples having very little slope

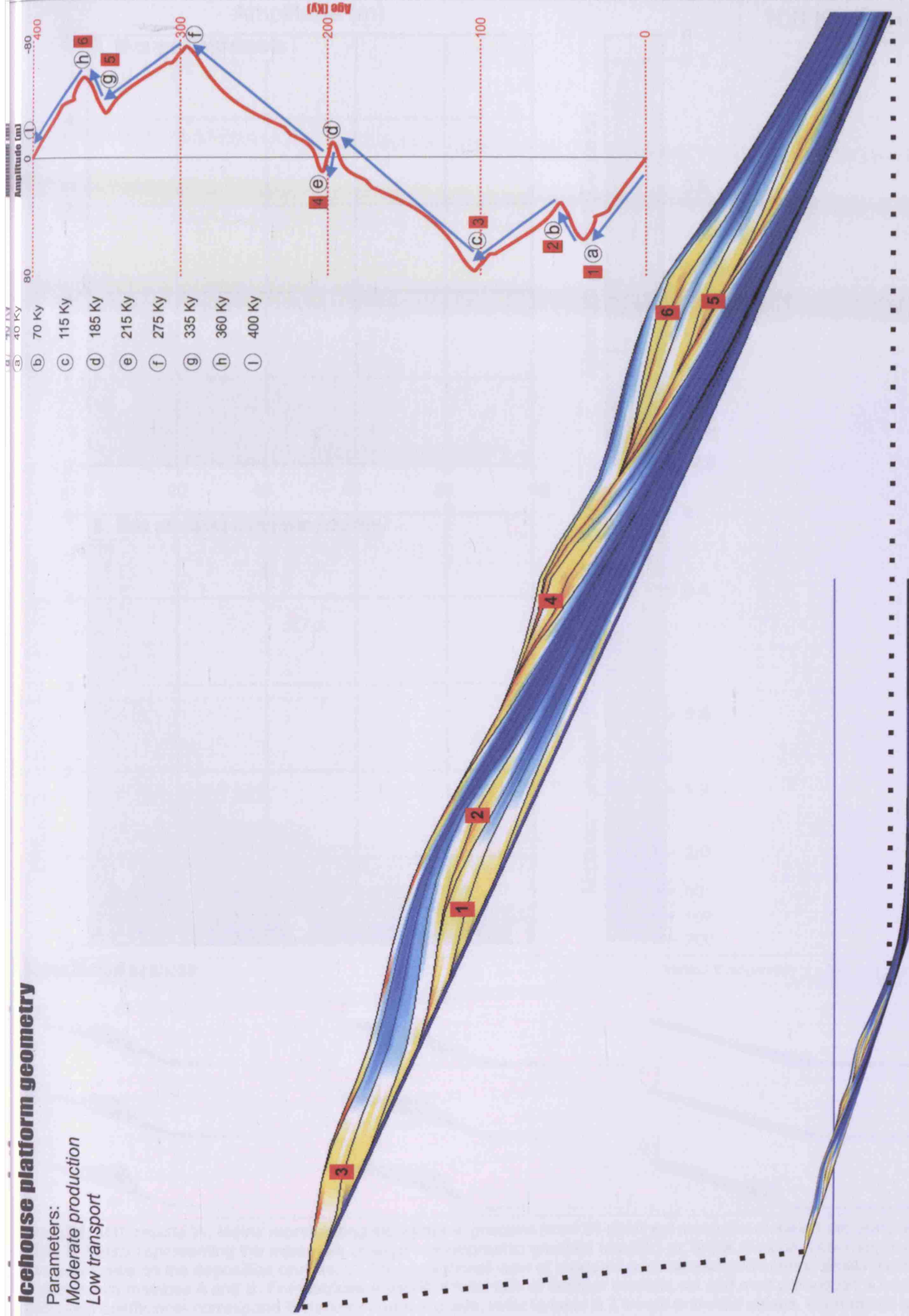
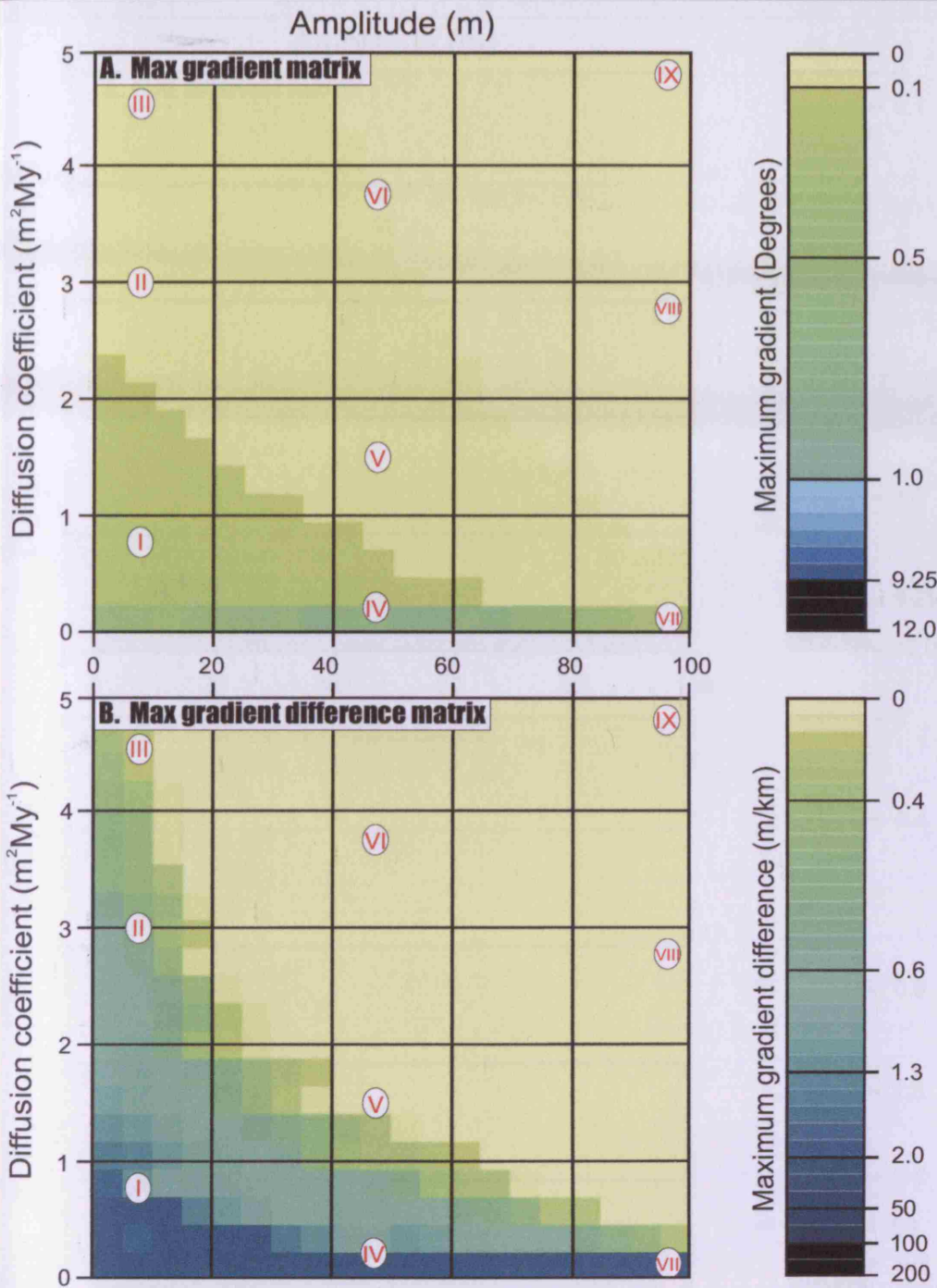


Figure 5.23. Magnified version of icehouse system run in figure 5.21C. The model was terminated at 400 Ky to depict effects of single 400 Ky cycle. Even under low transport conditions the overall geometry is ramp like in character due to the rapidly fluctuating water depths forcing the carbonate factory focal point to continuously migrate up and down the depositional geometry, thus suppressing long-term carbonate accumulation at any single point.

100 Ky Period



C. Depositional profiles

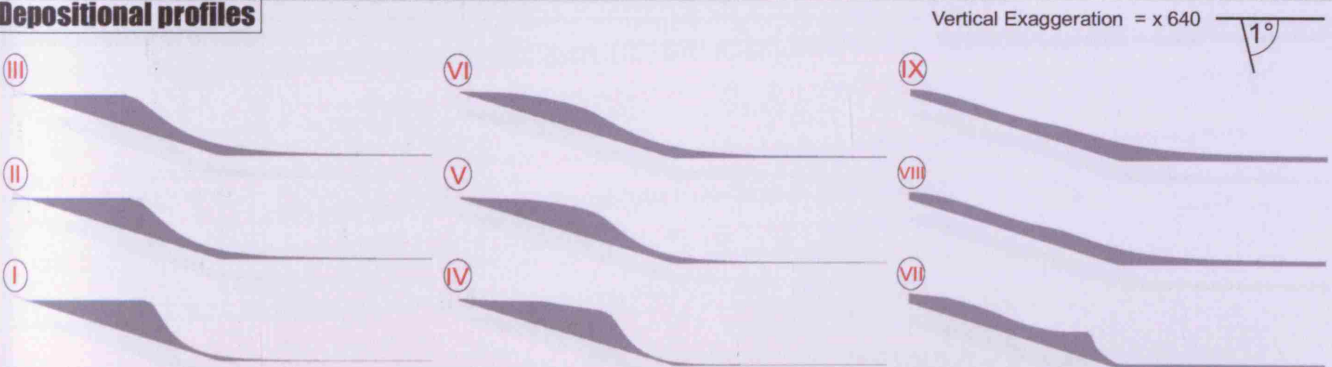
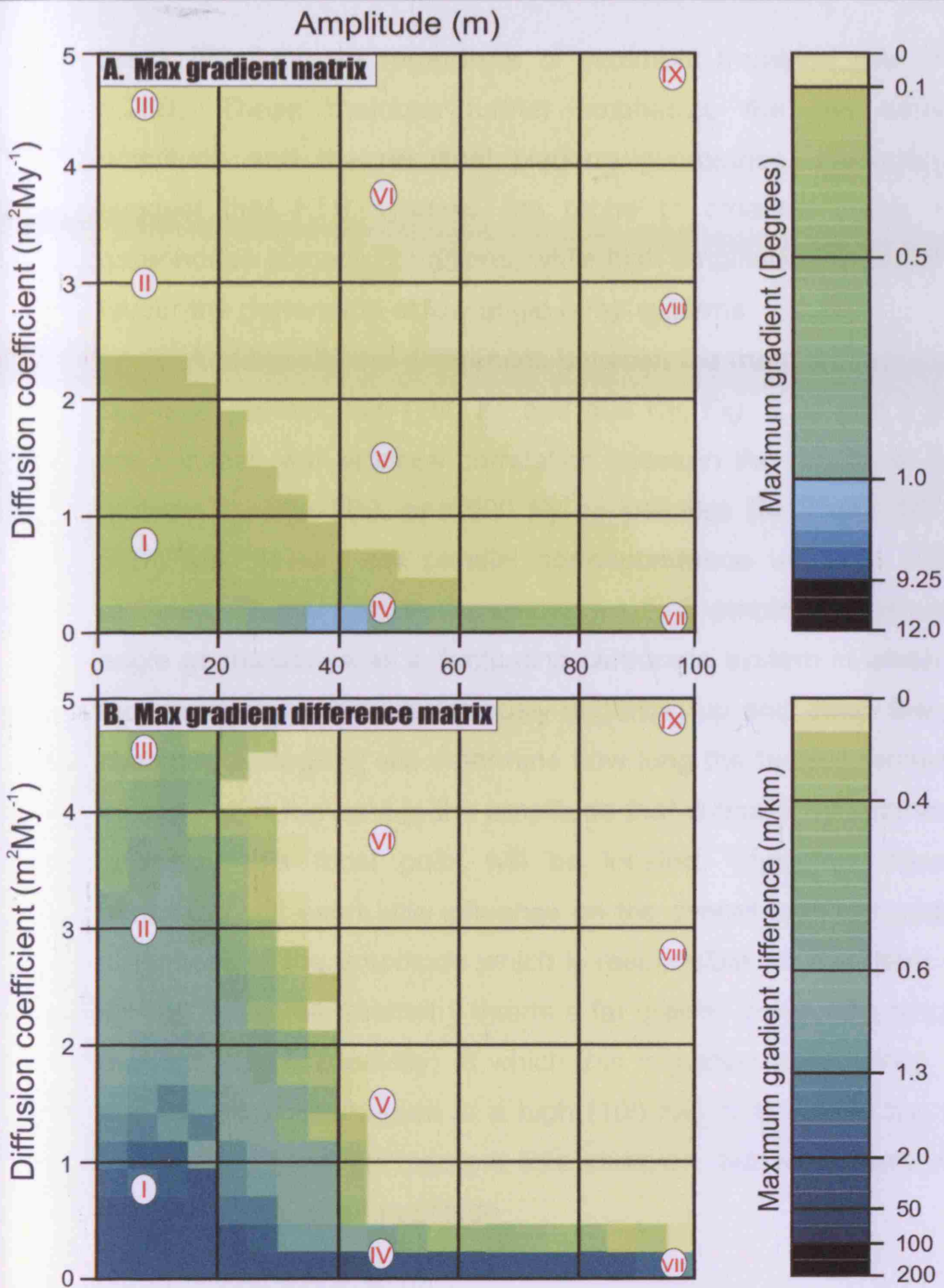


Figure 5.24. M16 results. A: Matrix representing topographic gradient (max S) obtained along the modeled depositional profiles. B: Matrix representing the maximum change in topographic gradient (max ΔS), or break of slope, occurring between two adjacent cells on the deposition profiles. C: Cross-sectional view of modeled depositional geometries, profile locations correspond with matrices A and B. For matrices A and B a fixed rate of sand or coarser, silt and mud production is used, and diffusion coefficients correspond to sand or coarser grade, refer to table 3.2 for silt and mud values. Each model is run with a 100 Ky periodicity and an increasing sea-level amplitude.

400 Ky Period



Depositional profiles

Vertical Exaggeration = x 640

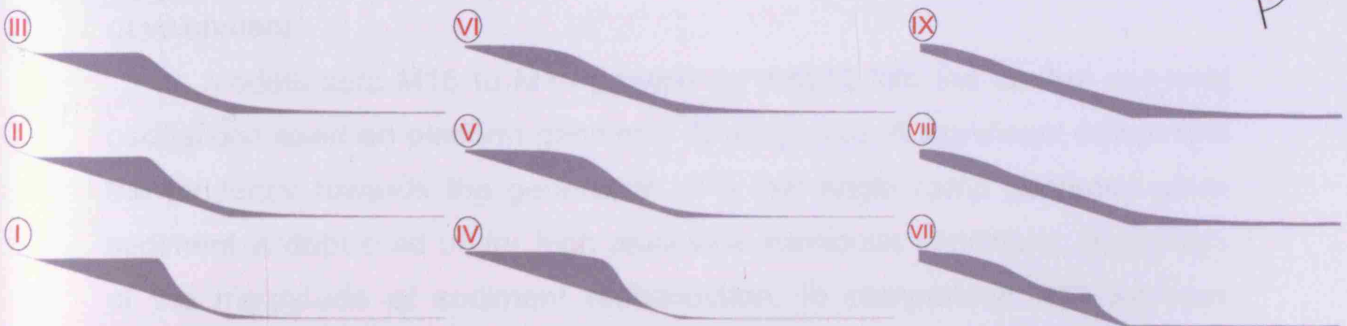


Figure 5.25. M17 results. Same as Figure 5.25 but models run with a 400 Ky periodicity.

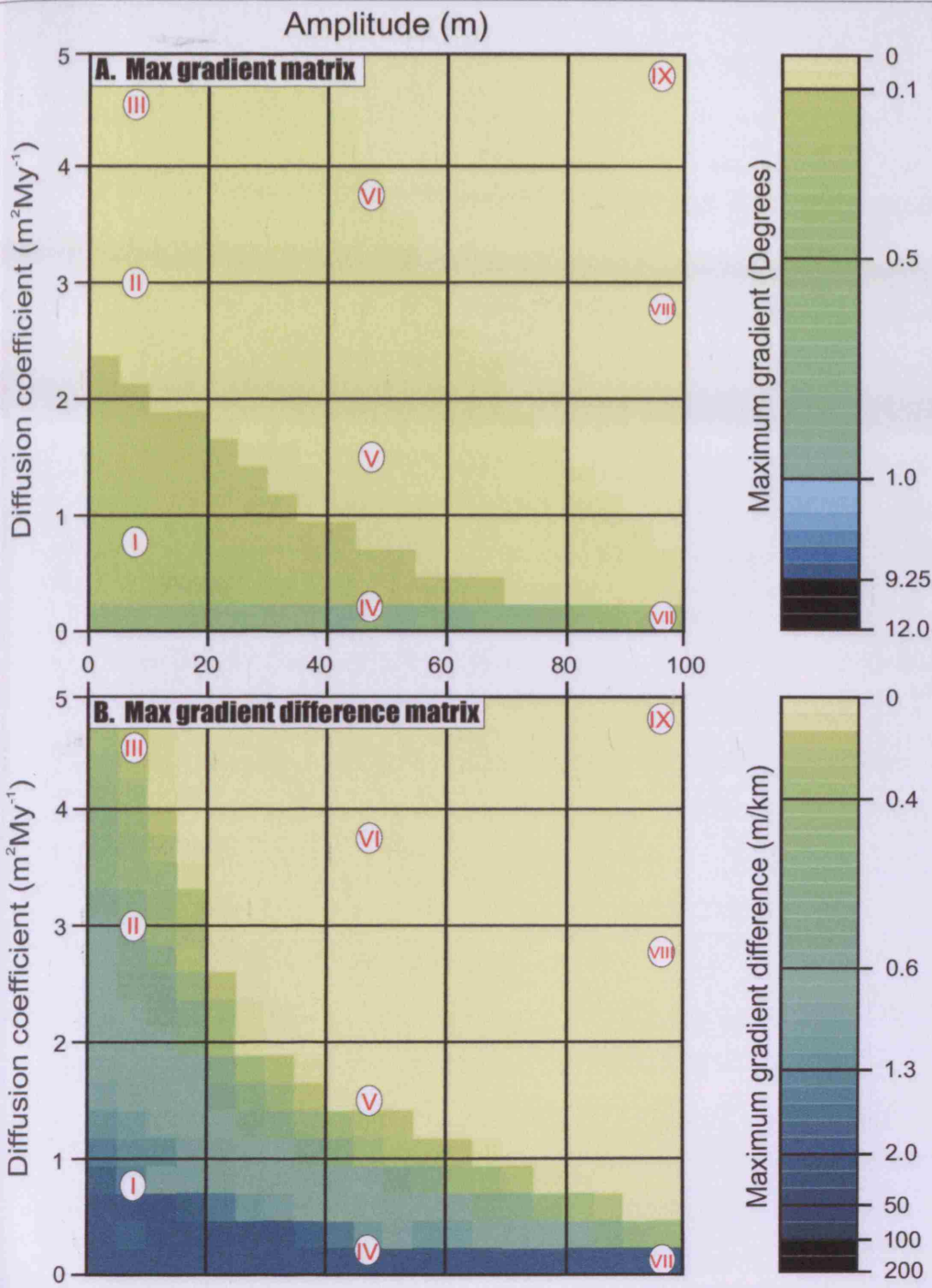
break development regardless of sediment transport rate (Fig 5.24B and 5.25B). These matrices further emphasize the link between sea-level amplitude and the resultant platform geometries, presenting evidence to suggest that FTP systems are prone to creation during low amplitude, greenhouse climatic conditions, while high amplitude ice-house conditions will favour the generation of low angle ramp systems.

Additionally the differences between the matrices representing different sea-level periodicities (100 Ky and 400 Ky, Fig. 5.24 and 5.25 respectively) are minimal, with a close correlation between the results of both. Additional matrices run for 200, and 500 Ky periodicities (M18 and 19, Figs 5.26 and 5.27) also show near parallel correspondence with the 100 and 200 Ky matrices. The explanation provided for high amplitude systems forming low angle geometries was a fluctuating carbonate system in which the carbonate factory focal point is continuously migrating up and down the geometry. The changing periodicity will determine how long the factory remains at a specific focal point; however it is the amplitude that critically determines where on the geometry this focal point will be located. Therefore minor changes in periodicity will exert little influence on the overall platform geometry, and the magnitude of the amplitude which is responsible for migrating this focal point up and down the geometry exerts a far greater control on resultant geometry than the rate (periodicity) at which this migration is occurring. Thus implying that the geometries seen in a high (100 Ky) or low (400 Ky) rate ice-house carbonate system will present little variation, but will in fact be governed by the rate of sea-level amplitude.

5.5.3. Summary of relative sea-level oscillation control on platform development

Models sets M15 to M19 provide an insight into the control sea-level oscillations exert on platform geometry development. A significant outcome is the tendency towards the generation of a low angle ramp geometry when sediment is deposited under high amplitude ice-house conditions, regardless of the magnitude of sediment redistribution. In comparison with previous investigations into similar controls, principally the work of Read (1998), the models presented here are in general agreement. Problematic terminology in

200 Ky Period



C. Depositional profiles

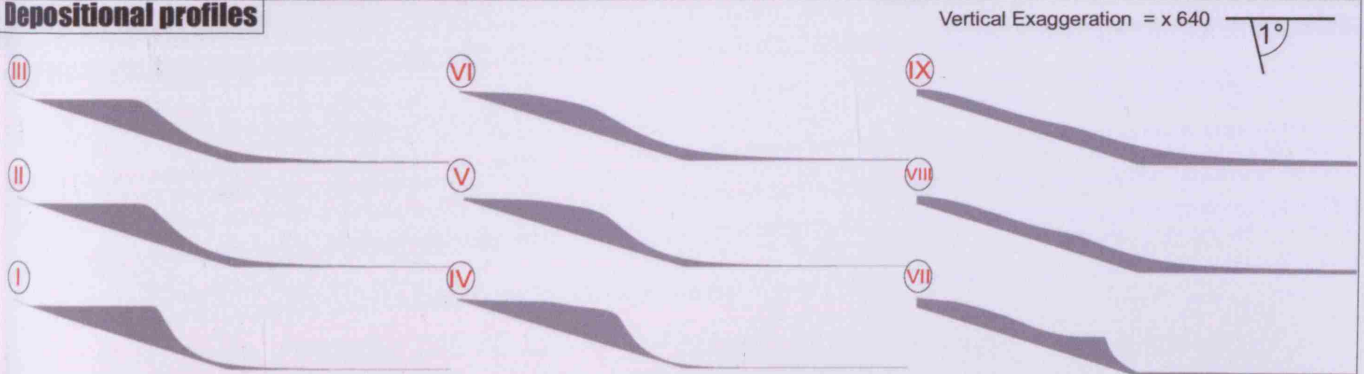
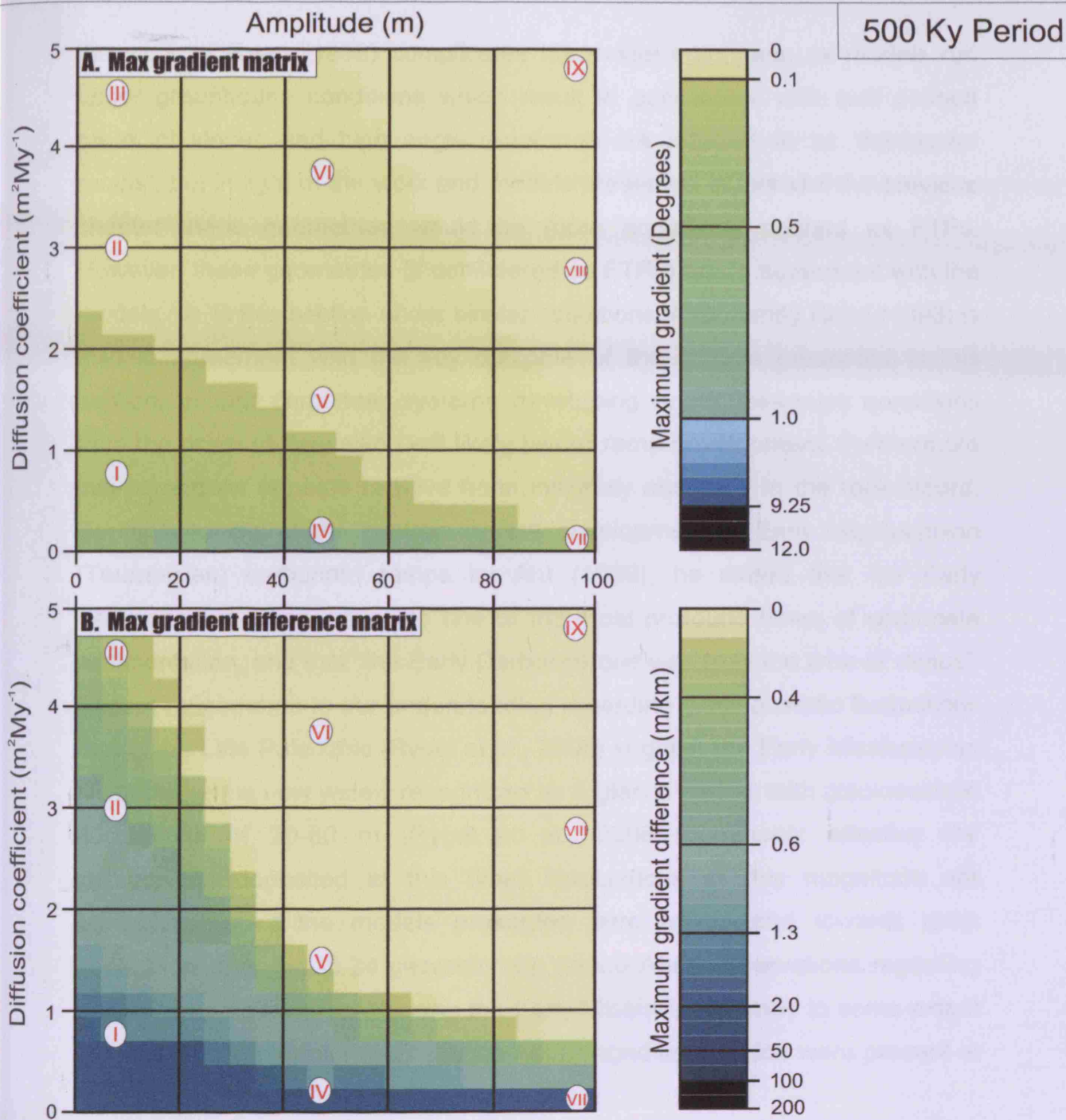


Figure 5.26. M18 results. Same as Figure 5.24 but models run with a 200 Ky periodicity.



C. Depositional profiles

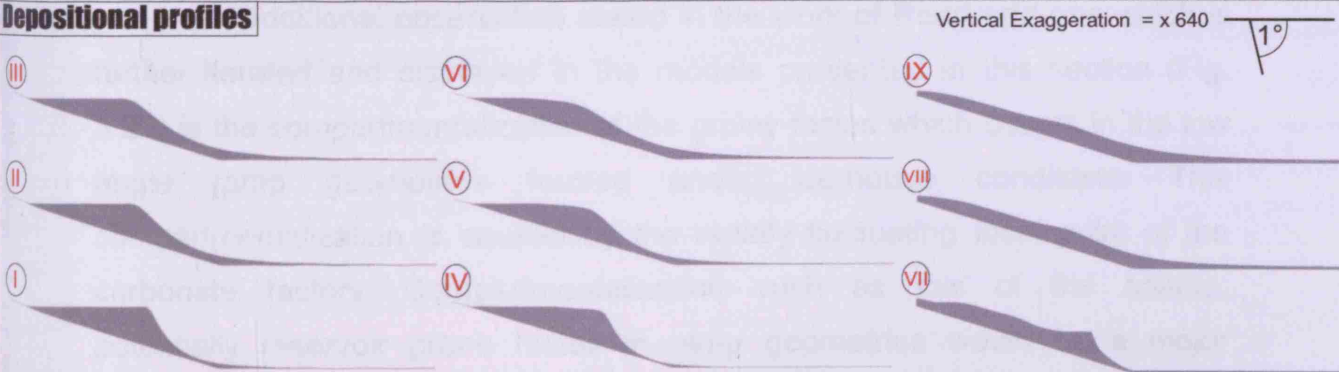


Figure 5.27. M19 results. Same as Figure 5.24 but models run with a 500 Ky periodicity.

the work of Read (1998) complicates his model outcomes, as models run under greenhouse conditions which result in geometries with well defined break of slopes and high angle clinoforms are referred to as 'flat-topped ramps', but in light of the work and models presented in this and the previous chapter these geometries would be more accurately defined as FTPs. However, these geometries (if considered as FTPs) are in agreement with the models run in this section under similar conditions. Importantly Read (1998) is also in agreement with the key outcome of the models presented in this section, in that carbonate systems developing under ice-house conditions from the onset of deposition will likely favour ramp development. Furthermore this correlation appears to have been indirectly observed in the rock record. During a review of the controls on the development of Early Mississippian (Tournaisian) carbonate ramps by Ahr (1989), he stated that the Early Carboniferous was world-wide one of the most profound times of carbonate sedimentation, and that "the Early Carboniferous was truly the time of ramps". Recent refinements to our understanding regarding glacioeustatic fluctuations during the Late Paleozoic (Rygel et al., 2008) suggest the Early Mississippian (Tournaisian) is now widely recognized as a glacial period, with glacioeustatic fluctuations of 20-60 m (Rygel et al., 2008) commonly affecting the successions deposited at this time. Fluctuations of this magnitude are representative of the models presented here which tend towards ramp generation (e.g. Fig. 5.24 geometry vi), hence Ahr's observations regarding prolific ramp development during the Early Mississippian may to some extent have been a consequence of the ice-house conditions which were present at the time.

An additional observation stated in the work of Read and one which is further iterated and displayed in the models presented in this section (Fig. 5.23) is the compartmentalization of the grainy facies which occurs in the low angle ramp geometries formed under ice-house conditions. This compartmentalization is caused by the rapidly fluctuating focal point of the carbonate factory. Compartmentalization such as this of the coarse, potentially reservoir prone facies in ramp geometries would be a major consideration when assessing any potential hydrocarbon play in such a geometry.

The observations and results discussed throughout section 5.5 appear to generally be in agreement with the work of Read (1998). The control sea-level oscillations exert on platform geometry were not however fully developed in this previous study, as the data set was limited to individual model runs, with less than 10 models in total analysed. The development of the APE modelling method (refer to section 3.3) has allowed over 800 model runs to be conducted through model sets M15 to M19. This significantly increased data set facilitated a greater number of parameter variations to be analysed, thus enhancing our understanding of relative sea-level oscillation control on platform geometry development.

In addition to the sediment transport and production regime (discussed in chapter 4, Fig 4.10), and the syndepositional control exerted by variances in basin subsidence (section 5.3.2, Fig 5.5), the magnitude of sea-level oscillation can also be considered an additional parameter influencing the multidimensional parameter space for carbonate platform development (refer to section 5.6.1). As with the previous parameters, it is likely a continuum of geometries exist, the development of which are controlled by the magnitude of sea-level amplitude (Fig. 5.28). The models presented in this section likely only provide us with small selection of the potential variances in platform geometry which may occur due to varying sea-level amplitude. The models do however illustrate the general trend of platform geometries; implying sediment deposited under low amplitude, greenhouse conditions will likely behave in a similar fashion to previous models, in that under low rates of sediment redistribution the most probable geometry development will be that of a steep margined FTP (Geometry I, Fig.5.28). Conversely, as sea-level amplitude increases, and becomes more representative of ice-house conditions, platform development will trend towards low angle ramp geometries, due to the rapidly fluctuating focal point of the carbonate factory, regardless of the magnitude of sediment redistribution (Geometry II and IV, Fig. 5.28). The parameter space developed through the models of this section, and presented in figure 5.28, provide an additional dimension in the multidimensional parameter space for carbonate platform development (section 5.6.1, Fig. 5.29).

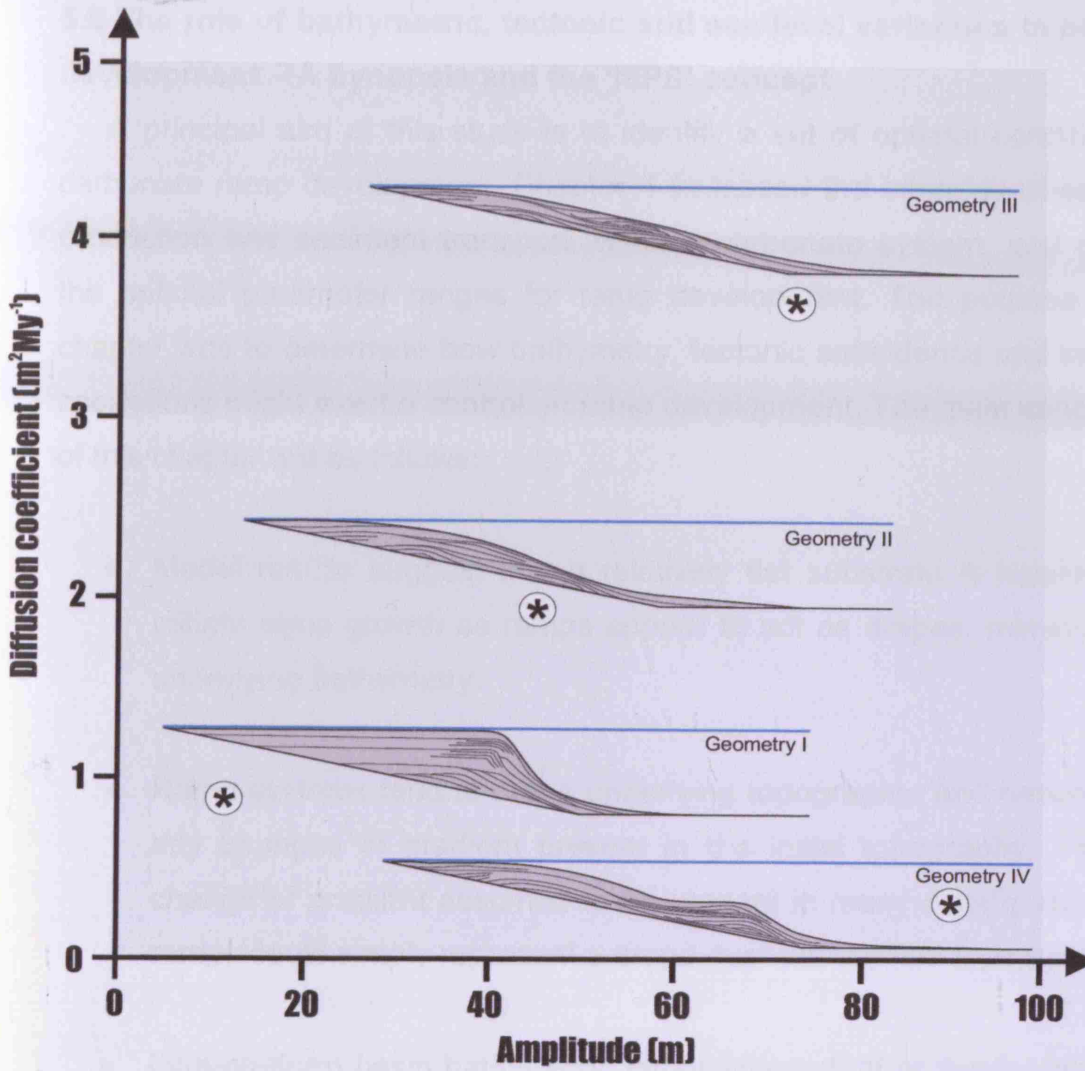


Figure 5.28. Representative gradational geometries created by interaction of sediment transport rate and the amplitude of relative sea-level change. Geometry I, a low amplitude (greenhouse) system with low sediment redistribution results in an FTP geometry, following the relationship seen in previous models. Geometry II has a higher amplitude of sea-level change, more akin to an ice-house system, and still a relatively low rate of sediment redistribution, however a low angle ramp geometry has developed. The fluctuating water depths due to the higher amplitude have forced the carbonate factory focal point to continuously migrate up and down the depositional geometry, resulting in carbonate deposition across the width of the platform, reducing aggradation of carbonate at any single point, suppressing long-term carbonate accumulation, preventing development of a steep platform-margin slope, resulting in the formation of a low angle ramp geometry. Geometry IV has almost zero sediment redistribution, however the high amplitude results in carbonate being deposited across the platform, preventing the development of a platform margin even with the significantly low rate of sediment transport.

5.6 The role of bathymetric, tectonic and sea-level variations in platform development – A synopsis and the ‘MPS’ concept

A principal aim of this study is to identify a set of optimal conditions for carbonate ramp development. Chapter 4 assessed the interplay of sediment production and sediment transport within a carbonate system, and outlined the optimal parameter ranges for ramp development. The purpose of this chapter was to determine how bathymetry, tectonic subsidence and sea-level oscillations might exert a control on ramp development. The main conclusions of this chapter are as follows:

- Model results suggest that a relatively flat substrate is necessary to initiate ramp growth as ramps appear to act as drapes, mimicking the underlying bathymetry.
- Ramp systems tend to drape underlying topography, and hence inherit any changes in gradient present in the initial topography. Thus the change of gradient assumed to be present in many distally steepened ramps could simply represent a drape over antecedent topography.
- Intra-platform basin bathymetry, either antecedent or syndepositionally generated, for example by faulting, may be an important control on platform geometry, but the degree of influence depends on rates of sediment production, rates of sediment transport and the magnitude of platform-basin relief. Model results suggest that high production rates, or high transport rates, or both, tend to negate the impact of an antecedent intraplatform basin physiography, while low production and/or low transport rate platform margins tend to stack aggradationally over an underlying margin that inhibits progradation further into the basin.
- Rotational subsidence tends to favour ramp development by increasing topographic gradient through time, leading to increased rates of sediment transport, suppressed in-situ accumulation, suppressed

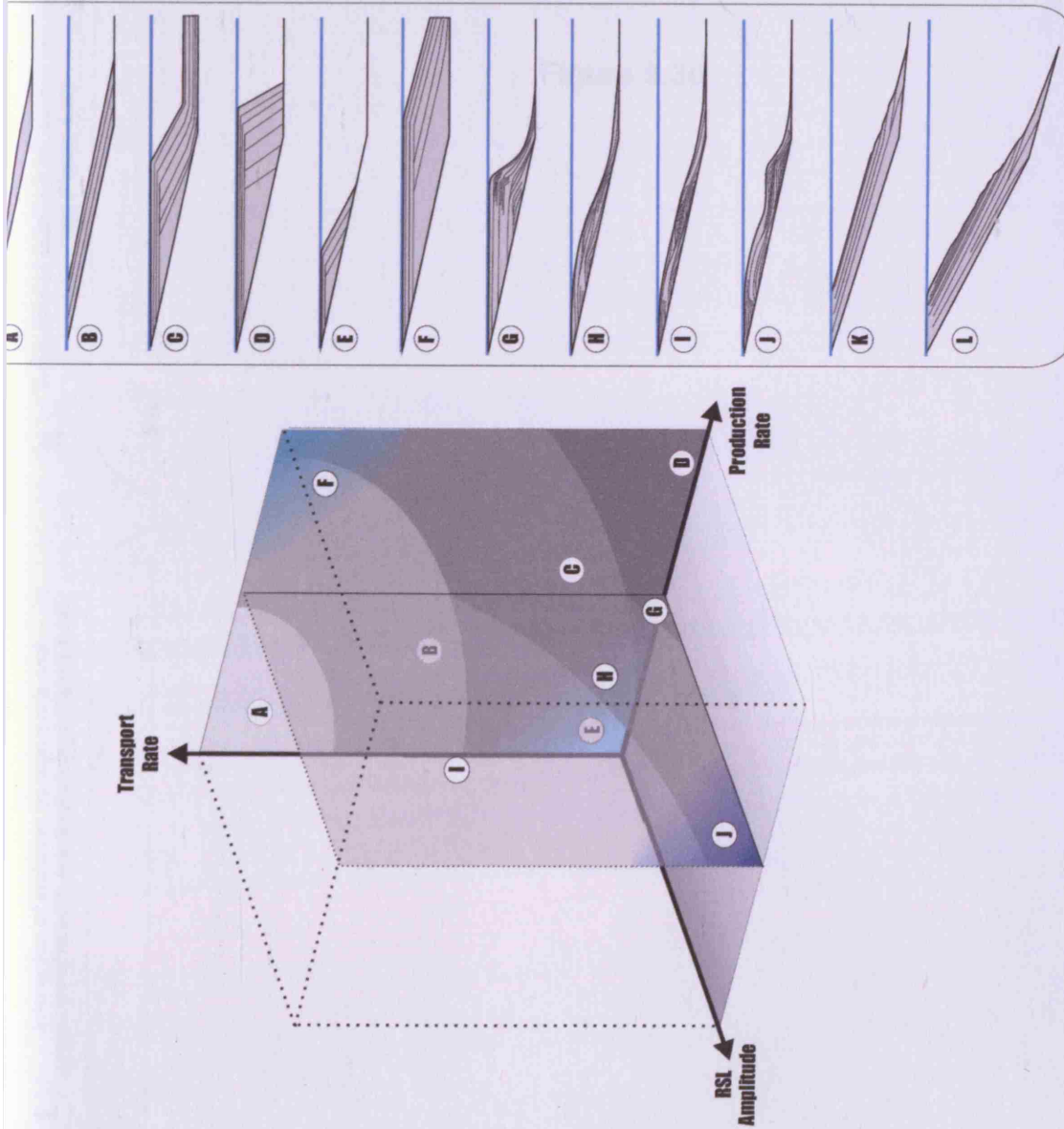
generation of constructional topography and a consequent low-gradient system lacking a significant slope break.

- Model results suggest that in carbonate systems developing in greenhouse climatic conditions (low amplitudes of eustatic sea-level oscillation) ramp growth is likely to be dependent on the sediment transport dynamics of the system, with ramp geometries developed at relatively high rates of sediment transport, and FTPs developed when transport rates are lower and in-situ accumulation dominates.
- However, modelling carbonate systems developed under ice-house conditions suggests a strong tendency towards ramp generation regardless of the carbonate systems sediment transport regime. Under these higher sea-level amplitudes the focal point of the carbonate factory continuously migrates across the substrate inhibiting deposition and margin development at any single point, and thus favouring the development of low angle ramp geometries.

If the parameter variations within this chapter shown to portray a tendency towards ramp development are combined with the results of chapter 4, we have a series of key parameter combinations with which optimal conditions for ramp generation can be predicted.

5.6.1. A *Multidimensional Parameter Space for carbonate platform development: 'MPS'*

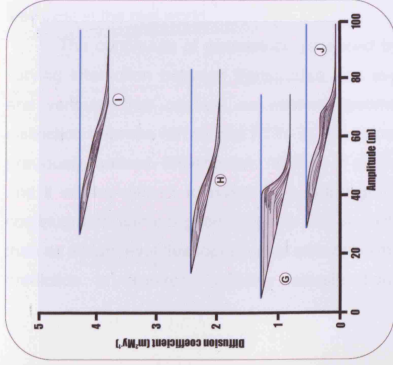
The numerical model results presented in chapters 4 and 5 suggest that carbonate platforms occur as a gradational series of geometries created by interacting processes of production and transport, plus the influence of other controls such as differential subsidence and relative sea-level oscillations. The individual parameter space plots identifying platform geometry variations controlled by sediment transport and amplitude of relative sea-level change (Fig. 5.30 i), sediment production and sediment transport (Fig. 5.30 ii), and sediment transport and rotational subsidence (Fig. 5.30 iii),



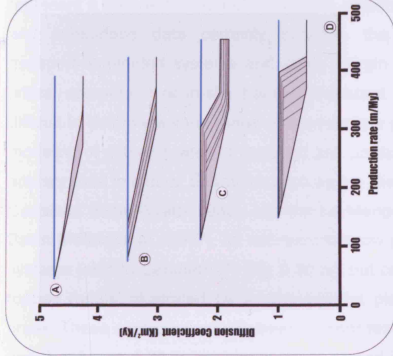
Multidimensional Parameter Space for carbonate platform development: 'MPS'

Figure 5.29. Multidimensional parameter space for carbonate platform development (for parameter space input data refer to Figure 5.30). Two sets of axes are shown representing an illustrative subset of the much larger multidimensional parameter space. Each set of axes is plotted as a three-dimensional cube and example platform geometries are shown in the positions they occur within each three-dimensional parameter space sample. Grey shades illustrate the gradation of geometries that occur and demonstrate hypothetically how these gradations of geometry link across the axes, for example from the transport rate axis to the rotational subsidence axis.

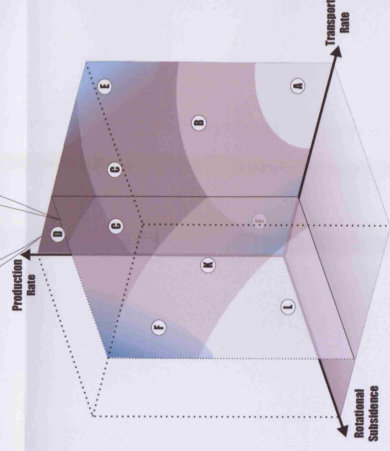
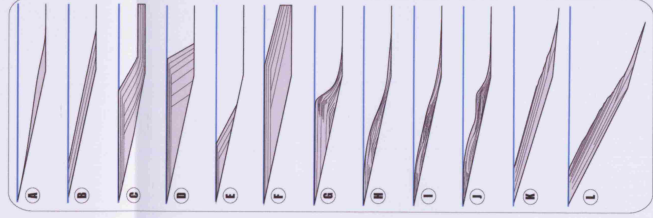
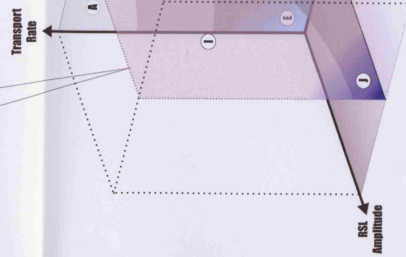
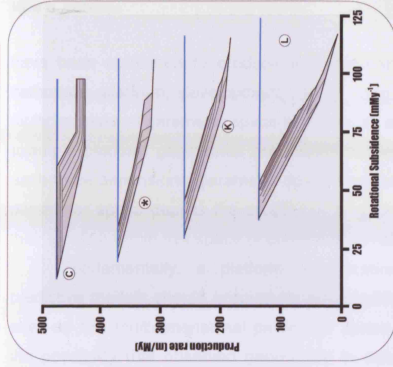
I. Interaction of sediment transport rate and amplitude of relative sea-level change (Figure 5.28)



II. Interaction of sediment production and transport rate (Figure 4.10)



III. Interaction of sediment production rate and rotational subsidence (Figure 5.5)



IV. Multidimensional Parameter Space for carbonate platform development: 'MPS'

Figure 5.30. Synthesis of controls on carbonate platform development. Parameter space plots (I) - (III) combine to produce multidimensional parameter space (IV). (I) Parameter space plot illustrating the control on platform development exerted by the interaction of sediment transport and amplitude of relative sea-level change (refer to figure 5.28 for description of geometries). (II) Same as (I) but illustrating interaction of sediment production and sediment transport (refer to figure 4.10 for description). (III) Same as (I) but illustrating interaction of sediment transport and rotational subsidence (refer to figure 5.5 for description). (IV) Multidimensional parameter space for carbonate platform development. Refer to Figure 5.29 for description.

have been combined to produce a multidimensional parameter space for carbonate platform development, 'MPS' (Fig. 5.29 and 5.30 iv). The multidimensional parameter space is plotted as a three-dimensional cube and example platform geometries are shown in the positions they occur within each three-dimensional parameter space sample (Fig. 5.29 and 5.30 iv). The parameter space depicts the continuum of geometries which may exist and their location within this space of controlling variables.

Fundamentally, a platform classification scheme and associated predictive models should account for any significant variability on any of the axes on this multidimensional parameter space, and also take into account the possibility that observed geometries in outcrop or the subsurface may represent a transient form, not in dynamic equilibrium. Evidence from outcrop and subsurface data certainly supports the existence of low-gradient transport-dominated systems and steep margin FTPs, the latter including a critical component of in-situ transport-resistant facies. However, it is more difficult to determine if the range of intermediate geometries suggested by the modeling of different rates of transport and production (e.g. Fig 5.30 ii and iv) actually exist in nature. Examples such as the Nisku Formation of the Western Canadian Basin (Watts 1988), and the La Manga Formation of the Neuquen Basin (Palma et al., 2007), do not resemble low gradient transport-dominated systems (akin to Geometry A, Fig. 5.30 iv), but can best be described as 'flat-topped ramps' illustrated by a relatively flat platform top and subtle slope break. These examples actually bear a closer resemblance with Geometries B and C of Figure 5.30 iv, implying these modelled intermediate geometries may well exist in the real world.

The continuum of geometries produced by the models in response to varying interaction between transported and in-situ sediment accumulation, and various other controls on platform geometry, suggests that a clear distinction between ramps and FTPs in nature may be more problematic than previously realised. Either a new method of making the distinction is required, and it will be difficult to make this meaningful and not arbitrary given the continuum of platform geometries, or the distinction should be avoided other than as a high-level descriptive label with only limited predictive power. Where prediction is required, arbitrary classification could be replaced with

recognition that ramps and flat-topped platforms are part of a process continuum in a multi axis platform parameter space (Fig. 5.29 and 5.30 iv), with a range of geomorphic forms, from transport-dominated low-gradient ramp (e.g. Geometries A and B, Fig. 5.29) to in-situ dominated steep-margined FTPs (e.g. Geometry D, Fig. 5.29), plus variants on these influenced by the other controlling parameters such as relative sea-level oscillations (e.g. Geometries G – J, Fig. 5.29) and differential subsidence (e.g. Geometries K and L, Fig. 5.29).

Additional work is required to map these parameter space volumes with more realistic process models, but a multidimensional platform parameter space such as the one presented here could provide the next generation of predictive facies and sequence stratigraphic models for carbonate platforms.

Chapter 6: SEDIMENT DYNAMICS OF A CARBONIFEROUS (MISSISSIPPIAN) CARBONATE RAMP: THE SOUTH WALES RAMP

Chapter 6 presents the results of a field analysis of the Mississippian aged carbonate ramp which outcrops in the South Wales region of the United Kingdom. The field investigation was conducted to test the results and applicability of the previous modelling chapters. Facies description and analysis for proximal and distal localities on the ramp example were carried out, and their significance with regards to the dynamics of the sediment on the carbonate ramp examined. The facies patterns displayed in the South Wales example further emphasize the importance of a high rate of sediment transport in the carbonate ramp environment, the frequency and mechanism of which in this example is analysed. The chapter concludes with a discussion of the applicability of the sediment dynamic regime displayed in the South Wales example to other carbonate ramp examples.

6.1 Introduction – Fieldwork Objectives

The purpose of conducting a field investigation on the carbonate ramp of South Wales was to test the key results and hypothesis presented in the modelling work of the previous chapters. The significant number of model runs and application of the APE modelling method in chapter 4 illustrated that the dominant controlling parameter in the development of low gradient carbonate geometries was a high rate of sediment transport. Conversely, the models demonstrated how a lack of transport combined with a coarse (framebuilding) factory resulted in the development of a slope margin and ultimately an FTP geometry. Additional parameter variations, such as changing factory location and bathymetric variances were tested throughout chapters 4 and 5, however in each example a high transport coefficient ultimately led to the development of a ramp system. Thus a principal outcome of the modelling results is that a high sediment transport regime is required for carbonate ramp development.

The aim of the fieldwork was to test this hypothesis of significant sediment redistribution resulting in low angle carbonate geometries by analysing a carbonate ramp outcrop example to see if characteristics are displayed which would imply significant sediment transport; the chosen outcrop example being the Mississippian aged carbonate ramp of South Wales. A comparison of the facies displayed in both proximal and distal locations on the ramp was conducted in an attempt to identify if outer ramp sediments are mainly composed of autochthonous or allochthonous material. A larger proportion of the field analyses were carried out on the distal or outer ramp section of the example, as it was considered to be the most likely location to confirm or disprove the hypothesis of significant sediment transport controlling ramp development. The reasoning behind this bias towards an understanding of the deeper water, outer ramp composition being that if the ramp had been influenced by high transport conditions this may be evidenced in the outer ramp sediments by the identification of shallow water derived material contained within these outer ramp facies.

The South Wales ramp example was selected due to the quality and extent of outcrop which can be traced from the most proximal, shallowest sections of the ramp all the way to the most distal region of the ramp, with relatively continuous sections between. The inner and middle ramp sections of the South Wales example have been the focus of considerable work (i.e. Wu, 1982; Beus, 1984; Wright, 1986; 1987; Ramsay, 1987; Faulkner, 1989; and Hennebert and Lees, 1991), however the outer ramp section lacks this detail of analysis, with the only notable work on the section conducted by Simpson (1985, 1987), along with a basic stratigraphic description by George et al., (1976), the reason for this being the restricted access to the succession due to the outcrops being located almost entirely within the Castlemartin Artillery Range. As outlined previously analysis of the distal facies was paramount for this field study, therefore special access was granted to the sections, and the relatively untouched outer ramp strata of the Castlemartin region provided the ideal sections for analysis.

6.2 The South Wales carbonate ramp

The South Wales Mississippian ramp has been the site of considerable work, therefore its regional, geological, tectonic and stratigraphic setting are relatively well understood. During the Early Mississippian Europe was influenced by the continuing affects of the Hercynian Orogeny. At this time much of Central and Northern Britain was experiencing an extensional regime in which carbonate sedimentation was predominantly governed by graben and half graben basins (Golonka, 2002), while the Southwest (Fig. 6.1) was likely to have been influenced by an incipient peripheral flexure during the earliest stages of the Hercynian foreland basin evolution (Burgess and Gayer, 2000).

The Early Mississippian (Tournaisian) is widely recognised as a glacial period (Haq and Schutter, 2008; Rygel et al., 2008) and was therefore affected by frequent glacioeustatic fluctuations to the magnitude of 20-60 metres (Rygel et al., 2008). One such fluctuation and associated relative sea-level rise led to the development of an extensive carbonate ramp over what is now the South Wales region. The ramp was bounded to the north by a small land mass known as St George's Land (Fig. 6.1) and to the south by the deep Cornubain or Culm Basin (Wright, 1986). This ramp is understood to have been dipping in a Southerly direction (Wright, 1986; Hennebert and Lees, 1991). A decrease in eustatic fluctuations (10-25 metres; Rygel et al., 2008) during the Middle Mississippian (mid-Chadian through Holkerian) resulted in the deposition of a 100 Km wide wedge of sediment across the ramp during this time, which is now displayed as the present Lower Carboniferous Limestone series of South Wales (Fig. 6.2 and 6.3).

The limestone sequence of South Wales has been attributed to deposition in a carbonate ramp setting as a consequence of two fundamental characteristics. The first is the gradual transition from very shallow water (peritidal) to mud-dominated deeper water facies displayed in the outcropping strata, a transition of facies such as this is commonly displayed in modern carbonate ramps (i.e. the Arabian Gulf). The second, as described in the original classification of the ramp is a lack of 'evidence of a shelf rim or shelf margin' (Wright, 1986), as indicated by the absence of typical slope deposits such as slumps and breccias. Furthermore, considerable data collection and analysis of the South Wales ramp has been carried out before and since, and

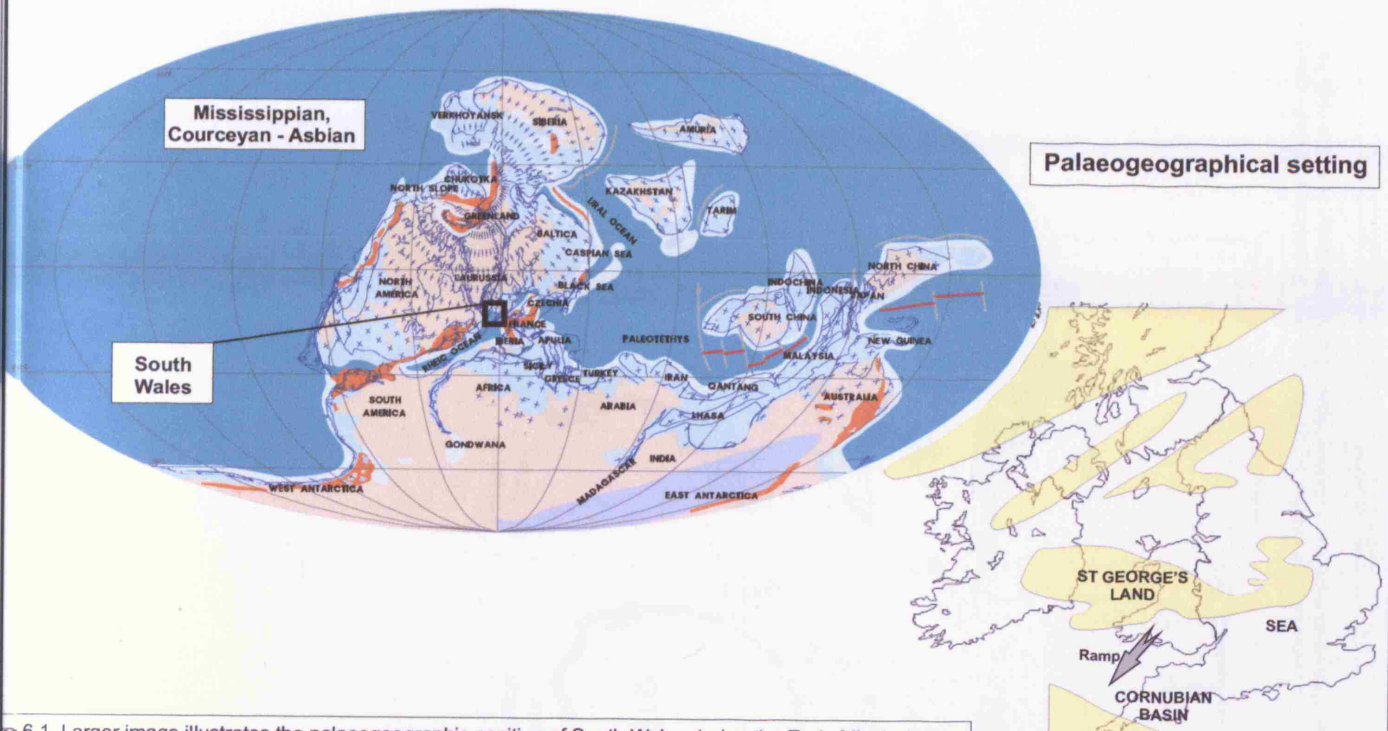


Figure 6.1. Larger image illustrates the palaeogeographic position of South Wales during the Early Mississippian, based on Golonka (2002). Smaller image depicts land distribution, and likely location and dip direction of a carbonate ramp in the South Wales area during the Early Mississippian, edited from Wright (1986).

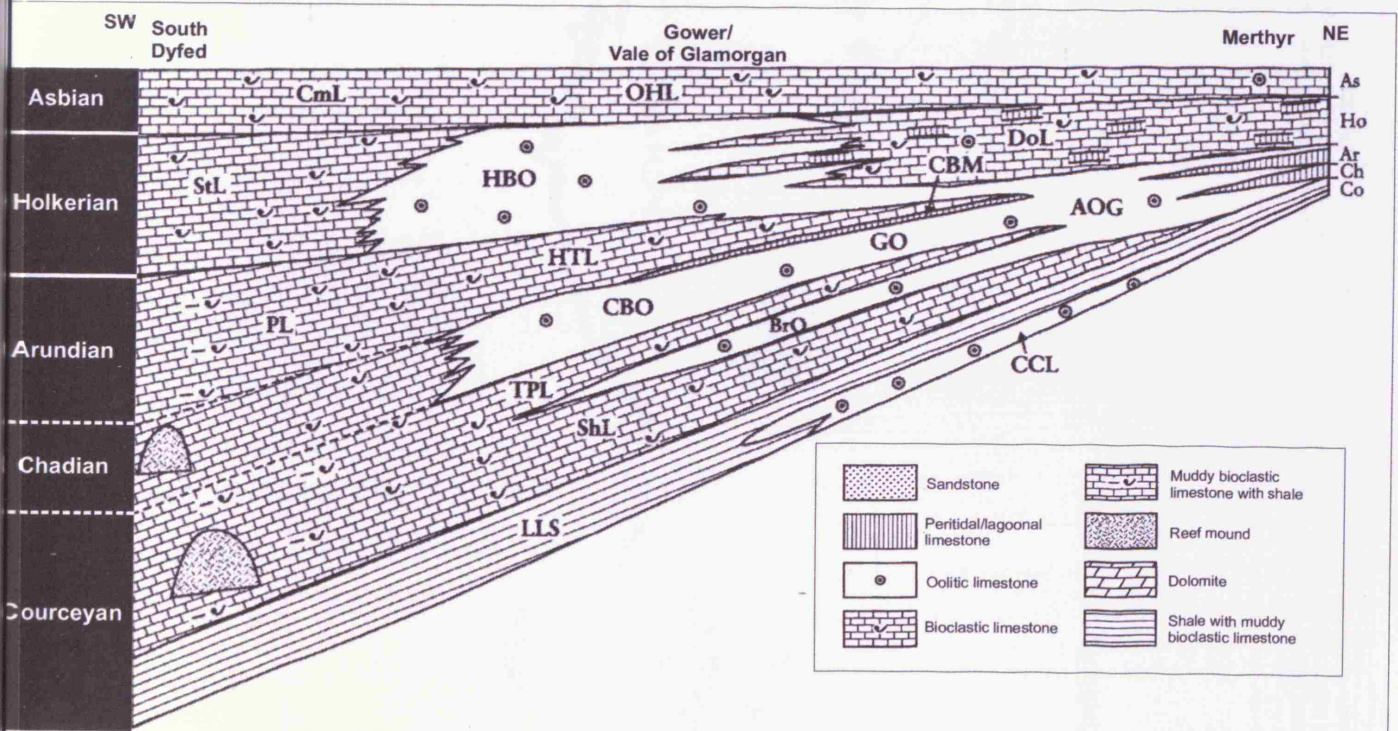


Figure 6.2. Stratigraphical section of the Dinantian strata in South Wales based on Wright (1986), section length is approximately 100 Km. CmL - Crickmail Limestone; OHL - Oxwich Head Limestone; StL - Stackpole Limestone; HBO - Hunts Bay Oolite; CBM - Caswell Bay Mudstone; DoL - Dowlais Limestone; HTL - Hylton Limestone; PL - Pen-y-Holt Limestone; CBO - Caswell Bay Oolite; GO - Gully Oolite; AOG - Abercrombie Oolite group; BrO - Brofiscin Oolite; TPL - Tears Limestone; ShL - Shipway Limestone; LLS - Lower Limestone Shale; CCL - Castell Coch Limestone. (Modified after Cossey et al., 2004).

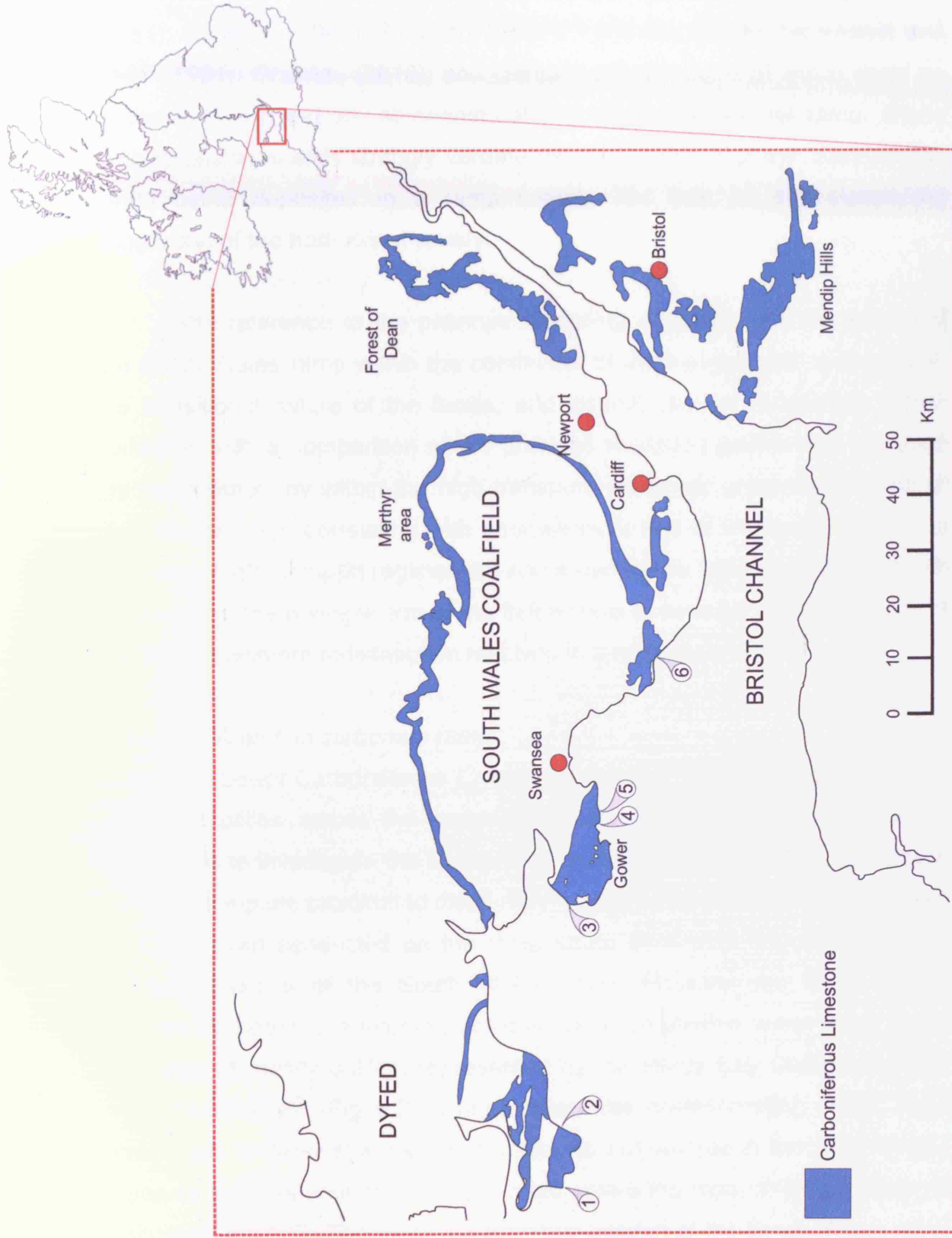


Figure 6.3. Location map of Southwest Britain showing the South Wales Coalfield (South Wales Synclinorium), the Forest of Dean and the Bristol/Mendips area. The outcrops of Carboniferous Limestone in the region are highlighted in Blue. Numbered localities identify sites of field investigation. Arundian Pen-y-Holt member - 1) Linney Head, 2) Stackpole Quay; Arundian High Tor Limestone Member - 3) Spaniard Rocks, 4) Three cliffs bay, 5) Foxhole, 6) Ogmore by Sea

a series of logged sections collected at various locations covering much of the ramp have been conducted in work by authors such as; Wu, (1982); Beus, (1984); Ramsay, (1987); Simpson, (1987); Faulkner, (1988); Hennebert and Lees, (1991); Ghamdi, (2010); and Qahtani, (2010), each of which show no evidence to suggest any steepening at any locality across the ramp. These outcrop characteristics strongly validate the interpretation of the South Wales strata being deposited in a ramp setting, the lack of any steepening suggesting of the homoclinal variety.

With reference to the previous modelling chapters and the locality of the South Wales ramp within the continuum of form suggested in chapter 4, the transitional nature of the facies, and distinct lack of steepening, which combined with a comparison of the previous modelled geometries suggests the ramp would lay within the high transport, moderate production region of the matrices (e.g. correlating with geometries II and III in Figure 4.2). Thus implying a high transport regime was active during the deposition of the South Wales ramp, the principle aim of the fieldwork is to assess if this hypothesis of significant sediment redistribution resulting in a ramp geometry is correct.

6.2.1. The Arundian carbonate ramp

The Lower Carboniferous Limestone series of South Wales outcrops at several localities across the region (Fig 6.3). As the principle aim of the fieldwork is to investigate the transport of sediment across this ramp system, the most complete proximal to distal ramp section was required. Considerable work has been conducted on the ramp strata from both the Holkerian and Chadian intervals of the South Wales ramp. However the South Wales outcrops for both these intervals are dominated by shallow water shoal facies consisting of mainly oolites, represented by the Hunts Bay Oolite and Gully Oolite respectively (Fig 6.2). Unfortunately the corresponding distal, outer ramp facies to these shallow water oolites do not outcrop in the South Wales region as their distribution is likely located where the modern Bristol Channel is situated (Fig 6.3). Therefore the Arundian section of the South Wales ramp has been selected due to its near complete outcropping sequence of proximal to distal strata. The inner to middle ramp environment is represented by the

High Tor Limestone Formation, while the Pen-y-Holt Limestone Formation represents the most distal, outer ramp deposits of the ramp during the Arundian (Fig 6.4). Palinspastic reconstructions (estimated from Hancock et al., 1983) suggest that the Pen-y-Holt Limestone was deposited around 20-30 km from the probable Arundian basin margin, and in a water depth of 100-200 metres (Simpson, 1987). The palaeodepth of the laterally equivalent High Tor Limestone is interpreted to be in the region of 10-20 metres (Simpson, 1987). Calculations incorporating the outcropping localities and suggested water depths for these laterally equivalent facies imply a ramp gradient of approximately 0.5 degrees, well below the 1 degree threshold commonly invoked for ramp classification (Burchette and Wright, 1992). The Arundian sequence of South Wales can thus be interpreted as the relatively shallow, wave agitated facies of the High Tor, passing gradually into the deeper water Pen-y-Holt facies across a gently dipping carbonate ramp (Fig 6.4).

6.3 Field and Laboratory Analysis Methods

6.3.1. *The Pen-y-Holt Limestone (PyH)*

The quantity of fieldwork conducted on the PyH was significantly greater than that carried out on the laterally equivalent High-Tor Limestone. The reason being that the purpose of the overall field study was to understand the dynamics of the ramp system, the hypothesis being that the outer ramp sections would yield a significantly greater insight into these processes than their shallower water equivalents. Therefore if a detailed understanding of the composition and bioclastic content of the outer ramp sediments could be achieved an assessment of the provenance of this material may be possible, thus leading to an enhanced understanding of the systems dynamics.

The PyH solely outcrops on the Pembrokeshire Peninsula of South Dyfed (Fig. 6.3 and 6.4), and is exposed in two principal locations. The first is a relatively small section at Stackpole Quay (GR SR 993956), however the section is incomplete and structurally complex so minimal analysis was conducted at the locality. The second is the Linney Head section between the east side of Hobbyhorse Bay (GR SR 888957) and the Wash (GR SR 918944). A near complete section of the PyH Formation is exposed at this locality; therefore it was selected as an appropriate section for the analysis of

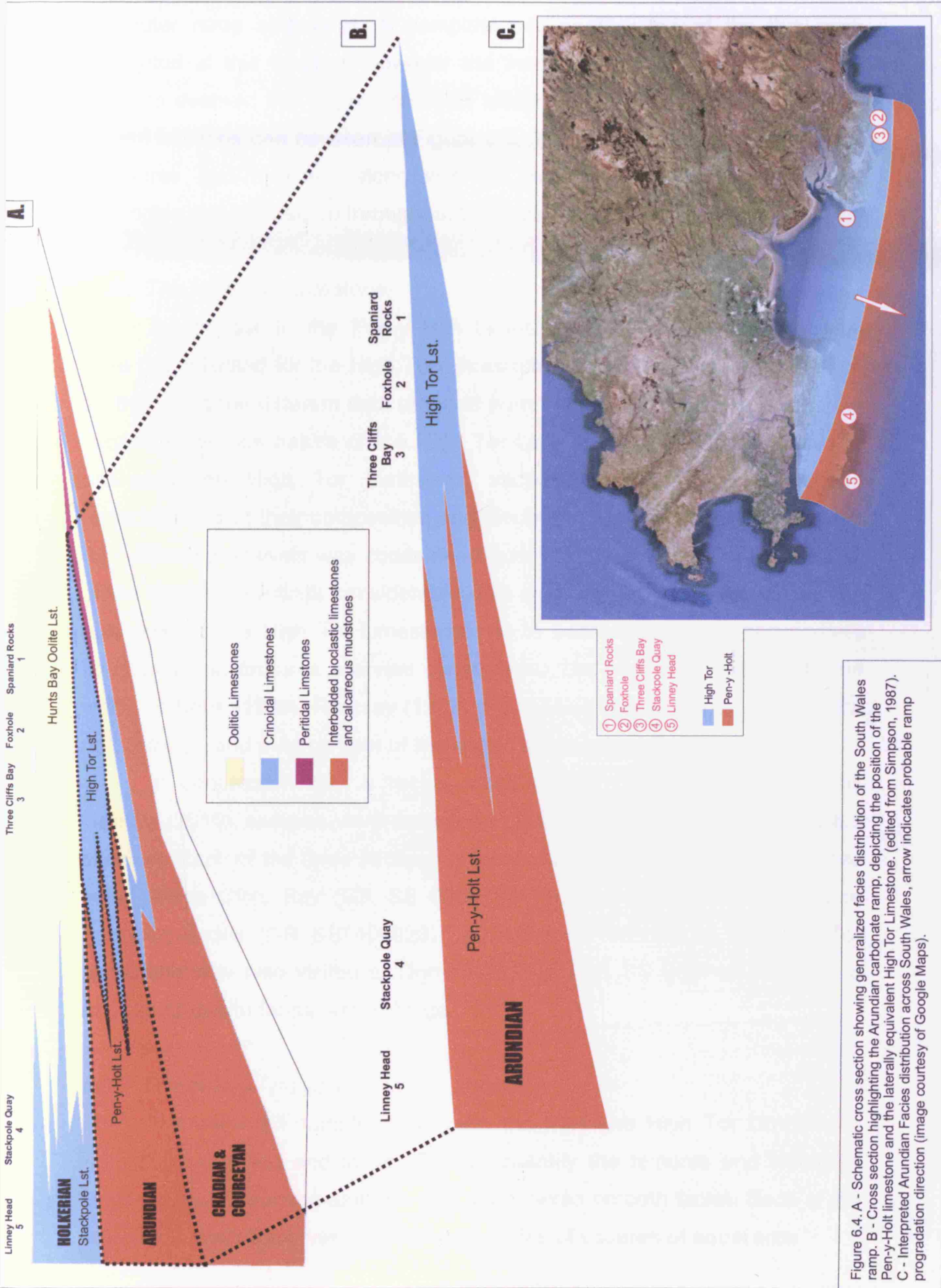


Figure 6.4. A - Schematic cross section showing generalized facies distribution of the South Wales ramp. B - Cross section highlighting the Arundian carbonate ramp, depicting the position of the Pen-y-Holt limestone and the laterally equivalent High Tor Limestone. (edited from Simpson, 1987). C - Interpreted Arundian Facies distribution across South Wales, arrow indicates probable ramp progradation direction (image courtesy of Google Maps).

the outer ramp sediments. A complete sedimentary log of the PyH was attempted at this location; however the inaccessibility of certain steep cliff sections deemed this impractical. The location and extent of the accessible logged sections can be seen in Figure 6.5. The identification of sedimentary structures and features, along with an evenly spaced sampling of the lithologies was conducted throughout the construction of the logs.

6.3.2. *The High Tor Limestone*

In contrast to the Pen-y-Holt Limestone detailed sedimentary logs were not collected for the High Tor Limestone sections. The principal reason for this being the different data required from the two limestone units, and the very homogenous nature of the High Tor Limestone. The main objective of analyzing the High Tor Limestone sections was to gain a detailed understanding of their composition and bioclastic content; therefore sampling for laboratory analysis was conducted throughout the sections. Furthermore, unlike the PyH sections considerable data and sedimentary logs have been published on the High Tor Limestone and its bedding patterns, sedimentary structures and features are well constrained. The reader is referred to the works of Beus (1984), Ramsay (1987) and more recently Qahtani (2010), for detailed logs and outcrop data of the High Tor Limestone sections.

In conjunction with a recent study of the High Tor Limestone by Qahtani (2010), samples were collected from three principal localities (Fig 6.3 and 6.4). Each of the three sections is located on the Gower peninsula, these being Three Cliffs Bay (GR SS 535876), Foxhole (GR SS 553872), and Spaniard Rocks (GR SS 403926). An additional outcrop of the High Tor Limestone was also visited at Ogmores-by-Sea (GR SS 865746) in order to analyse its in-situ faunal assemblage.

6.3.3. *Laboratory Analysis*

The collected samples from both the PyH and High Tor Limestones were thin sectioned and in an effort to quantify the textures and bioclastic content a point counting analysis was undertaken on both facies. Each of the selected thin sections was divided into a series of squares of equal area

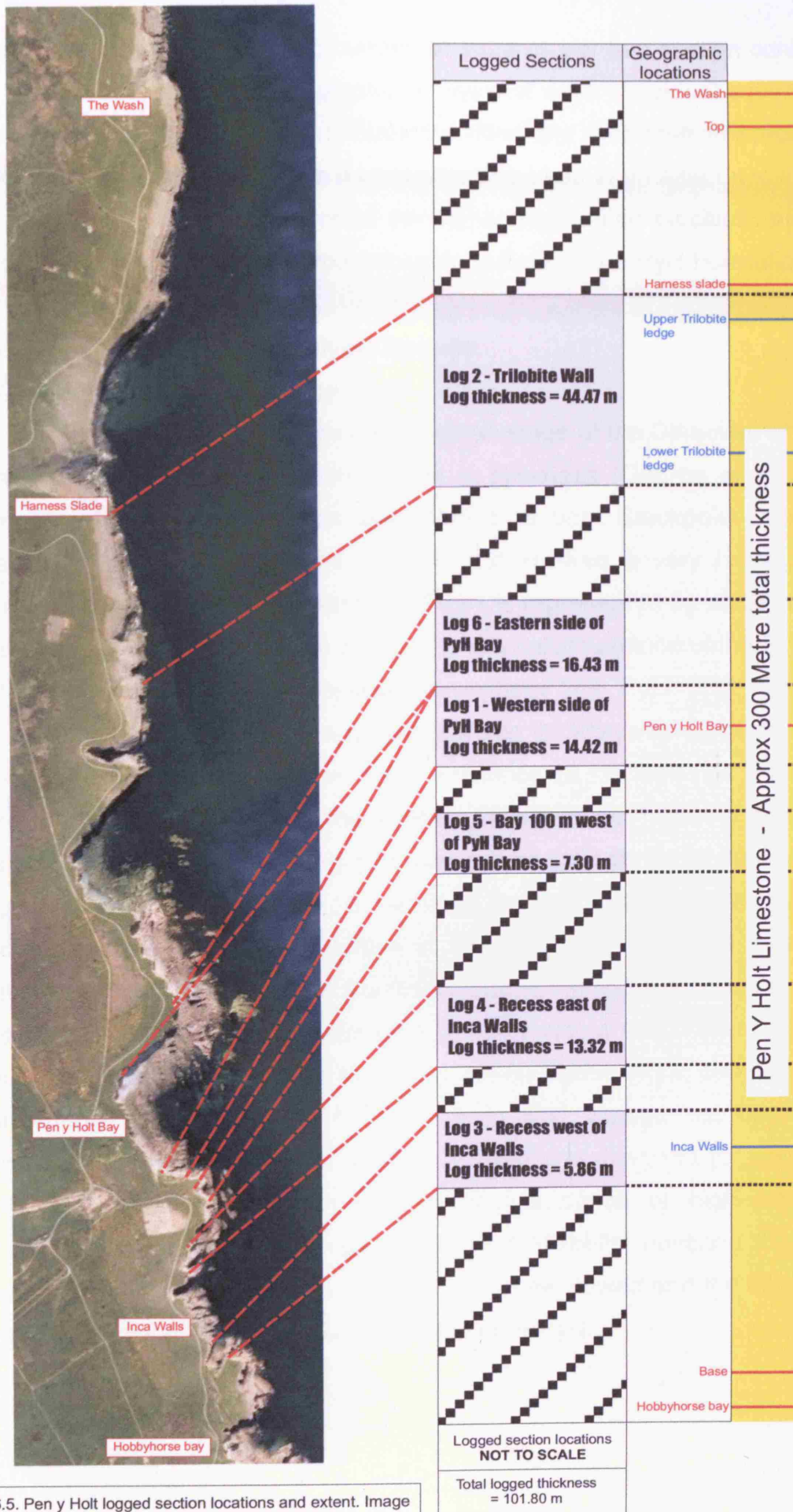


Figure 6.5. Pen y Holt logged section locations and extent. Image courtesy of Google maps.

measuring 5 mm by 5 mm, the number of squares per thin section controlled by the thin section size. Petrographic analysis of each individual square was conducted with all identifiable bioclasts identified and systematically recorded. Additionally a scanning electron microscope was used in an attempt to identify the provenance and composition of the highly fragmented bioclastic material which comprises the matrix of the wackestone beds in the PyH Formation.

6.4 Field and Laboratory Analysis Results

6.4.1. *The Pen-y-Holt Limestone (PyH)*

The PyH Formation spans the Arundian stage of the Dinantian of South Wales and is approximately 300 metres in thickness (George et al., 1976; Simpson, 1987). The formation was studied at both Stackpole Quay and predominantly the Linney Head section, and showed a very homogenous character throughout the formation. The PyH is represented by an alternation of two lithologies, a wackestone unit (L1) and a calcimudstone unit (L2), which outcrop in an alternating character throughout the PyH (Fig 6.6). The wackestone beds tend to have a greater outcrop thickness (average thickness of 40 – 50 cm) than the thinner calcimudstones (2 -10 cm). An attempt to construct a sedimentary log of the entire PyH was made, however due to the inaccessibility of certain sections just over a third (101.80 m) of the PyH was logged. A sample log covering 10 metres of the PyH is depicted in figure 6.7 and the complete logs are provided in Appendix 1. The failure to log the complete PyH was not deemed significant due to the extremely homogenous character of the formation, therefore the logged sections which cover a third of the formation are considered to be highly representative of the complete PyH. Furthermore the entire 300 m of the PyH was walked out on several occasions and the inaccessible sections viewed and analysed for anomalies from the cliff edges, which combined with a series of high resolution photographs (taken from sea, courtesy of Sid Howells) covering the entire section, the homogeneity of the formation could be viewed and the alternating pattern of bedding seen throughout the complete PyH.

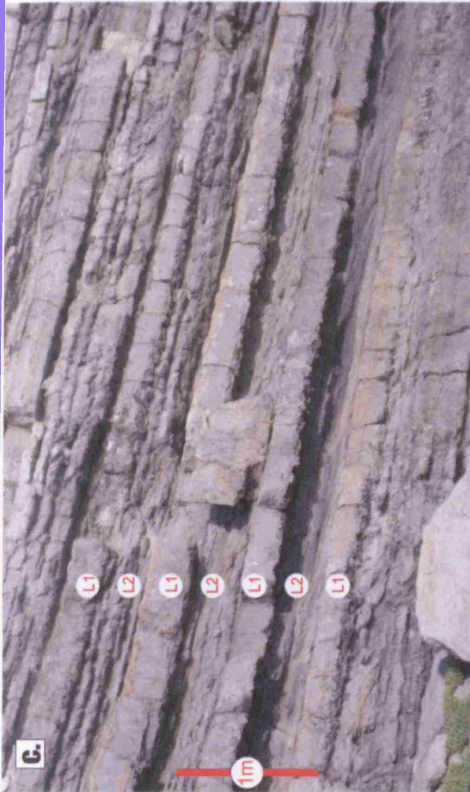


Figure 6.6. A - Overview of outcrop pattern of the Pen-y-Holt Limestone at the Linney Head section. Cliff section is approximately 500 m across and is taken in a northward looking direction. Photo courtesy of Sid Howells. B - Characteristic Pen-y-Holt outcrop pattern seen at the 'Inca Walls' section of the Linney Head region. Recessed units are the calcimudstones and prominent thick beds are wackestones. For scale person in photo is approximately 1.8 m tall. C - Close up of Pen-y-Holt bedding character showing alternating L1 (wackestone) and L2 (calcimudstone) lithologies.

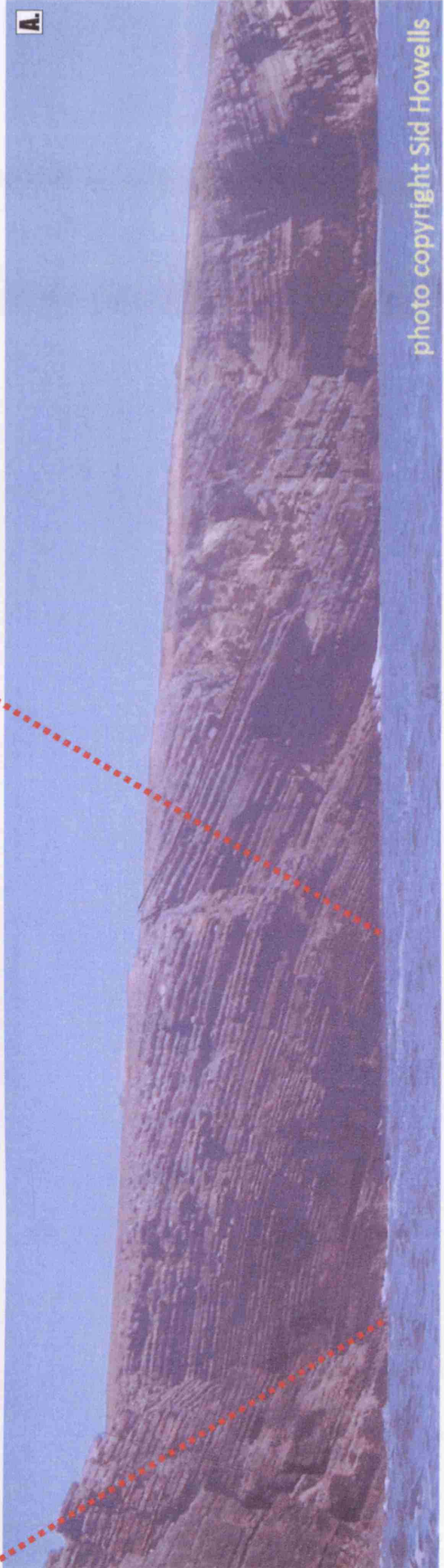
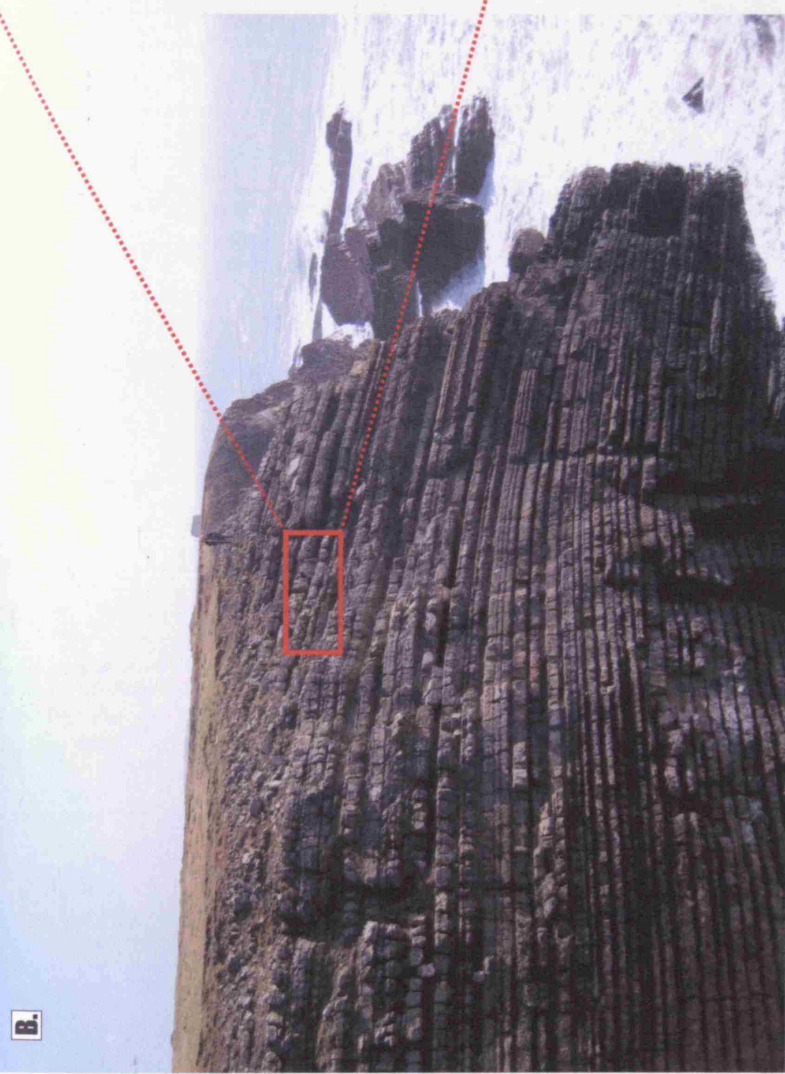


photo copyright Sid Howells



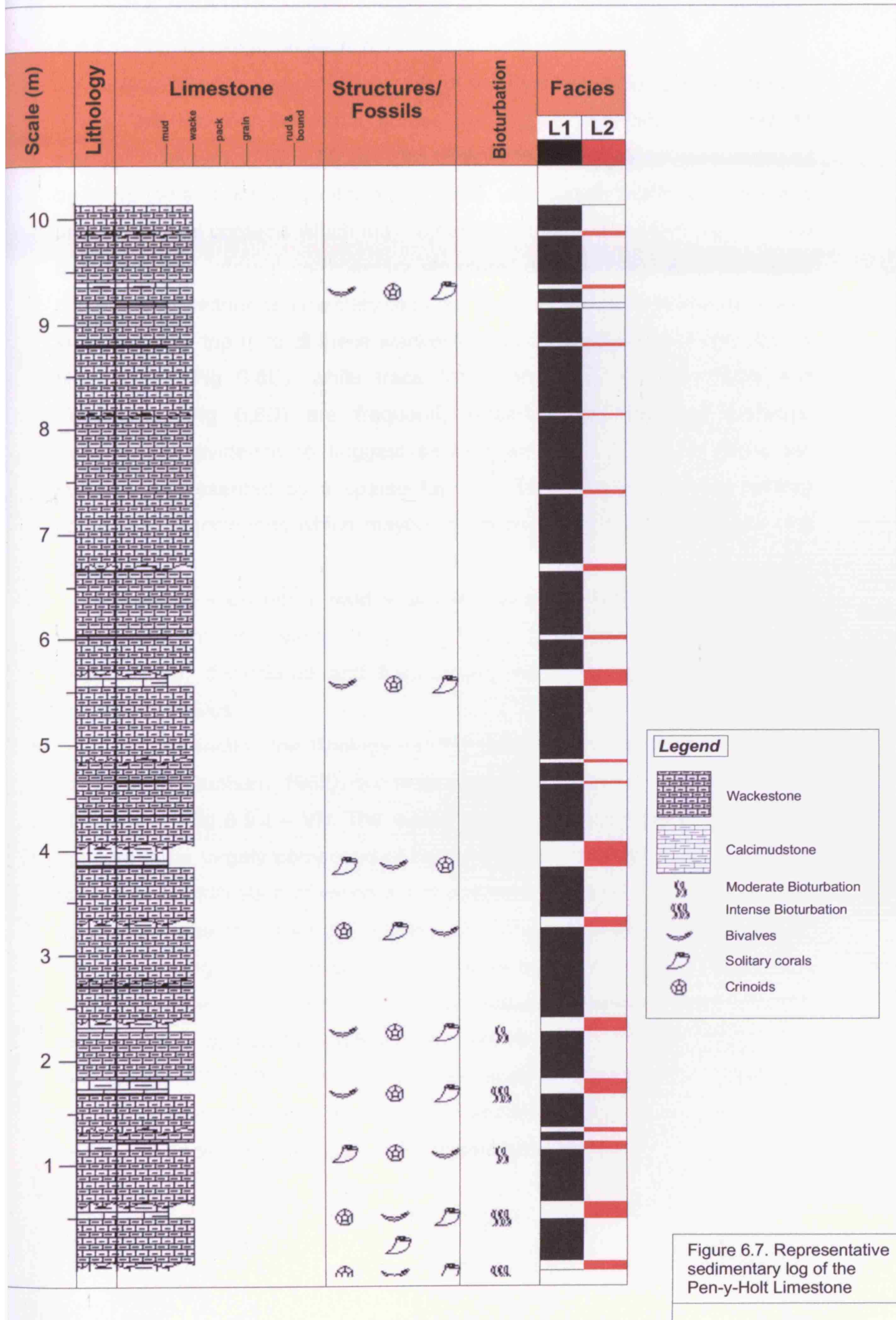


Figure 6.7. Representative sedimentary log of the Pen-y-Holt Limestone

6.4.1.1. *The Wackestone Beds (L1)*

At outcrop the wackestone beds of the PyH Formation are light grey in colour, are laterally persistent across the logged sections, and have an average thickness of 40 – 50 cm. The beds of this lithology are characterised by sharp top and bottom contacts (Fig 6.8A), with certain examples displaying undulose basal contacts which may represent primary erosion or loading. The beds lack any internal sedimentary structure, display little visible bioclastic content, and neither sedimentary lags nor hummocky cross-stratification was identified. The top third of these wackestone beds are commonly affected by bioturbation (Fig 6.8E), while trace fossils including *Thalassinoides* and *Zoophycos* (Fig 6.8D) are frequently observed on their top surfaces. Furthermore, evidence to suggest small colonisation areas on these top surfaces is presented by a sparse fauna of body fossils including solitary corals and brachiopods which maybe in life position on these surfaces (Fig 6.8 B and C).

In hand specimen a mud supported fabric can be observed, with little faunal element observable. Any identifiable body fossils are commonly disarticulated, dissociated and fragmented, including crinoid ossicles and brachiopod valves.

In thin section the lithology can be classified as having a wackestone composition (Dunham, 1962), due to its mud supported texture with more than 10% grains (Fig 6.9 I – VI). The matrix is not wholly composed of mud but appears to be largely composed of highly fragmented bioclastic material, the origin and identification of which is not possible with a standard petrographic microscope due to the very fine grain size, and has therefore been studied with a scanning electron microscope (refer to section 6.4.4). The identifiable bioclastic content of the wackestones is relatively varied including bivalves, brachiopods, ostracods, echinoderm plates and various algae and foraminifera (Fig 6.9 I – VI). A detailed analysis identifying the type and quantity of these bioclasts is provided in section 6.4.3 while the significance and provenance of these grains is discussed in section 6.5.



c



b



a



d



e

Figure 6.8. Lithology 1 (L1) outcrop characteristics. a) Typical bedform character of wackestone beds. Beds lack internal sedimentary structure, have little bioclastic content, depict a sharp top contact and a sharp to erosive base contact. For scale hammer is 28 cm in length. b) Giant Caniniod coral on top surface of wackestone bed. For scale hand lens is 5 cm in length. c) Brachiopods in colonising attitudes on top surface of wackestone beds may indicate small colonisation areas on these top surfaces. d) Zoophycos trace fossils on top surface of bed. e) Bioturbation and evident burrows originating from top surface of wackestone beds. Such effects commonly only effect the top third of the wackestone beds.

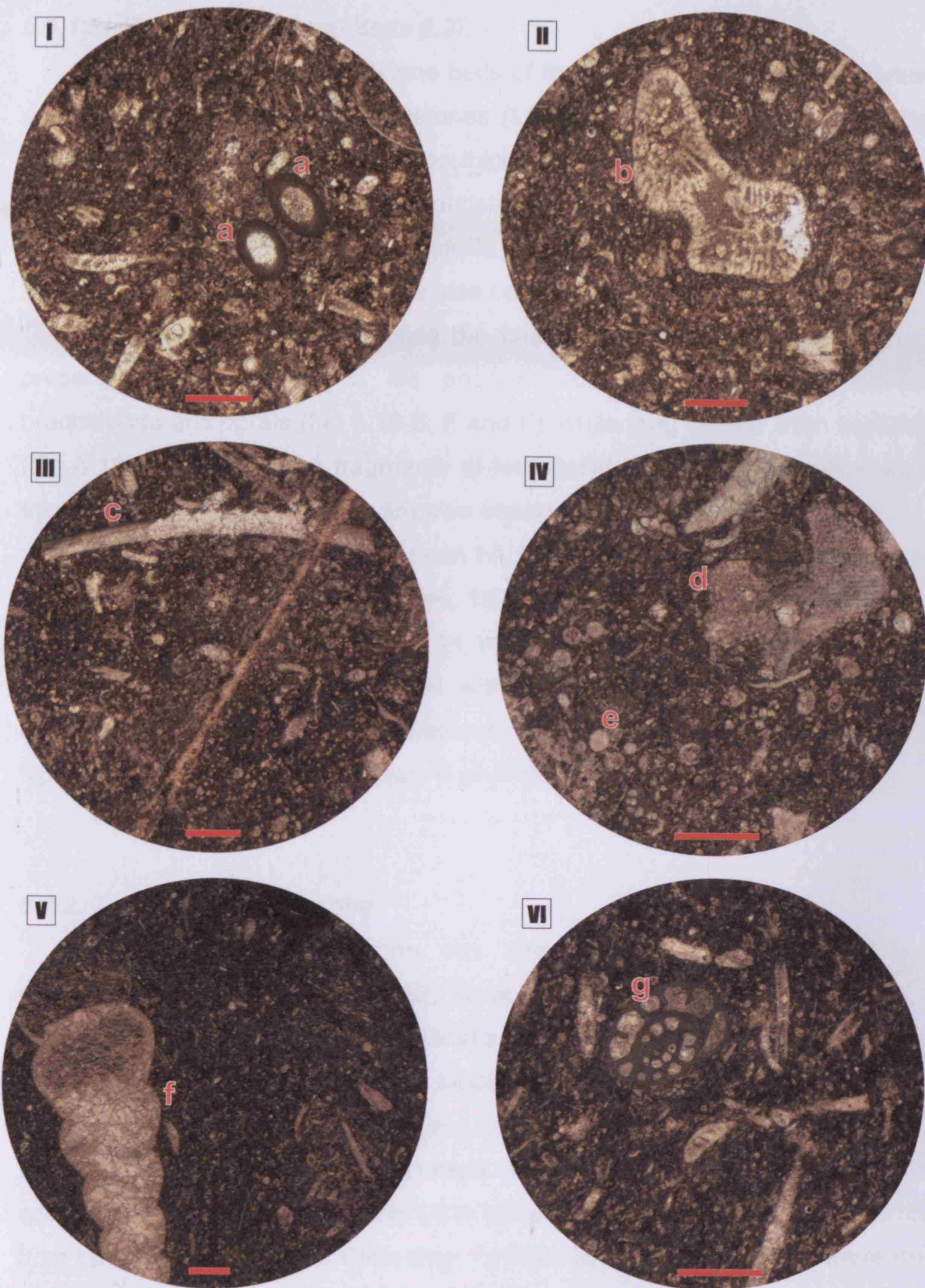


Figure 6.9. I-VI Photomicrographs of lithology 1 (L1). For scale red line at bottom of each image equals 1mm. Wackestone texture evident in each of the images, composed of a mud supported matrix which has a very fine grained highly fragmented bioclastic component, and more than 10% grains. Identifiable individual grains include: a - Earlandiid foraminifera, b - Epistacheoides Algae, c - Bivalve, d - Echinoderm plate; crinoid, e - Calcisphere, f - Microgastropod, g - Endothyrid Foraminifera.

6.4.1.2. *The Calcimudstone Beds (L2)*

At outcrop the calcimudstone beds of the PyH Formation have a darker grey colouration than the wackestones (L1) they are interbedded with (Fig 6.10 A). The beds have an average thickness of 2 – 10 cm, and commonly portray a thin lamination. The calcimudstones are typically heavily bioturbated (Fig 6.10H), while similar trace fossils to the wackestone beds including *Thalassinoides* and *Zoophycos* are also commonly observed.

Unlike the wackestone beds the fauna in the calcimudstones is well preserved and may be in life position. Autochthonous fauna include brachiopods and corals (Fig 6.10 B, E and F), while long crinoid stem sections (Fig 6.10 C and D), large fragments of fenestellid bryozoans and articulated trilobite carapaces (Fig 6.10G) are also observed.

In thin section the lithology can be classified as having a mudstone or calcimudstone composition (Dunham, 1962), due to its mud supported texture with less than 10% grains (Fig 6.11 I-IV). The bioclastic content of these calcimudstones is relatively limited with only brachiopods, ostracods, and echinoderm plates and spines observed. A detailed analysis identifying the type and quantity of these bioclasts is provided in section 6.4.3.

6.4.2. *The High Tor Limestone*

The High Tor Limestone has been studied and interpreted by numerous authors (e.g. Wu, 1982; Beus, 1984; Ramsay, 1987; Hennebert and Lees, 1991), and although peritidal sediments are present the succession is dominated by massively bedded bioclastic grainstones. In conjunction with a recent re-analysis of the High Tor Limestone by Qahtani (2010), samples were taken from the dominant High Tor facies (Facies Association A according to Ramsay, 1987; and Lithofacies H1 according to Qahtani, 2010) from three localities, Three Cliffs Bay, Foxhole and Spaniard rocks where the facies has a thickness of 48, 40 and 52 metres respectively.

At outcrop The High Tor is massively bedded, with bed thickness varying between 0.4 and 2 metres, and displays a distinct absence of sedimentary structures (Fig 6.12 A-C). The bedding planes of the High Tor typically display a varied faunal assemblage (particularly at the Ogmores-by-



Figure 6.10. Lithology 2 (L2) outcrop characteristics. a) Typical bedform character of calcimudstone beds. Red line illustrates extent of single L2 bed and for scale measures 20 cm. b) Brachiopods possibly in life positions. For scale hand lens is 5 cm in length. c & d) Intact long crinoid stems. e & f) Caninia corals in life position. g) Trilobite carapace. h) Calcimudstones are commonly heavily bioturbated.

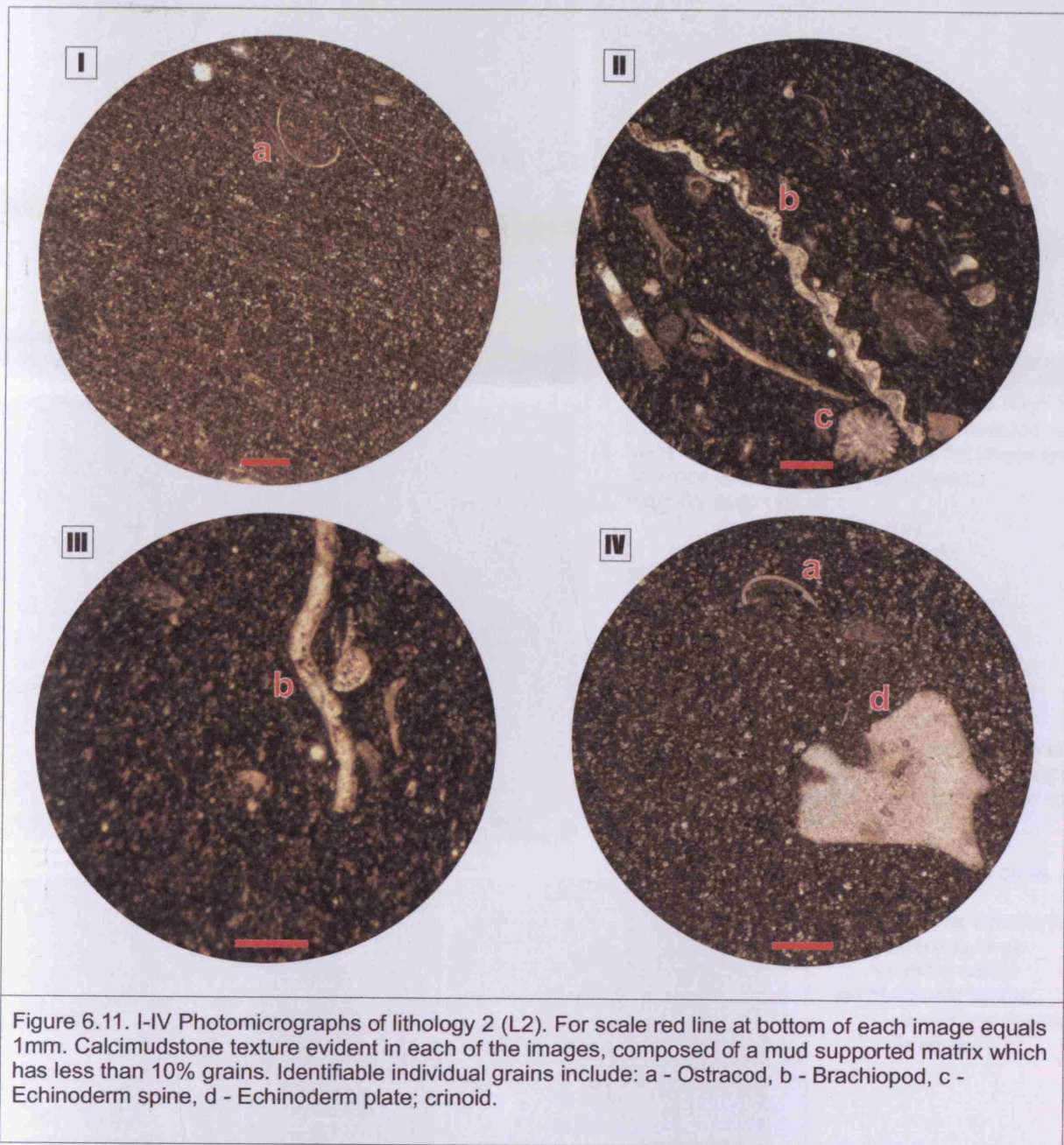




Figure 6.12. Outcrop character of the High Tor Limestone: Massively bedded succession with beds varying from 0.4 to 2 m in thickness and an absence of sedimentary structures.

High Tor outcrops at:

- a) Three Cliffs Bay
- b & c) Spaniard Rocks.

(For scale backpack in a and b is 45 cm in length, and stick in c is 2 m). Images courtesy of Qahtani (2010).

Fauna of the High Tor:

Images show probable in-situ faunal associations on the bedding planes of the High Tor. Images are from the Ogmore by Sea section. (For scale hand lens is 5cm in length).



- d) Syringoporida coral colony
- e) Michelinia coral colony
- f) Numerous large caninoid corals
- g&h) Crinoid stems, numerous ossicles in length

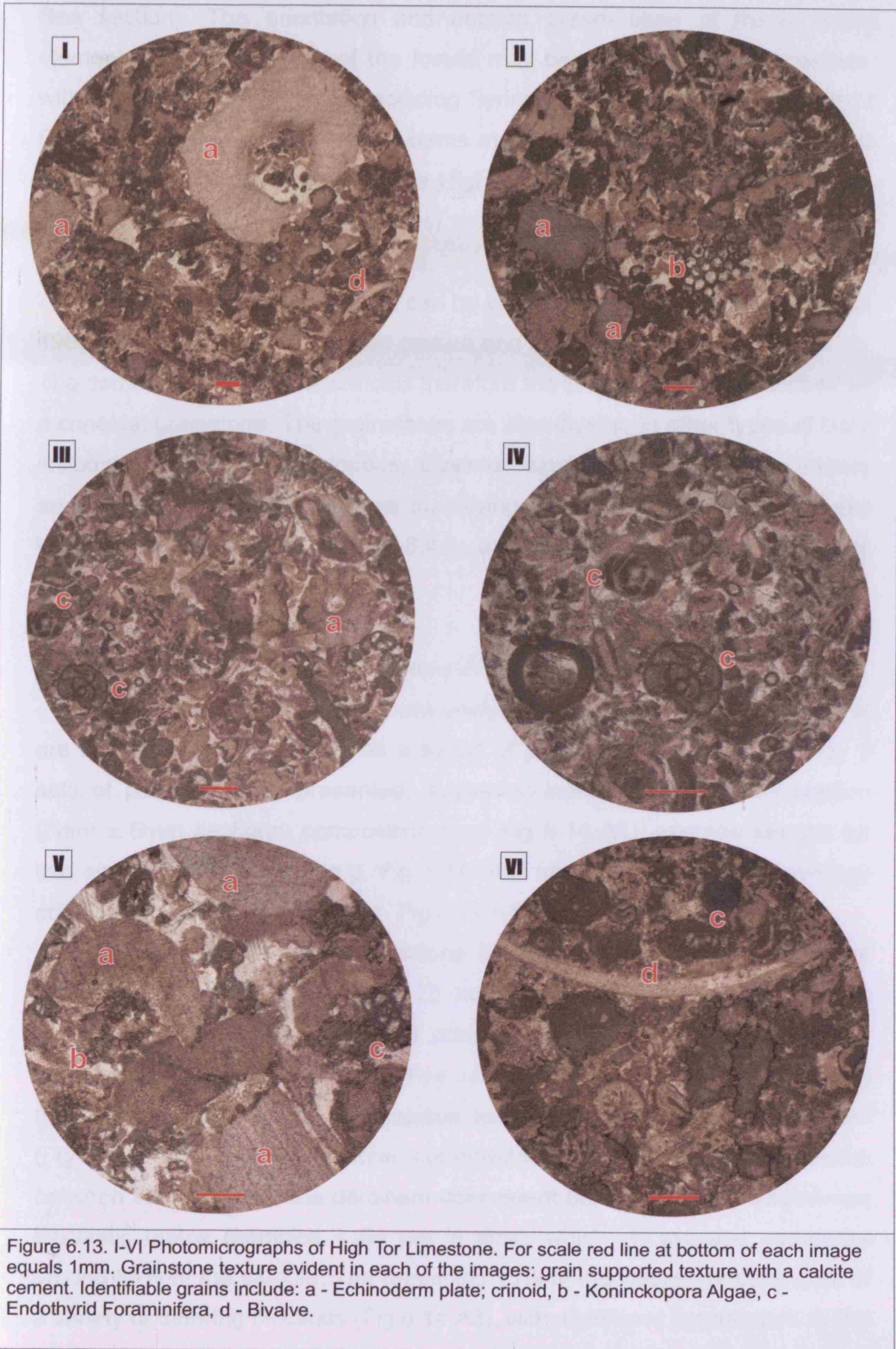


Figure 6.13. I-VI Photomicrographs of High Tor Limestone. For scale red line at bottom of each image equals 1mm. Grainstone texture evident in each of the images: grain supported texture with a calcite cement. Identifiable grains include: a - Echinoderm plate; crinoid, b - Koninckopora Algae, c - Endothyrid Foraminifera, d - Bivalve.

Sea section). The orientation and outcrop preservation of these faunal elements imply that many of the fossils may be preserved in life positions, with extensive coral colonies, including Syringoporid and *Michelinia* (Fig 6.12 D and E), and numerous crinoid stems many ossicles in length (Fig 6.12 G and H) observed on several of the High Tor bedding planes. Brachiopods, trace fossils (commonly *Zoophycos*) and significant bioclastic material are also present throughout the sections.

In thin section the lithology can be classified as a grainstone (Dunham, 1962), due to its grain supported texture and calcite cement (Fig 6.13 I – VI). The dominant grain type is crinoids therefore the lithology is best described as a crinoidal grainstone. The grainstones are also diverse in other types of biota including ostracods, brachiopods, bivalves, algae, and foraminifera (mainly endothyrids). A detailed analysis identifying the type and quantity of these bioclasts is provided in section 6.4.3, and their significance discussed in section 6.5.

6.4.3. Point count analysis of the Pen-y-Holt and High Tor

The results of the point count analysis on both the PyH and High Tor are illustrated in Figure 6.14 as a series of pie charts. For each lithology 3 sets of pie charts are presented, illustrating individual point count section (5mm x 5mm sections) composition (e.g. Fig 6.14 A1), average sample (or thin section) composition (e.g. Fig 6.14 A2), and finally the overall average composition for the lithology (e.g. Fig 6.14 A3).

For lithology 1, the wackestone beds of the PyH, 6 samples were examined with between 14 and 20 individual sections of 5mm by 5mm constructed and analysed for their composition (Fig 6.14 A1). An average sample composition for each of the six samples was worked out (Fig 6.14 A2) before an overall average composition for the wackestones was calculated (Fig 6.14 A3). The wackestone compositions are relatively homogenous between samples, with the dominant component being the highly fragmented bioclastic matrix (particles < 64 µm in size), which on average composes around 85% of the sample. The remaining 15% of the wackestones consist of a variety of differing bioclasts (Fig 6.14 A3), with significant contributors to this

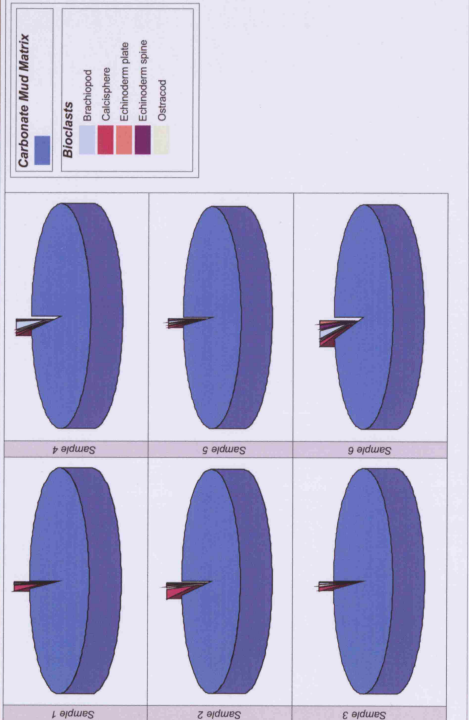
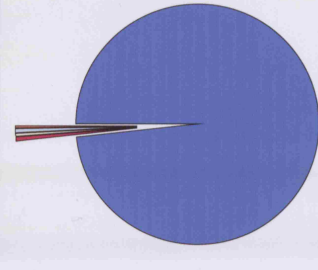
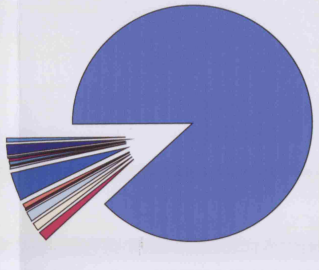
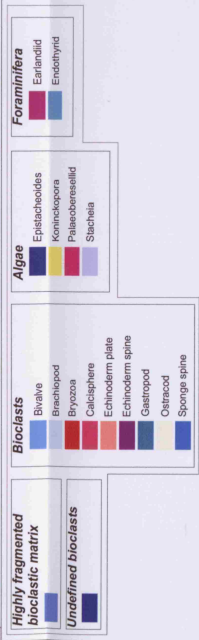
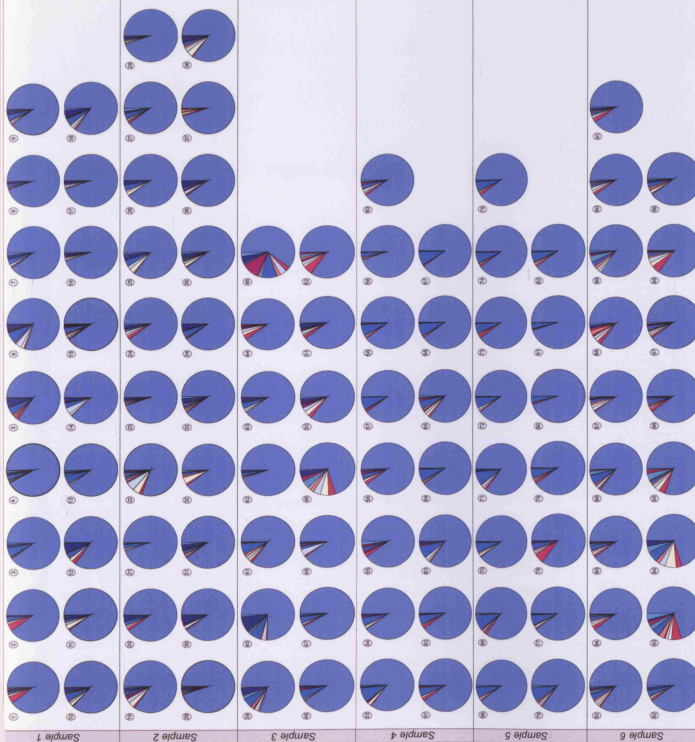
15% including ostracods, brachiopods, sponge spines and echinoderm fragments (> 64 μm in size).

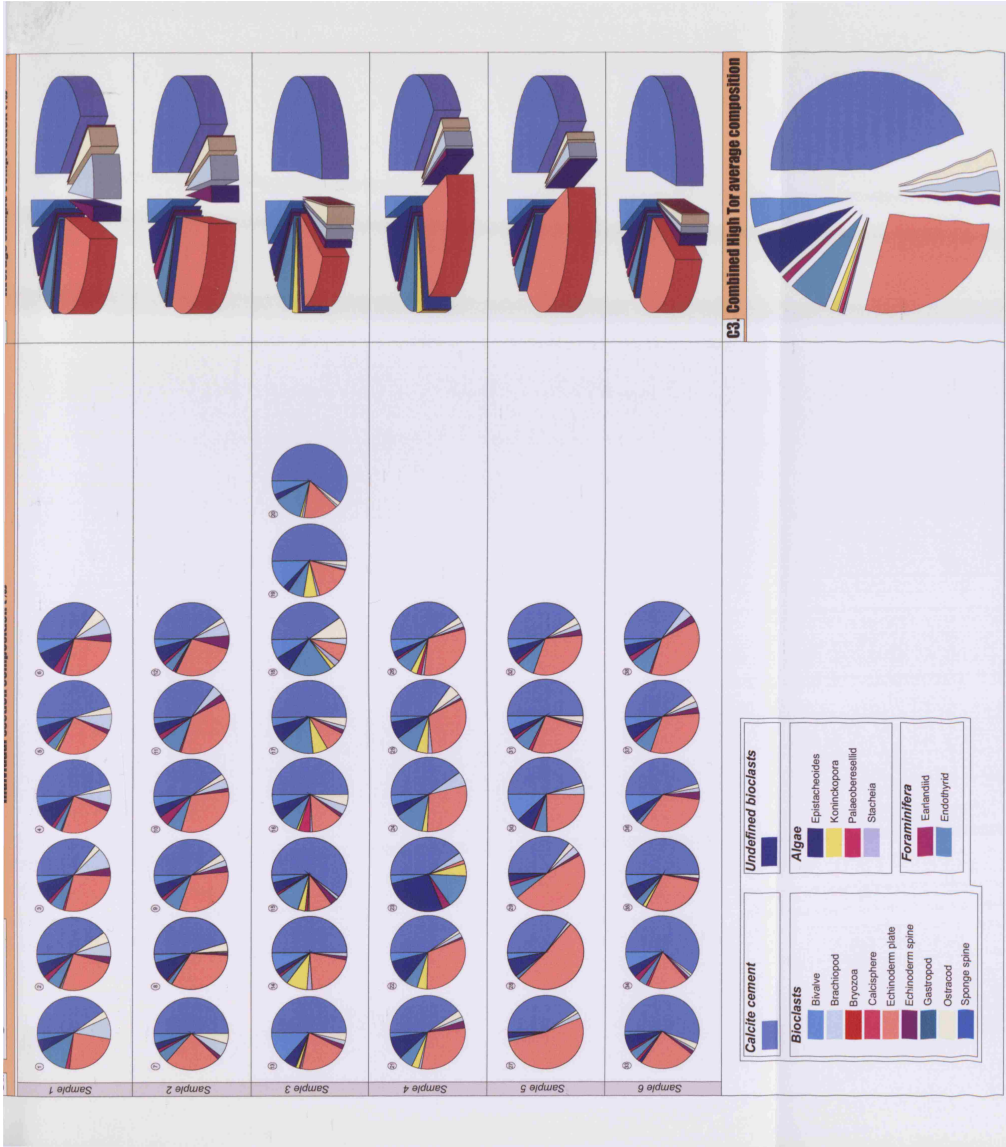
A slightly different approach was taken for lithology 2, the PyH calcimudstones, due to the extreme homogeneity of the samples. A point count analysis of individual 5mm x 5mm sections was initially attempted; however the very mud rich nature of the lithology and the sparseness of bioclasts resulted in the majority of sections displaying a 100% mud composition. It was therefore decided appropriate that an overall composition for the sample be calculated by point counting the identifiable bioclasts for the entire sample (Fig 6.14 B1), and an average overall composition for lithology 2 calculated from these (Fig 6.14 B2). The dominant component of the calcimudstones is carbonate mud, composing approximately 98% of the sample, with the remaining 2% consisting of bioclasts including calcispheres, brachiopods and echinoderm fragments.

The final lithology assessed using the point counting technique was the High Tor Limestone. The thin sections made for this lithology were not as large as those as of the other two lithologies therefore fewer individual point count sections could be constructed. In total 6 samples were examined with between 8 and 6 individual sections (5mm x 5mm) analysed for their composition (Fig 6.14 C1). An average sample composition for each of the six samples was worked out (Fig 6.14 C2) before an overall average composition for the High Tor was calculated (Fig 6.14 C3). The grainstones of the High Tor are considerably more heterogeneous in composition when compared with the other two lithologies, as they illustrate a significantly greater and varied bioclast content. The dominant bioclast of the High Tor are echinoderm plates (crinoids), composing on average 27% of the grainstones (Fig 6.14 C3), with other considerable contributing bioclasts including bivalves (5%), brachiopods (3%), ostracods (3%) and Endothyrid foraminifera (6%).

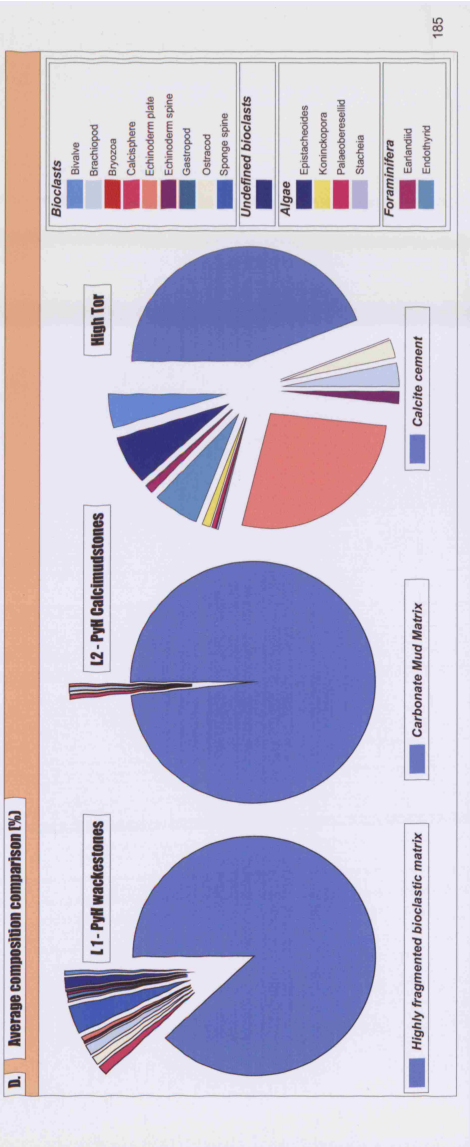
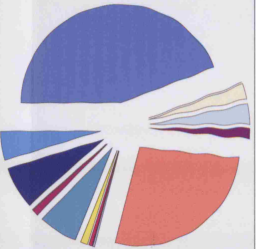
In order to compare and contrast the overall compositions for the three lithologies the overall composition pie chart for each of the respective lithologies is provided along side one another in figure 6.14 D.

Figure 6.14. Point count analysis Pie Charts for the Pen-y-Holt and High Tor Limestones. A1-3) Pie charts illustrate composition of wackestone beds from the PyH. B1-2) Pie charts illustrate composition of the calcimudstone beds from the PyH. C1-3) Pie charts illustrate composition of the High Tor. D) Comparison of average compositions for the three lithologies.





C3. Combined High Tor average composition



6.4.4. Scanning electron microscope analysis of the Pen-y-Holt Limestones

The Wackestone (L1) and Calcimudstone (L2) Beds of the PyH Formation were viewed under a scanning electron microscope (SEM) for two principle reasons; in an effort to identify the provenance and composition of the highly fragmented bioclastic material which comprises the matrix of the wackestone beds, and to identify if the strata have been affected by diagenetic remobilization of benthic skeletal aragonite (Wheeley et al., 2008).

Recently the diagenesis and mechanism of formation of Limestone-marl/shale alternations (LMA) has received considerable interest (e.g. Munnecke et al., 1997, 2001, Westphal and Munnecke, 2003; Westphal, 2006), largely in response to research developments in marine burial diagenesis (e.g. Melim et al., 2002) and efforts to understand their environmental records (e.g. Munnecke and Westphal, 2004, 2005). It has been argued that some LMA have originated solely by diagenetic processes acting on originally homogenous sediment (e.g. Hallam, 1986; Munnecke et al., 2001), while in other cases it has been suggested that diagenesis has acted only to enhance primary sedimentological features (e.g. Einsele et al., 1991; Ricken, 1996). It is likely that all LMA will have undergone some degree of differential diagenesis, whereby aragonite is dissolved from what become the shale layers (interbeds) and where the carbonate is reprecipitated as low-magnesium calcite microspar in limestone layers (beds). Questions still remain however with regards to the source of the primary aragonite, and Cherns and Wright (2000) and Wright et al., (2003) have documented the effects of large-scale, early diagenetic dissolution of molluscan shell aragonite from Silurian and Jurassic LMA, suggesting that 'missing molluscs' provided a benthic autochthonous source of carbonate for cementing limestones (wright and Cherns, 2004).

The wackestone and calcimudstone alternations (LMA) of the PyH may therefore be a product of diagenetic alteration, if so the same diagnostic features observed in the studies listed above would therefore expected to be identified in the PyH beds. A combined field (section 6.4) and SEM analysis of the PyH strata should therefore reveal evidence to infer the presence or absence of diagenetic bedding in the PyH.

Diagenetic bedding typically displays a distinct set of characteristics, most notably a nodular bedform is typically displayed in the limestone bed intervals. Nodular bedding was not observed in the wackestone beds (L1) in any of the logged sections (Fig. 6.5); however an ultrastructural analysis of the carbonate mineralogy of both the wackestone and calcimudstone beds should provide a clearer picture regarding the diagenetic history of the PyH beds.

Thin sections for both the wackestone and calcimudstone intervals were polished (up to carborundum 1000 granulation and finished with 0.5 µm aluminium oxide powder), cleaned with acetone and distilled water, and then etched in 1% acetic acid for up to 20 seconds. The sections were sputter coated with gold and examined with a scanning electron microscope (Philips XL30 ESEM) at 20kv in secondary electron mode at the School of Earth Sciences, Cardiff University.

6.4.4.1 PyH Wackestone (L1) under the SEM

At relatively low magnification the same microbioclasts viewed under a petrographic microscope could be identified (refer to section 6.4.3, and Fig. 6.14). Due to the extremely fragmented nature of the bioclastic material which composes the matrix of the wackestones, further identification of this bioclastic material was not possible. Under higher magnification the wackestone beds generally have a microspar texture (microspar crystals between 4-31 µm after Folk 1959; 1965), with relatively smooth surfaces and cleavage lines (Fig. 6.15 A-B). A size frequency histogram of the microspars is provided in Figure 6.16A. The surfaces of the smooth microspars are almost devoid of any pitting with only occasional single pits observed. Little to no clay was observed in the sections, while sporadic framboids of pyrite (<5 µm) were identified in certain microspars.

6.4.4.2 PyH Calcimudstones (L2) under the SEM

The dominant texture of the calcimudstones is similar to that of the wackestones in that it is composed of microspars (Fig. 6.15 C-D, Fig. 6.16 B). However the surfaces of these microspars are not smooth as in the

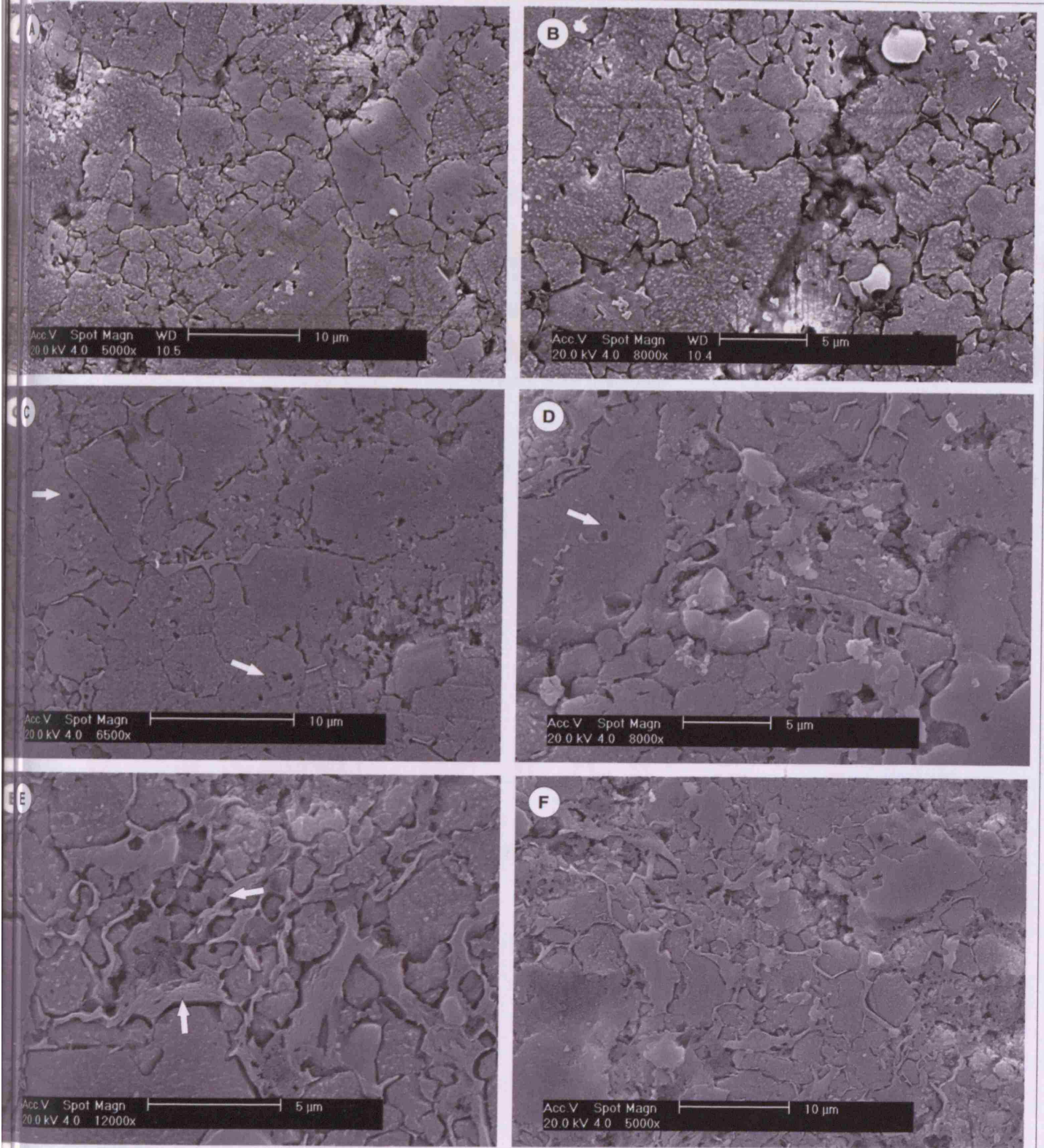


Figure 6.15. Texture of wackestone (L1) and calcimudstone (L2) intervals of the PyH under the SEM. (A-B). Wackestones generally display a microspar texture, with relatively smooth surfaces and cleavage lines. Note the lack of pitting on the microspar surfaces. C-D). Microspar texture of the calcimudstones. Arrows indicate the location of the square, rectangular to hexagonal shaped pits on the surface of the microspars. E-F). Micrite texture of the calcimudstones, with platy clays observed between the boundaries of the crystals (arrowed) forming partial to complete clay cages.

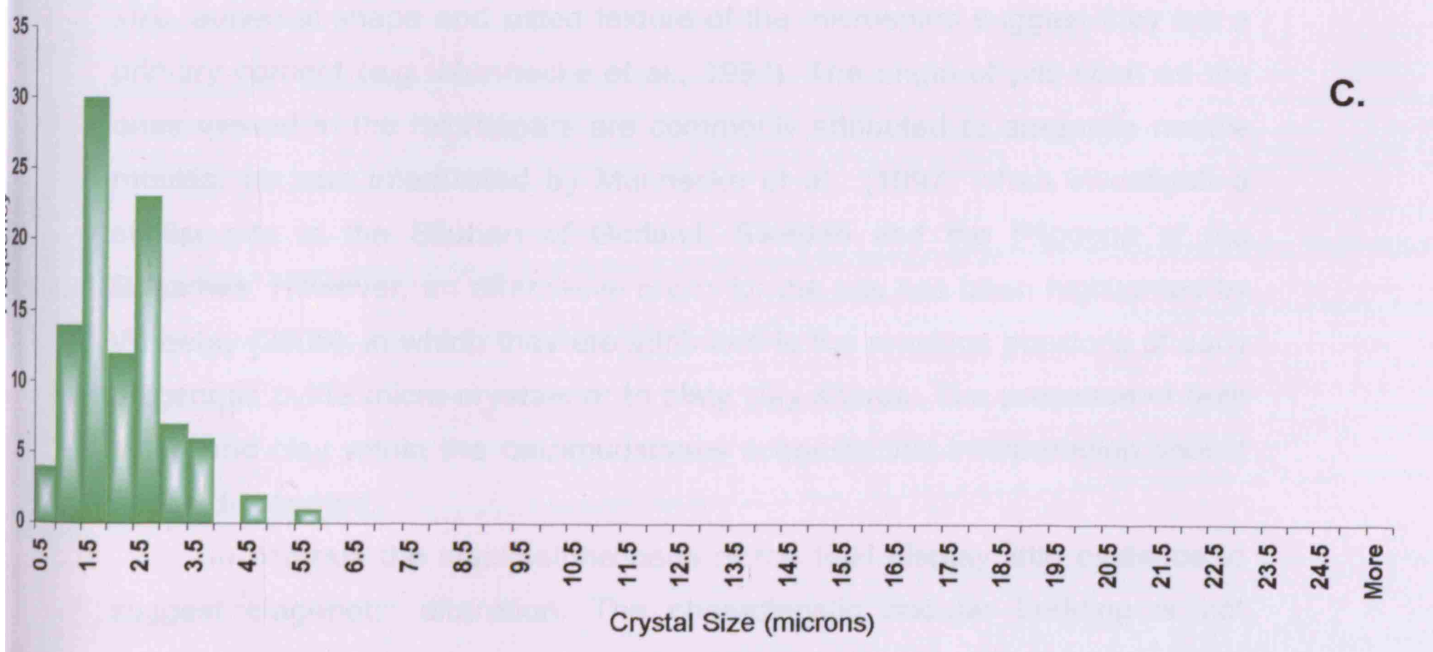
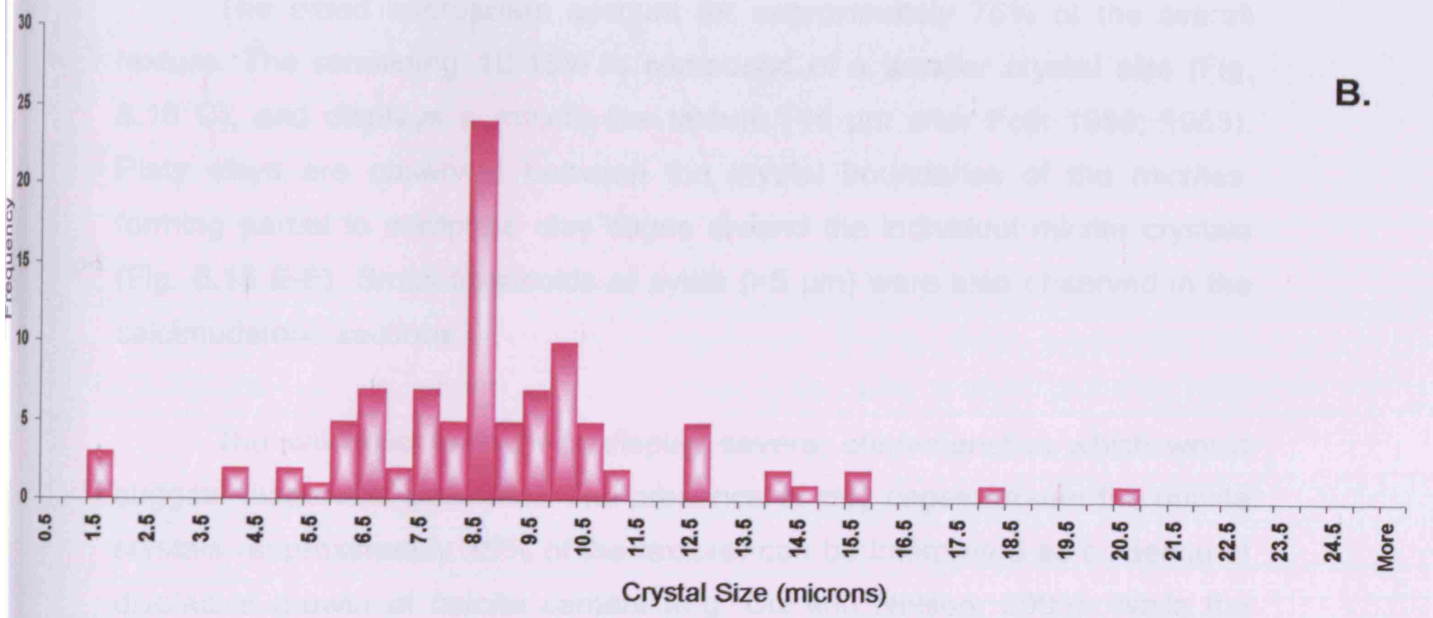
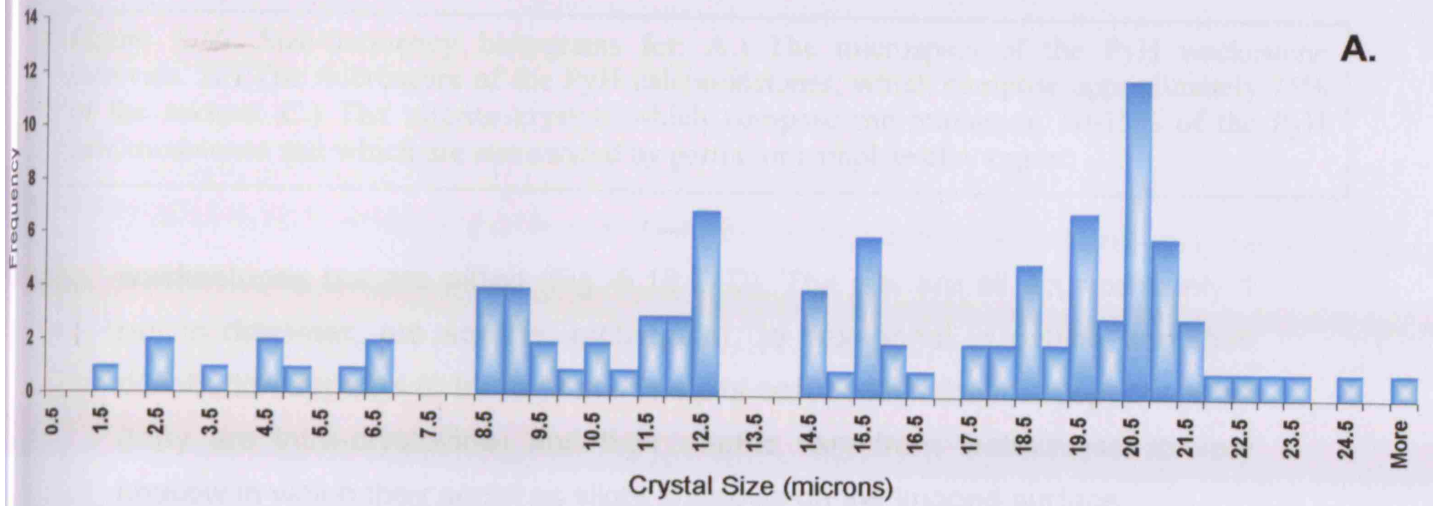


Figure 6.16. Size-frequency histograms for: A.) The microspars of the PyH wackestone intervals. B.) The microspars of the PyH calcimudstones, which compose approximately 75% of the texture. C.) The micrite crystals which compose the remaining 10-15% of the PyH calcimudstones and which are surrounded by partial or complete clay cages.

wackestones but are pitted (Fig. 6.15 C-D). The pits are all approximately 1 μm in diameter, are square, rectangular, to hexagonal in outline and their distribution appears to be random. The pits occur within the microspar crystals (they are intra-crystalline) and their depths vary from 'bottomless' to very shallow in which they occur as slight shadows on the imaged surface.

The pitted microspars account for approximately 75% of the overall texture. The remaining 10-15% is composed of a smaller crystal size (Fig. 6.16 C), and displays a micrite like texture (<4 μm after Folk 1959; 1965). Platy clays are observed between the crystal boundaries of the micrites, forming partial to complete clay cages around the individual micrite crystals (Fig. 6.15 E-F). Small framboids of pyrite (>5 μm) were also observed in the calcimudstone sections.

The calcimudstone beds display several characteristics which would suggest diagenetic alteration. The presence of clay cages around the micrite crystals (approximately 15% of the texture) can be interpreted as evidence of displacive growth of calcite cement (e.g. Dix and Nelson, 2006). While the size, euhedral shape and pitted texture of the microspars suggest they are a primary cement (e.g. Munnecke et al., 1997). The origin of pits such as the ones viewed in the microspars are commonly attributed to aragonite needle moulds, as was interpreted by Munnecke et al., (1997) when investigating similar pits in the Silurian of Gotland, Sweden and the Pliocene of the Bahamas. However, an alternative origin for the pits has been highlighted by Wheeley (2006), in which they are attributed to the previous positions of early diagenetic pyrite micro-crystals or to platy clay shards. The presence of both pyrite and clay within the calcimudstones suggests this interpretation should not be discounted.

In contrast the wackestone beds of the PyH display little evidence to suggest diagenetic alteration. The characteristic nodular bedding is not

present at outcrop, while pitting and clay cages are rare to absent when viewing the microspars under the SEM. It should be noted that the overall lack of clay within the sections renders the identification of clay cages difficult, however when combined with the absence of the other diagnostic features it seems likely that the wackestone beds of the PyH have been subject to little diagenetic alteration. In relation to the LMA discussed previously the wackestone beds do not appear to be the product of diagenetic bedding, therefore their mechanism of formation must be attributed to an alternative process, the mechanism and origin of which are discussed in the subsequent section.

6.5 Sediment dynamics on the South Wales ramp – Interpretations and discussion

An interpretation of the field, thin section and SEM results for the three studied lithologies can develop our understanding of the sediment dynamics and ultimately the development of the South Wales ramp. The High Tor Limestones are characterised by a coarse grainstone texture which displays an abundant faunal and floral assemblage, the bioclasts of which imply an open marine setting. Furthermore the algal and foraminifera assemblages of the High Tor Limestone provide evidence to suggest likely water depths for this marine setting. The most abundant alga observed within the High Tor Limestone (Fig 6.14 C) was *Koninckopora*, which in a study by Gallagher (1998) on the Lower Carboniferous of Ireland were interpreted as characteristically inhabiting water depths of less than 5 metres. This corresponds with water depth ranges of modern dasyclad algae which are found at depths down to about 30 metres, but are most commonly observed at depths of less than 5 metres (Flügel, 2004). Palaeoberesellids are also abundant and have been interpreted to have lived at water depths of around 10 metres (Adams et al., 1992; Horbury and Adams, 1996). Similarly endothyrid foraminifera, which on average compose over 6% of the High Tor composition (Fig 6.14 C3) are also described as a shallow water taxa, most likely occurring in water depths between 5-10 metres (Gallagher, 1998).

The relatively homogenous grainstone texture and lack of micrite within the High Tor Limestones would suggest a moderate to high energy environment. While the presence of abundant in-situ fossil assemblages (in the Ogmores-by-Sea sections, Fig 6.12) suggest the High Tor was the site of an active high producing carbonate factory during the Arundian. Combined with the water depth indicators derived from the algal and foraminifera assemblages this would imply that the High Tor was deposited in a very shallow water marine environment, and therefore represents the proximal (inner to middle) ramp deposits of the South Wales ramp.

The premise of this study is to identify if a similar high producing carbonate factory is observed in the more distal sections of the South Wales ramp, therefore indicating a more widespread carbonate production across the ramp environment (i.e. Wright and Faulkner, 1990), or if the shallow water bioclasts of the High Tor succession were in fact redistributed to these more distal localities, hence the necessity for a detailed understanding of the PyH.

The PyH illustrates markedly different textures to the High Tor; however it shares numerous similarities, most noticeably when comparing faunal assemblages. The PyH is characterised by an alternation of two lithologies, the possibility of this LMA being the result of diagenetic alteration has been discounted by an ultrastructural analysis of the carbonate mineralogy under the SEM (section 6.4.4.). The two lithologies of the PyH are therefore interpreted here as having contrasting modes of formation and are thus discussed separately. The wackestone beds of the PyH (L1) are interpreted as event deposits, numerous characteristics from both field and laboratory analysis present evidence to suggest this. At outcrop the wackestone units display distinctly sharp basal contacts, with the undulose bases of specific beds clearly being of erosional nature. Combined with the lack of para-autochthonous sediments at the base of the wackestone beds, these sharp bases likely represent the high energy, erosive phase of the event deposit. In contrast, the top surfaces of these beds are commonly heavily vertically bioturbated and display small colonisation surfaces, and may therefore represent post-event re-colonisation. However the most significant evidence to suggest considerable sediment redistribution and event deposits

is displayed when analysing the lithologies texture and bioclast content in thin section.

The identifiable bioclasts in thin section are typically fragmented, disarticulated and dissociated, while the matrix of the wackestones is dominated by unidentifiable, highly fragmented fine bioclastic material, both of which would suggest a significant degree of transport and reworking of the bioclasts contained within these units. Furthermore an analysis of the biotic assemblage and a comparison of the assemblage with that of the proximal, age equivalent High Tor (Fig 6.14) illustrates a significant correlation. A parallel comparison of the composition of the two lithologies (Fig 6.14 D) displays near identical bioclast types for both, in that similar bioclasts (i.e. ostracods, brachiopods, bivalves, echinoderm fragments etc) are observed in both lithologies. The proportions of these bioclasts varies greatly however and is likely to reflect their varied resistance to significant transport. Conversely this correlation is not seen in the algal and foraminiferal assemblages of the two lithologies, as the wackestones lack the same diversity seen in the High Tor Limestones. Algae such as *Koninickopora* are unlikely to have been resistant to the high degree of transport which affected the grains of these wackestone units, which may explain their lack of occurrence in the wackestone beds. Importantly very small quantities of both palaeoberesellid algae and endothyrid foraminifera were however identified in the wackestone thin sections, both of which were described previously as a shallow water taxa, most likely occurring in water depths between 5-10 metres (Gallagher, 1998).

The PyH is understood to have been deposited in water depths between 100 - 200 metres (Simpson, 1987), far too deep for these very shallow water taxa, and they must therefore have been transported from a more proximal section of the ramp. Combined with the close correlation seen in bioclast type between the High Tor and the wackestone beds of the PyH it would thus seem apparent that the source of much of the bioclastic material observed in these wackestone units may have been derived and transported from the shallow water, high producing carbonate factory of the High Tor. Consequently implying a mechanism of significant sediment redistribution may have been the controlling parameter on the development of the South

Wales ramp. The bedding and outcrop patterns suggest that this sediment redistribution occurred as a series of events, the nature and processes of which is discussed further in the subsequent section.

The second lithology of the PyH (L2), the calcimudstones, are interpreted as being representative of the background sedimentation which would have been deposited between events. Field and petrographic data suggest that the origin of mud which comprises the majority (>95%) of the calcimudstone intervals (L2) predominantly originated from inshore-derived muds, with a small contribution coming from *in situ* benthic production. The high energy and erosive nature of the storm driven events, and subsequent transport of coarser, shallow water derived grains would have resulted in significant quantities of mud being suspended within the water column. The lower energy, post event phase is likely to have resulted in much of this mud falling out of suspension, resulting in the deposition of the calcimudstone (L2) intervals upon the event bedding (L1). An absence of calcareous nannoplankton throughout the calcimudstones suggests minor, if any contribution to the outer ramp muds from pelagic sedimentation. While the identification of *in situ* fauna in the outcropping intervals of the calcimudstone beds (L2) implies a minor contribution from benthic production.

It should also be noted that the sediment dynamic regime suggested here to have been active during the Arundian was likely established and influencing the South Wales ramp prior to the Arundian. Work conducted on the Chadian and Courceyan aged sections of the South Wales ramp by Faulkner (1989) presented evidence to suggest high rates of sediment transport were also affecting the ramp at these times. The most distal beds of the Chadian and Courceyan aged sections (The Friars point limestone; Faulkner, 1989) depict a similar interbedded wackestone/mudstone character to those of the PyH; however pervasive bioturbation of these beds has obliterated much of the sedimentary structure and bedforms in these Limestones. One notable difference between the two distal sections is the absence of para-autochthonous sediment lags in the PyH wackestones, which may indicate that event bed deposition during the Arundian was higher energy and more erosive than those deposited during the Chadian and Courceyan.

6.5.1. *The event deposits of the PyH*

The previous section attributed the wackestone beds of the PyH to deposition as event deposits. Sedimentary events are defined as short (hours to days), usually rare intervals of rapid deposition within a system of relatively slow background sediment accumulation (Einsele et al., 1996). The recognition of event deposits has been studied by numerous authors (e.g. Einsele, 1982, 1996; Bourrouilh et al., 2007; Tappin, 2007), and a series of characteristics have been derived for the identification of these deposits. These characteristics include; erosional and depositional structures which reflect the onset and waning of water turbulence, sharp bases marking abrupt, lithological, textural and faunal changes (the sediment often being allochthonous), sharp tops often marked by re-colonisation surfaces where bioturbation is downward, and minor to no impact on the background bioturbation and sedimentation rate, all of which are displayed in the PyH wackestone beds thus substantiating their classification as event deposits.

The provenance of the sediment contained within these event beds was discussed when looking at the results of the thin section analysis. The majority of the material was interpreted to have been derived from the proximal, age equivalent High Tor Limestone, and was likely transported to the more distal sections of the ramp by a series of bottom water traction currents. However the initiation of these currents requires a trigger, the most likely in the marine realm being wind-induced storm waves or tsunami waves, both of which have long wave-lengths and thus an increased depth range below sea level to stir up and transport sediment accumulated in the pre-event period. With regards to the PyH this trigger is unlikely to be tsunami waves, as these waves typically leave behind a characteristic set of features (Cantalamesa and Di Celma, 2005; Dawson and Stewart, 2007; Tappin, 2007), one of which are distinctive beds in the shallow water sections due to tsunami backflow, none of which have been recorded in the Arundian sections. Storm waves would therefore appear to be the most likely trigger, and it should be noted that many heavy storms last longer than tsunamis, thus the effects of storms are likely to be more significant in the coastal zone than that of tsunamis. The principal mechanisms of resedimentation by storm waves are mass flows and traction current transport (Einsele et al., 1996).

These processes are controlled by the transformation of the storm waves into currents flowing alongshore, landward or seaward, with these turbulent flows typically reaching sufficient velocities to erode and transport coarse grained sediment.

The efficacy of this storm wave transport is defined by two parameters; the extent or reach of the wave, therefore storm-wave base, and the duration of these storms. Placing an exact value on storm-wave base is somewhat impractical, as the wave base will directly correlate to the magnitude of the storm, which itself is controlled by varied climatic conditions. Therefore storm-wave base is likely to vary significantly from one example to another. Tentative estimates at storm wave base have been presented by numerous authors, with values lying anywhere between 30 and 150 metres (e.g. Sami and Desrochers, 1992; Reading 1996; Nichols, 1998; Mohseni and Al-Asam, 2004); while other authors have suggested that stronger storms may in fact have wave bases of 200 metres or more (Komar et al., 1972).

A precise calculation of storm wave-base depth on the South Wales Arundian ramp is therefore not possible. It is however possible to decipher if the PyH was deposited above or below this level. Sediments deposited below fair weather wave base but above storm wave-base illustrate distinct sedimentary structures due to the interaction of storm waves, the most characteristic being hummocky cross stratification or HCS (Hamblin and Walker, 1979; Dott and Bourgeois, 1982). HCS was not identified within the PyH, suggesting it was therefore deposited below storm wave base. Waning bottom water traction currents derived from these storm waves would have thus been the most likely process controlling PyH event bed transport and deposition. HCS has however been identified at a more proximal location on the Arundian ramp of South Wales. Wu (1982) documented HCS outcropping in a section of High Tor Limestone at Three Cliffs Bay (Fig 6.3). This HCS was not observed in the proximal High Tor Limestone outcrops discussed in sections 6.4.2 and 6.4.3, but in a more distal location to these outcrops. The presence of this HCS advocates significant storm influence on the Arundian South Wales ramp, and its location in the proximal High Tor Limestones suggests storm-wave base was likely located somewhere between the most

distal deposits of the High Tor (middle ramp) and the PyH (outer ramp) deposits.

In contrast to our understanding of storm wave base our knowledge of storm duration is significantly greater due to modern studies of storm activity. Evidence from palaeosols, palaeokarsts and styles of meteoric diagenesis (Wright, 1990) suggest that the early carboniferous climate of southern Britain was strongly seasonal, and was affected by monsoonal systems, furthermore the South Wales region during the Arundian was located very near the equator (Fig 6.1), which by analogy to the present day would have been well within the tropical hurricane belt. A useful analogy would be with a region located in a present tropical hurricane belt. The south-east States of the USA (e.g. Louisiana, Florida etc) are one such region currently located within the Atlantic tropical hurricane belt, and The National Ocean and Atmospheric Administration (NOAA) provides extensive details of climatic conditions for this region over the last 200 years. Data sourced from NOAA suggests that typical thunder storms rarely exceed 24 hours in duration, while hurricane duration can be anything between 1 week and 1 month at the very maximum. By combining this data with the thickness distributions derived from the logged sections of the PyH, it may be possible to calculate estimates for the frequency of the events which formed the event bedding observed in the PyH sections.

6.5.2. The frequency of the PyH event deposits

An analysis of the frequency and duration of the events that influenced the PyH deposits can be estimated via a series of calculations. The principle input parameters and assumptions, and the source of parameters for these calculations are:

- 1.) *The length of the Arundian = 3.5 My (Concise geologic time scale, Ogg et al., 2008).*
- 2.) *The PyH represents deposition throughout the Arundian therefore represents 3.5 My of deposition (Simpson, 1987).*
- 3.) *Estimate of the total PyH thickness = 300 m (George et al., 1976).*

- 4.) *Number of wackestone event beds (L1) in 101.8 m of the PyH = 204.*
Sourced from own sedimentary logs.
- 5.) *Total actual thickness of wackestone event beds (L1) in 101.8 m of the PyH = 78.84 m.* Sourced from own sedimentary logs.
- 6.) *Total actual thickness of calcimudstone beds (L2) in 101.8 m of the PyH = 22.96 m.* Sourced from own sedimentary logs.
- 7.) *Of the logged 101.8 m of the PyH 77.5% of the total thickness was composed of wackestone event beds.*

Calculation 1 – Event bed frequency

For logged section –

Logged section = 101.8 m
Total PyH Thickness = 300 m

Thus logged section represents 33.9 % of the total PyH
33.9% of the Arundian = 1.19 My

Total number of event beds in logged section = 204

Frequency of events = Duration / number of events
= 1.19 My / 204 events
= 5833.33 years
~ **Event approximately every 6000 years**

Calculation 2 – Event bed duration

Assuming homogeneity throughout the PyH, the logged section can be scaled up to represent the total PyH

The 101.8 m logged section shows 204 event beds in 1.19 My (33.9% of Arundian duration)

Scaled up for the total PyH
= 600 Events in 300 m over 3.5 My

Storm derived event beds –

Average storm duration does not exceed 24 hours

If each event bed is deposited in one day:
Total duration of event deposition = 1 day x 600 events
= 600 days / 365
= 1.64
~ **Approximately 2 years for total event bed deposition**

If storm driven, the event beds were deposited in just 2 years of the total 3.5 My over which the PyH was deposited.
Therefore event deposits represent just $5.7 \times 10^{-7}\%$ of the total depositional time of the PyH

Hurricane derived event beds –

Maximum hurricane duration is approximately 30 days

If each event bed is deposited over 30 days

Total duration of event deposition = 30 days x 600 events

= 18000 days / 365

= 49.3

~ Approximately 50 years for total event bed deposition

If hurricane driven, the event beds were deposited in 50 years of the total 3.5 My over which the PyH was deposited.

Therefore event deposits represent just $1.5 \times 10^{-5}\%$ of the total depositional time of the PyH

Calculation 3 – Background sedimentation rate

The very short duration of event bed deposition (Storm derived =2 Yrs, Hurricane derived = 50 yrs) means the majority of the 3.5 My would have been dominated by background sedimentation.

Logged section = 101.8 m

Logged section represents 33.9 % of the total PyH

33.9% of the Arundian = 1.19 My

Thickness of calcimudstones in logged section = 22.96 m

= Approximately 23 m of deposition in 1.19 My

= 19.33 m in 1 Ma

Net accumulation rate = Approximately 20 m/My

The calculations provide us with some tentative estimates regarding the frequency of the events which affected the PyH. The logged sections illustrate how the majority (>75%) of the PyH is composed of these wackestone event beds, however Calculation 2 implies that these event beds represent a very minor (<1%) period of the total PyH deposition. The very short duration for the total deposition of the event beds (2 or 50 years for storms and hurricanes respectively) would indicate that much of the 3.5 My

over which the PyH was deposited would have been influenced by background sedimentation. Data extracted from the logged thickness of the calcimudstones provides an approximation for this background accumulation rate, which has been calculated at 20 m/My (Calculation 3). This rate of accumulation is not dissimilar to the value (15 m/My) assigned to modern pelagic production rates by Warrlich et al., in a recent modelling study of carbonate platform stratigraphies (2008). It should however be noted that an absence of calcareous nannoplankton would suggest that outer ramp pelagic production in the South Wales Arundian ramp was minimal, and the majority of this background accumulation is likely derived from mud deposited out of suspension as energy levels decreased post event.

The frequency of the PyH events has been calculated as a single event approximately every 6000 years (Calculation 1). Frequencies of a similar order have been calculated for ancient storm events by several authors, notably an estimated frequency of 2500-5000 years for Upper Triassic calcareous storm deposits by Aigner (1982). However, these frequencies do not correlate with those of major modern storms. As previously mentioned a suitable analogy for the climatic conditions affecting South Wales during the Arundian is the present day south-east States of the USA. These States are currently located within a tropical hurricane belt, and according to data obtained from the NOAA database the State of Florida has been the most frequently hurricane affected State since records began, with 113 hurricanes recorded in Florida since 1851. This would equate to an approximate frequency of a hurricane every 1.4 years, and even if only considering the major hurricanes that have reached Category 5 status (the strongest and most destructive of hurricanes), of which there have been 37 since 1851, this would still result in an approximate frequency of a hurricane every 4.3 years. Thus there is a considerable difference between the calculated event frequency of the PyH and that of modern storms.

This variation in frequencies could simply indicate that the Arundian experienced a considerably more stable climate than that which is observed in modern storm affected regions, with these major storms/events simply occurring less frequently than is presently observed. Alternatively, the currents responsible for the significant offshore sediment transport could have

been triggered by rarer events, one such possibility being sediment transport via geostrophic currents. These currents result from unidirectional wind forced surface currents diverging from deeper layers of water which have been deflected by the Coriolis force. The currents initially move obliquely offshore but subsequently veer around, owing to the Coriolis force to assume a direction roughly parallel to the bathymetric contours. Sediment transport via such currents has been recorded in examples such the Northern KwaZulu-Natal shelf of south-east Africa (Ramsay et al., 1996), and off the Southern Greenland Margin (Hunter et al., 2007). However, due to the directional trends of these currents they tend not to transport sediment any great distance offshore, but principally redistribute the sediment more laterally along the bathymetric contours. They are therefore unlikely to be responsible for the significant offshore transport of sediment viewed in the Arundian South Wales ramp.

The most probable reason for the significant variation between the calculated event frequency of the PyH and that of modern storms is a lack of event bed preservation. A review of depositional events by Einsele et al., (1996) stated that environments subject to permanent or frequent current reworking, such as shallow seas, generally have a low preservation potential for event deposits. This lack of preservation may be due to numerous factors, including extensive post-event bioturbation destroying the event bed structure, and erosion of event bedding by a subsequent event. The PyH event beds present considerable evidence to suggest they were deposited under high energy, erosive conditions (sharp undulose basal contacts and a lack of parautochthonous sediments at the base of the event deposits); hence considerable erosion of the underlying substrate during event bed deposition is likely. Furthermore the preservation of only the largest events or the amalgamation of numerous smaller events into a single condensed composite event bed would both significantly skew the calculated event frequency. In addition, if the event beds in the logged sections of the PyH only represent a fraction of the actual events which occurred (due to a lack of preservation), then the estimate for the total duration of event bed deposition (Calculation 2) would also be significantly increased.

6.6 Carbonate ramp sediment dynamics – Applications

The results of the combined field and laboratory analysis on the South Wales Arundian ramp provide evidence to suggest significant sediment redistribution across the system. A high sediment producing carbonate factory was likely located on the proximal section of the ramp, with intermittent storms transporting significant portions of this shallow water derived material into the deeper, more distal sections of the ramp, depositing it as a series of event beds. This continuous redistribution of sediment across the geometry is likely to have inhibited significant sediment build-up at any single point, ultimately preventing the development of a slope break or platform margin, and thus forming a very low angle depositional geometry.

With reference to the modelling work of the previous chapters, a principle outcome and hypothesis presented by the results of these numerous model runs was that the dominant controlling parameter in the development of low gradient carbonate geometries was a high rate of sediment transport. The results of the fieldwork conducted on the South Wales Arundian sections present considerable evidence in agreement with this hypothesis, as significant transport was certainly a dominant control on the development of the low gradient carbonate geometry. With regards to the continuum of form presented in chapter 4, this high transport regime and distinct lack of steepening, which combined with a comparison of the previous modelled geometries suggests the South Wales carbonate geometry would lay within the high transport, moderate production region of the matrices (e.g. correlating with geometries II and III in Figure 4.2).

One example does not however prove a hypothesis, and if sediment redistribution is in fact a major controlling parameter on the development of low gradient carbonate geometries it would be expected that similar characteristics to the ones observed in the South Wales example will be seen in numerous other low gradient carbonate systems. A review of the considerable literature covering the many carbonate ramp examples reveals that several of these characteristics are in fact present in numerous if not the majority of low gradient carbonate systems. In several examples the diagnostic features which suggest significant offshore sediment transport are

present, but have either been misinterpreted by the authors, or more commonly the significance of this sediment redistribution on the development of the system simply overlooked. One important ramp example in which the significance of these resedimentation processes has not been underestimated is the Kimmeridgian aged ramp in the northern part of the Iberian basin, upon which considerable work has been conducted by Aurell and Badenas (Aurell et al., 1995; 1998; Aurell and Badenas, 2004; Badenas et al., 2003; Badenas and Aurell, 2001; 2008; 2010).

The authors recognised that the factors controlling the sedimentation in carbonate ramps is poorly understood, and by means of a detailed analysis on the shallow to relatively deep environments of the extensive outcrops of the Kimmeridgian ramp were able to deduce a model for the sediment dynamics and development of this system. They concluded that carbonate production was higher in the proximal areas of the ramp than in the distal sections, where there was little indication of significant pelagic or benthic production, and that the activity of unidirectional return flows induced by winter storms and hurricanes played an important role in the redistribution of sediment across the ramp. A comparison with the South Wales system shows numerous similarities between the two examples, notably the likeness of the outer ramp facies. Similar to that seen in the South Wales example the most distal facies of the Kimmeridgian ramp are composed of interbedded lime mudstones and marls. The lime mudstones typically display erosive bases, and contain fragmented ooids, bioclasts and scattered skeletal and terrigenous grains, the presence of which are thus interpreted to have originated from shallower-ramp areas, and would therefore likely be comparable with the wackestone event beds of the South Wales PyH succession.

The origin of the muds in the Kimmeridgian ramp, likely akin to the calcimudstones of the PyH, is interpreted to have been predominately derived from shallow water domains and transported offshore by storm generated turbidity currents, while a small fraction is thought derived from calcareous nanoplankton. In contrast the identification of in-situ fauna in the calcimudstones of the PyH may indicate a slightly increased benthic contribution of mud to the PyH section when compared with that of the

Kimmeridgian ramp; however the majority of the mud in the PyH is also interpreted to have been derived and transported from shallower waters.

As previously mentioned the driving process behind this significant sediment redistribution across the Kimmeridgian ramp is thought to be major storms and hurricanes. The authors infer that storm surges would result in higher water elevations which in turn would result in bottom return flow. These return currents would eventually generate turbidity density currents that involved the offshore resedimentation of the carbonate grains produced in the shallow areas, the pathway of which would be driven downslope by gravity and follow the general inclination of the ramp.

The presence of this example is significant as it shares numerous similarities with the South Wales example, and more importantly the authors are in agreement with the principal control on ramp development which has been presented in this chapter for the South Wales example, in that considerable sediment redistribution of shallow water derived material is essential in maintaining low angle carbonate geometries.

The detailed analysis of the South Wales example (and to some extent the Kimmeridgian ramp) provides us with a potential list of criteria for identifying significant sediment redistribution in other low angle carbonate geometry examples. If other ramp examples have been subject to significant quantities of offshore sediment transport it would be expected that the characteristics displayed in the South Wales section will also be observed in these additional examples. As briefly mentioned previously, a search of the extensive carbonate ramp literature suggests that these properties are in fact evident in many, if not the majority of examples, yet the significance of which with regards to the development of these geometries has been underestimated. Details of several low gradient carbonate geometries which display similar evidence for significant sediment redistribution to that which is observed in the South Wales example are provided below:

1. *Becscie and Merrimack Formations, Anticosti Island Canada (Sami and Desrochers, 1992).*

The Silurian aged Formations are interpreted to have been deposited on an open marine carbonate ramp which was exposed to short-lived,

episodic high-energy cyclonic storms. This has produced a distinct outer ramp facies pattern, very similar to the one seen in the South Wales example. The strata of this facies is represented by an alternation of mudstones and packstones. The packstones contain fragmented shell assemblages and have sharp erosive bases. They are interpreted as storm event beds, and as in the South Wales example the restriction of bioturbation to the bed tops supports deposition from a single event. The interbedded muds are thought to represent intervening fair-weather sedimentation.

2. Pabdeh Formation, Zagros Basin, SW Iran (Mohseni and Al-Aasm, 2004).

The Late Paleocene to Late Eocene aged Formation is interpreted to have been deposited on a storm dominated ramp. The outer ramp facies are once more represented by an alternation of bioclastic packstones, which are rich in pelagic microfauna and have a sharp erosional base, and interbedded mudstones. Palaeogeographic reconstructions for the Formation indicate it was situated in tropical, storm-dominated palaeolatitudes during deposition.

3. Paine Member, Lodgepole Formation, SW Montana, USA (Elrick et al., 1991).

The Lower Mississippian aged deposits of the Paine Member are understood to represent distal outer ramp sedimentation and depict a bedding character very similar to that seen in the South Wales PyH. The Paine Member is composed of interbedded packstone and wackestones; the packstones are interpreted to represent distal storm deposits, whereas the wackestones which contain abundant whole, delicate fossils (akin to the PyH calcimudstones) are thought to represent quiet-water deposition during times of little or no storm activity.

4. Buah Formation, Oman (Cozzi et al., 2004).

The Neoproterozoic aged Lower Buah Formation is interpreted to have been deposited in a storm-dominated ramp environment. The mid ramp setting is characterised by the deposition (in an estimated water depth of 150 m) of abundant resedimented material of shallow-water origin, including ooids and stromatolites. While the outer ramp setting, which is interpreted to be

distally steepened, is dominated by resedimentation processes such as turbidity currents and debris flows.

5. *Vysoka Formation, Western Carpathians (Michalik, 1997).*

The Middle Triassic aged Formation is interpreted to have been deposited on a very shallow water carbonate ramp which was frequently affected by storms and occasional tsunami derived tidal waves. The distal packstone storm deposits (akin to the PyH event beds) display sharp, erosive bases and contain fragmented bioclasts of shallow marine organisms and occasional clasts of the underlying strata. The tsunamites exhibit a structureless character with large extraclasts indicating a rapid, single depositional event, and are typically accompanied by sigmoidal deformation (“rope-ladder structure”) of the underlying beds, formed by the on-shore and returning off-shore deformation of the tsunami wave. These deposits are interbedded with thin isolated beds containing a more in-situ fauna (akin to the PyH calcimudstones) and are likely representative of fair-weather conditions.

Additional low gradient carbonate geometries which present evidence to suggest significant sediment redistribution include the Upper Kimmeridgian storm-dominated ramp deposits of the Boulonnais, Northern France (Proust et al., 1995), the Lower Triassic storm-dominated ramp sequence of Northern Hungary (Hips, 1998), the Proterozoic storm-dominated ramp deposits of the Nama Group, Namibia (Dibenedetto and Grotzinger, 2005), and the Late Cenomanian-Turonian muddy ramp of the Kaskapau Formation, Western Canada (Bogdan and Plint, 2008), in which sediment is estimated to have been transported considerable distances (>250 km) offshore by storm induced currents.

These are just a selection of the ramps affected by considerable sediment redistribution which were discovered when reviewing the carbonate ramp literature. The presence of these several other transport dominated ramp systems to some extent validates the interpretation for the sediment dynamics of the South Wales example presented in this chapter. Furthermore they are in agreement with the modelling work presented in the previous chapters, in that as had previously been thought widespread carbonate

production does not appear to be occurring across the geometry (evidenced by the lack of distal carbonate factories, but significant quantities of transported material in the distal sections of each of the examples), but in fact appears to principally be occurring in shallow waters, much of which is transported offshore by storm and hurricane derived currents. While accumulation and storage of this transported sediment appears to of been relatively rare due to the high energy, highly erosive nature of the process.

A comprehension of the sediment dynamics for the examples discussed here has important implications for our broader understanding of the dominant controls on the development and maintenance of low angle carbonate geometries. This example also provides a set of criteria for comparison when interpreting (or reinterpreting) the controlling parameters on the development of other low angle carbonate geometry examples.

Chapter 7: THE SEISMIC VISIBILITY OF CARBONATE GEOMETRIES: CAN THE MPS PLATFORM GEOMETRIES BE VIEWED IN SEISMIC?

Chapters 4 and 5 presented Dionisos modelling results illustrating the control on platform geometry exerted by a range of parameters. Platform geometries formed by these models were analysed in terms of a multidimensional parameter space (MPS) to demonstrate the main controlling factors. This chapter investigates how some of these platform geometries might appear on 2D seismic lines by creating synthetic seismic for each geometry. Two methods were used, one based on simple 1D convolution, and the other based on a more realistic 2D convolution. Results from both methods were then used to analyse possible subsurface seismic expression of the platform geometries modelled in Dionisos. Scaling effects and seismic resolution are considered. The chapter concludes by discussing how the continuum of platform geometries may be identified on seismic.

7.1 Introduction

Dionisos models presented in Chapters 4 and 5 produced a variety of platform geometries within the multidimensional parameter space (MPS) (Fig. 5.30). These models are very useful for assessing the controlling parameters which produce these platform geometries. However, a key question is how such platform geometries are imaged on seismic, how different parts of a platform can be identified and thus how likely gross depositional environments and presence of petroleum system elements such as reservoir and source rock predicted. Synthetic seismic generated from numerical stratigraphic models has been used previously as a tool to extend relatively small-scale stratal geometries observed in outcrop to the relatively large-scale stratal geometries preserved in the subsurface (Helland-Hansen et al., 1994; Hodgetts and Howell, 2000; Chapin and Tiller, 2007). The assumption is that generating synthetic seismic can provide insights into understanding and interpreting stratal geometries observed on real seismic by indicating how known geometries from outcrop and stratigraphic forward models might

appear in seismic images (Sullivan et al., 2004; Janson et al., 2007; Schwab et al., 2007). More specifically, this kind of modelling can help determine what scale of features can be resolved on a particular seismic data set (Larue, 2004; Schwab et al., 2007) as well as providing insight into possible imaging artefacts (Stafleu et al., 1994).

The aim of the work presented in this chapter is to produce synthetic seismic for selected Dionisos models from Chapters 4 and 5, and investigate which geometries and architectures are well imaged and which are not. The synthetic seismic models will be analysed to see if the continuum of geometries presented in the MPS have distinguishing seismic character allowing recognition and identification of the geometries when viewed on a typical seismic line (Sheriff, 1991).

7.2 Synthetic seismic

Synthetic seismic represents the seismic response to vertical propagation of an assumed source wavelet through a model of the subsurface composed of a series of horizontal layers of differing acoustic impedance. Each layer boundary reflects some energy back to the surface, the amplitude and polarity of the reflection being determined by the acoustic impedance contrast. The synthetic seismogram comprises the sum of the individual reflections in their correct travel-time relationships (Kearey et al., 2002).

7.2.1 Calculating synthetic seismic from sonic and density log data – 1D convolution

Synthetic seismograms derived from well data are a widely useful way of providing a tie between changes in rock properties in a borehole and seismic reflection data at the same location. Seismic reflection data is initially only available in the time domain. In order that the geology encountered in a borehole can be tied to the seismic data, a 1D synthetic seismogram is generated. This is important in identifying the origin of seismic reflections seen on the seismic data. The synthetic seismogram is generated using the density and velocity data derived from the borehole logs. The data derived from these logs is used to calculate the variation in acoustic impedance down the well bore using the Zoeppritz equations (Costain and Coruh, 2004). The

acoustic impedance data is then combined with the velocity data to generate a reflection coefficient series in time. This series is convolved with a seismic wavelet to produce the synthetic seismogram. The input seismic wavelet is chosen to match as closely as possible to that produced during the original seismic acquisition.

7.2.2 Velocity and density parameters

Synthetic seismic calculated from well data is generated using the density and velocity data which is routinely measured down the borehole using wireline logging tools. Well log data of this kind can be used as a guide to what velocities should be, assigning to synthetic lithologies produced by forward models like Dionisos is more difficult. However, assigning appropriate velocity values also requires consideration of the resolution of the model, the way in which lithology is represented in the model, and which method is applied to generate the synthetic seismic. The generation of synthetic seismic for the platform geometries of the MPS has been carried out using two different software packages, both of which require the input of density and velocity data to produce the seismograms. In these synthetic seismograms density and velocity values have been assigned to individual carbonate grain types, the values of which (Table 7.1) have been determined from Rider (1986) and Janson et al. (2007).

	Sand or coarser	Silt	Mud	Shale overburden	Granite Basement
Velocity (m/s)	4100	5250	5850	3300	6500
Density (ρ)	2.45	2.58	2.6	2.27	2.75

Table 7.1. Seismic parameters used for the creation of synthetic seismic in both Dionisos and Madagascar. Values from Rider (1986) and Janson et al., (2007).

7.2.3 Calculating synthetic seismic in Dionisos – 1D convolution

The generation of synthetic seismic using the Dionisos software package uses a very similar 1D convolution technique to that used for data derived from borehole logs (section 7.2.1). Stratigraphic geometries produced in Dionisos are modelled as individual columns of stratal data, each of which are akin to a borehole log. As a result, the seismograms generated for each individual stratal column in Dionisos are calculated following a method comparable to the method used to generate a synthetic seismogram from well data.

The generation of synthetic seismic in Dionisos requires no conversion of the Dionisos models, as the original model files can be loaded and the synthetic seismic function in Dionisos utilised. Density and velocity values (Table 7.1) are specified for the seismic parameters of each grain type, and an average value determined for each cell of the Dionisos model based on the proportion of each grain present per cell. A shale overburden was also added to the original Dionisos models in an attempt to replicate post-depositional burial and generate a more realistic seismic section. In relation to the geometries presented in the MPS (Figure 6.30), geometries A, B, C, D, G, I, J and L were selected and synthetic seismograms were generated for each using a wavelet frequency of 60 and 120 Hz.

7.2.4 Calculating synthetic seismic in Madagascar – 2D convolution

The generation of synthetic seismic using a 2D convolution requires a different approach to that used for 1D. The method requires the construction of a cross-section which is populated with density and seismic velocities values for each of the individual layers. A geophysical software program (Madagascar in this example) can then run a synthetic acquisition across the model to produce a set of 'shot gathers' that can be processed as if they were real seismic data to produce a synthetic 2D seismic section. The synthetic record in this example is then generated using the exploding reflector algorithm of Lowenthal et al (1976).

The 2D convolution synthetic seismograms of the MPS geometries were generated using 'Madagascar', an open-source software package developed at the BEG (Fomel et al., 2006). In order to utilise the Madagascar

software the Dionisos models of the MPS were exported as a series of stratigraphic grids. Madagascar requires an equally spaced grid of acoustic impedance values, however Dionisos stores and outputs stratigraphy as time surfaces, each with an associated variable thickness of deposited strata and liable to be truncated or pinchout laterally, thus a conversion of the file formats was required. To achieve compatibility with Madagascar the Dionisos layers were exported as a text file, imported into an Excel work sheet, and then converted into an equally spaced grid using a linear interpolation routine implemented in Visual Basic for Excel.

These equally spaced grids were populated with density and velocity values (Table 7.1), before two grids of acoustic impedance and velocity were exported from the excel file and formatted to the standard Madagascar type file format (SEP). It should be noted that a granite basement and shale overburden were added to the original Dionisos grids in an attempt to produce realistic seismic sections. The SEP input files then implement the exploding reflector modelling module in Madagascar to generate synthetic seismograms for each Dionisos model using a wavelet frequency of 60 and 120 Hz.

As with the 1D convolution, geometries A, B, C, D, G, I, J and L were selected from the MPS (Figure 6.30), and seismograms generated for each.

7.3 Synthetic seismic results and discussion

The synthetic seismograms generated via the Dionisos 1D convolution method are presented in Figure 7.1. The original Dionisos model profile is presented for comparison with the seismograms (Fig 7.1 i). The dashed box around this profile indicates the region used in the synthetic seismic modelling, which has been selected in order to capture the carbonate platform (and platform break) and not the basinal region. Seismic images are presented at 160 times (Figure 7.1 II and III) and 640 times (Figure 7.1 IV and V) vertical exaggeration, and derived with a wavelet frequency of 60 (Figure 7.1 II and IV) and 120 Hz (Fig 7.1 III and V). Synthetic seismic generated with a 2D convolution in Madagascar are presented in Figure 7.2, which depict the Dionisos profile (Fig 7.2 I) alongside seismograms at wavelet frequencies of 60 and 120 Hz (Fig 7.2 II and III) all with a vertical exaggeration of 640 times.

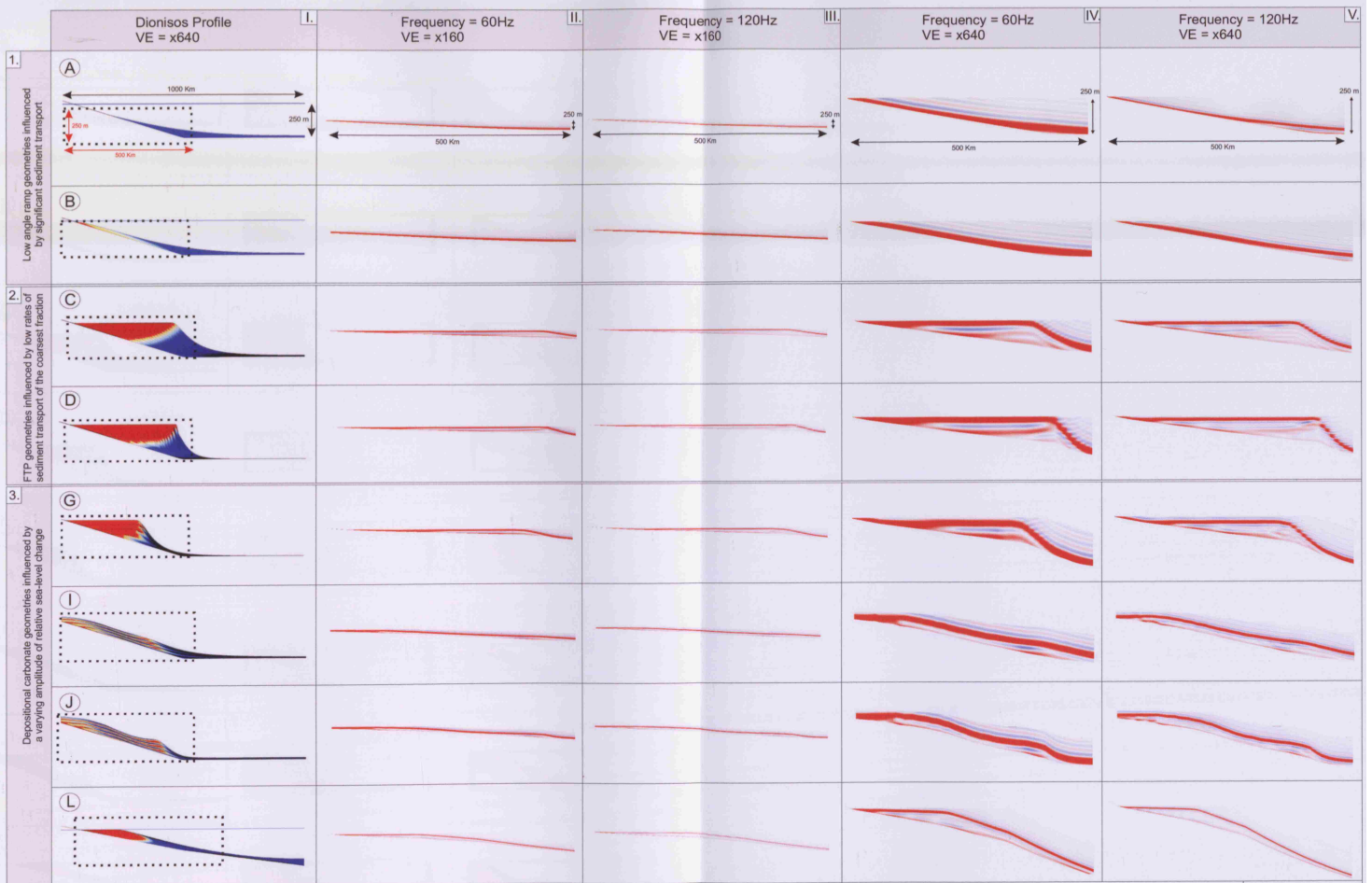


Figure 7.1

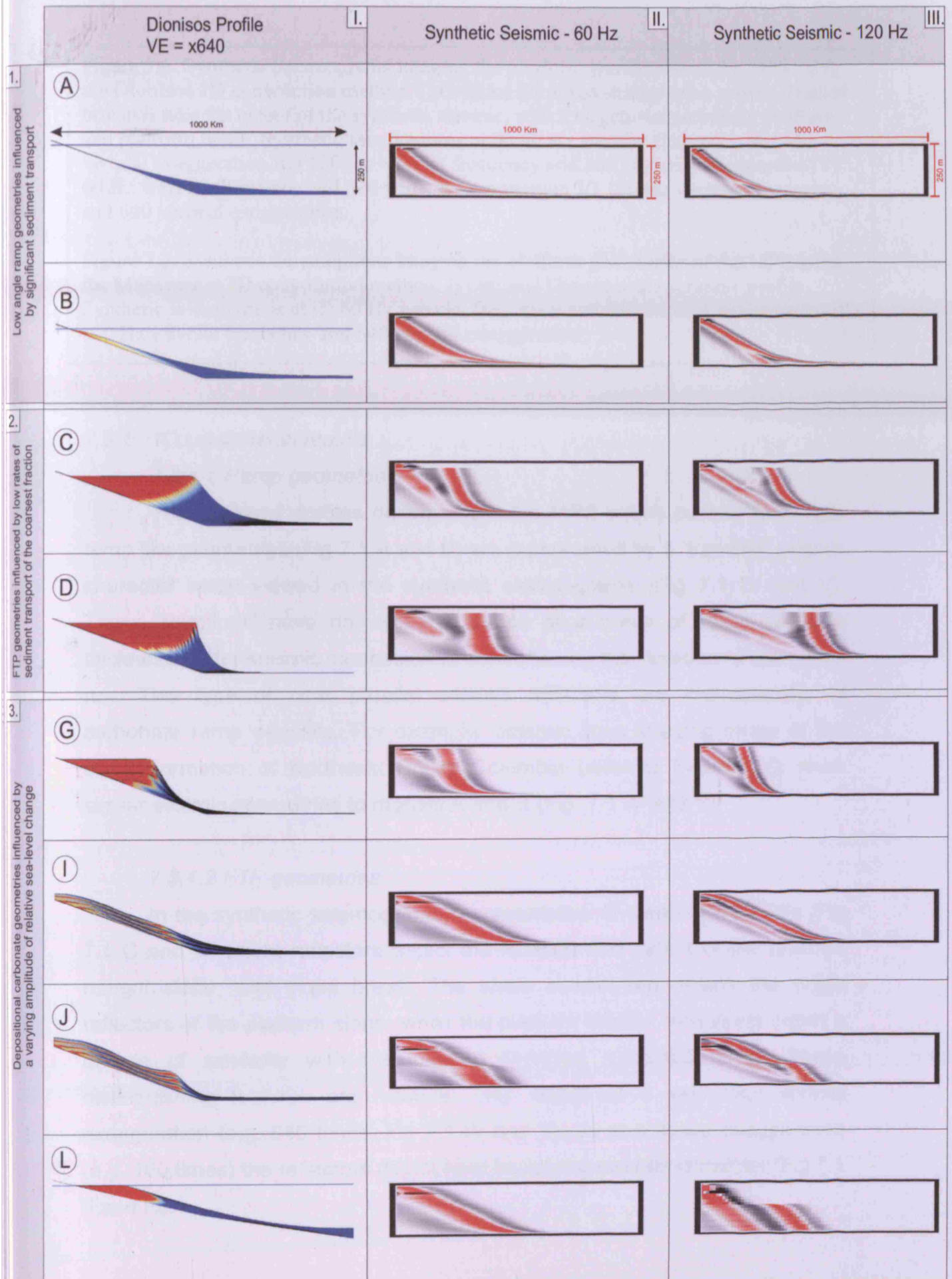


Figure 7.2

Figure 7.1. Synthetic Seismograms imaging the platform geometries of the MPS using the Dionisos 1D convolution method. I) Original Dionisos stratigraphic profile. Dashed box indicates the extent of the synthetic seismic, which targets the carbonate platform, and platform break. Synthetic seismograms at II) 60 Hz wavelet frequency and 160 vertical exaggeration III) 120 Hz wavelet frequency and 160 vertical exaggeration IV) 60 Hz wavelet frequency and 640 vertical exaggeration V) 120 Hz wavelet frequency and 640 vertical exaggeration.

Figure 7.2. Synthetic Seismograms imaging the platform geometries of the MPS using the Madagascar 2D convolution method. I) Original Dionisos stratigraphic profile. Synthetic seismograms at II) 60 Hz wavelet frequency and 640 vertical exaggeration III) 120 Hz wavelet frequency and 640 vertical exaggeration.

7.3.1 1D convolution results

7.3.1.1 Ramp geometries

The Dionisos profiles derived from the MPS which portray low angle ramp like geometries (Fig 7.1 A and B) are represented by a 'tramline' seismic character when viewed in the synthetic seismograms (Fig 7.1 IV and V). These 'tramlines' have no visible evidence of a break of slope, and the thickness of the seismic expression is controlled by the duration of the model run. This type of near parallel seismic reflectors are characteristic of carbonate ramp deposits. For example, seismic lines imaging strata of the Banff Formation of Northeast British Columbia (refer to Figure 2.5) show similar seismic geometries to models A and B (Fig. 7.1 IV and V).

7.3.1.2 FTP geometries

In the synthetic seismograms representative of steep sided FTPs (Fig 7.1 C and D) bright reflectors depict the location and extent of the platform margin slope, and slope break. The shale overburden onlaps the bright reflectors of the platform slope, while the platform interior reflections depict a degree of similarity with the original Dionisos modelled strata. These distinguishing features are however only visible at a very high vertical exaggeration (e.g. 640 times, Fig 7.1 IV and V), as at a lesser exaggeration (e.g. 160 times) the reflectors depict near horizontal seismic character (Fig 7.1 II and III).

Seismic stratigraphic interpretation commonly interprets bright reflector geometries such as the ones defining the platform margin and slope break in these examples as timelines (e.g. Vail, 1987; Posamentier et al., 1988; Van Wagoner et al., 1988). Significantly however these reflectors are unlikely to represent timelines in these synthetic seismograms (Fig 7.1 IV and V; Geometries C and D). In these examples the reflections are generated by lithological boundaries related to the platform margin trajectory of the developing FTP. Since a founding assumption of the seismic stratigraphic method is that reflections are timelines, this result may have significant implications with regards to future seismic stratigraphic interpretation, and it is therefore important to rule out other factors which may have resulted in these reflectors. One important factor to eliminate is the possibility that these continuous reflectors are an artefact of constructive interference during the 1D convolution models; 2D convolution modeling (section 7.3.2), provides some independent constraint to check this possibility.

7.3.1.3 Relative sea-level influenced examples

The synthetic seismic generated for the Dionisos geometries modelled with a high-amplitude glacio-eustatic control (Fig 7.1 I and J) depict near horizontal continuous reflectors (Fig 7.1 IV and V) similar to those seen in the seismograms representative of ramp geometries (section 7.3.1.1). These reflectors are disturbed however by a mounded feature in the more distal sections of the seismogram, which is particularly prominent in profile J (Figure 7.1). A 'bump' feature such as this viewed on a prospective seismic line might be interpreted as indicative of an offshore isolated carbonate buildup and therefore a potential hydrocarbon target. However, the original Dionisos models reveal (refer to section 5.5) how this distal 'bump' is not the result of an offshore buildup, but instead is due to the continual migration of the carbonate factory focal point across the low angle geometry. Significantly, distal bump like features similar to those viewed in the seismograms have been viewed in several glacio-eustatic effected carbonate ramp examples, such as the Permian San Andreas Formation (Kerans et al., 1994), and the Permian Grayburg Formation (Barnaby and Ward, 2007). The term 'ramp crest' has commonly been used to describe these subtle slope changes which

are recognisable on some regional seismic lines (Burchette and Wright 1992, Kerans et al., 1994).

The 1D convolution modelling illustrates the differences in seismic character displayed by differing platform geometries. Low angle carbonate geometries display a characteristic tramline like character, while FTP geometries can be distinguished by the bright reflectors attributed to their platform margin slope break. Each of the synthetic seismograms in Figure 7.1 are representative of a relatively thin depositional relief, with approximately 200-300 metres of strata deposited over 5 My. Consequently this results in relatively thin seismic expressions only a couple of reflectors in thickness. However when compared with the seismic expression of actual platform examples the characteristics displayed by these synthetic seismograms are comparable. For example, the Gialo Formation of the Sirte basin, Libya was deposited over approximately 10 My (Fiduk, 2009), with an overall average thickness of 500 to 600 metres (Hallett, 2002; Fiduk, 2009). When viewed on seismic (refer to Figures 5.17 and 5.18) the Gialo Formation is represented by several prominent reflectors, with a slope break distinguishable by means of bright reflectors. Similarly the Natih Formation of Northern Oman, specifically the E member, was deposited over approximately 4.6 My (Van Buchem et al., 2002), and has an average thickness of just 150 metres (Van Buchem et al., 2002). Viewed on seismic (refer to figure 5.20) the Natih E member is represented by just one or two prominent reflectors; however a break of slope is still interpreted at this resolution (Droste and Van Steenwinkel, 2004; Droste 2010). The similarity of these examples with the synthetic seismograms presented here suggest the seismic expression displayed in the synthetic seismic is to some degree analogous with actual carbonate platform seismic geometries.

7.3.2 2D convolution results

The synthetic seismic (Fig 7.2) created using the Madagascar 2D convolution method share numerous similarities with those produced with a 1D convolution (section 7.3.1). As with the 1D convolutions the models representative of low angle ramp geometries (Fig 7.2 A and B) portray a

'tramline' like seismic character, while the glacio-eustatic effected ramp geometries (Fig 7.2 I and J) contain the same bump like feature in the distal portion of the seismogram. Similarly the seismograms representative of FTP geometries have bright reflectors depicting the location and extent of the platform margin slope, and slope break.

The presence of these continuous bright reflectors in both the 1D and 2D convolution FTP examples suggests they are unlikely to be an artefact of constructive interference in the 1D convolution models, and significantly may represent diachronous boundaries. Unfortunately the poor resolution of the 2D convolutions means that further analysis of these reflectors is not possible, and additional detailed 2D analysis of these geometries is required to fully understand the origin of the seismic character depicted by these FTP geometries in the synthetic seismograms presented here.

The major difference between the two sets of seismograms is the seismic character of the platform interior reflectors in the FTP examples. The reflectors of the 1D examples show a horizontal, 'layer-cake' character in the platform interior, which terminate with dipping reflectors at the slope break. In contrast, in the 2D FTP examples there is a lack of interior reflectors (Fig 7.2 II and III; Geometries C and D). The seismic character of the 1D interior reflectors may therefore be an artefact of the 1D convolution method, however the disparity maybe a consequence of the poor resolution of the 2D convolution examples. An analysis of platform interior facies heterogeneity therefore requires a more comprehensive 2D analysis of the platform strata.

7.3.3 Smaller-scale models and synthetic seismic

A principal aim for creating the synthetic seismic was to investigate which geometries and architectures from the MPS have distinguishing seismic character allowing recognition and identification of the geometries when viewed on a typical seismic line. A distinguishing characteristic separating low angle carbonate geometries and FTPs is the presence and extent of a platform margin slope break, therefore a key question is when is the platform margin identifiable, and when is it not? Furthermore how steep does this platform margin have to be before it is seismically resolvable when viewed on a typical seismic line?

The seismograms presented in Figures 7.1 and 7.2 are based on a large scale carbonate system (100s of Km) and would unlikely be resolvable even on the most extensive of regional seismic lines. An additional set of synthetic seismograms has therefore been produced for a system one tenth of the scale, using the Dionisos 1D convolution method (section 7.2.3). The model is based on Geometry C from Figures 7.1 and 7.2 and the stratal and seismic geometries are near identical to those viewed in Geometry C, except at a finer scale. This allows the seismic character of the model to be viewed at a significantly lesser vertical exaggeration ($\times 30$) and seismic sections to be extracted which replicate a typical seismic line of approximately 10 Km in length (refer to Fig 7.3).

A series of synthetic seismograms depicting geometry development at 2 My time slices have been created (Fig 7.3). The seismograms are plotted alongside the original Dionisos geometries for comparison, while a maximum gradient value for each geometry is provided and a 10 Km seismic section extracted from each (Fig 7.3). The location of this extracted section is significant as a 10 Km section located in the platform interior or in the basal facies would depict considerably different seismic attributes to those depicted in the 10 Km seismic line which has been sampled. The sampled section targets the location of the platform margin slope break, and it is important to understand at what stage an interpretation of the overall platform geometry and the location of the slope margin could be made if this was the only available seismic section.

The seismogram results (Fig 7.3) illustrate how the clear identification of a slope break would be unlikely until the later stages of the model (after 6.5 My) when a steep platform margin had developed (margin gradient $> 5^\circ$). Slope breaks of a similar magnitude have been imaged and identified on seismic in the Natih Formation of Northern Oman ($2- 3^\circ$) (Droste and Van Steenwinkel, 2004), and the Smackover Formation of South Texas (4 to 7°) (Handford and Baria, 2007). Prior to this magnitude of margin gradient a reliable identification of the platform margin would be unlikely (i.e. 2.5 My; Fig 7.3), thus the synthetic seismic results demonstrate the relationship between platform margin development and the visibility of slope break on seismic. It

Figure 7.3

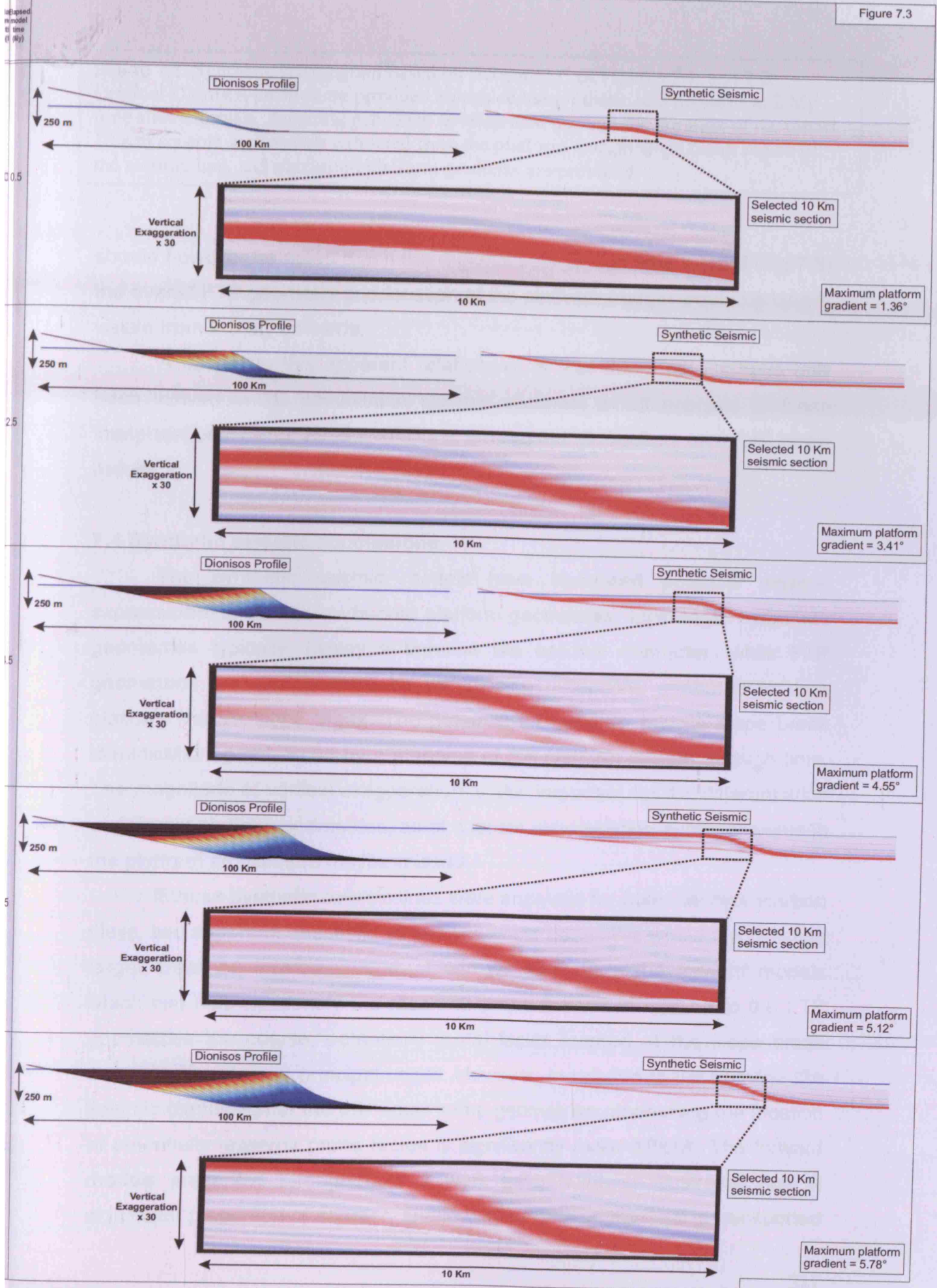


Figure 7.3. Synthetic seismogram based on Geometry C of Figures 7.1. and 7.2. Original Dionisos profiles are provided alongside the synthetic seismograms at 2 My time slice intervals, depicting geometry development through the duration of the model. 10 Km seismic sections are extracted from the platform margin slope break region of the seismic line, and maximum platform gradients are provided.

should however be noted that if the regional seismic line was viewed (Fig 7.3) the overall FTP geometry and location of the platform margin would be clearly visible from 2.5 My onwards.

A caveat to this apparent relationship is that these results have only been viewed in 1D convolution seismic sections; a full analysis of these interpretations using 2D convolutions is required to confirm or refute these results.

7.4 Synthetic seismic conclusions

The synthetic seismic models have illustrated potential seismic expressions for various carbonate platform geometries. Low angle carbonate geometries typically display a tramline like seismic character, while FTP geometries are distinguished by the dipping reflections attributed to their platform margin slope break. The potential for platform margin slope break identification is enhanced by a steeping of the platform margin through time. The magnitude of vertical exaggeration is also important for the differentiation of different platform geometries, as at a lesser exaggeration subtle changes in the platform architecture maybe missed.

If these synthetic seismic lines were analysed for potential hydrocarbon plays, two important questions to answer would be; where would the principle target areas be located, and what can we learn from the forward models which can help us identify the reservoir prone facies? In relation to the FTP geometries the coarse, potentially reefal facies located at the slope break would be the obvious principal target. However, in relation to the tramline like seismic expression of the low angle ramp geometries pinpointing the location of potentially reservoir prone facies is significantly more difficult. The forward models presented throughout this work have however illustrated how a significant proportion of coarser, shallow water derived material is transported

offshore and is deposited in the 'outer' ramp sections of the system. An observation justified by the presence of coarse, shallow water derived material in the wackestone/packstone beds located in the distal strata of the Arundian South Wales ramp (refer to chapter 6), and several other ramp examples. These outer ramp intervals could potentially present a prospective target, which due to a previous lack of understanding regarding ramp dynamics, and a bias towards shallow water facies, may have been previously overlooked. Unfortunately the resolution of the synthetic seismic presented here is unable to illustrate the stratal architecture of the outer ramp. However as we now understand these intervals may exist, high resolution seismic specifically targeting these areas may well be able to image these intervals, which potentially would be viewed on seismic passing laterally and pinching out into the more proximal middle and inner ramp facies of the system.

In relation to the low angle carbonate geometries influenced by high-amplitude glacio-eustatic variations, these systems will have a significantly greater lateral facies variation, and will therefore present distinctly different potential reservoir targets. A uniform facies distribution in which one grades laterally into another (as typically viewed in transport dominated systems) is unlikely. The forward models display how the facies will vary considerably in relation to the magnitude of relative sea-level change, and that significant coarse potential reservoir units are likely to be located offshore. These mounded features are however identifiable on seismic as convex upward features that disturb the otherwise continuous tramline reflectors. The facies heterogeneity of these mounded features is likely to vary significantly between examples, and a refined, higher resolution synthetic seismic is required to understand these features fully, they are nevertheless of significant importance with regards reservoir targets in what are otherwise featureless, tramline like seismic expressions.

These synthetic seismograms provide us with a useful insight into the seismic character of a range of carbonate platform geometries. In order to fully appreciate the location of reservoir prone facies in these geometries a more refined synthetic seismic modelling method is required. These refined models would ideally incorporate a diagenetic influence on reservoir potential and provide more realistic lithological and facies distributions, from which

reservoir facies and even potential stratigraphic traps could be identified. Such models require a higher resolution 2D convolution model than is currently able to be conducted using the Madagascar software.

Chapter 8: CONCLUSIONS AND FUTURE WORK

8.1 Conclusions

In attempting to address the objectives outlined in Chapter 1, several conclusions can be drawn from the results of the combined outcrop and modelling studies presented here.

8.1.1. Forward modelling conclusions

A principal aim of this study was to use forward modelling to identify a set of optimal conditions for carbonate ramp development. The main results obtained from these forward models are:

1. Carbonate platform strata are the result of multiple interacting controls, including sediment transport, sediment production, differential subsidence and relative sea-level oscillations. These controls and the resulting platform geometries can be understood in terms of a platform parameter space (Figure 8.1), and different platform geometries will occur in different parts of the parameter space, with a continuum of forms in between.

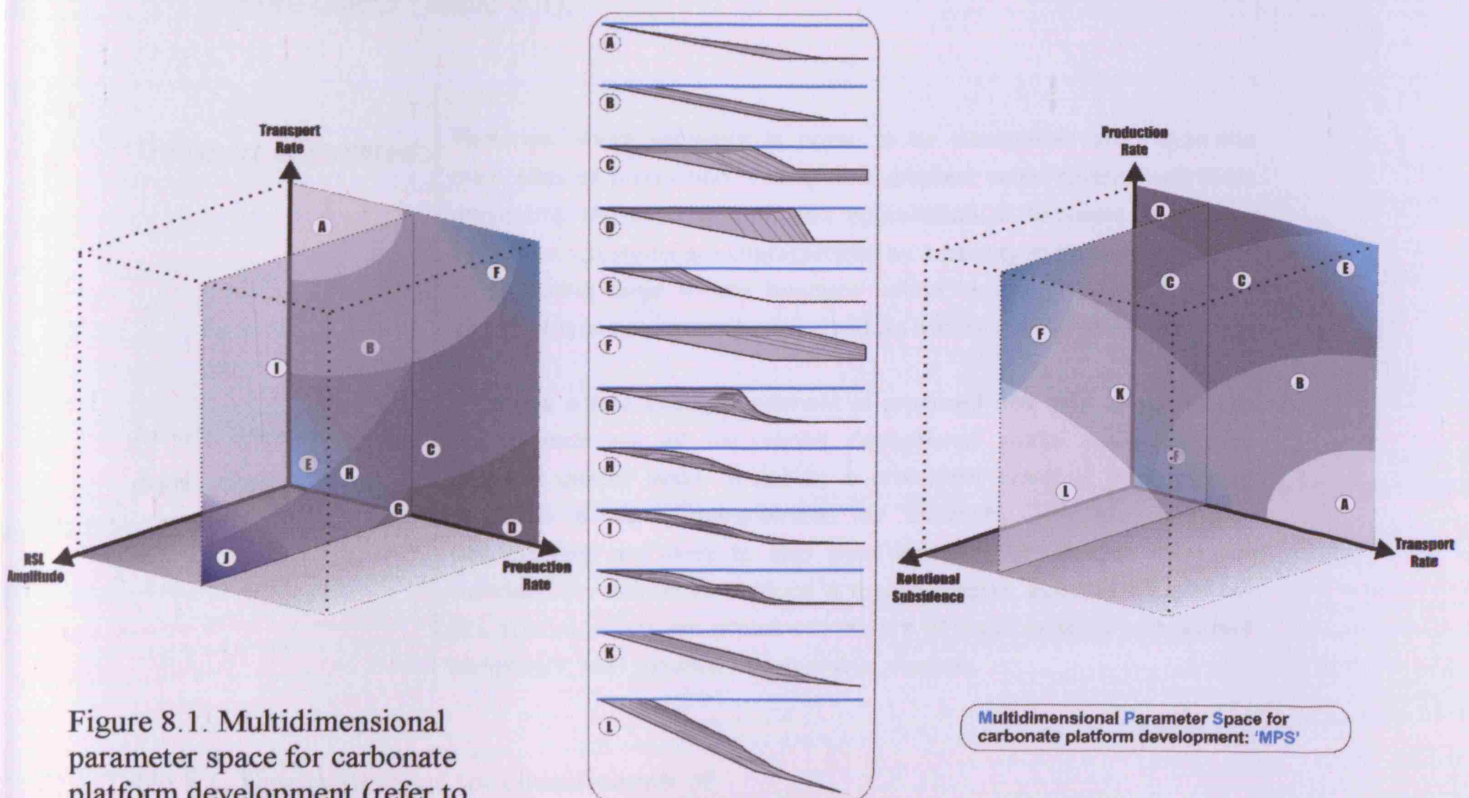


Figure 8.1. Multidimensional parameter space for carbonate platform development (refer to Fig. 5.30)

Multidimensional Parameter Space for carbonate platform development: 'MPS'

2. Rates of sediment transport exert a major control on carbonate platform development. Transport dominated systems with easily transportable carbonate grains, efficient offshore transport processes, and relatively low production rates, will maintain low-gradient ramp profiles. Systems dominated by in-situ production and accumulation will rapidly evolve into FTPs. Systems with intermediate rates of transport and production will show intermediate forms (commonly referred to as 'flat-topped ramps'), but will tend to evolve towards FTP forms.

3. While ramp and FTP are useful general descriptive terms, classification of any single example into a discrete platform type such as a ramp is often based on rather subjective criteria, for example a gradient cutoff value of 1°. Such classifications applied to specific outcrop or subsurface examples may not be particularly useful given a continuum of geometries. The distinction could be replaced with the recognition that ramps and flat-topped platforms are a process continuum, representing different balances between sediment production and sediment transport rates. Therefore a distinction between in-situ accumulation dominated, and transport dominated systems may be more useful (Table 8.1).

<i>Transport dominated</i>	Platforms where sediment is prone to be transported away from the main sites of production. Favour low gradient ramp systems, normally preventing the accumulation and aggradation of sediment to produce FTP's. Such systems are characterized by a paucity of organisms capable of producing large in-situ buildups unless in deeper waters, and by sediment types more easily dispersed by normal marine processes.
<i>In-situ accumulation dominated</i>	Platforms where enough sediment is produced and retained to lead to the development of flat-topped depositional profile separated from adjacent deeper water areas by a prominent break of slope beyond which is a zone characterized by instability and gravity flows. Deposystems are likely to also shed sediment into deeper water but sufficient is retained to produce a topographically elevated margin. In-situ accumulations are prominent feature of these systems such as reef complexes, reef mounds and microbial mounds.

Table 8.1. New definitions for classification of large-scale carbonate deposystems

4. Transport dominated systems tend to drape underlying topography, so that low-gradient platforms lacking steep margins and other elements of constructional topography may often be transport dominated systems with overall gradients controlled by a low-gradient antecedent bathymetry. 'Distally steepened ramps' may often simply represent a drape over an underlying antecedent topography.

5. Oligophotic production-depth curves tend towards flat-topped platform development, not ramps, as previously suggested. The shape and dominant loci of production curves (e.g. euphotic versus oligophotic) are not a major control on platform geometry. In the absence of high transport rates, oligophotic production curves produce flat-topped steep-margin platforms likely to be indistinguishable from platform geometries produced by euphotic curves (Figure 8.2), at least in terms of their overall geometry.

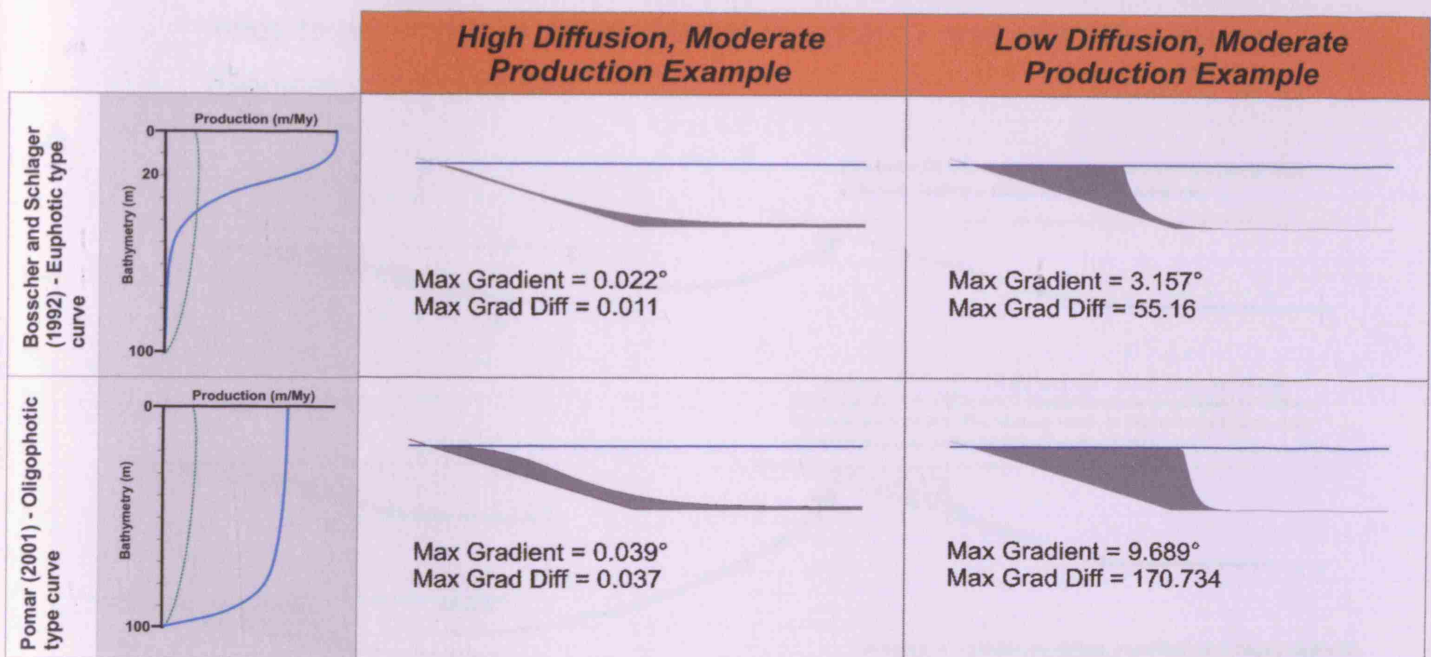


Figure 8.2. Under ramp prone (high diffusion) conditions both euphotic (Bosscher and Schlager curve) and oligophotic (Pomar curve) production-depth profiles produce low angle ramp geometries (refer to Fig. 4.5).

6. Rotational subsidence tends to favour ramp development by increasing topographic gradient through time, thus leading to increased rates of sediment transport which suppresses the generation of a constructional topography, and typically results in a low-gradient system lacking a significant slope break.
7. A relatively flat initial substrate combined with a suitable subsidence regime (preferably rotational) facilitates ramp development in passive, foreland and extensional basins. Differential subsidence forming highs with adjacent shallow depressions can affect platform progradation, or under suitable sediment transport and production rates result in distally steepened ramp geometries in the intraplatform basin setting.
8. High-amplitude glacio-eustatic oscillations tend to create low-gradient ramp systems by distributing sediment accumulation across a range of bathymetric depths, thereby preventing concentration of production that leads to generation of constructional topography and over steepening (Geometry IV, Figure 8.3).

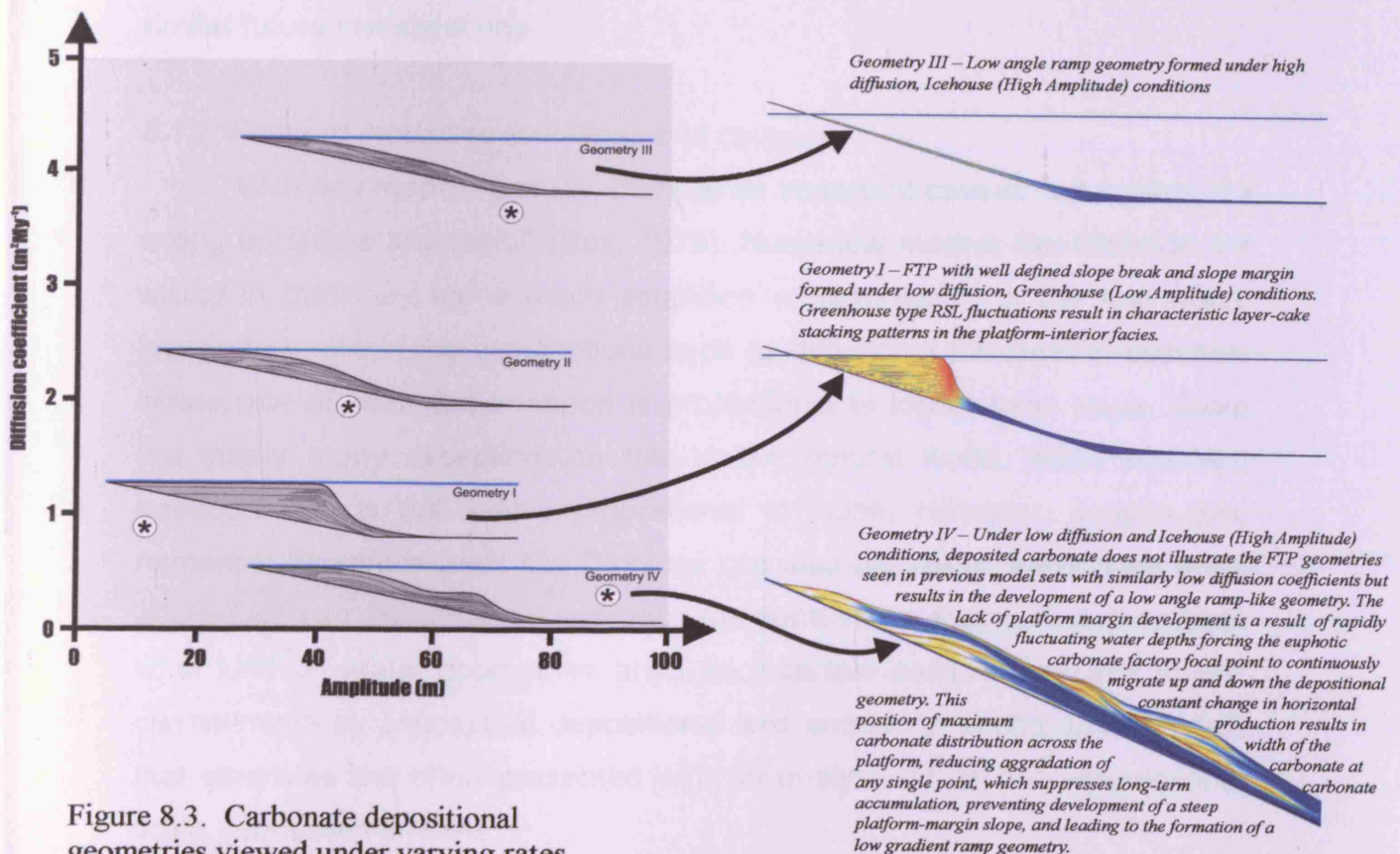


Figure 8.3. Carbonate depositional geometries viewed under varying rates of RSL change (refer to Figures. 5.22 and 5.28).

Models sets analysing the control sea-level oscillations exert on platform geometry development illustrate how sediment deposited under low amplitude, greenhouse conditions will likely behave in a similar fashion to previous models, in that under low rates of sediment redistribution the most probable geometry development will be that of a steep margined FTP (Geometry I, Figure 8.3). Conversely, as sea-level amplitude increases, and becomes more representative of ice-house conditions, platform development will trend towards low angle ramp geometries (Geometry IV, Figure 8.3), due to the rapidly fluctuating focal point of the carbonate factory, regardless of the magnitude of sediment redistribution. This correlation is also likely observed in the rock record, as the Early Carboniferous (a period significantly affected by Icehouse conditions) was a time of prolific ramp development.

The major outcomes of the modelling results listed above were made possible by the development of the APE modelling method. The creation and refinement of this analytical method is also a significant outcome of this study, and the detailed method provided will hopefully be implemented by others in similar future investigations.

8.1.2. Forward modelling limitations and caveats

With any modeling study, there is an important caveat; “all models are wrong but some are useful” (Box, 1979). Numerical models like Dionisos are wrong in that they are a much simplified representation of the real world, founded on simplifying assumptions such as diffusional transport of sediment where rate of sediment transport is proportional to topographic slope. There are surely many exceptions to this in the natural world, when sediment transport rate is not simply proportional to slope. However, despite this, numerical forward models like Dionisos can also be useful, particularly when applied with an experimental approach (as done in this study), to demonstrate what kind of stratal geometries arise from certain assumptions and to test claims made by conceptual depositional and sequence stratigraphic models that otherwise are often presented with no analysis of implicit assumptions, scale, processes or rates.

In this thesis, a numerical forward model has been used in an experimental mode to investigate, and in a limited sense at least to test, some of the current concepts of carbonate platform evolution. Two important simplifications which have facilitated this experimental modelling are that pelagic sedimentation only occurs up to a depth of 100 metres and that sedimentation is taking place upon a relatively flat, low angled substrate. Both simplifications are based on, and constrained by modern examples, with the pelagic production profile based on the commonly used curve of Bosscher and Schlager (1992), the data for which has been derived from modern carbonate production rates, while the initial basement bathymetry was constructed to be representative of the modern Arabian Gulf bathymetric profile.

Although based on modern rates and examples these simplifying model assumptions may still however have impacted the final modelled geometries. The lack of pelagic sedimentation beyond 100 metres is a consequence of the interaction between the initial basement configuration and the depth-production curve. This relationship is complicated further by the modelled subsidence rates, and rate of relative sea-level change, both of which alter the active zone of pelagic sedimentation in each respective model. These variations may result in differing modelled depositional geometries to those viewed in real world examples in which pelagic sedimentation is more widespread and occurring at greater depths. It should however be noted that rates of pelagic carbonate sedimentation are likely to be significantly less than carbonate production rates occurring in the more proximal areas of the carbonate system (Tucker and Wright, 1990), therefore the impact of pelagic sedimentation on overall gross platform geometry is likely to be minimal. Furthermore the field analysis of the Arundian aged South Wales ramp (see Chapter 6) presented evidence to suggest minimal, if any pelagic production and contribution to the outer ramp sediments of the Pen Y Holt Formation. The Pen y Holt beds are understood to have been deposited at a depth of between 100 and 200 metres (Simpson, 1987), further implying the model assumptions of pelagic sedimentation occurring only to a depth of 100 metres utilized within this modelling study may be accurate.

Additional model runs in which the rate of active pelagic sedimentation was extended to greater depths would however be beneficial in understanding the impact of pelagic production on overall platform morphology. Interestingly, models testing the influence of pelagic sedimentation on the Kimmeridgian aged ramp of the Iberian basin (Aurell et al., 1998) have already been run. The modelled geometries resulting from: 1) outer ramp facies derived from significant pelagic production, and 2) outer ramp facies derived from erosion and redeposition from inshore areas, showed similar depositional geometries. However, the models derived from significant offshore transport were deemed to be a closer match to the actual outcropping facies, further iterating the lack of influence pelagic sedimentation likely exerts on gross platform morphology, and that sediment redistribution is likely the dominant control on platform geometry development.

8.1.3. Outcrop analysis conclusions

The results obtained from the forward modelling work were tested and validated by a field analysis of the South Wales carbonate ramp. The important results achieved during this field work are:

1. A combined field and laboratory analysis of the South Wales example suggests the Arundian aged carbonate ramp was subject to significant sediment redistribution across the system.
2. A high sediment producing carbonate factory was likely located on the proximal section of the ramp, with intermittent storms transporting significant portions of this shallow water derived material into the deeper, more distal sections of the ramp, depositing it as a series of event beds.
3. There was no significant offshore carbonate factory on the South Wales ramp. The fine grained, laminated mud's which are interbedded with the event beds are representative of minor background sedimentation, deposited in the outer ramp environment between events. The outer ramp calcimudstone beds are dominantly composed of mud, the origin of which is interpreted to have predominantly

originated from inshore-derived muds deposited out of suspension during the lower energy post event phase. Muds derived from minor benthic production are evidenced by the sparse in situ fauna, while an absence of calcareous nanoplankton throughout the calcimudstones suggests minor, if any contribution to the outer ramp muds from pelagic sedimentation

4. Calculations imply an approximate frequency of 6000 years for the sediment redistributing (storm) events. However the highly erosive nature of these events and the considerable potential for lack of preservation suggest a significantly shorter duration between events, and a frequency more comparable with modern storm frequency rates.
5. The continuous redistribution of sediment across the Arundian geometry likely inhibited significant sediment build-up at any single point, ultimately preventing the development of a slope break or platform margin, and thus forming a very low angle carbonate ramp depositional geometry (Figure 8.4).
6. The observations made during the analysis of the South Wales carbonate ramp validate a principle outcome of the forward modelling results in that one of the dominant controlling parameters in the development of low gradient carbonate geometries is a high rate of sediment transport (Figure 8.4).

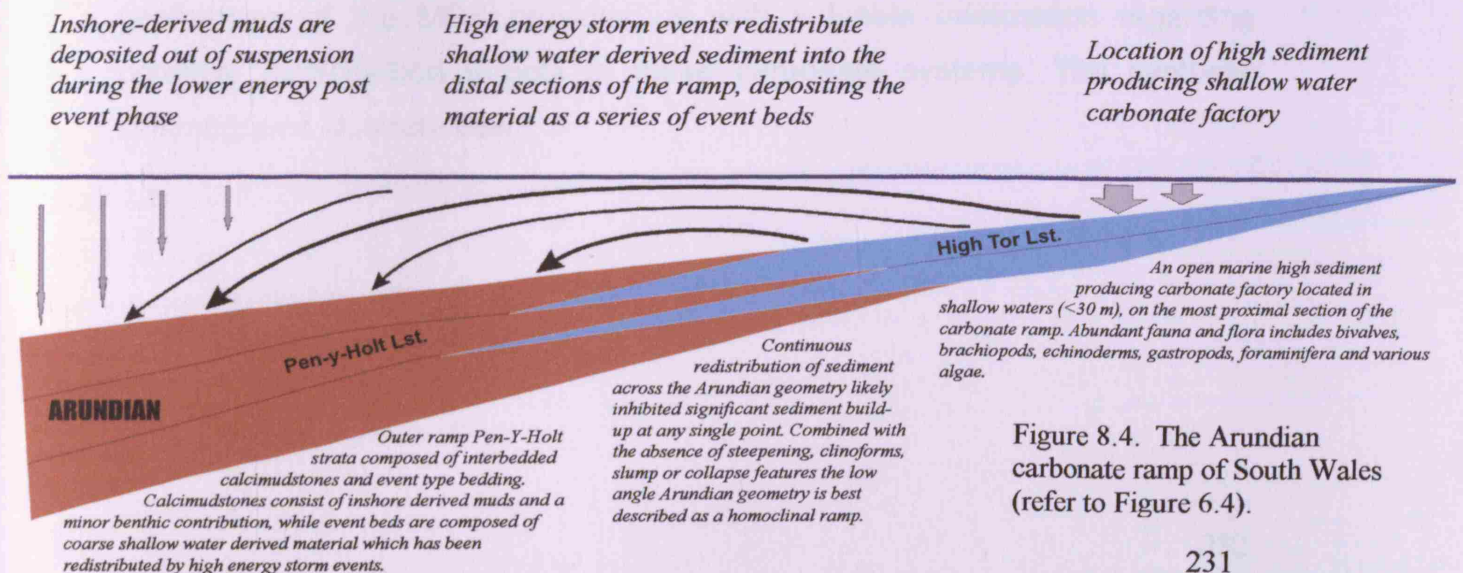


Figure 8.4. The Arundian carbonate ramp of South Wales (refer to Figure 6.4).

In addition, the South Wales ramp has been compared with numerous other carbonate ramp examples, each of which display similar diagnostic features to imply a significant magnitude of sediment transport was present during the development of each of these low angle carbonate geometries.

8.2 Wider implications of results

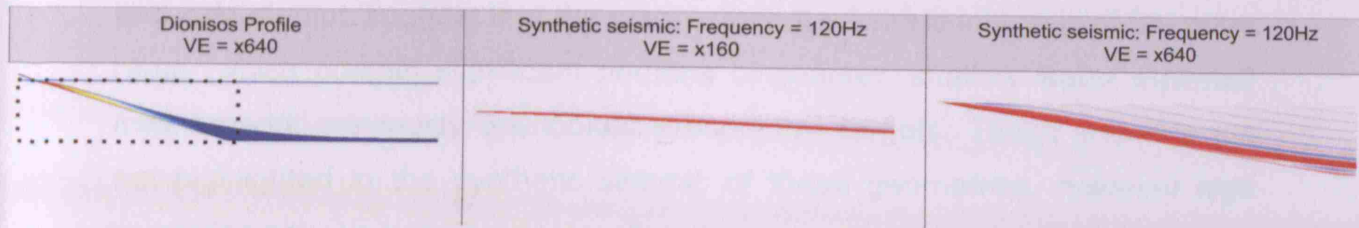
Understanding the sediment dynamics of the South Wales ramp (and the additional examples discussed) has important implications for our broader understanding of the dominant controls on the development and maintenance of low angle carbonate geometries. These examples provide us with a set of criteria for comparison when interpreting (or reinterpreting) the controlling parameters on the development of other low angle carbonate geometry examples.

The forward modelling results imply that carbonate platforms occur as a gradational series of geometries created by interacting processes of production and transport, plus the influence of other controls such as differential subsidence and relative sea-level oscillations. Combining the parameter plots for these individual controls generates an overall multidimensional parameter space for carbonate platform development (MPS, Figure 8.1). The forward models suggest that classification of any single geometry into a discrete platform type may not be particularly useful given the continuum of geometries and the transient nature of many forms. A more useful approach may be to try to determine where the system sits in the MPS taking into account as many controlling factors as possible.

Synthetic seismic investigating the seismic expression of the geometries of the MPS provides us with valuable information regarding potential hydrocarbon targets in these carbonate systems. The synthetic seismograms illustrate how:

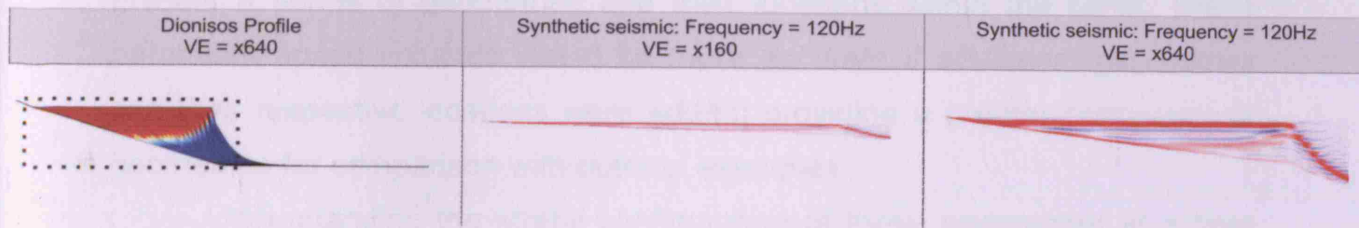
C

1. Low angle carbonate geometries typically display tramline like seismic character.



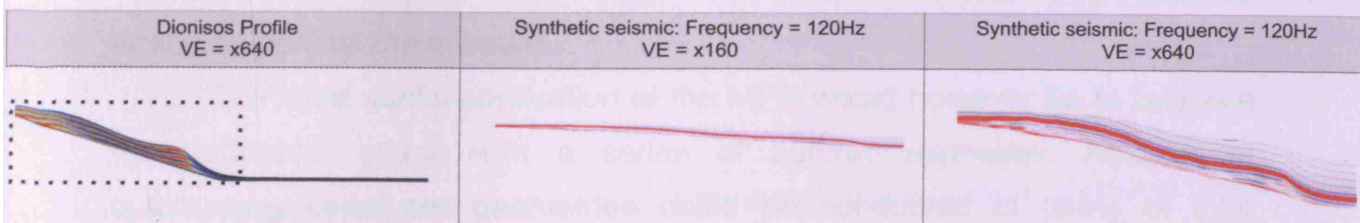
In synthetic seismic low angle ramp geometries depict 'tramline' like character with little other discernable seismic attributes

2. FTP geometries are distinguished by the bright reflectors attributed to their platform margin slope break.



FTP geometries are identifiable in synthetic seismic due to the bright reflectors attributed to the location of the platform margin slope break

3. Low angle carbonate geometries influenced by high-amplitude glacio-eustatic variations display mounded features in the distal sections of otherwise continuous seismic reflectors.



The otherwise continuous reflectors of carbonate geometries influenced by high-amplitude glacio-eustatic variations are disrupted by 'mounded' features in the distal sections of these geometries. These 'mounds' are a consequence of a rapidly fluctuating carbonate factory focal point, and may indicate the location of coarser outer ramp facies which have previously been overlooked.

The identification of potential hydrocarbon targets in the synthetic seismic of low angle carbonate systems is somewhat difficult due to the tramline like seismic expression. However, the combined forward modelling and field studies suggest that the wackestone/packstone intervals of the outer ramp (which contain significant portions of coarser, shallow water material) may present previously overlooked prospective targets. These intervals are not highlighted in the synthetic seismic of these geometries, however high resolution seismic specifically targeting these areas may prove beneficial.

8.3 Future work

A primary outcome of the work presented here was the generation of a multidimensional parameter space for carbonate platform development. A logical step would be to develop this parameter space further. The models present a series of geometries and their locations within the MPS. These parameter space volumes would be more accurate if additional geometries and their respective locations were added, providing a greater continuum of geometries for comparison with outcrop examples.

Understanding the stratal configuration of these geometries at a finer scale may also be advantageous with regards to reservoir prediction. However such a study would require use of a different forward model with more detailed representation of sediment production and transport processes, and probably an associated significant increase in computational cost. A refined model could also incorporate a diagenetic influence on reservoir potential which would provide more realistic lithological and facies distributions, which in turn would aid reservoir facies and potential stratigraphic trap identification.

The most useful application of the MPS would however be to populate the parameter space with a series of outcrop examples. Analysis of outcropping carbonate geometries could be conducted in terms of their controlling parameters, with reference to the diagnostic set of characteristics presented here. Field examination of carbonate systems from several tectonic settings would be beneficial in accurately mapping out the MPS with outcrop examples. In light of the data presented here for the misinterpretation of carbonate geometries in the intraplatform basin setting, additional

investigation into this tectonic setting would be favourable. It is proposed that the Natih Formation represents an ideal system for such a study, as the extensive exposures of this Formation, combined with the abundance of sub-surface data available would provide a good quality dataset. It is suggested that previous interpretations for the overall geometry and controlling parameters of this Formation be re-evaluated, facilitating an accurate mapping of its locality within the MPS.

In relation to fully understanding the seismic expression of these carbonate geometries a more refined synthetic seismic modelling method is required. Furthermore, a series of higher resolution 2D convolutions focusing on the distal sections of low angle carbonate systems would be advantageous in understanding the location of potential reservoir prone facies in these systems.

References

- Adams, A.E. Horbury, A.D. and Ramsay, A.T.S. 1992. Significance of palaeoberesellids (Chlorophyta) in Dinantian sedimentation, UK. *Lethaia* **25**(4), pp. 375-382
- Adams, E.W. and Schlager, W. 2000. Basic types of submarine slope curvature. *Journal of Sedimentary Research* **70**, pp. 814-828
- Ahr, W.M. 1971. Paleoenvironment, algal structures, and fossil algae in the upper Cambrian of central Texas. *Journal of Sedimentary Petrology* **41**(1), pp. 205-216
- Ahr, W.M. 1973. Carbonate Ramp - Alternative to Shelf Model. *American Association of Petroleum Geologists Bulletin* **57**, pp. 1826-1826
- Ahr, W.M. 1989. Sedimentary and tectonic controls on the development of an Early Mississippian carbonate ramp, Sacramento Mountains area, New Mexico. In: Crevello, P.D. et al. eds. *Controls on Carbonate Platforms and Basin Development*. SEPM Special Publication **44**, pp. 203-212
- Aigner, T. 1982. Calcareous tempestites: Storm-dominated stratification in Upper Muschelkalk Limestones (Middle Trias, SW-Gemany). In Einsele, G. and Seilacher A. eds. *Cyclic and Event Stratification*. New York: Springer, pp. 180–198
- Aigner, T. 1983. Facies and origin of Nummulitic buildups: an example from the Giza Pyramids Plateau, (Middle Eocene, Egypt). *Neues Jahrbuch für Geologie und Palaeontologie Abhandlungen* **166**, pp. 347-368
- Aigner, T. 1984. Dynamic stratigraphy of epicontinental carbonates, Upper Muschelkalk (M. Triassic), South-German Basin. *Neues Jahrbuch für Geologie und Palaeontologie Abhandlungen* **169**, pp. 127-159
- Alhbrandt, T.S. 2001. *The Sirte basin province of Libya - Sirte - Zelten total petroleum system*. U.S Geological Survey Bulletin, 2202 –F
- Allen, P.A. Burgess, P.M. Galewsky, J. and Sinclair, H.D. 2001. Flexural-eustatic numerical model for drowning of the Eocene perialpine carbonate ramp and implications for Alpine geodynamics. *Bulletin of the Geological Society of America* **113**(8), pp. 1052-1066
- Allen, P.A. and Allen, J.R. 2005. *Basin analysis: principles and applications*. Oxford: Blackwell Publications.

- Alsharhan, A.S. 1985. Depositional environment, reservoir units evolution, and hydrocarbon habitat of Shuaiba Formation, Lower Cretaceous, Abu Dhabi, United Arab Emirates. *American Association of Petroleum Geologists Bulletin* **69**(6), pp. 899-912
- Alsharhan, A.S. 1995. Facies variation, diagenesis, and exploration potential of the Cretaceous rudist-bearing carbonates of the Arabian Gulf. *American Association of Petroleum Geologists Bulletin* **79**(4), pp. 531-550
- Al-Tawil, A. Wynn, T.C. and Read, J.F. 2005. Sequence response of a distal-to-proximal foreland ramp to glacio-eustasy and tectonics: Mississippian, Appalachian Basin, West Virginia-Virginia, U.S.A. In: Ahr, W.M. et al. eds. *Permo-Carboniferous carbonate platforms and reefs*. American Association of Petroleum Geologists, Memoir **83**, pp. 11-34
- Anketell, J.M. 1996. Structural history of the Sirt basin and its relationship to the Sabratah basin and Cyrenaican platform, northern Libya. In: Salem M.J. et al. eds. *Geology of the Sirt Basin*. Amsterdam: Elsevier, pp. 57-89
- Aurell, M. Bosence, D. and Waltham, D. 1995. Carbonate ramp depositional systems from a late Jurassic epeiric platform (Iberian Basin, Spain): a combined computer modelling and outcrop analysis. *Sedimentology* **42**, pp. 75-94
- Aurell, M. Bádenas, B. Bosence, D.W.J. and Waltham, D.A. 1998. Carbonate production and offshore transport on a Late Jurassic carbonate ramp (Kimmeridgian, Iberian basin, NE Spain): evidence from outcrops and computer modeling. In: Wright, V.P. and Burchette, T.P. eds. *Carbonate ramps*. The Geological Society, Special Publication **149**, pp. 137-161
- Aurell, M. and Bádenas, B. 2004. Facies and depositional sequence evolution controlled by high-frequency sea-level changes in a shallow-water carbonate ramp (late Kimmeridgian, NE Spain). *Geological Magazine* **141**(6), pp. 717-733
- Azerêdo, A.C. Silva, R.L. Duarte, L.V. and Cabral, M.C. 2009. Subtidal stromatolites from the Sinemurian of the Lusitanian Basin (Portugal). *Facies* **56**(2), pp. 1-20
- Bachmann, M. and Kuss, J. 1998. The Middle Cretaceous carbonate ramp of the northern Sinai: sequence stratigraphy and facies distribution. In: Wright, V.P. and Burchette, T.P. eds. *Carbonate ramps*. The Geological Society, Special Publication **149**, pp. 253-280
- Bádenas, B. and Aurell, M. 2001. Proximal-distal facies relationships and sedimentary processes in a storm dominated carbonate ramp (Kimmeridgian, Northwest of the Iberian Ranges, Spain). *Sedimentary Geology* **139**(3-4), pp. 319-340

- Bádenas, B. Aurell, M. Rodríguez-Tovar, F.J. and Pardo-Igúzguiza, E. 2003. Sequence stratigraphy and bedding rhythms of an outer ramp limestone succession (Late Kimmeridgian, Northeast Spain). *Sedimentary Geology* **161**(1-2), pp. 153-174
- Bádenas, B. and Aurell, M. 2008. Kimmeridgian epeiric sea deposits of northeastern Spain: Sedimentary dynamics of a storm-dominated carbonate ramp. *Geological Association of Canada - Special Paper* **48**, pp. 55-71
- Bádenas, B. and Aurell, M. 2010. Facies models of a shallow-water carbonate ramp based on distribution of non-skeletal grains (Kimmeridgian, Spain). *Facies*, **56**(1) pp. 89-110
- Bahamonde, J.R. Kenter, J.A.M. Della Porta, G. Keim, L. Immenhauser, A. and Reijmer, J.J.G. 2004. Lithofacies and depositional processes on a high, steep-margined Carboniferous (Bashkirian-Moscovian) carbonate platform slope, Sierra del Cuera, NW Spain. *Sedimentary Geology* **166**(1-2), pp. 145-156
- Barnaby, R.J. and Read, J.F. 1990. Carbonate Ramp to Rimmed Shelf Evolution - Lower to Middle Cambrian Continental-Margin, Virginia Appalachians. *Geological Society of America Bulletin* **102**, pp. 391-404
- Barnaby, R.J. and Ward, W.B. 2007. Outcrop Analog for Mixed Siliciclastic - Carbonate Ramp Reservoirs - Stratigraphic Hierarchy, Facies Architecture, and Geologic Heterogeneity: Grayburg Formation, Permian Basin, U.S.A. *Journal of Sedimentary Research* **77**(1), pp. 34-58
- Barnett, A.J. Burgess, P.M. and Wright, V.P. 2002. Icehouse world sea-level behaviour and resulting stratal patterns in late Visean (Mississippian) carbonate platforms: Integration of numerical forward modelling and outcrop studies. *Basin Research* **14**, pp. 417-438
- Batten Hender, K.L. and Dix, G.R. 2008. Facies development of a Late Ordovician mixed carbonate-siliciclastic ramp proximal to the developing Taconic orogen: Lourdes Formation, Newfoundland, Canada. *Facies* **54**(1), pp. 121-149
- Beavington-Penney, S. J. Wright, V.P. and Racey, A. 2005. Sediment production and dispersal on foraminifera-dominated early tertiary ramps: the Eocene El Garia Formation, Tunisia. *Sedimentology* **52**, pp. 537-569
- Beus, S.S. 1984. Fossil Associations in the High Tor Limestone (Lower Carboniferous) of South Wales. *Journal of Paleontology* **58**(3), pp. 651-667

- Bice, D. 1988. Synthetic stratigraphy of carbonate platform and basin systems. *Geology* **16**, pp. 703-706
- Bice, D. 1991. Computer simulation of carbonate platform and basin systems. In: Franseen, E.K. et al. eds. *Sedimentary modeling: Computer simulations and methods for improved parameter definition*. Kansas Geological Survey Bulletin **233**, pp. 431-447
- Bishop, W.F. 1969. Environmental control of porosity in the Upper Smackover Limestone, North Haynesville Field, Claiborne Parish, Louisiana. *Transactions, Gulf Coast Association of Geological Societies* **19**, pp. 155-169
- Bogdan, L.V. and Plint, A.G. 2008. Palaeoenvironments, palaeogeography, and physiography of a large, shallow, muddy ramp: Late Cenomanian-Turonian Kaskapau Formation, Western Canada foreland basin. *Sedimentology* **55**(1), pp. 201-233
- Bosence, D.W.J. and Waltham, D. 1990. Computer modeling the internal architecture of carbonate platforms. *Geology* **18**, pp. 26-30
- Bosence, D.W.J. Pomar, L. Waltham, D.A. and Lankester, T.H.G. 1994. Computer modeling a Miocene carbonate platform, Mallorca, Spain. *American Association of Petroleum Geologists Bulletin* **78**(2), pp. 247-266
- Bosence, D. Cross, N. and Hardy, S. 1998. Architecture and depositional sequences of Tertiary fault-block carbonate platforms; an analysis from outcrop (Miocene, Gulf of Suez) and computer modelling. *Marine and Petroleum Geology* **15**(3), pp. 203-221
- Bosence, D. 2005. A genetic classification of carbonate platforms based on their basinal and tectonic settings in the Cenozoic. *Sedimentary Geology* **175**, pp. 49-72
- Bosscher, H. and Schlager, W. 1992. Computer simulation of reef growth. *Sedimentology* **39**, pp. 503-512
- Bosscher, H. and Southam, J. 1992. CARBPLAT - a computer model to simulate the development of carbonate platforms. *Geology* **20**(3), pp. 235-238
- Bosscher, H. and Schlager, W. 1993. Accumulation rates of carbonate platforms. *Journal of Geology* **101**(3), pp. 345-355
- Bourrouilh-Le Jan, F.G. Beck, C. and Gorsline, D.S. 2007. Catastrophic events (hurricanes, tsunamis and others) and their sedimentary records: Introductory notes and new concepts for shallow water deposits. *Sedimentary Geology* **199**(1-2), pp. 1-11

- Bowman, S.A. and Vail, P.R. 1999. Interpreting the stratigraphy of the Baltimore Canyon section, offshore New Jersey with PHIL, a stratigraphic simulator. In: Harbaugh, J.W. et al. eds. *Numerical Experiments in Stratigraphy: Recent Advances in Stratigraphic and Sedimentologic Computer Simulations*. SEPM, Special Publication **62**, pp. 117–138
- Box, G.E.P. 1979. Robustness in the strategy of scientific model building. In: Launer, R.L. and Wilkinson, G.N. eds. *Robustness in Statistics*. New York, Academic Press, pp. 202
- Boylan, A.L. Waltham, D.A. Bosence, D.W.J. Badenas, B. and Aurell, M. 2002. Digital rocks: Linking forward modelling to carbonate facies: *Basin Research* **14**, pp. 401-415
- Buckovic, D. Cvetko Tesovic, B. Jelaska, V. and Gusic, I. 2003. Evolution of Depositional Environments from the Palaeozoic to the Quaternary in the Karst Dinarides and the Pannonian Basin. In: Vlahovic, I. and Tislar, J. eds. *The Jurassic Succession of Mt. Svilaja - Field Trip Guidebook*. Opatija.
- Budd, D.A. and Loucks, R.G. 1981. *Smackover and Lower Buckner Formations, South Texas: Depositional systems on a Jurassic Carbonate Ramp*. The University of Texas at Austin, Bureau of Economic Geology. Report of Investigations No. **112**
- Burchette, T.P. 1981. European Devonian reefs: a review of current concepts and models. In: Toomey, D. ed. *European Reef Models*. SEPM Special Publication **30**, pp. 85-142
- Burchette, T.P. and Britton, S.R. 1985. Carbonate facies analysis in the exploration for hydrocarbons: a case study from the Cretaceous of the Middle East. In: Brenchley, P.J. and Williams, B.P.J. eds. *Sedimentology, Recent Developments and Applied Aspects*. Oxford: Blackwell, pp. 311-338
- Burchette, T.P. 1988. Tectonic control on carbonate platform facies distribution and sequence development: Miocene, Gulf of Suez. *Sedimentary Geology* **59**, pp. 179-204
- Burchette, T.P. Wright, V.P. and Faulkner, T.J. 1990. Oolitic sandbody depositional models and geometries. Mississippian of southwest Britain: implications for petroleum exploration in carbonate ramp settings. *Sedimentary Geology* **68**, pp. 87-115
- Burchette, T.P. and Wright, V.P. 1992. Carbonate Ramp Depositional Systems. *Sedimentary Geology* **79**, pp. 3-57

- Burchette, T.P. 1993. Mishrif Formation (Cenomanian-Turonian), Southern Arabian Gulf: Carbonate Platform Growth Along a Cratonic Basin Margin. In: Simo, J.A.T. et al. eds. *Cretaceous carbonate platforms*. American Association of Petroleum Geologists, Memoir **56**, pp. 185-200
- Burgess, P.M. 2001. Modeling carbonate sequence development without relative sealevel oscillations. *Geology* **29**, pp. 1127–1130
- Burgess, P.M. 2006. The signal and the noise: forward modelling of autocyclic and allocyclic processes influencing peritidal stacking patterns. *Journal of Sedimentary Research* **76**, pp. 962–977
- Burgess, P.M. 2008. Phanerozoic evolution of the sedimentary cover of the North American Craton. In: Miall, A. eds. *The Sedimentary Basins of the United States and Canada*. Volume **5**, Elsevier, pp. 31-63
- Burgess, P.M. 2009, In Press. A Brief Review of Developments in Stratigraphic Forward Modelling 2000-2009. In: Bally, A.W. and Roberts, D.G eds. *Phanerozoic Regional Geology of the World, Volume 1*. Elsevier.
- Burgess, P.M. and Gayer, R.A. 2000. Late Carboniferous tectonic subsidence in South Wales: Implications for Variscan basin evolution and tectonic history in SW Britain. *Journal of the Geological Society* **157**(1), pp. 93-104
- Burgess, P.M. Wright, V.P. and Emery, D. 2001. Numerical forward modeling of peritidal carbonate parasequence development: implications for outcrop interpretation. *Basin Research* **13**, pp. 1–16
- Burgess, P.M. and Wright, V.P. 2003. Numerical forward modelling of carbonate platform dynamics: an evaluation of complexity and completeness in carbonate strata. *Journal of Sedimentary Research* **73**, pp. 637–652
- Burgess, P.M. and Emery, D.J. 2004. Sensitive dependence, divergence and unpredictable behaviour in a stratigraphic forward model of a carbonate system. In: Curtis, A. and Wood, R. eds. *Geological Prior Information: Informing Science and Engineering*. The Geological Society, Special Publication **239**, pp. 77–94
- Buxton, M.W.N. and Pedley, M.H. 1989. A standardized model for Tethyan carbonate ramps. *Journal of the Geological Society London* **146**, pp. 746-748.
- Cabaleri, N.G. Armella, C. Cagnoni, M. Ramos, A. and Valencio, S.A. 2003. Carbonate ramp facies at the Calabozo Formation (Middle Jurassic), Mendoza, Argentina. *Revista Geologica de Chile* **30**(2), pp. 205-214

- Čadjenović, D. Kilibarda, Z. and Radulović, N. 2008. Late Triassic to Late Jurassic evolution of the Adriatic Carbonate Platform and Budva Basin, Southern Montenegro. *Sedimentary Geology* **204**, pp. 1-17
- Calvet, F. and Tucker, M.E. 1988. Outer ramp carbonate cycles in the Upper Muschelkalk, Catalan Basin, N.E. Spain. *Sedimentary Geology* **57**, pp. 185-198
- Cantalamesa, G. and Di Celma, C. 2005. Sedimentary features of tsunami backwash deposits in a shallow marine Miocene setting, Mejillones Peninsula, northern Chile. *Sedimentary Geology* **178**(3-4), pp. 259-273
- Chapin, M. and Tiller, G. 2007. Synthetic seismic modeling of turbidite outcrops. In: Nielsen, T.H. et al. eds. *Atlas of deep-water outcrops*. American Association of Petroleum Geologists Studies in Geology **56**, chapter 119.
- Chatellier, J. Y. 1988. Carboniferous carbonate ramp, the Banff formation, Alberta, Canada. *Bulletin des centres de recherches exploration-production Elf Aquitaine* **12**, pp. 569-599
- Cherns, L. and Wright, V.P. 2000. Missing molluscs as evidence of large-scale, early skeletal aragonite dissolution in a Silurian sea. *Geology* **28**(9), pp. 791-794
- Cherns, L. Wheeley, J.R. and Wright, V.P. 2008. Taphonomic windows and molluscan preservation. *Palaeogeography, Palaeoclimatology, Palaeoecology* **270**(3-4), pp. 220-229
- Cossey, P. J. Adams, A. E. Purnell, M. A. Whiteley, M. J. Whyte, M. A. and Wright, V. P. 2004. *British Lower Carboniferous Stratigraphy*. Geological Conservation Review Series Volume **29**. Peterborough: Joint Nature Conservation Committee.
- Contreras, J. Zühlke, R. Bowman, S. Bechstädt, T. 2010. Seismic stratigraphy and subsidence analysis of the southern Brazilian margin (Campos, Santos and Pelotas basins). *Marine and Petroleum Geology*, Article in press.
- Costain, J.K. and Coruh, C. 2004. *Basic theory of exploration seismology*. Elsevier.
- Cowie, P. A. and G. P. Roberts. 2001. Constraining Slip Rates and Spacings of Active Normal Faults. *Journal of Structural Geology* **23**, pp. 1901-1903
- Cozar, P. Somerville, I.D. Rodriguez, S. Mas, R. and Medina-Varea, P. 2006. Development of a late Viséan (Mississippian) mixed carbonate/siliciclastic platform in the Guadalquivir Valley (southwestern Spain). *Sedimentary Geology* **183**(3-4), pp. 269-295

- Cozzi, A. Allen, P.A. and Grotzinger, J.P. 2004. Understanding carbonate ramp dynamics using $\delta^{13}\text{C}$ profiles: Examples from the Neoproterozoic Buah Formation of Oman. *Terra Nova* **16**(2), pp. 62-67
- Cross, T.A. 1990. *Quantitative dynamic stratigraphy*. New Jersey: Prentice Hall.
- Cuevas Castell, J.M. Betzler, C. Rossler, J. Hussner, H. and Peinl, M. 2007. Integrating outcrop data and forward computer modelling to unravel the development of a Messinian carbonate platform in SE Spain (Sorbas Basin). *Sedimentology* **54**(2), pp. 423-441
- Cutler, W. G. 1983. Stratigraphy and sedimentology of the Upper Devonian Grosmont Formation, northern Alberta. *Bulletin of Canadian Petroleum Geology* **31**, pp. 282-325
- Davies, P.J. Symonds, P.A. Feary, D.A. and Pigram, C.J. 1989. The evolution of the carbonate platforms of northeast Australia. In: Crevello, P.D. et al. eds. *Controls on Carbonate Platforms and Basin Development*. SEPM Special Publication **44**, pp. 233-258
- Dawson, A.G. and Stewart, I. 2007. Tsunami deposits in the geological record. *Sedimentary Geology* **200**(3-4), pp. 166-183
- Della Porta, G. Kenter, J.A.M. Bahamonde, J.R. Immenhauser, A. and Villa, E. 2003. Microbial boundstone dominated carbonate slope (Upper Carboniferous, N Spain): microfacies, lithofacies distribution and stratal geometry. *Facies* **49**, pp. 175-208
- Della Porta, G. Kenter, J.A.M. and Bahamonde, J.R. 2004. Depositional facies and stratal geometry of an Upper Carboniferous prograding and aggrading high-relief carbonate platform (Cantabrian Mountains, NW Spain). *Sedimentology* **51**, pp. 267-295
- Demicco, R.V. 1998. CYCOPATH 2D - A two-dimensional, forward model of cyclic sedimentation on carbonate platforms. *Computers and Geosciences* **24**, pp. 405-423
- Demicco, R.V. and Hardie, L.A. 2002. The "carbonate factory" revisited: A re-examination of sediment production functions used to model deposition on carbonate platforms. *Journal of Sedimentary Research* **72**(6), pp. 849-857
- Dibenedetto, S. and Grotzinger, J. 2005. Geomorphic evolution of a storm-dominated carbonate ramp (c. 549 Ma), Nama Group, Namibia. *Geological Magazine* **142**(5), pp. 583-604
- Dix, G.R. and Nelson, C.S. 2006. Diagenetic potential for lithification of cool-water carbonate shelf mud. *Sedimentary Geology* **185**(1-2), pp. 41-58

- Doherty, P.D. Soreghan, G.S. and Castagna, J.P. 2002. Outcrop-based reservoir characterization: A composite phylloid-algal mound, western Orogrande basin (New Mexico). *American Association of Petroleum Geologists Bulletin* **86**(5), pp. 779-795
- Dorobek, S.L. 1995. Synorogenic carbonate platforms and reefs in foreland basins: controls on stratigraphic evolution and platform/reef morphology. In: Dorobek, S.L. and Ross, G.M. eds. *Stratigraphic Evolution of Foreland Basins*. SEPM Special Publication **52**, pp. 127-147
- Dorobek, S.L. 2008. Tectonic and depositional controls on syn-rift carbonate platform sedimentation. In: Lukasik, J. and Simo, J.A. eds. *Controls on Carbonate Platform and Reef Development*. SEPM Special Publication **89**, pp. 57-81
- Dott Jr, R.H. and Bourgeois, J. 1982. Hummocky stratification: significance of its variable bedding sequences. *Geological Society of America Bulletin* **93**(8), pp. 663-680
- Droste, H. 1990. Depositional Cycles and Source Rock Development in an Epeiric Intra-Platform Basin - the Hanifa Formation of the Arabian Peninsula. *Sedimentary Geology* **69**, pp. 281-296
- Droste, H. 2010. High-resolution seismic stratigraphy of the Shu'aiba and Natih formations in the Sultanate of Oman: implications for Cretaceous epeiric carbonate platform systems. In: Van Buchem, F.S.P. et al eds. *Mesozoic and Cenozoic Carbonate Systems of the Mediterranean and the Middle East: Stratigraphic and Diagenetic Reference Models*. The Geological Society, Special Publication **329**, pp. 145-162
- Droste, H. and Van Steenwinkel, M. 2004. Stratal Geometries and Patterns of Platform Carbonates: The Cretaceous of Oman. In: Eberli, G.P. et al. eds. *Seismic imaging of carbonate reservoirs and systems*. American Association of Petroleum Geologists, Memoir **81**, pp. 185-206
- Drummond, C.N. and Dugan, P.J. 1999. Self-organizing models of shallow-water carbonate accumulation. *Journal of Sedimentary Research* **69**, pp. 939-946
- Dunham, R.J. 1962. Classification of carbonate rocks according to depositional texture. In: Ham, W.E. ed. *Classification of carbonate rocks: a symposium*. American Association of Petroleum Geologists Memoir **1**, pp. 108-122
- Einsele, G. 1982. Limestone-marl cycles (periodites): diagnosis, significance, causes - a review. In: Einsele, G. and Seilacher, A. eds. *Cyclic and event stratification*. Springer-Verlag, pp. 8-53
- Einsele, G. 1996. Event deposits: The role of sediment supply and relative sea-level changes – Overview. *Sedimentary Geology* **104**(1-4), pp. 11-37

- Einsele, G. Ricken, W. and Seilacher, A. 1991. *Cycles and events in stratigraphy*. New York: Springer-Verlag.
- Einsele, G. Chough, S.K. and Shiki, T. 1996. Depositional events and their records - an introduction. *Sedimentary Geology* **104**(1-4), pp. 1-9
- Elrick, M. Read, J.F. and Coruh, C. 1991. Short-term paleoclimatic fluctuations expressed in lower Mississippian ramp-slope deposits, southwestern Montana. *Geology* **19**(8), pp. 799-802
- Evans, G. 1995. The Arabian Gulf: a modern carbonate-evaporite factory; a review. *Cuadernos de Geologia Iberica* **19**, pp. 61-96
- Faulkner, T.J. 1988. The Shipway Limestone of Gower: sedimentation on a storm-dominated early Carboniferous ramp. *Geological Journal* **23**, pp. 85-100.
- Faulkner, T.J. 1989. *Carbonate facies on a Lower Carboniferous storm-influenced ramp in SW Britain*. PhD Thesis, University of Bristol, Bristol (unpublished).
- Fiduk, J.C. 2009. Evaporites, petroleum exploration, and the Cenozoic evolution of the Libyan shelf margin, central North Africa. *Marine and Petroleum Geology* **26**(8), pp. 1513-1527
- Flügel, E. 2004. *Microfacies of Carbonate Rocks. Analysis, Interpretation and Application*. New York: Springer-Verlag.
- Folk, R.L. 1959. Practical petrographic classification of limestones. *American Association of Petroleum Geologists Bulletin* **43**, pp. 1-38
- Folk, R.L. 1965. *Petrology of sedimentary rocks*. Texas: Hemphill's.
- Fomel, S. Sava, P. and Hermann, F. 2006. Introducing RSF, a computational platform for geophysical data Processing and reproducible numerical experiments. *Vienna EAGE workshop 2, Open-source E&P software*. Program with abstract.
- Gaetani, M. Gnaccolini, M. Poliani, G. Grignani, D. Gorza, M. and Martellini, L. 1991. An anoxic intraplatform basin in the Middle Triassic of Lombardy (southern Alps, Italy): anatomy of a hydrocarbon source. *Rivista Italiana di Paleontologia e Stratigrafia* **97**(3-4), pp. 329-353
- Galewsky, J. 1998. The dynamics of foreland basin carbonate platforms: Tectonic and eustatic controls. *Basin Research* **10**(4), pp. 409-416

- Gallagher, S.J. 1998. Controls on the distribution of calcareous Foraminifera in the Lower Carboniferous of Ireland. *Marine Micropaleontology* **34**(3-4), pp. 187-211
- George, T.N. Johnson, G.A.L Mitchell, M. Prentice, J.E. Ramsbottom, W.H.C. Sevastopulo, G.D. and Wilson, R.B. 1976. *A correlation of the Dinantian rocks of the British Isles*. The Geological Society, Special Publication **7**, pp. 1-87
- Gerber, T.P. Pratson, L.F. Wolinsky, M.A. Steel, R. Mohr, J. Swenson, J.B. and Paola, C. 2008. Clinof orm Progradation by Turbidity Currents: Modeling and Experiments. *Journal of Sedimentary Research* **78**, pp. 220-238
- Ghamdi, M. 2010. *The Sedimentology, sea-level history and porosity evolution of the Holkerian (Lower Carboniferous) of Gower*. MPhil Thesis, University of Cardiff, Cardiff (unpublished).
- Gilham, R.F. and Bristow, C.S. 1998. Facies architecture and geometry of a prograding carbonate ramp during the early stages of foreland basin evolution: Lower Eocene sequences, Sierra del Cadí, SE Pyrenees, Spain. In: Wright, V.P. and Burchette, T.P. eds. *Carbonate ramps*. The Geological Society, Special Publication **149**, pp. 181-203
- Ginsburg, R.N. and James, N.P. 1974. Holocene carbonate sediments of continental shelves. In: Burk, C.A. and Drake, C.L. eds. *The Geology of Continental Margins*. New York: Springer-Verlag.
- Ginsburg, R.N. Gischler, E. and Kiene, W.E. 2001. Partial mortality of massive reef-building corals: An index of patch reef condition, Florida Reef Tract. *Bulletin of Marine Science* **69**(3), pp. 1149-1173
- Glennie, K.W. 1995. *The geology of the Oman Mountains: An outline of their origin*. Bucks: Scientific Press Ltd.
- Goldhammer, R.K. Dunn, P.A. and Hardie, L.A. 1987. High frequency glacio-eustatic sealevel oscillations with Milankovitch characteristics recorded in Middle Triassic platform carbonates in northern Italy. *American Journal of Science* **287**(9), pp. 853-892
- Goldhammer, R.K. Oswald, E.J. and Dunn, P.A. 1991. Hierarchy of stratigraphic forcing: example from Middle Pennsylvanian shelf carbonates of the Paradox Basin. In Franseen, E.K. et al. eds. *Sedimentary Modeling: Computer Simulations and Methods for Improved Parameter Definition*. Kansas Geological Survey, Bulletin **233**, pp. 361-413
- Goldhammer, R.K. Lehmann, P.J. and Dunn, P.A. 1993. The origin of high-frequency platform carbonate cycles and third-order sequences (Lower Ordovician El Paso Gp, west Texas): constraints from outcrop data and stratigraphic modeling. *Journal of Sedimentary Petrology* **63**, pp. 318-359

- Golonka, J. 2002. Plate-tectonic maps of the Phanerozoic. In: Kiessling, W. et al. eds. *Phanerozoic reef patterns*. SEPM Special Publication **72**, pp. 21-75
- Graham, J.R. and Sevastopulo, G.D. 2008. Mississippian Platform and basin successions from the Todrha Valley (northeastern Anti-Atlas), southern Morocco. *Geological Journal* **43**(2-3), pp. 361-382
- Granjeon, D. and Joseph, P. 1999. Concepts and applications of a 3-D multiple lithology, diffusive model in stratigraphic modeling. In: Harbaugh, J.W. et al. eds. *Numerical experiments in stratigraphy: Recent advances in stratigraphic and sedimentologic computer simulations*. SEPM, Special Publication **62**, pp. 197-210
- Granjeon, D. Casa, M. C. Eschard, R. and Joseph, P. 2002. Stratigraphic modeling: A new tool to construct 3-D geological models for basin modeling purposes. *American Association of Petroleum Geologists Annual Meeting Program* **11**, pp. A66
- Grotzinger, J.P. 1989. Facies and evolution of Precambrian carbonate depositional systems: emergence of the modern platform archetype. In: Crevello, P.D. et al. eds. *Controls on Carbonate Platforms and Basin Development*. SEPM Special Publication **44**, pp. 79-106
- Gutteridge, P. 1989. Controls on carbonate sedimentation in a Brigantian intrashelf basin (Derbyshire). In: Arthurton, R.S. et al. eds. *The Role of Tectonics in Devonian & Carboniferous Sedimentation in British Isles*. Yorkshire Geological Society Occasional Publication **6**, pp. 171-187
- Hallam, A. 1986. Origin of minor limestone shale cycles: climatically induced or diagenetic? *Geology* **14**(7), pp. 609-612
- Hallett, D. 2002. *Petroleum Geology of Libya*. Elsevier.
- Hamblin, A.P. and Walker, R.G. 1979. Storm-dominated shallow marine deposits: the Fernie- Kootenay (Jurassic) transition, southern Rocky Mountains. *Canadian Journal of Earth Sciences* **16**(9), pp. 1673-1690
- Hancock, P.L. Dunne, W.M. and Tringham, M.E. 1983. Variscan deformation in southwest Wales. In: Hancock, P.L. ed. *The Variscan fold belt in the British Isles*. Bristol: Adam Hilger, pp. 47-73
- Handford, C.R. and Baria, L.R. 2007. Geometry and seismic geomorphology of carbonate shoreface clinofolds, Jurassic Smackover Formation, north Louisiana. In: Davies, R.J. et al. eds. *Seismic Geomorphology: Applications to Hydrocarbon Exploration and Production*. Geological Society, London, Special Publication **277**, pp. 171-185

- Haq, B.U. Hardenbol, J. and Vail, P.R. 1988. Mesozoic and Cenozoic chronostratigraphy and cycles of sea-level change. In: Wilgus, C.K. et al. eds. *Sea-Level Changes - An Integrated Approach*. SEPM, Special Publication **42**, pp. 71-108
- Haq, B.U. and Al-Qahtani, A.M. 2005. Phanerozoic cycles of sea-level change on the Arabian platform. *GeoArabia* **10**(2), pp. 127-160
- Haq, B.U. and Schutter, S.R. 2008. A chronology of paleozoic sea-level changes. *Science* **322**, pp. 64-68
- Helland-Hansen, W. Helle, H.B. and Sunde, K. 1994. Seismic modeling of Tertiary sandstone clinothems, Spitsbergen. *Basin Research* **6**, pp. 181-191
- Helland-Hansen, W. and Hampson, G.J. 2009. Trajectory analysis: Concepts and applications. *Basin Research* **21**(5), pp. 454-483
- Hennebert, M. and Lees, A. 1991. Environmental gradients in carbonate sediments and rocks detected by correspondence analysis: examples from the Recent of Norway and the Dinantian of southwest England. *Sedimentology* **38**(4), pp. 623-642
- Hips, K. 1998. Lower Triassic storm-dominated ramp sequence in northern Hungary: An example of evolution from homoclinal through distally steepened ramp to Middle Triassic flat-topped platform. In: Wright, V.P. and Burchette, T.P. eds. *Carbonate ramps*. The Geological Society, Special Publication **149**, pp. 315-338
- Hodgetts, D. and Howell, J.A. 2000. Synthetic seismic modeling of a large-scale geological cross-section from the Book Cliffs, Utah, U.S.A. *Petroleum Geoscience* **6**, pp. 221-229
- Hogg, S.L. 1993. Geology and hydrocarbon potential of the Neuquen Basin. *Journal of Petroleum Geology* **16**(4), pp. 383-396
- Horbury, A.D. and Adams, A.E. 1996. Microfacies associations in Asbian carbonates: An example from the Urswick Limestone Formation of the southern Lake District, northern England. In: Strogon, I.D. et al. eds. *Recent Advances in Lower Carboniferous Geology*. The Geological Society, Special Publication **107**, pp. 221-237
- Hunter, S. Wilkinson, D. Louarn, E. McCave, N.I. Rohling, E. Stow, D.A.V. and Bacon, S. 2007. Deep western boundary current dynamics and associated sedimentation on the Eirik Drift, Southern Greenland Margin. *Deep-Sea Research Part I: Oceanographic Research Papers* **54**(12), pp. 2036-2066

- James, N.P. and Kendall, A.C. 1992. Introduction to carbonate and evaporite facies models In: Walker, R.G. and James, N.P. eds. *Facies Models: Response to Sea Level Change*. Geological Association of Canada, pp. 265-275
- James, N.P. Collins, L.B. Bone, Y. and Hallock, P. 1999. Subtropical carbonates in a temperate realm: Modern sediments on the southwest Australian shelf. *Journal of Sedimentary Research* **69**, pp. 1297-1321
- Janson, X. Eberli, G.P. Bonnaffe, F. Gaumet, F. and Casanove, V. 2007. Seismic expressions of a Miocene prograding carbonate margin, Mut Basin, Turkey. *American Association of Petroleum Geologists Bulletin* **91**, pp. 685-713
- Kassler, P. 1973. The Structural and geomorphic evolution of the Persian Gulf. In: Purser, B.H. ed. *The Persian Gulf: Holocene carbonate sedimentation and diagenesis in a shallow epicontinental sea*. Berlin: Springer-Verlag, pp. 11-32
- Kastner, M. Schuke, I. and Winsemann, J. 2008. Facies architecture of a Late Jurassic carbonate ramp: The Korallenoolith of the Lower Saxony Basin. *International Journal of Earth Sciences* **97**(5), pp. 991-1011
- Keary, P. Brooks, M. and Hill, I. 2002. *An introduction to Geophysical Exploration*. Wiley: Blackwell.
- Keeley, M.L. 1994. Phanerozoic evolution of the basins of Northern Egypt and adjacent areas. *Geologische Rundschau* **83**(4), pp. 728-742
- Kendall, C.G.St.C. and Schlager, W. 1981. Carbonates and relative changes in sea level. *Marine Geology* **44**, pp. 181-212
- Kenter, J. A. M. 1990. Carbonate platform flanks: Slope angle and sediment fabric. *Sedimentology* **37**, pp. 777-794
- Kenter, J.A.M. Harris, P.M. and Porta, G. 2005. Steep microbial boundstone-dominated platform margins; examples and implications, *Sedimentary Geology* **178**, pp. 5-30
- Kenyon, P.M. and Turcotte, D.L. 1985. Morphology of a delta prograding by bulk sediment transport. *Bulletin of Geological Society of America* **96**, pp. 1457-1465
- Kerans, C. Lucia, F.J. and Senger, R.K. 1994. Integrated Characterization of Carbonate Ramp Reservoirs Using Permian San-Andreas Formation Outcrop Analogs. *American Association of Petroleum Geologists Bulletin* **78**, pp. 181-216

- Kirkland, D.W. and Evans, R. 1981. Source-Rock Potential of Evaporitic Environment. *American Association of Petroleum Geologists Bulletin* **65**, pp. 181-190
- Kjennerud, T. Lippard, S.J. and Vanhauwaert, P. 2001. Short term development of intracontinental rifts, with reference to the late Quaternary of the Rukwa Rift (East African Rift System). *Marine and Petroleum Geology* **18**(3), pp. 307-317
- Komar, P.D. Neudeck, R.H. and Kulm, L.D. 1972. Observations and significance of deep water oscillatory ripple marks on the Oregon Continental shelf. In: Swift, P.J.P et al. eds. *Shelf Sediment Transport: Process and Pattern*. Dowden, Hutchinson and Ross, pp. 601-619
- Ku, T.C.W. Walter, L.M. Coleman, M.L. Blake, R.E. and Martini, A.M. 1999. Coupling between sulfur recycling and syndepositional carbonate dissolution: Evidence from oxygen and sulfur isotope composition of pore water sulfate, South Florida Platform, U.S.A. *Geochimica et Cosmochimica Acta*, **63**(17), pp. 2529-2546
- Lachkar, N. Guiraud, M. El Harfi, A. Dommergues, J.-L. Dera, G. and Durllet, C. 2009. Early Jurassic normal faulting in a carbonate extensional basin: Characterization of tectonically driven platform drowning (High Atlas rift, Morocco). *Journal of the Geological Society* **166**(3), pp. 413-430
- Larue, D. 2004. Outcrop and waterflood simulation modeling of the 100-foot channel complex, Texas and the Ainsa II channel complex, Spain: Analogs to multistory and multilateral channelized slope reservoirs. In: Grammer, G.M. et al. eds. *Integration of outcrop and modern analogs in reservoir modelling*. American Association of Petroleum Geologists, Memoir **80**, pp. 337-364
- Lehrmann, D.J. and Goldhammer, R.K. 1999. Secular variation in parasequence and facies stacking patterns of platform carbonates: A guide to application of stacking pattern analysis in strata of diverse ages and settings. In Harris, P.M. et al. eds. *Advances in Carbonate Sequence Stratigraphy: Applications to Reservoirs, Outcrops, and Models*. SEPM, Special Publication **63**, pp. 187-225
- Lerche, I. Dromgoole, E. Kendall, C.G.St.C. Walter, L.M. and Scaturro, D. 1987. Geometry of carbonate bodies: A quantitative investigation of factors influencing their evolution. *Carbonates and Evaporites* **2**(1), pp. 15-42
- Lindsay, R.F. and Kendall, C.G.St.C. 1985. Depositional facies, diagenesis, and reservoir character of Mississippian cyclic carbonates in the Mission Canyon Formation, Little Knife Field, Williston Basin, North Dakota. In: Roehl, P.O. and Choquette, P.W. eds. *Carbonate Petroleum Reservoirs*. New York: Springer-Verlag, pp. 175-190

- Liu, K. Pigram, C.J. Paterson, L. and St. Kendall, C.G.C. 1998. Computer simulation of a Cainozoic carbonate platform, Marion Plateau, northeast Australia. In: Camoin, G.F and Davies, P.J. eds. *Reefs and Carbonate Platforms in the Pacific and Indian Oceans*. International Association of Sedimentologists Special Publication **25**, pp. 145–161
- Lokier, S. and Steuber, T. 2008. Quantification of carbonate-ramp sedimentation and progradation rates for the late Holocene Abu Dhabi shoreline. *Journal of Sedimentary Research* **78**, pp. 423-431
- Loosveld, R.J.H. Bell, A. and Terken, J.J.M. 1996. The tectonic evolution of interior Oman. *GeoArabia* **1**(1), pp. 28-51
- Loreau, J.P. and Purser, B.H. 1973. Distribution and ultrastructure of Holocene ooids in the Persian Gulf. In: Purser, B.H. ed. *The Persian Gulf: Holocene carbonate sedimentation and diagenesis in a shallow epicontinental sea*. Berlin: Springer-Verlag, pp. 279-328
- Lowenthal, D. Lu, L. Roberson, R. and Sherwood, J.W.C. 1976. The wave equation applied to migration. *Geophysical Prospecting* **24**, pp. 380-399
- Mancini, E.A. Parcell, W.C. Ahr, W.M. Ramirez, V.O. Llinas, J.C. and Cameron, M. 2008. Upper Jurassic updip stratigraphic trap and associated Smackover microbial and nearshore carbonate facies, eastern Gulf coastal plain. *American Association of Petroleum Geologists Bulletin* **92**(4), pp. 417-442
- Markello, J.R. and Read, J.F. 1981. Carbonate ramp to deeper shale shelf transitions of an Upper Cambrian intrashelf basin, Nolichucky Formation, southwest Virginia Appalachians. *Sedimentology* **28**, pp. 573-597
- Markello, J.R. and Read, J.F. 1982. Upper Cambrian intrashelf basin, Nolichucky Formation, southwest Virginia Appalachians. *American Association of Petroleum Geologists Bulletin* **66**(7), pp. 860-878
- Melim, L.A. Westphal, H. Swart, P.K. Eberli, G.P. and Munnecke, A. 2002. Questioning carbonate diagenetic paradigms: Evidence from the Neogene of the Bahamas. *Marine Geology* **185**(1-2), pp. 27-53
- Merino-Tome, O. Bahamonde, J.R. Samankassou, E. and Villa, E. 2009. An example from a thrust-top carbonate ramp (Upper Pennsylvanian foreland basin, Picos de Europa, NW Spain). *Palaeogeography, Palaeoclimatology, Palaeoecology* **278**(1-4), pp. 1-23
- Michalik, J. 1997. Tsunamites in a storm-dominated Anisian carbonate ramp (Vysoká Formation, malé Karpaty Mts., western Carpathians). *Geologica Carpathica* **48**(4), pp. 221-229

- Mitchell, N.C. 1996. Creep in pelagic sediments and potential for morphological dating of marine fault scarps. *Geophysical Research Letters* **23**, pp. 483-486
- Mitchum, R. M. and Uliana, M. A. 1985. Seismic stratigraphy of carbonate depositional sequences, Upper Jurassic-Lower Cretaceous, Neuquen Basin, Argentina. In: Berg, O.R. and Woolverton, D.G. eds. *Seismic Stratigraphy II: an Integrated Approach to Hydrocarbon Exploration*. American Association of Petroleum Geologists, Memoir **39**, pp. 255-274
- Mohseni, H. and Al-Asam, I.S. 2004. Tempestite deposits on a storm-influenced carbonate ramp: An example from the Pabdeh Formation (Paleogene), Zagros Basin, SW Iran. *Journal of Petroleum Geology* **27**(2), pp. 163-178
- Moore, C. H. 2001. *Carbonate Reservoirs. Porosity Evolution and Diagenesis in a Sequence Stratigraphic Framework*. Elsevier.
- Mougenot, D. 1999. Seismic imaging of a carbonate reservoir: The Dogger of the Villeperdue oil field, Paris Basin, France. *Petroleum Geoscience* **5**(1), pp. 75-82
- Munnecke, A. Westphal, H. Reijmer, J.J.G. and Samtleben, C. 1997. Microspar development during early marine burial diagenesis: A comparison of Pliocene carbonates from the Bahamas with Silurian limestones from Gotland (Sweden). *Sedimentology* **44**(6), pp. 977-990
- Munnecke, A. Westphal, H. Elrick, M. and Reijmer, J.J.G. 2001. The mineralogical composition of precursor sediments of calcareous rhythmites: A new approach. *International Journal of Earth Sciences* **90**(4), pp. 795-812
- Munnecke, A. and Westphal, H. 2004. Shallow-water aragonite recorded in bundles of limestone-marl alternations - The Upper Jurassic of SW Germany. *Sedimentary Geology* **164**(3-4), pp. 191-202
- Munnecke, A. and Westphal, H. 2005. Variations in primary aragonite, calcite, and clay in fine-grained calcareous rhythmites of Cambrian to Jurassic age - An environmental archive? *Facies* **51**(1-4), pp. 592-607
- Murris, R.J. 1980. Middle East: stratigraphic evolution and oil habitat. *American Association of Petroleum Geologists Bulletin* **64**, pp. 597-618
- Mutti, M. and Bernoulli, D. 2003. Early marine lithification and hardground development on a Miocene ramp (Maiella, Italy): Key surfaces to track changes in trophic resources in montropical carbonate settings. *Journal of Sedimentary Research* **73**(2), pp. 296-308

- Nichols, G. 1998. *Sedimentology and Stratigraphy*. London: Wiley-Blackwell.
- Ogg, J.G. Ogg, G. and Gradstein, F.M. 2008. *The Concise Geologic Time scale*. Cambridge University Press.
- Osleger, D.A. Barnaby, R. and Kerans, C. 2004. A Laterally Accreting Grainstone Margin from the Albian of Northern Mexico: Outcrop Model for Cretaceous Carbonate Reservoirs. In: Grammer, G.M. et al. eds. *Integration of outcrop and modern analogs in reservoir modelling*. American Association of Petroleum Geologists, Memoir **80**, pp. 93-107
- Palma, R.M. López-Gómez, J. and Piethé, R.D. 2007. Oxfordian ramp system (La Manga Formation) in the Bardas Blancas area (Mendoza Province) Neuquén Basin, Argentina: Facies and depositional sequences. *Sedimentary Geology* **195**(3-4), pp. 113-134
- Pedley, M. 1998. A review of sediment distributions and processes in Oligo-Miocene ramps of southern Italy and Malta (Mediterranean divide). In: Wright, V.P. and Burchette, T.P. eds. *Carbonate ramps*. The Geological Society, Special Publication **149**, pp. 163-179
- Perissoratis, C. and Van Andel, T.H. 1991. Sea-level changes and tectonics in the Quaternary extensional basin of the South Evvoikos Gulf, Greece. *Terra Nova* **3**(3), pp. 294-302
- Playton, T.E. Janson, X. and Kerans, C. In press. Carbonate Slopes. In: James, N.P. and Dalrymple, R.W. *Facies models*. Geological Association of Canada, GeoText **6**
- Pomar, L. 2001a. Types of carbonate platforms: a genetic approach. *Basin Research* **13**, pp. 313-334
- Pomar, L. 2001b. Ecological control of sedimentary accommodation: Evolution from a carbonate ramp to rimmed shelf, Upper Miocene, Balearic Islands. *Palaeogeography, Palaeoclimatology, Palaeoecology* **175**(1-4), pp. 249-272
- Pomar, L. Obrador, A. and Westphal, H. 2002. Sub-wavebase cross-bedded grainstones on a distally steepened carbonate ramp, Upper Miocene, Menorca, Spain. *Sedimentology* **49**(1), pp. 139-169
- Pomar, L. Brandano, M. and Westphal, H. 2004. Environmental factors influencing skeletal grain sediment associations: A critical review of Miocene examples from the western Mediterranean. *Sedimentology* **51**(3), pp. 627-651
- Pomar, L. and Hallock, P. 2008. Carbonate factories: A conundrum in sedimentary geology. *Earth-Science Reviews* **87**(3-4), pp. 134-169

- Posamentier, H.W. Jervy, M.T. and Vail, P.R. 1988. Eustatic controls on clastic deposition I – conceptual framework. In: Wilgus, C.W. et al. eds. *Sea-level changes: an integrated approach*. SEPM, Special Publication **42**, pp. 109-124
- Posamentier, H.W. and Allen, G.P. 1993. Siliciclastic sequence stratigraphic patterns in foreland ramp-type basins. *Geology* **21**(5), pp. 455-458
- Proust, J.N. Deconinck, J.F. Geysant, J.R. Herbin, J.P. and Vidier, J.P. 1995. Sequence analytical approach to the upper Kimmeridgian-lower tithonian storm-dominated ramp deposits of the Boulonnais (Northern France). A landward time-equivalent to offshore marine source rocks. *Geologische Rundschau* **84**(2), pp. 255-271
- Proust, J.N. 1998. Carbonate platform drowning in a foreland setting: The mid-Carboniferous Platform in Western Urals (Russia). *Journal of Sedimentary Research* **68**(6), pp. 1175-1188
- Purser, B.H. 1973. *The Persian Gulf: Holocene carbonate sedimentation and diagenesis in a shallow epicontinental sea*. New York: Springer-Verlag.
- Purser, B.H. 1985. Dedolomite porosity and reservoir properties of Middle Jurassic Carbonates in the Paris Basin, France. In: Roehl, P.O. and Choquette, P.W. eds. *Carbonate Petroleum Reservoirs*. Berlin, Springer-Verlag, pp. 341-355
- Purser, B.H. and Evans, G. 1973. Regional sedimentation along the Trucial Coast, SE Persian Gulf. In: Purser, B.H. ed. *The Persian Gulf: Holocene carbonate sedimentation and diagenesis in a shallow epicontinental sea*. Berlin: Springer-Verlag, pp. 211-233
- Purser, B.H. and Seibold, E. 1973. The principal environmental factors influencing Holocene sedimentation and diagenesis in the Persian Gulf. In: Purser, B.H. ed. *The Persian Gulf: Holocene carbonate sedimentation and diagenesis in a shallow epicontinental sea*. Berlin: Springer-Verlag, pp. 1-11
- Qahtani, N. 2010. *Mode and tempo of sea-level changes during the Arundian of Gower and their effects on depositional architecture and porosity evolution*. MPhil Thesis, University of Cardiff, Cardiff (unpublished).
- Quesada, S. Dorronsoro, C. Rubles, S. Chiar, R. and Grimalt, J.O. 1997. Geochemical correlation of oil from the ayoluengo field to liassic black shale units in the southwestern Basque-Cantabrian Basin (northern Spain). *Organic Geochemistry* **27**(1-2), pp. 25-40
- Ramsay, A.T.S. 1987. Depositional environments of Dinantian limestones in Gower, South Wales. In: Miller, J. et al. eds. *European Dinantian Environments*. London: J. Wiley and Sons, pp. 265-308

- Ramsay, P.J. Smith, A.M. and Mason, T.R. 1996. Geostrophic sand ridge, dune fields and associated bedforms from the Northern KwaZulu-Natal shelf, south-east Africa. *Sedimentology* **43**(3), pp. 407-419
- Rankey, E. C. 2004. On the interpretation of shallow shelf carbonate facies and habitats: How much does water depth matter? *Journal of Sedimentary Research* **74**, pp. 2-6
- Read, J.F. 1982. Carbonate Platforms of Passive (Extensional) Continental Margins - Types, Characteristics and Evolution. *Tectonophysics* **81**, pp. 195-212
- Read, J.F. 1985. Carbonate Platform Facies Models. *American Association of Petroleum Geologists Bulletin* **69**, pp. 1-21
- Read, J.F. 1989. Controls on evolution of Cambrian-Ordovician passive margin, U.S. Appalachians. In: Crevello, P.D. et al. eds. *Controls on Carbonate Platforms and Basin Development*. SEPM Special Publication **44**, pp. 147-165
- Read, J.F. 1998. Phanerozoic carbonate ramps from greenhouse, transitional and ice-house worlds: clues from field and modelling studies. In: Wright, V.P. and Burchette, T.P. eds. *Carbonate ramps*. The Geological Society, Special Publication **149**, pp. 107-135
- Reading, H.G. 1996. *Sedimentary Environments: Processes, Facies and Stratigraphy*. Blackwell Publishing Limited
- Reid, S.K. and Dorobek, S.L. 1993. Sequence stratigraphy and evolution of a progradational, foreland carbonate ramp, Lower Mississippian Mission Canyon Formation and stratigraphic equivalents, Montana and Idaho. In: Loucks, J. and Sarg, J.F. eds. *Carbonate Sequence stratigraphy*. American Association of Petroleum Geologists, Memoir **57**, pp. 327-352
- Ricken, W. 1996. Bedding rhythms and cyclic sequences as documented in organic carbon - Carbonate patterns, Upper Cretaceous, Western Interior, U.S. *Sedimentary Geology* **102**(1-2), pp. 131-154
- Rider, M.H. 1996. *Geological interpretation of well logs, Second edition*. Houston: Gulf Publishing Company.
- Rosales, I. Quesada, S. and Robles, S. Geochemical arguments for identifying second-order sea-level changes in hemipelagic carbonate ramp deposits. *Terra Nova* **18**(4), pp. 233-240
- Rygel, M.C. Fielding, C.R. Frank, T.D. and Birgenheier, L.P. 2008. The magnitude of late paleozoic glacioeustatic fluctuations: A synthesis. *Journal of Sedimentary Research* **78**(7-8), pp. 500-511

- Saller, A.H. Walden, S. Robertson, S. Nims, R. Schwab, J. Hagiwara, H. and Mizohata, S. 2005. Three-dimensional seismic imaging and reservoir modeling of an upper paleozoic "reefal" buildup, reinecke field, west Texas, United States. In: Eberli, G.P. et al. eds. *Seismic imaging of carbonate reservoirs and systems*. American Association of Petroleum Geologists, Memoir **81**, pp. 107-122
- Sami, T. and Desrochers, A. 1992. Episodic sedimentation on an early Silurian, storm-dominated carbonate ramp, Becscie and Merrimack formations, Anticosti Island, Canada. *Sedimentology* **39**(3), pp. 355-381
- Sassen, R. Moore, C.H. and Meendsen, F.C. 1987. Distribution of hydrocarbon source potential in the Jurassic Smackover formation. *Organic Geochemistry* **11**(5), pp. 379-383
- Scheibner, C. Kuss, J. and Speijer, R.P. 2003. Stratigraphic modelling of carbonate platform-to-basin sediments (Maastrichtian to Paleocene) in the Eastern Desert, Egypt. *Palaeogeography, Palaeoclimatology, Palaeoecology* **200**(1-4), pp. 163-185
- Schlager, W. 1981. The paradox of drowned reefs and carbonate platforms. *Geological Society of America, Bulletin* **92**(4), pp. 197-211
- Schlager, W. 2000. Sedimentation rates and growth potential of tropical, cool water and mud-mound carbonate systems. In: Insalaco, E. et al. eds. *Carbonate Platform Systems: Components and Interactions*. The Geological Society, Special Publication **178**, pp. 317-227
- Schlager, W. 2003. Benthic carbonate factories of the Phanerozoic. *International Journal of Earth Sciences* **92**(4), pp. 445-464
- Schlager, W. 2005. *Carbonate Sedimentology and Sequence Stratigraphy*. SEPM Concepts in Sedimentology and Paleontology Series no. 8. Tulsa: SEPM
- Schwab, A.M. Cronin, B.T and Ferreira, H. 2007. Seismic expression of channel outcrops: Offset stacked versus amalgamated channel systems. *Marine and Petroleum Geology* **24**, pp. 504-514
- Seibold, E. Diester, L. Futterer, D. Lange, H. Muller, P. and Werner, F. 1973. Holocene sediments and sedimentary processes in the Iranian part of the Persian Gulf. In: Purser, B.H. ed. *The Persian Gulf: Holocene carbonate sedimentation and diagenesis in a shallow epicontinental sea*. Berlin: Springer-Verlag, pp. 57-80
- Sheriff, R.E. 1991. *Encyclopedia dictionary of exploration geophysics*. Geophysical reference series, Society of Exploration Geophysics. American Association of Petroleum Geologists: Tulsa

- Simpson, J. 1985. *The Sedimentology of the Arundian (Dinantian) of Gower and South Dyfed*. PhD Thesis, University of Reading, Reading (unpublished).
- Simpson, J. 1987. Mud-dominated storm deposits from a Lower Carboniferous ramp. *Geological Journal* **22**(3), pp. 191-205
- Sinclair, H.D. 1997. Tectonostratigraphic model for underfilled peripheral foreland basins: An Alpine perspective. *Bulletin of the Geological Society of America* **109**(3), pp. 324-346
- Sivils, D.J. 2005. An upper Mississippian carbonate ramp system from the Pedregosa Basin, Southwestern New Mexico, U.S.A.: An outcrop analog for middle carboniferous carbonate reservoirs. In: Grammer, G.M. et al. eds. *Integration of Outcrop and Modern Analogs*. American Association of Petroleum Geologists, Memoir **80**, pp. 109-128
- Sonnenfeld, P. 1985. Evaporites as oil and gas source rocks. *Journal of Petroleum Geology* **8**, pp. 28-42
- Stafleu, J. Everts, A.J.W. and Kenter, J.A.M. 1994. Seismic models of a prograding carbonate platform: Vercors, southeast France. *Marine and Petroleum Geology* **11**, pp. 513-527
- Stanton Jr, R.J. and Flugel, E. 1995. An accretionary distally steepened ramp at an intrashelf basin margin: an alternative explanation for the Upper Triassic Steinplatte "reef" (Northern Calcareous Alps, Austria). *Sedimentary Geology* **95**(3-4), pp. 269-286
- Steuber, T. 2000. Skeletal growth rates of Upper Cretaceous rudist bivalves: Implications for carbonate production and organism-environment feedbacks. In: Insalaco, E. et al. eds. *Carbonate Platform Systems: Components and Interactions*. The Geological Society, Special Publication **178**, pp. 21-32
- Sullivan, M. Foreman, J.L. Jennette, D.C. Stern, D. Jensen, N.G and Goulding, F.J. 2004. An integrated approach to characterization and modeling of deep-water reservoirs, Diana field, western Gulf of Mexico. In: Gramer, M. et al. eds. *Integration of outcrop and modern analogs in reservoir modeling*. American Association of Petroleum Geologists, Memoir **80**, pp. 215-234
- Swift, D.J.P. and Thorne, J.A. 1991. Sedimentation on Continental Margins, I: A General Model for Shelf Sedimentation. In Swift, J. P. et al. eds. *Shelf Sand and Sandstone Bodies*. International Association of Sedimentologists, Special Publication **14**, pp.1-31
- Tappin, D.R. 2007. Sedimentary features of tsunami deposits - Their origin, recognition and discrimination: An introduction. *Sedimentary Geology* **200**(3-4), pp. 151-154
- Terken, J. M. J. 1999. The Natih Petroleum of north Oman. *GeoArabia* **4**, pp. 157-180

- Thorne, J.A. and Swift, D.J.P. 1991. Sedimentation on Continental Margins, II: Application of the Regime Concept. In: Swift, J. P. et al. eds. *Shelf Sand and Sandstone Bodies*. International Association of Sedimentologists, Special Publication **14**, pp. 59-81
- Tinker, S.W. Caldwell, D.H. Cox, D.M. Zahm, L.C. and Brinton, L. 2005. Integrated reservoir characterization of a carbonate ramp reservoir, South Dagger Draw field, New Mexico: Seismic data are only part of the story. In: Eberli, G.P. et al. eds. *Seismic imaging of carbonate reservoirs and systems*. American Association of Petroleum Geologists, Memoir **81**, pp. 91-105
- Tisljar, J. Igor Vlahović, I.V. Matěec, D. and Robson, J. 1998. Carbonate facies evolution from the late albian to middle cenomanian in southern istria (Croatia): Influence of synsedimentary tectonics and extensive organic carbonate production. *Facies* **38**, pp. 137-152
- TomasĽovýĽ, A. 2004. Microfacies and depositional environment of an Upper Triassic intra-platform carbonate basin: The Fatric Unit of the West Carpathians (Slovakia). *Facies* **50**(1), pp. 77-105
- Torok, A. 1998. Controls on development of Mid-Triassic ramps: examples from southern Hungary. In: Wright, V.P. and Burchette, T.P. eds. *Carbonate ramps*. The Geological Society, Special Publication **149**, pp. 339-367
- Tucker, M.E. and Wright, V.P. 1990. *Carbonate Sedimentology*. London: Wiley-Blackwell.
- Urien, C.M. and Zambrano, J.J. 1994. Petroleum systems in the Neuquen Basin, Argentina. In: Magoon, L.B. and Dow, W.G. eds. *The petroleum system - from source to trap*. American Association of Petroleum Geologists, Memoir **60**, pp. 513-534
- Vail, P.R. 1987. Seismic stratigraphic interpretation using sequence stratigraphy. Part 1: Seismic stratigraphy interpretation procedure. In: Bally, A.W. ed. *Atlas of Seismic Stratigraphy*. American Association of Petroleum Geologists Studies in Geology **27**(1), pp. 1-10
- Van Buchem, F.S.P. Razin, P. Homewood, P.W. Philip, J.M. Eberli, G.P. Platel, J.P. Roger, J. Eschard, R. Desaubliaux, G.M.J. Boisseau, T. Leduc, J.P. Labourdette, R. and Cantaloube, S. 1996. High resolution sequence stratigraphy of the Natih Formation (Cenomanian/Turonian) in northern Oman: distribution of source rocks and reservoir facies. *GeoArabia* **1**(1), pp. 65-91
- Van Buchem, F. S. P. Razin, P. Homewood, P. W. Oterdoom, W. H. and Philip, J. 2002. Stratigraphic organization of carbonate ramps and organic-rich intrashelf basins: Natih Formation (middle Cretaceous) of northern Oman. *American Association of Petroleum Geologists Bulletin* **86**, pp. 21-53

- Van Wagoner, J.C., Posamentier, H.W., Mitchum, R.M., Vail, P.R., Sarg, J.F., Loutit, T.S. and Hardenbol, J. 1988. An overview of the fundamentals of sequence stratigraphy and key definitions. In: Wilgus, C.W. et al. eds. *Sea-level changes: an integrated approach*. SEPM, Special Publication **42**, pp. 39-45
- Van Wagoner, J.C., Mitchum, R.M., Campion, K.M. and Rahmanian, V.D. 1990. Siliciclastic sequence stratigraphy in well logs, core, and outcrops: Concepts for High-Resolution Correlation of Time and Facies. *American Association of Petroleum Geologists Special Volume 7*, pp. 1-55
- Wagner, C.W. and Van Der Togt, C. 1973. Holocene sediment types and their distribution in the southern Persian Gulf. . In: Purser, B.H. ed. *The Persian Gulf: Holocene carbonate sedimentation and diagenesis in a shallow epicontinental sea*. Berlin: Springer-Verlag, pp. 123-156
- Walkden, G. and Williams, A. 1998. Carbonate ramps and the Pleistocene-Recent depositional systems of the Arabian Gulf. In: Wright, V.P. and Burchette, T.P. eds. *Carbonate ramps*. The Geological Society, Special Publication **149**, pp. 43-53
- Walter, L.M. and Bruton, E.A. 1990. Dissolution of recent platform carbonate sediments in marine pore fluids. *American Journal of Science* **290**(6), pp. 601-643
- Warren, J.K. 1986. Perspectives: shallow-water evaporitic environments and their source rock potential. *Journal of Sedimentary Petrology* **56**, pp. 442-454
- Warrlich, G.M.D., Waltham, D.A. and Bosence, D.W.J. 2002. Quantifying the sequence stratigraphy and drowning mechanisms of atolls using a new 3-D forward stratigraphic modelling program (CARBONATE 3D). *Basin Research* **14**, pp. 379-400
- Warrlich, G., Bosence, D., Waltham, D., Wood, C., Boylan, A. and Badenas, B. 2008. 3D stratigraphic forward modelling for analysis and prediction of carbonate platform stratigraphies in exploration and production. *Marine and Petroleum Geology* **25**, pp. 35-58
- Watney, W.L., Wong, J.C. and French Jr. J.A. 1991. Computer simulation of Upper Pennsylvanian (Missourian) carbonate-dominated cycles in western Kansas. In: Franseen, E.K. et al. eds. *Sedimentary modeling: Computer simulations and methods for improved parameter definition*. Kansas Geological Survey, Bulletin **233**, pp. 415-430
- Watney, W.L., Rankey, E.C. and Harbaugh, J. 1999. Perspectives on stratigraphic simulation models: current approaches and future opportunities. In: Harbaugh, J.H. et al. eds. *Numerical Experiments in Stratigraphy*. SEPM, Special Publication **62**, pp. 3-21

- Watts, K.F. and Blome, C.D. 1990. Evolution of the Arabian carbonate platform margin slope and its response to orogenic closing of a Cretaceous ocean basin, Oman. In: Tucker, M.E. et al. eds. *Carbonate Platforms, Facies, Sequences and Evolution*. International Association of Sedimentologists. Special Publication 9, pp. 291–323
- Watts, N.R. 1988. The role of carbonate diagenesis in exploration and production from Devonian pinnacle reefs, Alberta, Canada. *Geological Society of Malaysia Bulletin* 22, pp. 1-2
- Weber, J.L. Francis, B.P. Harris, P.M. and Clark, M. 2003. Stratigraphy, lithofacies, and reservoir distribution, Tengiz Field, Kazakhstan. In: Ahr, W.M. et al. eds. *Permo-Carboniferous carbonate platforms and reefs*. American Association of Petroleum Geologists, Memoir 83, pp. 351-394
- Westphal, H. 2006. Limestone-marl alternations as environmental archives and the role of early diagenesis: A critical review. *International Journal of Earth Sciences* 95(6), pp. 947-961
- Westphal, H. and Munnecke, A. 2003. Limestone-marl alternations: A warm-water phenomenon? *Geology* 31(3), pp. 263-266
- Wheelely, J. 2006. Taphonomy, sedimentology and palaeoenvironmental interpretation of Middle Ordovician Limestones, Jämtland, Sweden. PhD Thesis, University of Cardiff, Cardiff (unpublished).
- Wheelely, J. R. Cherns, L. and Wright, V.P. 2008. Provenance of microcrystalline carbonate cement in limestone–marl alternations (LMA): aragonite mud or molluscs? *Journal of the Geological Society* 165, pp. 395-403
- Williams, H.D. Burgess, P.M. Wright, V.P. Della-Porta, G. and Granjeon, D. 2009 (In review). Investigating Carbonate platform types: multiple controls and a continuum of geometries. *Journal of Sedimentary Research*
- Wilson, J.L. 1975. *Carbonate Facies in Geologic History*. New York: Springer-Verlag
- Wright, V.P. 1986. Facies sequences on a carbonate ramp: the Carboniferous Limestone of South Wales. *Sedimentology* 33, pp. 221-241
- Wright, V.P. 1987. The evolution of the early Carboniferous limestone province in southwest Britain. *Geological Magazine* 124(5), pp. 477-480
- Wright, V.P. 1990. Equatorial aridity and climatic oscillations during the early Carboniferous, southern Britain. *Journal of the Geological Society* 147(2), pp. 359-363

- Wright, V.P. 1994. Early carboniferous carbonate systems: an alternative to the cainozoic paradigm. *Sedimentary Geology* **93**(1-2), pp. 1-5
- Wright, V.P. and Faulkner, T.J. 1990. Sediment Dynamics of Early Carboniferous Ramps - a Proposal. *Geological Journal* **25**, pp. 139-144
- Wright, V. P. Ries, A. C. and Munn, S. G. 1990. Intraplatformal basin-fill deposits from the Infracambrian Huqf Group, east Central Oman. In: Robertson, A.H.F. et al. eds. *The Geology and Tectonics of the Oman Region*. The Geological Society, Special Publication **49**, pp. 601-616
- Wright, V.P. and Burchette, T.P. 1998. Carbonate ramps: an introduction. In: Wright, V.P. and Burchette, T.P. eds. *Carbonate ramps*. The Geological Society, Special Publication **149**, pp. 1-5
- Wright, V.P. Chernes, L. and Hodges, P. 2003. Missing molluscs: Field testing taphonomic loss in the Mesozoic through early large-scale aragonite dissolution. *Geology*, **31**(3), pp. 211-214
- Wright, V.P. and Chernes, L. 2004. Are there "black holes" in carbonate deposystems? *Geologica Acta* **2**(4), pp. 285-290
- Wright, V.P. and Burgess, P.M. 2005. The carbonate factory continuum, facies mosaics and microfacies: An appraisal of some of the key concepts underpinning carbonate sedimentology. *Facies* **51**(1-4), pp. 17-23
- Wu, X.T. 1982. Storm-generated depositional types and associated trace fossils in Lower Carboniferous shallow-marine carbonates of Three Cliffs Bay and Ogmores-by-Sea, South Wales. *Palaeogeography, Palaeoclimatology, Palaeoecology* **39**(3-4), pp. 187-202
- Wyatt, R.J. and Cave, R. 2002. The Chalfield Oolite Formation (Bathonian, Middle Jurassic) and the Forest Marble overstep in the South Cotswolds, and the stratigraphical position of the Fairford Coral Bed. *Proceedings of the Geologists' Association* **113**(2), pp. 139-152
- Yang, W. Mazzullo, S.J. and Teal, C.S. 2004. Sediments, facies tracts, and variations in sedimentation rates of Holocene platform carbonate sediments and associated deposits, northern Belize - Implications for "representative" sedimentation rates. *Journal of Sedimentary Research* **74**(4), pp. 498-512

Appendix 1:

Sedimentary logs of the Pen y Holt Formation, Castlemartin, UK

Sedimentary log legend

Lithology

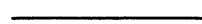


Wackestone



Calcimudstone

Contacts



Sharp



Erosional

Bioturbation



Moderate Bioturbation



Intense Bioturbation

Fossils



Bivalves



Brachiopod



Crinoids



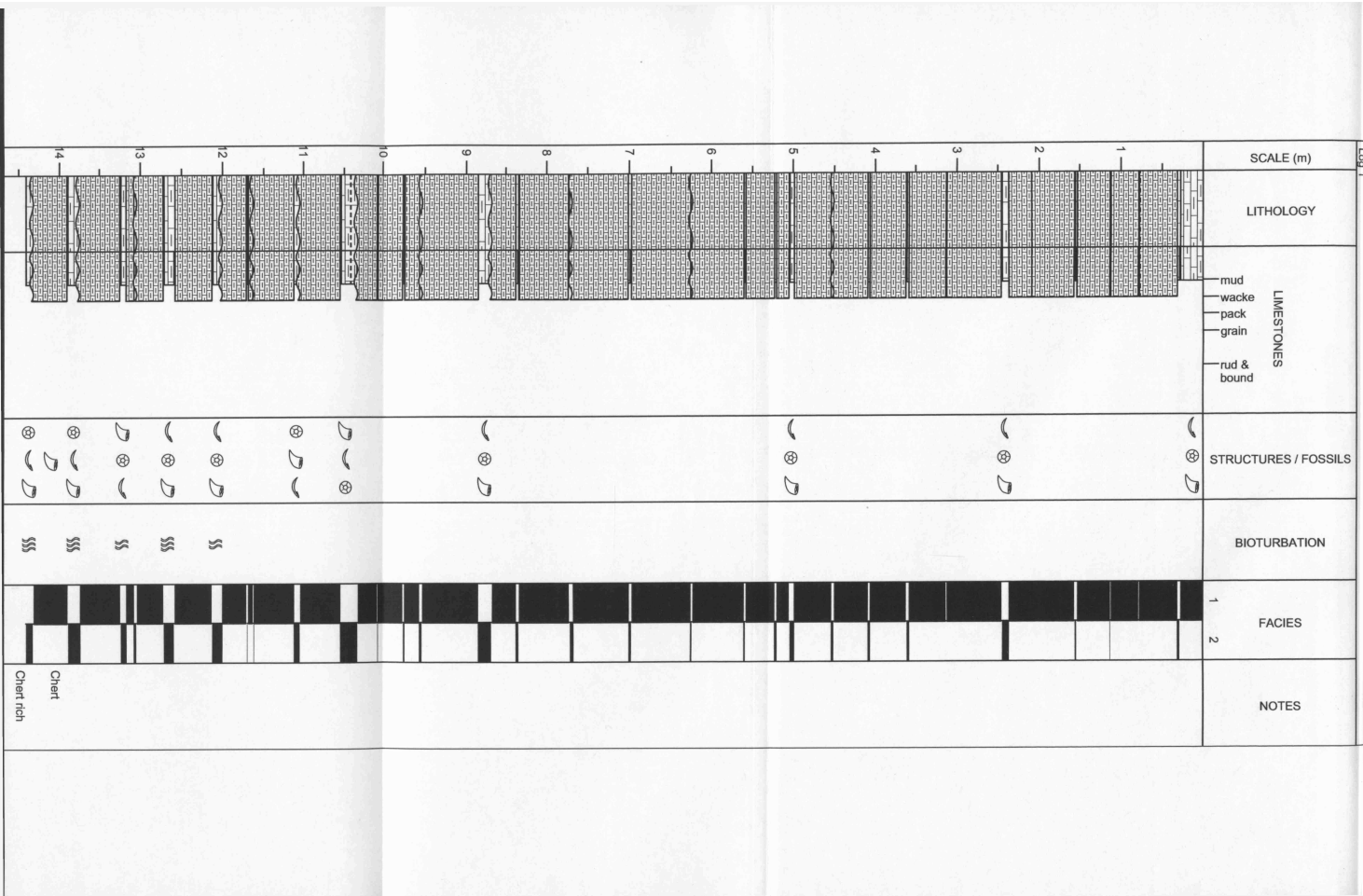
Gastropod



Solitary corals

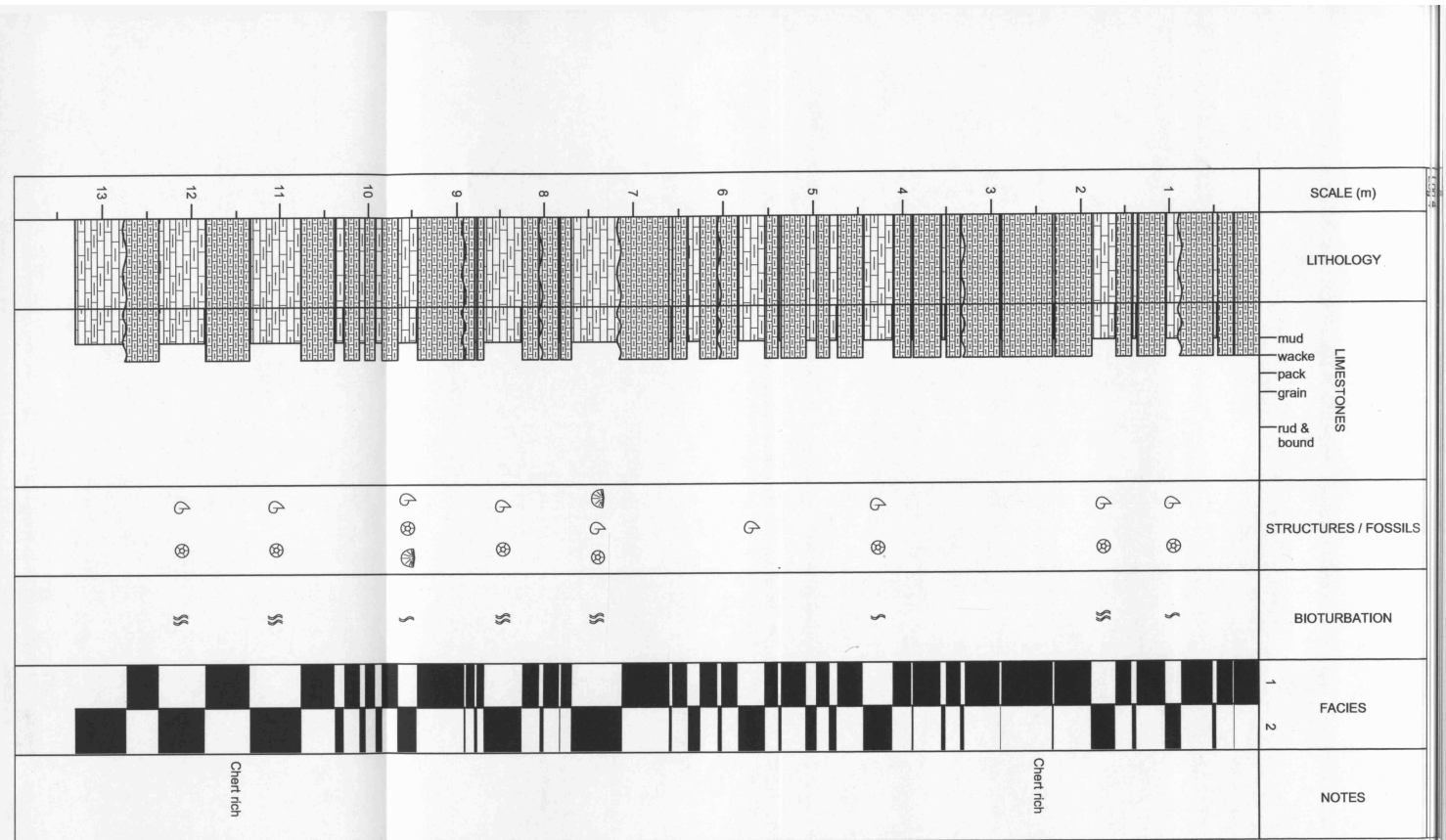


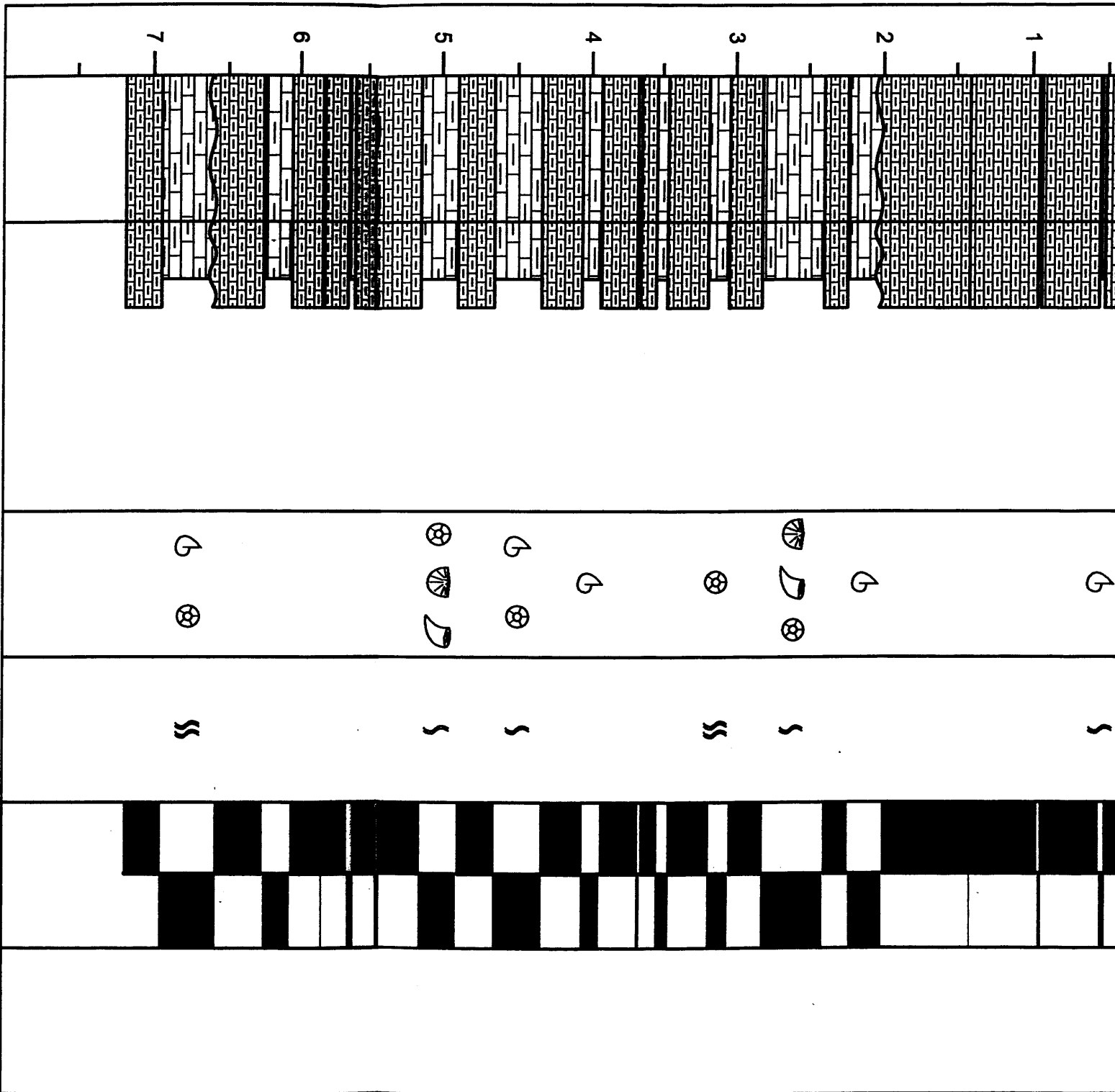
Shell fragments

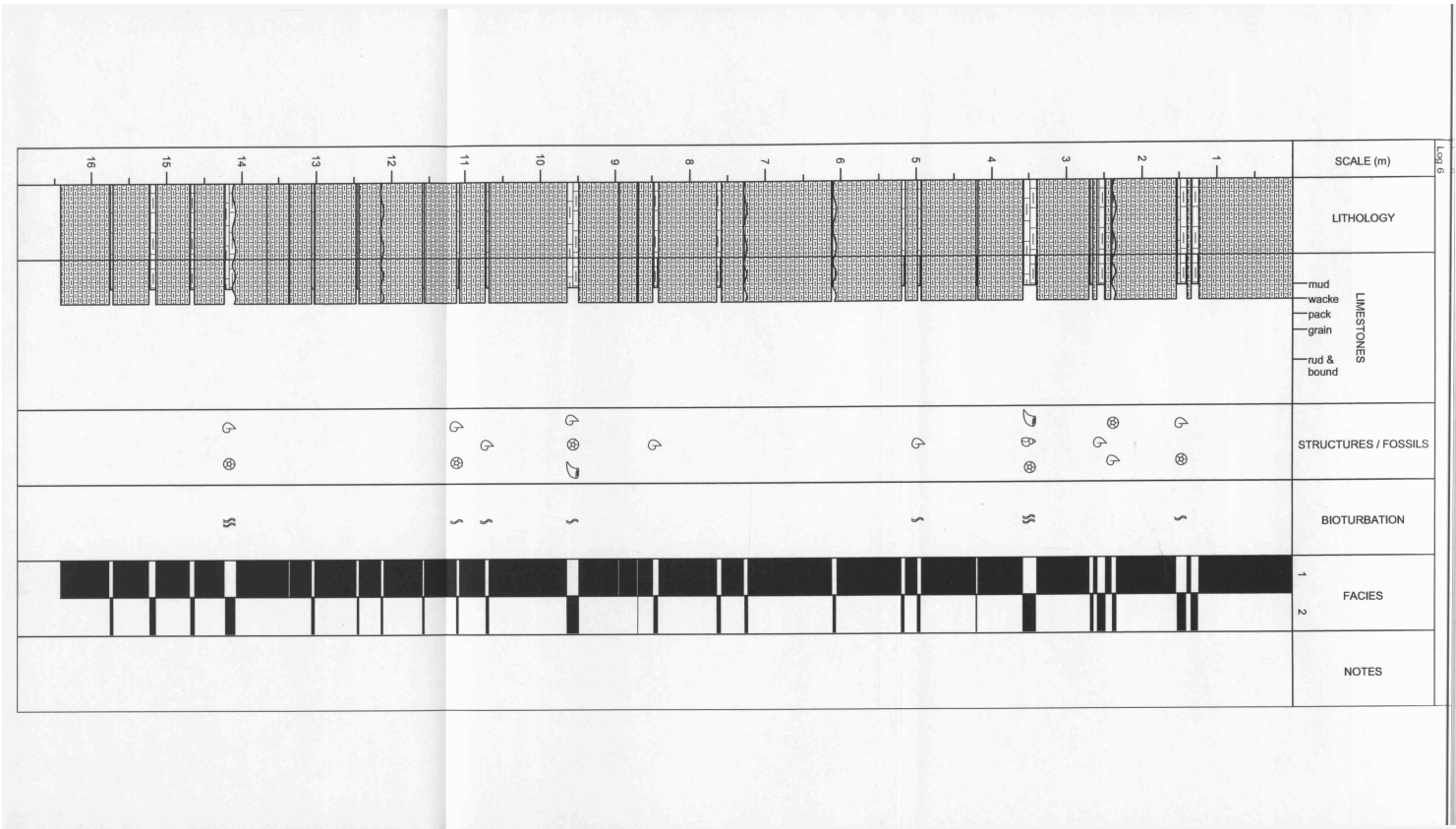


<p>SCALE (M)</p>										
<p>LITHOLOGY</p> <p> </p>										
<p>STRUCTURES (FOLIA)</p> <p> </p>										
<p>BOTANICAL</p> <p> </p>										
<p>FACES</p> <p> </p>										
<p>NOTES</p>										

SCALE (m)	LITHOLOGY	LIMESTONES	STRUCTURES / FOSSIL	BIOTURBATION	FACIES	NOTES
<p>5</p> <p>4</p> <p>3</p> <p>2</p> <p>1</p>		<p>mud wacke pack grain</p> <p>rud & bound</p>			<p>1</p> <p>2</p>	<p>Chert rich</p> <p>Chert rich</p> <p>Chert rich</p>







Lith 6

SCALE (m)

LITHOLOGY

LIMESTONES
 mud wacke
 pack
 grain
 rud & bound

STRUCTURES / FOSSILS

BIOTURBATION

FACIES

NOTES

